

**AUTOMATIC TUNING PID CONTROLLER FOR DISSOLVED OXYGEN
CONCENTRATION IN FERMENTATION PROCESSES.**

by

KARL OWEN JONES B.Eng. (Hons)

**This thesis is submitted in partial fulfilment of the
requirements of Liverpool John Moores University
for the degree of Doctor of Philosophy (PhD).
in
Control Engineering**

July 1995.

**Liverpool John Moores University
in collaboration with
LIFE SCIENCE LABORATORIES Ltd.**

**This copy of the thesis has been supplied on condition
that anyone who consults it is understood to recognise
that its copyright rests with its author and that no
quotation from the thesis and no information derived
from it may be published without the author's prior
written consent.**

ABSTRACT.**Automatic Tuning PID Controller For Dissolved Oxygen Concentration in Fermentation Processes.**

Manual and semi-automatic control of fermentation process loops have been used for many years, however there are now cost incentives and environmental considerations for improving overall process efficiency. Fermentation systems are multivariable, nonlinear and time-varying and consequently difficult to control optimally. One of the significant process variables is the dissolved oxygen concentration in the medium, since there is a requirement for adequate dissolved oxygen to ensure the correct conditions for efficient growth.

Although systematic techniques exist for tuning conventional three term (Proportional + Integral + Derivative) controllers, the problem of finding an optimum set of controller constants can be both difficult and time consuming, when applied to a *Saccharomyces cerevisiae* batch or fed-batch fermentation. The time-variant nature of a fermentation can result in a relatively poor control performance over the process run-time when PID controllers are used. The performance can be improved by the application of adaptive techniques which monitor the time-varying process dynamics and subsequently adjust the controller tuning parameters to continuously improve the system performance.

The research work was the investigation of applying a novel automatic tuner to the control of dissolved oxygen concentration in a Bakers' Yeast fermentation. The tuning technique was chosen from a number of possible control algorithm approaches, because of the minimum knowledge required by the operator. The chosen technique was applied to computer simulations to ascertain its suitability and to evaluate its performance.

The automatic tuner retains the standard PID controller structure, and is designed to retune either periodically, or automatically when a significant error is detected in the regulation of dissolved oxygen concentration. The tuner forces the dissolved oxygen concentration into 'controlled' oscillations without the system becoming unstable. By monitoring the oscillatory response of the process, the automatic tuning procedure determines suitable PID parameters to meet an appropriate design specification. To improve the robustness of the automatic tuner, a noise rejection mechanism is employed to counteract problems caused by erroneous spikes on the measurement signal.

The thesis will demonstrate how the proposed automatic tuner was developed, tested and validated using mathematical models of batch and fed-batch *S. cerevisiae* fermentations. The model of the *S. cerevisiae* fermentation includes the effects of excess glucose with a controlled dissolved oxygen loop. Simulation results are presented showing the performance of the automatic tuner, highlighting the tuner's ability to produce suitable controller parameters, for a range of operating conditions, in a relatively short time. Additionally, on-line results of the automatic tuner on *S. cerevisiae* batch and fed-batch fermentations will be shown, using a laboratory scale vessel. An assessment and comparison of the performance of the automatic tuner with a conventionally tuned PID controller will be made, for off-line and on-line implementations.

The automatic tuner has also been successfully tested on-line by its application to a chemical reaction, in which the broth dissolved oxygen is removed by sodium sulphite (Na_2SO_3) in a conversion to sodium sulphate (Na_2SO_4). This was in effect a 'black-box' application since no mathematical model existed for simulations to be carried out to ascertain the automatic tuner performance.

Karl Owen Jones.
20th July, 1995.

ACKNOWLEDGEMENTS

I would like to express my thanks to my supervisors, Prof. D. Williams, Dr. D. Phipps and Dr. P.A. Montgomery; for their continued support and encouragement.

In addition I would like to thank Dr. J. Adamson of Life Science Laboratories Ltd. for his technical assistance on the MENTOR software and the fermentation industry in general.

I would like to acknowledge the assistance and encouragement provided by all the members of the Control Systems Research Group and the staff of the School of Electrical and Electronic Engineering, in particular Mr. A.V. Goodier.

Finally, I could not have embarked on a project of this magnitude without the love and support of my parents and my fiancée.

Karl O. Jones.

CONTENTS

NOMENCLATURE	viii
CHAPTER 1.	
INTRODUCTION.	
1.1. FOREWORD.	1
1.2. FERMENTATION PROCESSES.	3
1.2.2. Why Bakers' Yeast?	3
1.2.3. Fermentation Process Control.	3
1.3. METHODS OF CONTROLLING DISSOLVED OXYGEN.	5
1.4. PRACTICAL CONTROL METHODOLOGIES.	7
1.4.1. Adaptive Control.	10
1.5. SCOPE OF THE INVESTIGATION.	12
1.5.1. Statement of Problem Addressed.	12
1.5.2. Aims of the Project.	14
1.5.3. Approach to the Investigation.	14
1.5.4. Originality of the Research.	15
1.6. REVIEW OF THE THESIS.	15
1.7. REFERENCES.	16
CHAPTER 2.	
MATERIALS AND EQUIPMENT EMPLOYED.	
2.1. INTRODUCTION.	21
2.2. EQUIPMENT REQUIREMENTS.	22
2.2.1. Microprocessor System and Peripherals.	22
2.2.2. Laboratory Scale Fermentation Vessel.	24
2.2.3. Sensors and Probes.	26
2.2.3.a. Dissolved Oxygen Measurement.	26
2.2.3.b. Input Air Flow Control.	27
2.2.3.c. Temperature Measurement and Control.	29
2.2.3.d. pH Measurement and Control.	29
2.2.3.e. Foam Control.	31
2.2.3.f. Feed Pumps.	31
2.2.4. 3D-Interface Unit.	32
2.3. COMPUTER SOFTWARE UTILISED.	32
2.3.1. Fermentation Control Software (MENTOR).	32
2.3.1.a. Data Logging.	32
2.3.1.b. Process Control.	33
2.3.2. Computer Aided Design Software.	35
2.3.3. Custom Written Software (QuickBASIC).	35
2.4. CHEMICAL COMPOUNDS.	36
2.4.1. Fermentation Experiments.	36
2.4.2. Sodium sulphite Experiments.	37
2.5. DISCUSSION.	37
2.6. REFERENCES.	37
CHAPTER 3.	
AUTOMATIC TUNING PROCEDURE : THEORY AND IMPLEMENTATION.	
3.1. INTRODUCTION.	38
3.2. THE THREE TERM REGULATOR.	42
3.3. MANUAL TUNING PROCEDURES.	42
3.3.1. Closed-Loop Tuning Method.	44
3.3.2. Phase Margin and Gain Margin.	45
3.3.3. Phase Margin Design.	47

3.3.4. Gain Margin Design.	51
3.4. RELAY CONTROL.	53
3.4.1. Limit Cycles.	53
3.4.2. Describing Function Technique.	53
3.4.3. Stability Analysis using Describing Functions.	58
3.5. DEVELOPMENT OF THE AUTOMATIC TUNER.	60
3.5.1. Choice of Nonlinear Element.	60
3.5.2. Analysis of the Describing Function of a Nonlinear Element with Hysteresis.	62
3.5.3. Analysis of a System Containing a Nonlinear Element with Hysteresis.	67
3.6. IMPLEMENTATION OF THE AUTOMATIC TUNING PROCEDURE.	69
3.6.1. Estimation of Process Response Amplitude and Frequency.	70
3.6.1.a. Amplitude Estimation.	70
3.6.1.b. Frequency Estimation.	71
3.6.1.c. Practical Implementation.	72
3.7. TUNING RULES.	73
3.7.1. Using the Nonlinear Element with Hysteresis.	76
3.7.1.a. Criteria for Ending the Tuning Phase.	77
3.8. DISCUSSION.	78
3.9. REFERENCES.	80
CHAPTER 4.	
MATHEMATICAL MODELS OF FERMENTATION PROCESSES.	
4.1. INTRODUCTION.	84
4.2. CELL GROWTH.	84
4.3. DISSOLVED OXYGEN IN THE FERMENTER.	87
4.3.1. Oxygen Transfer Rate.	88
4.3.2. Oxygen Uptake Rate.	89
4.3.3. Volumetric Oxygen Transfer Coefficient.	90
4.3.4. Oxygen Partial Pressure.	91
4.3.5. Factors affecting $K_{L,a}$ values in fermentation vessels.	92
4.3.5.a. Effect of air-flow rate on $K_{L,a}$	92
4.3.5.b. Effect of the degree of agitation on K	92
4.4. FED-BATCH FERMENTATION (MODEL I).	93
4.4.1. Cell Growth Rate.	93
4.4.2. Specific Growth Rate.	94
4.4.3. Glucose Feed Rate.	95
4.4.4. Substrate Concentration.	96
4.4.5. Dissolved Oxygen Concentration.	97
4.5. OXYGEN DEMAND FOR GROWTH.	98
4.6. GROWTH YIELD.	99
4.7. BATCH FERMENTATION (MODEL II).	99
4.7.1. Cell Mass Concentration.	99
4.7.2. Substrate Concentration.	100
4.7.3. Ethanol Concentration.	102
4.7.3.a. Specific Ethanol Production Rate, π_e	102
4.7.3.b. Specific Ethanol Consumption Rate, v_e	103
4.7.4. Growth Inhibitory Substances.	104
4.7.5. Specific growth rate.	104
4.7.6. Dissolved Oxygen Concentration.	105
4.7.7. Glucose Feed Rate.	105
4.8. DISCUSSION.	105
4.9. REFERENCES.	109

CHAPTER 5.**SIMULATION OF THE AUTOMATIC TUNING PROCEDURE.**

5.1. INTRODUCTION.	110
5.2. CHOICE OF NONLINEAR ELEMENT.	111
5.2.1. Advantage of using the Hysteresis Nonlinearity.	117
5.3. IMPLEMENTATION OF THE AUTOMATIC TUNING PROCEDURE.	118
5.4. ADAPTION OF NONLINEARITY CHARACTERISTICS.	124
5.4.1. Regula-Falsi.	121
5.5. COMPARISON OF CONTROLLER RESPONSES.	124
5.5.1. Manual Tuning Methods.	127
5.5.1.a. Ziegler-Nichols Open-Loop Method.	127
5.5.1.b. Ziegler-Nichols Closed-Loop Method.	127
5.5.2. Automatic Tuning Procedure.	128
5.5.2.a. Modified Tuning Procedure.	130
5.5.3. Summary of Transfer Function Results.	132
5.6. APPLICATION TO A FED-BATCH FERMENTATION (MODEL I).	135
5.6.1. Manually Tuned Controller.	135
5.6.1.a. Inclusion of Gaussian Noise.	135
5.6.2. Automatic Tuning Procedure: Single Tuning.	137
5.6.3. Automatic Tuning Procedure: Multiple Tuning.	142
5.6.4. Disturbance Tests.	142
5.7. ENHANCEMENT OF PROCESS REPRESENTATION.	147
5.7.1. Use of Stirrer Speed as Manipulated Variable.	147
5.7.2. Use of Air Flow Rate as Manipulated Variable.	149
5.8. APPLICATION TO A BATCH FERMENTATION (MODEL II).	150
5.8.1. Manual Tuning of the Dissolved Oxygen Loop.	150
5.8.2. Single Application of the Tuning Procedure.	151
5.8.3. Multiple Application of the Tuning Procedure.	156
5.8.3.a. Multiple Application on a Time Basis.	156
5.8.3.b. Multi-tuning on Process Performance.	159
5.8.4. Disturbance Tests.	159
5.8.5. Multi-tuning on Stirrer Speed.	162
5.8.6. Multi-tuning using Air Flow Rate.	162
5.9. DISCUSSION.	162
5.10. REFERENCES.	167

CHAPTER 6.**ON-LINE EXPERIMENTATION.**

6.1. INTRODUCTION.	173
6.2. SOFTWARE IMPLEMENTATION OF THE TUNING PROCEDURE.	174
6.2.1. Comparison of PID Implementations.	175
6.2.2. Activating the Tuning Procedure.	177
6.2.3. Procedure 'Algorithm'.	177
6.2.4. Estimation of Oscillation Period and Amplitude.	178
6.2.5. Terminating the Tuning Phase.	178
6.3. FERMENTATION PROCESS CONTROL.	181
6.3.1. Effect of Temperature and pH on Growth.	181
6.3.2. Agitation Control.	182
6.4. BAKERS' YEAST FERMENTATION.	182
6.4.1. Experimental Method.	182
6.4.2. Glucose feed.	184
6.4.3. Process Control by MENTOR.	185
6.5. BATCH FERMENTATION RESULTS.	186
6.5.1. Manual Tuning.	187
6.5.2. Automatic Tuning.	188

6.5.3. Controller Modification.	194
6.6. FED-BATCH FERMENTATION RESULTS.	198
6.6.1. Manual Tuning.	198
6.6.2. Automatic Tuning.	200
6.7. SODIUM SULPHITE RESULTS.	203
6.7.1. Experimental method.	203
6.7.2. Experimental Results.	203
6.7.2.a. Manual Tuning.	204
6.7.2.b. Automatic Tuning.	206
6.7.2.c. Tuning using Stirrer Speed.	207
6.7.2.d. Effect of Nonlinearity Characteristic.	211
6.7.2.e. Change-over from Tuning to PID Control.	214
6.7.2.f. On-line Multiple Tuning.	215
6.8. DISCUSSION.	217
6.9. REFERENCES.	218

CHAPTER 7.

CONCLUSIONS AND RECOMMENDATIONS.

7.1. INTRODUCTION.	224
7.2. DISCUSSION.	224
7.3. CONCLUSIONS OF THE WORK.	224
7.4. RECOMMENDATIONS FOR FURTHER WORK.	226
7.4.1. Automatic Tuning Procedure Operation.	230
7.4.2. Application to Other Processes.	230
7.5. REFERENCES.	231

APPENDICES.

A. DISSOLVED OXYGEN PROBE STEP RESPONSE.	A-1
B. DATA FILTERS FOR NOISE SUPPRESSION.	B-1
C. MENTOR ANALOG LOOP DATABASE ARRANGEMENT.	C-1
D. AUTOMATIC TUNING PROCEDURE FLOWCHARTS	D-1
E. PUBLICATIONS PRODUCED.	E-1

FIGURES.

Figure 1.1 Normalised oxygen demand during a fed-batch fermentation.	13
Figure 1.2 Normalised oxygen demand during a batch fermentation.	13
Figure 1.3 Basic fermentation plant layout.	15
Figure 2.1 Laboratory Scale Fermentation Plant.	23
Figure 2.2 Computer controlled fermentation process.	24
Figure 2.3 Biolaftte Fermentation Vessel.	25
Figure 2.4 Flowsensor Operational Diagram.	28
Figure 2.5 Mass Flow Control System.	28
Figure 2.6 Mass Flowmeter Calibration Chart.	29
Figure 2.7 Temperature Control Loop.	30
Figure 2.8 pH Control Loop.	31
Figure 3.1 Closed-loop system including a nonlinear element.	40
Figure 3.2 Self-oscillating adaptive control loop.	41
Figure 3.3 The principle of the PID-tuner.	41
Figure 3.4 Gain margin and phase margin.	46
Figure 3.5 Nyquist diagram for phase and gain margin design.	48
Figure 3.6 Phase-margin-designed PID controllers for process of equation (3.16).	50
Figure 3.7 Gain-margin-designed PID controllers for process of equation (3.16).	52
Figure 3.8 Block diagram representing a nonlinear system.	54
Figure 3.9 Generalized form of signals at each system component.	56
Figure 3.10 Prediction and stability of limit cycle.	59

Figure 3.11 Example of a frequency response curve $G(j\omega)$ and the negative inverse describing function $-1/N(a,\omega)$.	60
Figure 3.12 Nonlinear element with hysteresis.	60
Figure 3.13 Comparison of nonlinearity outputs.	61
Figure 3.14 Input-output characteristics for a nonlinear element with hysteresis.	62
Figure 3.15 Ideal nonlinearity.	65
Figure 3.16 Nonlinearity with dead-band.	65
Figure 3.17 Saturation nonlinear element with hysteresis.	65
Figure 3.18 Nonlinear element with hysteresis.	65
Figure 3.19 Saturation nonlinearity.	65
Figure 3.20 Saturation nonlinearity with dead-band.	65
Figure 3.21 Saturation nonlinearity with dead-band and hysteresis.	65
Figure 3.22 Nonlinearity with dead-band and hysteresis.	65
Figure 3.23 Block diagram for process of section 3.5.3.	67
Figure 3.24 Nyquist diagram for equation (3.48) and the describing function.	68
Figure 3.25 Nonsymmetrical oscillation waveform.	73
Figure 3.26 Correct position of the nonlinear element with hysteresis.	76
Figure 3.27 Output from the nonlinear element with hysteresis.	76
Figure 3.28 Location of the $-1/N(a)$ and $G(j\omega)$ -loci.	77
Figure 4.1 Microorganism growth phases.	85
Figure 4.2 Influence of low and high levels of Glucose and Oxygen.	87
Figure 4.3 Cell mass concentration.	93
Figure 4.4 Substrate concentration.	96
Figure 4.5 Saturation oxygen concentration.	97
Figure 4.6 Cell mass concentration.	100
Figure 4.7 Glucose substrate concentration.	101
Figure 4.8 Ethanol concentration.	102
Figure 4.9 Ethanol production rate, π_e .	103
Figure 4.10 Concentration of growth inhibitory substances.	103
Figure 4.11 Cell mass concentration for two values of μ_{max} .	105
Figure 4.12 Oxygen demand for two values of μ_{max} .	106
Figure 5.1 Simple control system.	112
Figure 5.2 Response for first-order type 0 system including nonlinearity with hysteresis.	114
Figure 5.3 Response for second-order type 0 system including nonlinearity with dead-band.	115
Figure 5.4 Response for second-order type 1 system including nonlinearity with dead-band and hysteresis.	115
Figure 5.5 Response for third-order type 0 system including nonlinearity with hysteresis.	116
Figure 5.6 Response for third-order type 1 system including nonlinearity with dead-band and hysteresis.	116
Figure 5.7 Response for third-order type 2 system including ideal nonlinearity.	117
Figure 5.8 Composite period determination.	121
Figure 5.9 Comparison of controller responses.	122
Figure 5.10 Application of the automatic tuning procedure.	125
Figure 5.11 Inclusion of Regula-Falsi into the tuning procedure.	126
Figure 5.12 Tuned PID controller responses.	129
Figure 5.13 Simulation of the tuning operation for equation (5.9).	131
Figure 5.14 Responses of automatically tuned PID controller.	132
Figure 5.15 Effect of applying Regula-Falsi on tuning procedure transient.	133
Figure 5.16 Comparison of tuned PID controller characteristics.	134
Figure 5.17 Manually tuned PI controller on a fed-batch fermentation.	136
Figure 5.18 Manually tuned controller on process with simulated noise.	136
Figure 5.19 Single application of the automatic tuning procedure.	139

Figure 5.20	Operational view of the automatic tuning procedure.	140
Figure 5.21	Automatically tuned controller on fed-batch process with noise. . . .	141
Figure 5.22	Multiple tuned fed-batch process with noise.	143
Figure 5.23	Multi-tuning of the automatic tuning procedure on a fed-batch simulation.	144
Figure 5.24	Change in PID values.	145
Figure 5.25	Response for a set-point change.	146
Figure 5.26	Automatic Tuning Procedure applied during load disturbances.	148
Figure 5.27	Inclusion of stirrer speed as the manipulated variable.	149
Figure 5.28	Inclusion of gas velocity as the manipulated variable.	150
Figure 5.29	Manually tuned PI controller for each phase.	152
Figure 5.30	Same nonlinear element applied for both growth phases (including noise).	154
Figure 5.31	Modified nonlinearity for second tuner application.	155
Figure 5.32	Specific time retuning of a batch fermentation (no noise).	157
Figure 5.33	Change in PID value during a batch fermentation.	158
Figure 5.34	Multiple tuning on the dissolved oxygen concentration performance.	160
Figure 5.35	Automatic Tuning Procedure applied during set-point changes.	161
Figure 5.36	Positive load disturbance test.	163
Figure 5.37	Negative load disturbance test.	164
Figure 5.38	Inclusion of stirrer speed with multiple tuning.	165
Figure 5.39	Inclusion of air flow rate as the manipulated variable.	166
Figure 5.40	Flowchart for simulated automatic tuning procedure on generalized transfer functions.	168
Figure 5.41	Flowchart for the determination of the oscillation amplitude.	169
Figure 5.42	Flowchart for the determination of the oscillation period.	170
Figure 6.1	Block diagram of dissolved oxygen control loop.	174
Figure 6.2	Plot of oscillation amplitude and period estimation.	180
Figure 6.3	Total ammonia added and pH level during a batch fermentation.	183
Figure 6.4	Exponential glucose substrate feed profile.	186
Figure 6.5	Manually tuned proportional controller response.	189
Figure 6.6	Final manually tuned PID controller response.	190
Figure 6.7	Single tuning during a batch fermentation.	192
Figure 6.8	Auto-tuning during both growth phases.	193
Figure 6.9	Auto-tuning with increased sampling rate.	195
Figure 6.10	Dissolved oxygen response for final sampling rate.	196
Figure 6.11	Response for controller modification.	197
Figure 6.12	Fed-batch fermentation with a manually tuned PID controller.	199
Figure 6.13	Fed-batch fermentation with automatic tuning.	201
Figure 6.14	Fed-batch fermentation with multiple tunings.	202
Figure 6.15	Sodium sulphite reaction with binary air flow rate.	205
Figure 6.16	Response of a manually tuned PID controller on the chemical reaction.	206
Figure 6.17	Automatically tuned P and P+I controller responses.	208
Figure 6.18	Auto tuned PID and modified Ziegler-Nichols PID responses.	209
Figure 6.19	Application of automatic tuner using stirrer speed.	210
Figure 6.20	Effect on the dissolved oxygen concentration of varying the nonlinearity output.	212
Figure 6.21	Response of auto-tuned controller: 2-3 l/min.	212
Figure 6.22	Response of auto-tuned controller: 1-2 l/min.	213
Figure 6.23	Response of auto-tuned controller: 3-6 l/min.	213
Figure 6.24	On-line adjustment of nonlinearity output value.	214
Figure 6.25	Change from automatic tuning procedure to tuned PID control.	215
Figure 6.26	Multiple tuning during the sodium sulphite reaction.	216
Figure 6.27	Flowchart for the MENTOR to Amstrad communication routine.	219
Figure 6.28a	Flowchart for the procedure 'Algorithm'.	220

Figure 6.28b Flowchart for the procedure 'Algorithm' (continued). 221
 Figure 6.28c Flowchart for the procedure 'Algorithm' (continued). 222
 Figure 6.28d Flowchart for the procedure 'Algorithm' (continued). 223
 Figure A.1 Probe step response from 0% to 100%. A-2
 Figure A.2 Probe step response from 100% to 0%. A-2

TABLES.

Table 2.1 Initial fermentor contents. 36
 Table 2.2 Sodium sulphite chemicals. 37
 Table 3.1 Ziegler-Nichols Recommended Parameter Settings. 44
 Table 3.2 Phase-margin-design rules for a PID controller. 49
 Table 3.3 Tuning parameters for G(s). 49
 Table 3.4 Tuning parameters for gain margin design. 51
 Table 3.5 Describing functions for various nonlinearities. 66
 Table 3.6 Automatic Tuner Parameter Settings. 74
 Table 4.1 Equations used for Model I. 1
 Table 4.2 Equations used for Model II. 1
 Table 4.3 Model constant values used for simulations. 1
 Table 4.4 Saturation constant, K_s , for growth of organisms on diverse substrates. . . 1
 Table 5.1 Transfer functions used for nonlinear element tests. 113
 Table 5.2 Summary of Nonlinearity Simulation Tests. 114
 Table 5.3 Calculated PID tuning parameters. 124
 Table 5.4 Open-loop response tuning parameters. 127
 Table 5.5 Closed-loop response tuning parameters. 128
 Table 5.6 Automatic tuning procedure developed tuning parameters 130
 Table 5.7 Automatic tuning procedure PID parameter values. 130
 Table 5.8 Statistical analysis results for noise data. 137
 Table 5.9 Summary of tuning parameters used. 138
 Table 5.10 Derived PID values. 151
 Table 6.1 Oxygen consumption and critical concentration for various
 microorganisms. 174
 Table 6.2 PID parameter equations. 176
 Table 6.3 Bakers' Yeast fermentation components. 184
 Table 6.4 Sodium sulphite solution recipe (For each litre of solution required). . . 203
 Table 6.5 Calculated PID controller parameters. 207
 Table 6.6 Change in nonlinearity output value. 211

PROGRAM LISTINGS.

Listing 5.1. ACSL coding for hysteresis nonlinearity simulation. 119
 Listing 5.2. ACSL code for multiple auto tuning on a fed-batch fermentation. . . . 171
 Listing 5.3. ACSL code for batch fermentation with automatic tuning procedure. . 172
 Listing 6.1 Program listing for oscillation and period estimation. 179
 Listing 6.2 Sequence commands for a fed-batch fermentation. 187
 Listing 6.3 Sequence commands for a batch fermentation. 187

NOMENCLATURE.

α	Portion of oxygen in dry gas mixture (%)
$\pm\beta$	Width of relay element with hysteresis
δ	Phase shift ($^{\circ}$)
ε	Gas hold up constant
$\varepsilon(s)$	Process error
f	Gas flow rate (l/hr)
κ	Proportionality constant
σ_p	Statistical standard deviation of data
v	Constant used by automatic tuner
v_e	Specific rate of ethanol consumption (g-EtOH/g-cells.hr)
v_{e0}	Specific rate of ethanol consumption when available sugar concentration approaches zero (g-EtOH/g-cells.hr)
π_e	Specific rate of ethanol production (g-EtOH/g-cells.hr)
μ	Specific growth rate of yeast (hr^{-1})
μ_{\max}	Maximum specific growth rate of yeast (hr^{-1})
μ_p	Statistical mean of data
ζ	Process response damping ratio
ω_1	Gain crossover frequency (Hz)
ω_c	Oscillation frequency (Hz)
ω_n	Natural oscillation frequency (Hz)
$\hat{\omega}$	Estimate of oscillation frequency (Hz)
ϕ	Phase margin ($^{\circ}$)
ϕ_1	Phase shift of fundamental harmonic ($^{\circ}$)
ϕ_1	Correction phase margin ($^{\circ}$)
ϕ_m	Required phase margin ($^{\circ}$)
\hat{T}	Estimate of oscillation period (seconds, minutes)
τ_s	Sample time (seconds, minutes)
τ	Oscillation period
γ	Proportionality constant
a	Oscillation amplitude
\hat{a}	Estimate of oscillation amplitude
a_{gl}	Gas-liquid interfacial area (m^2)
a_1, a_2	Binary switching constants

A	Amplitude of oscillation of process variable
A_B	Total area of gas bubbles (m^2)
A_n	Fourier series coefficient
A^*	Maximum amplitude of oscillation
B_n	Fourier series coefficient
C^*	Dissolved oxygen concentration at saturation ($g-O_2/l$)
C_E	Concentration of ethanol in the culture broth (g/l)
C_L	Dissolved oxygen concentration ($g-O_2/l$)
CER	Carbon Dioxide evolution rate (% of saturation)
d_B	Average oxygen bubble diameter (m)
D_i	Impeller diameter (m)
DOT	Dissolved oxygen tension in fermentation vessel (%)
$\pm E$	Output level of relay element
F	Glucose solution feed rate (l/hr)
G_m	Gain margin (dB)
G(s)	Process transfer function
G(j ω)	Process transfer function
H	Henry's constant
j	Imaginary operator ($\sqrt{-1}$)
k_1, k_2	Constant for growth associated formation of inhibitory substances (l/g-cells.hr)
K	Process gain
K_A	Automatic tuner gain
K_c	Critical gain of process
K_d	Derivative gain
K_i	Integral gain
K_L	Mass-transfer coefficient (min^{-1})
$K_{L,a}$	Volumetric oxygen transfer coefficient (min^{-1})
K_P	Proportional gain
K_s	Monod saturation constant for substrate (g -substrate/l)
K_z	Zeigler-Nichols tuning method gain
L_{O_2}	Power factor with respect to oxygen ($Ws.g^{-1}$)
m_t	Maintenance coefficient of yeast (g substrate/g cells.hr)
n	Real number

N	Impeller tip rotational speed (s^{-1})
N(a)	Describing function
N(a,ω)	Describing function
O_{2in}	Oxygen concentration in inlet gas (g/l)
O_{2out}	Oxygen concentration in outlet gas (g/l)
OTR	Oxygen transfer rate (% of saturation) ($g/m^3.s$)
OUR	Oxygen uptake rate (% of saturation)
P	Dimensionless concentration of inhibitory substances
P(t)	Relay action time ratio
P_i	Power input (W)
PID	Proportional + Integral + Derivative controller
pO₂	Oxygen partial pressure (mg/l)
R	Empirical coefficient characteristic of a fermenter
s	Laplacean operator
S	Concentration of limiting feeding substrate (g/l)
S_{in}	Feed substrate concentration (g/l)
S_{gln}	Glucose concentration (g/l)
t	Time (seconds, minutes or hours)
t_c	Limit cycle oscillation period
T	Temperature ($^{\circ}C$)
T_A	Period of oscillation for automatic tuner (seconds, minutes)
T_d	Derivative action time (seconds)
T_D	Derivative action time (seconds)
T_I	Integral action time (seconds)
T₁	Integral action time (seconds)
T_s	Total sugar added (g)
T_{st}	Process settling time
T_u	Ultimate period of oscillation (seconds, minutes)
T_z	Zeigler-Nichols tuning method period of oscillation (seconds, minutes)
T₂	Biomass doubling time (hr)
U	Glucose feed rate (g/hr)
U_{ref}	Relative input for nonlinear element
v_s	Superficial gas velocity (m/s)
V	Broth volume (l)

V_G	Volume of gas in the broth (m^3)
V_L	Volume of liquid in the broth (m^3)
x	Empirical exponent
x_n	Process variable measured value
x_n'	Filtered value for process variable
X	Cell mass concentration - dry weight (g/l)
X_0	Initial cell mass concentration (g/l)
y	Empirical exponent
$y(s)$	PID controller output
Y_1	Amplitude of fundamental harmonic
Y_G	Overall process yield (g)
Y_{eo}	Ethanol yield on oxygen (g-EtOH/g-oxygen)
Y_{es}	Ethanol yield on substrate (g-EtOH/g-substrate)
Y_{O_2}	Cell yield on oxygen (g-cells/g-oxygen)
Y_{peak}	Process peak overshoot
Y_{ref}	Relative output value for nonlinear element
Y_{xc}	Cell yield on ethanol (g-cells/g-EtOH)
Y_{xs}	Cell yield on substrate (g-cells/g-substrate)

CHEMICALS.

Ag	Silver	N_2	Nitrogen
Cl	Chlorine	Na	Sodium
$C_6H_{12}O_6$	Glucose	NH_3	Ammonia
CO_2	Carbon dioxide	O^\bullet	Oxygen radical
Cu	Copper	O_2	Oxygen
e^-	Free electron	Pt	Platinum
C_2H_5OH	Ethanol (EtOH)	S	Sulphur
H_2	Hydrogen		

ABBREVIATIONS.

ACSL	Advanced Continuous Simulation Language
LSL	Life Science Laboratories
PC	Personal computer

CHAPTER 1.

INTRODUCTION.

When considering biotechnological engineering, it is useful to bear in mind the principle of Occam's Razor, taken from the writings of the 14th-Century philosopher, William of Ockham: "*entia non sunt multiplicanda praeter necessitatem*". Thus this law can be expressed as "systems should be no more complicated than really necessary".

1.1. FOREWORD.

In 1980, the Spinks Report [1.1] defined biotechnology as "the application of biological organisms, systems or processes to manufacturing and service industries". Fermentation processes form an important part of the area known as 'biotechnology'. The term 'fermentation' is derived from the Latin verb *fervere* - to boil. This is an apt description of the appearance of the broth during an aerobic fermentation of yeast. Fermentation can be utilised for:

- a) the preparation of biomass - this is primarily concerned with obtaining yeast from the process. Typical processes include Bakers' and Brewers' yeast cultivation.
- b) the preparation of alcohol - this involves the formation of some biomass, however the principal process product is ethanol.
- c) the production of secondary metabolites - this refers to products which are not essential for biomass growth but are the primary reason for the fermentation system. Typical secondary metabolites include the antibiotics and gibberellins. Generally, secondary metabolites are not synthesized in substantial quantity during rapid growth.

Fermentative processes are involved in the production of bulk enzymes, pharmaceuticals and numerous foods and beverages [1.2]. Products as diverse as sherry and antibiotics owe their origins to biotechnology, having been derived from the controlled application of living organisms (specifically, yeasts). There are more stringent requirements for purity in therapeutic products, which raises their unit cost above those of food additives, and the regulatory authorities set strict

requirements for manufacturing practice. This is an important constraint that is not always present, to the same extent, in other process industries.

Fermentation processes have two basic operating modes: continuous and batch. The continuous reactor is primarily used for large-scale operations, such as the treatment of waste water or the production of single cell-proteins (SCP), where nutrients are fed endlessly into the vessel and a constant product stream flows from the fermentation vessel. Continuous fermentations can be considered to be at a stationary or equilibrium state as far as process control is concerned. The batch reactor is used for the production of enzymes and metabolites, where the fermenter vessel is charged with both microorganisms and nutrients. Conditions within the vessel change as nutrients are consumed and products are formed; once the required degree of reaction has occurred, the vessel is discharged, cleaned and sterilized and the process repeated. Thus batch processes are non-steady-state processes. A variance of the batch reactor is the fed-batch reactor, which is fed with nutrient medium throughout the fermentation period. The first definition of a fed-batch system was proposed by Pirt [1.3] who described the process by means of equations referring to a steady-state. It is from these equations that the mathematical models presented in Chapter 4 have been derived.

The fermentation process should be controlled in such a way that in the shortest time the maximum amount of biomass is produced using the minimum amount of raw materials, such as substrate and oxygen. The optimization of cell production involves numerous factors with the final yield being affected by [1.4]:

- a) Age profile of the initial cell concentration
- b) Initial medium composition
- c) Changes in the rate of growth during the fermentation period, and
- d) Dissolved oxygen concentration during the fermentation period

Obviously, the initial choice of raw materials and oxygen supply, has a major influence on the quality and quantity of the final product. The ability to accurately control a fermentation process has been the subject of significant interest for a number of years, since the optimization of such processes can have a considerable effect on the cost, quantity and quality of the final product. The major disadvantage with conventional control methods is that they have no on-line optimization or adaptive attributes. Therefore, they cannot provide an optimized control

performance throughout the duration of a fermentation. This is true only for batch and fed-batch processes, since a continuous fermentation can be considered as a stable and well controlled process. Previously the research into fermentation processes has been centred around improving equipment design and into microbiological investigation. It was through these efforts that the production of penicillin at Gist-Brocades, in The Netherlands, improved 3 to 4 times between 1970 and 1985 [1.5].

1.2. FERMENTATION PROCESSES.

1.2.1. Why Bakers' Yeast?

Since the initial use of computers in the 1960's for modelling fermentation processes [1.6] and in process control for the production of glutamic acid [1.7] and penicillin [1.8], there have been numerous publications on computer applications in fermentation technology [1.9, 1.10 & 1.11]. The reduction in cost of large computers and the availability of low cost, efficient minicomputers has rendered their use for pilot plants and larger laboratory systems economical since in these cases the financial investment for the on-line computer amounted to a relatively insignificant part of the whole system [1.12].

Although numerous genera and species of yeast exist in nature and many are used industrially, the yeasts of greatest technical importance for fermentations are the species of the genera *Saccharomyces*. They are used in the production of beer and wine (*Saccharomyces carlsbergensis*), and in the leavening of bread, for example *Saccharomyces cerevisiae* (Bakers' Yeast). *S. cerevisiae* is probably the most widely investigated yeast since it is able to use glucose as the sole metabolic source of carbon and energy, however it requires other non-carbon nutrients for growth. It is a 'glucose sensitive' yeast, which exhibits ethanol production in the presence of glucose in excess quantities. *S. cerevisiae* and related species contribute the majority of alcoholic fermentations.

1.2.2. Fermentation Process Control.

Until recently the commercial cultivation of Bakers' Yeast, that is the accumulation of yeast biomass, has been an aerobic fed-batch fermentation under substrate limited growth. In approximate terms, the profit for the process is related to the biomass produced and the substrate consumed. For optimal control of the process, it is necessary to have on-line measurement of the process variables such as

biomass, specific growth rate and the yield of cells on the substrate. However, no such sensors are commercially available for industrial applications. In response to the need for on-line growth data, attention has focused on procedures providing indirect estimates by obtaining related process data such as the carbon dioxide evolution rate (CER) and the oxygen uptake rate (OUR). The other area of research interest has been the control of the fermentation broth environment, since if the biomass is contained within a liquid at the correct pH, temperature etc. then the conditions should allow optimum cell growth.

In order to improve the quantity and quality of the fermentation products, it is advantageous to have an accurate control system [1.13], which can be achieved using one or more of the following methods:

- a) By controlling the chemical environment inside the fermenter vessel;
- b) By standard closed loop control of measurable variables (for example pH and temperature),
- c) By estimating the values of unmeasurable variables and controlling the process using a mathematical model.

The first method refers to the chemicals used in the preparation of the initial broth media and any chemicals subsequently fed into the fermentation broth, such as the glucose substrate or ammonia solution. This can only be performed prior to the start of the fermentation by assaying the chemicals prior to use. The second method proves difficult in fermentation processes owing to the nonlinear and time-varying dynamics inherent in the system. Also, the important process variables, such as cell mass concentration, cannot be directly measured on-line. This leads to the last method, whereby factors such as oxygen uptake rate are measured and a mathematical model of the process used to provide an estimate of the cell mass concentration. This estimation is then used as part of a closed-loop control procedure to determine the substrate input flow rate.

The need to continually supply a fed-batch process with nutrient in response to cell demand, has led to the use of on-line closed-loop control algorithms [1.14]. These controllers utilise the information provided by a limited number of sensors, for example pH, temperature and dissolved oxygen, in conjunction with a model of the process. A drawback of this method is the dependency of the control algorithm on the accuracy of the measured variables and the inflexibility of the model to time-varying process dynamics.

Ideally the fermentation broth should be maintained at the required temperature and pH, and contain the required concentration of nutrients, free from any growth inhibitory substances. Whereas most soluble nutrients are placed in the broth prior to the addition of the microorganism, the maintenance of an adequate level of oxygen dissolved in the medium is one of the major problems facing the fermentation operator. Owing to the low solubility of oxygen gas, it must be supplied continuously to the fermentation vessel. It is only since the development of stable membrane-covered oxygen electrodes, which can be sterilized, that dissolved oxygen concentration became an acceptable control variable in fermentation processes. For fermentations of small volume culture, for example less than 1 litre, the oxygen demand may be satisfied by surface aeration. However for larger scale processes, other means of meeting the demand must be used, primarily by agitation and/or pumped aeration. Industrial scale fermentations are typically operated on a 100 m³ scale, hence it is uneconomical to use either excessive agitation or oxygen gas.

The oxygen concentration within the broth has to be kept within specific limits, if not, then the process might exhibit either the Crabtree Effect [1.15] or the Pasteur Effect [1.16]. The former is the production of ethanol under the condition of adequate oxygen concentration, if the glucose concentration is also high. Thus if biomass production is required, a fed-batch strategy offers the best result as ethanol production is inefficient and may also be inhibitory. If the supply of oxygen is limited, for example the air flow is reduced or the metabolic rate increases so that the oxygen input cannot satisfy the demand, then the fermentation will turn anaerobic (Pasteur Effect).

1.3. METHODS OF CONTROLLING DISSOLVED OXYGEN.

The dynamics of the fermentation process change gradually with the increase in cell mass concentration and with varying glucose and ethanol concentrations. Additionally, there are sudden changes resulting from the addition of external agents (such as anti-foam) making it difficult to obtain optimal closed-loop control performance by using constant controller tuning parameters. A number of nonlinear controllers have been proposed by Wang *et al* [1.17] and Aiba *et al* [1.18] for the control of fermentation processes, however, closed-loop control performance could not be maintained overall and during the changes within each phase of the process. Instead each phase requires different controller parameters, which are not

easily determined *a priori*. Optimal control may only be accomplished by continually adapting the control parameters to the actual system behaviour [1.19]. Recent years have seen significant improvements in the technology of fermentation processes, in particular for the production of antibiotics. These developments have increased the demand for oxygen in the process; some antibiotic production systems have progressed to a point where the oxygen demand exceeds the oxygen transfer capability of existing fermentation equipment. A consequence of this is that the oxygen transfer rate, OTR, has become a growth limiting factor for many such fermentation processes.

Researchers have investigated a variety of methods to maintain adequate levels of dissolved oxygen concentration in the fermenter. The use of the input air flow rate to maintain dissolved oxygen can frequently cause excess foaming of the broth. Further, it is suggested that the volumetric oxygen transfer coefficient, $K_{L,a}$, is not as sensitive to changes in aeration as it is to agitation [1.20]. To avoid these problems, Flynn and Lilly [1.21] suggested a method of altering the vertical position of the sparger outlet within the vessel. A drawback of the system was that the mechanics and electronics needed to accomplish this control strategy were complicated. In comparison, Fuchs and Wang [1.22] constructed a simple system for dissolved oxygen concentration control based on the modification of the oxygen partial pressure in the input air flow. In this system, air recycling was employed, with enrichment of the recirculated air with pure oxygen. For each different fermentation process, appropriate values of oxygen and air flow rates must be determined. Besides the usual dissolved oxygen monitoring equipment, additional hardware must be used, such as a recirculating air pump. Lengyel and Nyiri [1.23] used the agitation speed alone to control dissolved oxygen concentration. The associated electronics and control system were complex and not easily adapted for different sized fermentation units.

Cell cultivation in an oxygen rich environment allows an increase in the efficiency of Bakers' Yeast production [1.24], hence the dissolved oxygen concentration in culture broth must be maintained at a suitable level. In an effort to accomplish this, Sigell and Gaden [1.25] controlled dissolved oxygen concentration using an oxygen rich gas with a constant agitation speed, while Yano *et al* [1.26] changed both the inlet oxygen flow rate and the agitation speed to control the dissolved oxygen concentration. Earlier Yano *et al* [1.27] had suggested using On-Off control

of agitation using two impeller speeds; additionally pure oxygen mixed with air was supplied to the fermenter. For industrial scale fermentation vessels this system was difficult to implement owing to the difficulty in changing the impeller rotation speed. Yano *et al* [1.28] also constructed a dissolved oxygen controller - referred to by the authors as 'DO-Stat' - in which the aeration and agitation rates were used as the control variable. However, these systems required manual intervention during the fermentation to change the preset controller values. Later work by Kobayashi *et al* [1.29] describes a specifically designed piece of apparatus, interfaced with a computer, which was used to control the level of dissolved oxygen concentration during a fermentation. The system operated by varying the air and oxygen flow rates and also the agitation speed. A limitation of the system was that it only operated optimally when air was supplied to the fermenter. The preset values for the 'DO-Stat' had to be determined by the fermenter operator prior to being entered into the 'DO-Stat' system.

A flexible dual-action dissolved oxygen monitor-controller was developed by Archibald [1.30] which was capable of measuring and controlling the dissolved oxygen concentration by varying either the agitation, aeration or both. A disadvantage of this particular system was the need to build additional hardware onto an existing fermentation vessel. McInnis *et al* [1.31] suggested using a least-mean-squares algorithm to estimate the parameters of a minimum variance controller. Its attractiveness for industrial application was the ease with which it could be implemented on a computer. At the heart of the controller was a linear model representation of the oxygen concentration which naturally has a bilinear term [1.32]. The controller could only operate correctly if the vessel conditions varied slowly over time.

1.4. PRACTICAL CONTROL METHODOLOGIES.

The development of control theory has been characterized by algorithmic development for both on-line control and controller design. These methods require knowledge of the control problem including estimates of the process dynamics and disturbances. It is this knowledge requirement that has posed the largest problem in the control of nonlinear, time-varying, multivariable processes, such as batch and fed-batch fermentation.

Most processes may be divided into two generalized areas; constant and varying. Over time, the response of a constant process does not alter nor is it affected by changed process conditions, for example temperature control. These constant processes may be controlled by use of a standard PID controller, with optimal performance achieved when the controller parameters have been correctly tuned. The use of any form of adaptive control would therefore provide no further improvement in controller performance. The generalized group of varying processes may be further divided into those which have predictable variations and those which have non-predictable variations. Processes with non-predictable variations, have responses which change over time and which cannot be related to some measurable quantity. This group of processes may be adequately controlled by an adaptive control scheme which continually monitors all measurable process variables, forms a model of the process and thus 'learns' the process dynamics. Varying processes having variations in response, which can be attributed to some measurable influence, form the predictable variation group. An example of such a process is one which uses a nonlinear control valve. This type of process lends itself easily to adaptive control, however the continual modelling of the process by adaptive techniques can be tedious and a waste of computational resources. Instead, the process may be more efficiently controlled by a combination of standard PID control and gain scheduling [1.33]. The area of automatically tuning PID controllers has received a great deal of attention in the literature because of its ideally suited application in reducing process start-up time and in particular, in improving process response by retuning the controller on-line [1.34 to 1.38]. Adaptive control techniques will be described in detail in section 1.4.1.

In 1979, Wang *et al* [1.39] were amongst the first to illustrate the usefulness of computer control for the production of yeast. Since then, many investigations have been carried out to improve the control of these nonlinear time-varying processes. One of the traditional methods of controlling nonlinear processes is to base the three term controller on a linearized model of the process about a nominal set-point. This form of controller can be expected to operate acceptably only when the process operating point is sufficiently close to the set-point used for the tuning of the controller. If the process is to be operated over a larger range, the controller parameters must be altered to accommodate the change in process dynamics [1.40]. Dairaku *et al* [1.41] developed a PID controller which included automatic parameter tuning using a microcomputer, in an attempt to overcome this problem.

Three term (Proportional plus Integral plus Derivative) controllers are extremely popular for industrial applications, where any of the subset of terms (P, PI, PD and PID) are used [1.42]. Although the PID controller is usually found in single-loop applications, it can be used for multivariable loops [1.43]. The ability to tune a PID controller to achieve a desired closed loop response specification is often considered more of an art than a science. Often the controller is tuned by an operator who has more of an intuitive feel for the process than a theoretical understanding of it; this is especially true where the process has no mathematical model or where the process is difficult to model accurately. It is common to find that each shift operator has a different set of controller settings for the same process. In these situations, the optimal response is considered as the one which "looks best" to the operator concerned, and are not based on any mathematical theory. In fact, some mathematically derived tuning parameters actually produce unacceptable transient responses [1.44].

Andreiev [1.45] has stated that for industrial applications, the dissatisfaction with PID controller performance and the inability to easily tune the controller means that up to 50% of the control loops are operated in open-loop mode. One of the major reasons for operator dissatisfaction with three-term controller performance is caused by the nonlinear dynamics of the processes they handle. The PID tuning parameters may be acceptable for one point of the operating range but will be unsatisfactory for another.

It has been proposed by Tan [1.46] that a PID controller may be combined with an Artificial Neural Network (ANN) to form an on-line hybrid control scheme. The reasoning behind this scheme is that a fixed PID controller can adequately control a dynamic process over a small operating range. Outside this area the ANN can be used to reduce the performance error so that the PID controller may once again operate.

The Foxboro EXACT auto-tuning controller was based on pattern recognition, where the process response to a step change or disturbance is observed and the controller parameters adjusted accordingly. The approach mimics the procedure used by an experienced process control engineer. The method does however require that reasonable controller settings are known prior to implementation. Retuning could be operator invoked when desired, or by continuous monitoring of the process

and activating when the controller performance deteriorated. Although the Foxboro EXACT could cope with large disturbances, its major disadvantage was that unless the disturbance was of the right pattern, then retuning of the system could not take place [1.47].

1.4.1. Adaptive Control.

Where control loops involve either large time lags or interactions with other loops, then owing to lack of time or experience the tuning procedure is often prematurely terminated. Consequently the loop operates with tuning parameters which are not optimum. In an attempt to overcome these tuning problems many loop controller manufacturers have developed products which can automatically tune the PID parameters to the ideal settings for each application. There is growing interest in the use of these automatic tuning techniques. However, there are a number of potential problems associated with their use, and prospective users should be aware of the basis of the controller tuning principles when selecting a controller.

There are numerous automatic tuners available, many of these continuously adjust the tuning parameters to follow changes in the process characteristics. Almost all use different approaches to loop tuning, with these approaches varying in both concept and complexity. In the majority of cases an adaptive controller comprises a standard PID algorithm with adjustable tuning parameters, together with some high level software used to adjust the parameters in order to improve overall control performance. The various methods differ in the way in which the controller performance is assessed and the way in which the new controller tuning parameters are calculated. A number of procedures are used to perform these functions, ranging from highly theoretical approaches involving mathematical modelling of the process, through to heuristic approaches where the parameters are adjusted using 'rules of thumb'.

Within the area of continuous adaptive controllers there are a number of approaches which could be used, however it is possible to identify four distinct classifications. These are:

- ★ Gain scheduling
- ★ Explicit self-tuning
- ★ Implicit self-tuning
- ★ Auto-tuning

In the gain scheduling, or adaptive gain controller, the gain, and in some cases also the integral and derivative terms, are altered on-line. These adjustments are pre-defined by the operator as simple functions of either the measured variable, controller output or error signal. Once defined, this pre-programmed schedule remains fixed and is defined to adjust the loop tuning parameters to compensate for known nonlinearities in the process. The full benefits of gain scheduling can only be achieved if the changes in the process dynamics, with respect to the measured variables, are well understood and if these relationships do not change with time.

An explicit self-tuner performs two distinct functions. Firstly, it uses a knowledge of the past values of the process input and output to develop a mathematical model of the process. Secondly, it uses a conventional design procedure to compute the tuning parameters of a controller, based on the description of the process embodied in the model. In an explicit self-tuner the model generation and controller design functions are separate and the controller is usually based on the conventional PID algorithm.

The implicit self-tuner combines the model development and controller design procedures, thus a generalised control algorithm with an arbitrary structure is used. This allows a freedom to tune the controller parameters more accurately to compensate for high order dynamics and time delays.

Self-tuners are worthy of consideration as there are many different methods of performing the various functions. It is essential that the construction of the mathematical model, which is used to describe the process dynamics, has the required number of terms to fully describe the process. Clearly, if the model does not provide a sufficient number of terms to describe the process dynamics, then an appropriate controller cannot be designed. Given the model structure, the system needs to estimate the model coefficients. A number of ways of achieving this are used, ranging from statistical techniques, some of which can handle significant measurement noise, through Fourier analysis to simple adjustment of the parameters of an internal model to fit the data. The estimation requires process data, in some implementations normal process variations are used, whilst others inject significant perturbations in order to excite the process.

An adaptive controller, as the name suggests, controls a process by adjusting itself to any change in the process conditions. As the dynamics of the process change with time or as nonlinearities or noise disturbances take effect, then the controller reassesses its concept of the process model accordingly. The important assumption that lies behind many adaptive control techniques is that the inferential model used is an accurate representation of the actual process. A variety of different techniques exist for obtaining an adaptive controller, such as Model Reference Control, Stochastic Control and Deterministic Control.

1.5. SCOPE OF THE INVESTIGATION.

1.5.1. Statement of Problem Addressed.

When designing a controller system for bioreactors the following must be taken into consideration:

- a) There is a lack of mathematical models which accurately describe cell growth and metabolic production.
- b) The process is time-varying and nonlinear during the exponential growth phase.
- c) There is a lack of on-line sensors which can measure important process variables such as the cell mass and substrate concentrations.

In batch or fed-batch cultures, both the temperature and the pH of the broth are usually regulated. However, the dissolved oxygen concentration is seldom controlled even though oxygen is an important variable in cell growth and can become a growth limiting factor.

During an industrial fed-batch fermentation, the glucose substrate is supplied to the broth by following a standard feed profile. Since cell growth follows an exponential increase there is a corresponding exponential demand for oxygen (Figure 1.1).

In comparison, for a batch fermentation the complete glucose substrate is introduced to the broth at the start of the fermentation period. Cell growth in batch culture, under aerobic conditions, comprises two growth phases known as diauxic growth (Figure 1.2). The first phase involves the consumption of the glucose substrate with the formation of ethanol as a by-product; with a high demand for oxygen. A change in oxygen demand occurs when the substrate concentration falls

below a critical level. From this point the ethanol is utilised as the growth substrate, during this phase the demand for oxygen decreases dramatically.

Further, the conditions within the fermentation vessel can vary from batch to batch, requiring different controller tuning parameters for each fermentation started. The additional problems encountered, such as measurement noise and external environmental disturbances, may frequently result in poor closed loop performance.

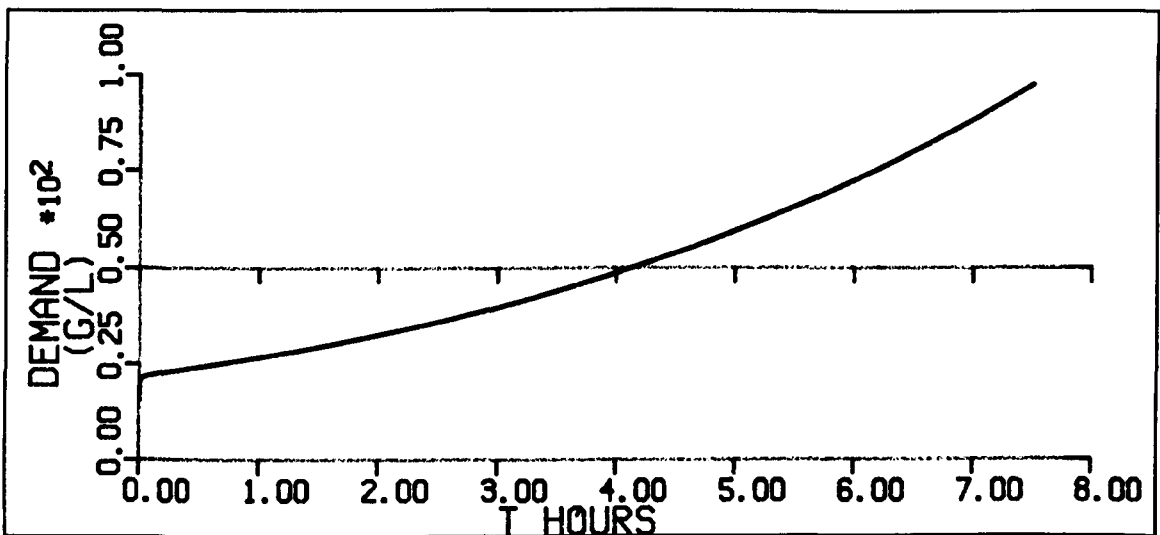


Figure 1.1 Normalised oxygen demand during a fed-batch fermentation.

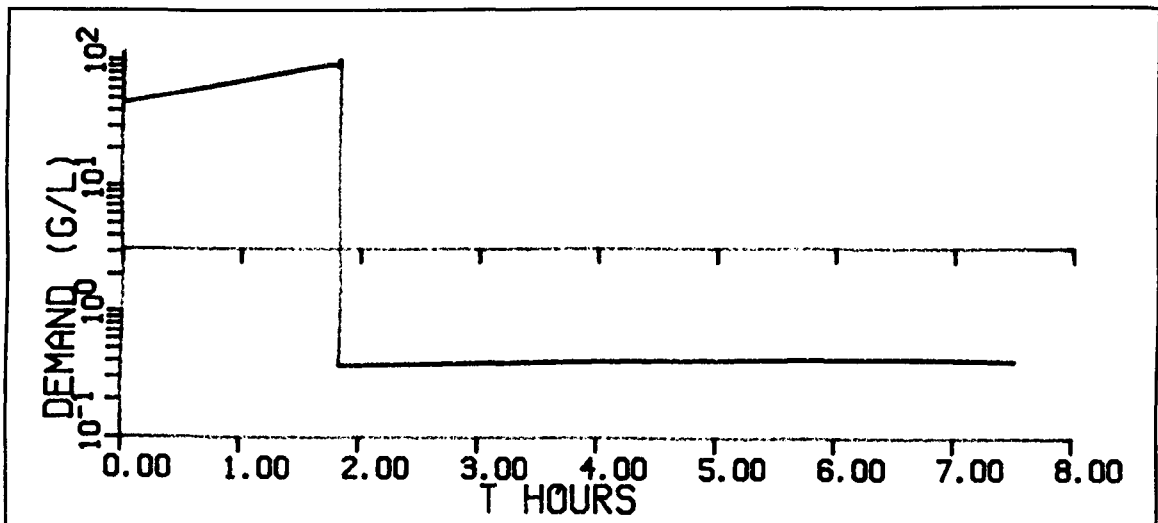


Figure 1.2 Normalised oxygen demand during a batch fermentation.

When a controller is applied to the dissolved oxygen loop, it will often be a PID with a fixed set of tuning parameters. This will not provide an optimum controller performance for the duration of the fermentation. Hence a means whereby the tuning parameters of a three term controller may be changed during the duration

of a fermentation should be investigated. The alteration to the values of the tuning parameters should:

1. Require minimal or (ideally) no manual intervention.
2. Make adjustments so as to maintain an optimum controller performance.
3. Require little computational power.
4. Maintain the familiar structure of the PID controller, with the manual override facility.
5. Use a minimum amount of *a priori* knowledge about the process.

1.5.2. Aims of the Project.

The aims of the research in relation to the problems outlined in section 1.5.1 were to:

- a) Investigate the practicality of an industrial application of the proposed automatic tuning procedure.
- b) Develop a technique for adapting a three term PID controller to maintain an optimum regulation during a time varying, nonlinear fermentation process.

Obviously, the two objectives are associated, however, one can view the second as the tool with which to test the first. A secondary requirement of the work was to ensure that the system developed was compatible with the Department's fermentation equipment; and any software written must interact with the MENTOR fermentation process control package. Both the hardware and the software used were for a commercially available small scale process.

1.5.3. Approach to the Investigation.

The automatic tuning procedure will initially be investigated on simple mathematical models using a simulation package. Having determined the operational concepts of the automatic tuner, the procedure will be applied, in simulation, to mathematical models of fed-batch and batch fermentations. The first model to be used describes a fed-batch fermentation with aerobic cell growth without excess glucose addition. The second, more complex model, covers the case of a batch fermentation with ethanol production, this also includes a step nonlinearity caused by the sudden change from cell growth on a glucose substrate to growth on the ethanol produced.

Once the tuning procedure has been verified, a series of on-line fed-batch and batch Bakers' Yeast fermentations will be performed to ascertain the applicability of using the method during industrial situations. The equipment used for the experiments will be a small scale pilot plant, fitted with all necessary instrumentation and computer systems (Figure 1.3). For the work described in this thesis, the important components are the dissolved oxygen probe, the air flow meter and the computer running the MENTOR process control software.

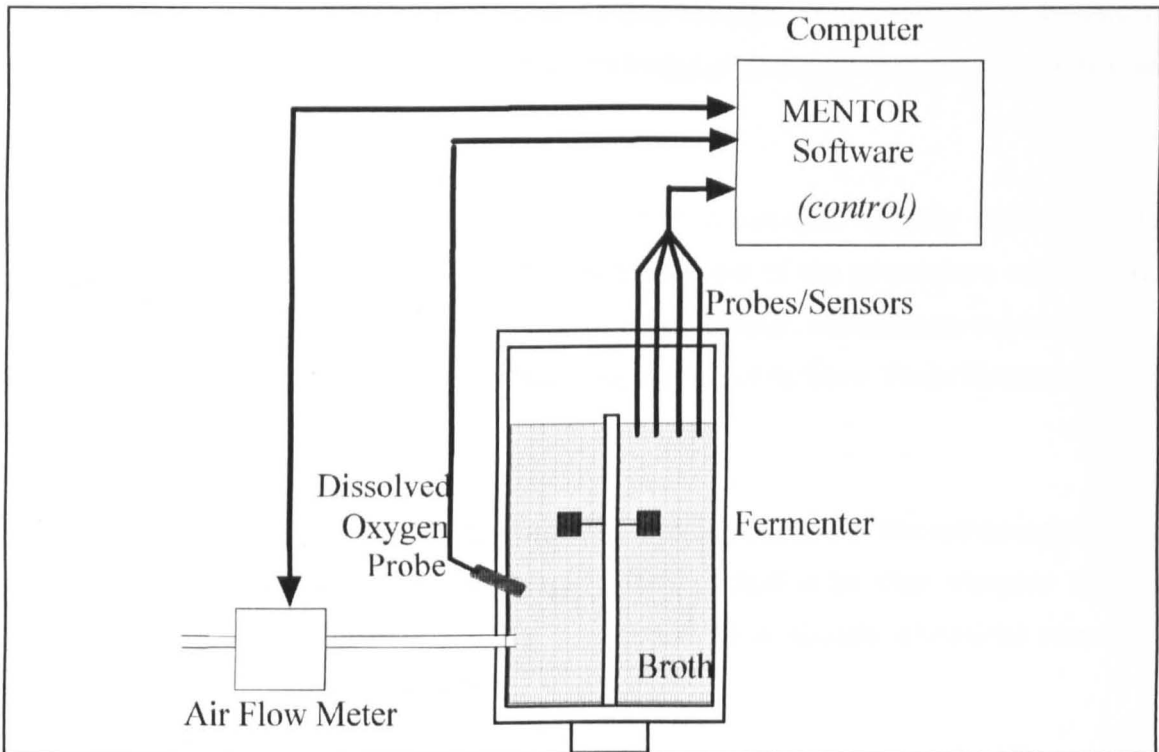


Figure 1.3 Basic fermentation plant layout.

1.5.4. Originality of the Research.

The ingenuity of the work lies in that it is the application of a relatively recently suggested controller tuning scheme to a industrial process. Additionally, current literature, related to the automatic tuning procedure, does not highlight the application of the procedure to nonlinear, multivariable, time-varying processes. It is anticipated that this thesis will represent one of the earliest of these applications, and will provide a comprehensive study of the system chosen.

1.6. REVIEW OF THE THESIS.

An overview of the materials utilised for the research work is given in Chapter 2. This includes descriptions of the software employed and the hardware used; both the computers and the laboratory scale fermentation process system.

The theory behind the operation of the automatic tuning procedure is described in Chapter 3. Comparison of the chosen automatic tuner with other adaptive control techniques is also presented here. An explanation of how the theory has been practically applied in both simulation and experimental work will also be given.

The two mathematical models of Bakers' Yeast fermentations used in the work are highlighted in Chapter 4. This includes batch and fed-batch fermentations, as well as an introduction to the theory of yeast fermentation. The concept of dissolved oxygen concentration and its importance to fermentation processes is described in this chapter.

An investigation into the performance of the automatic tuning procedure is presented in Chapter 5. This comprises simulations of the procedure using first, second and third order transfer functions. Additionally, simulation results of the automatic tuner applied to the mathematical models of Bakers' Yeast fermentations are presented.

Chapter 6 contains the results of the on-line implementation of the automatic tuner for batch and fed-batch fermentations. Also included in this chapter is the application of the automatic tuning procedure to a simple chemical reaction process, for which *a priori* knowledge was unknown.

Finally, Chapter 7 presents the conclusions of the research and recommendations for further work which should be investigated; this includes general work on the tuning procedure and specific work on fermentation applications.

1.7. REFERENCES.

- 1.1. Spinks, A. Biotechnology, report of a Joint Working Party, HMSO London. (Joint Working Party - Advisory Council for Applied Research and Development, Advisory Board for the Research Councils, and The Royal Society). March, 1990.
- 1.2. Thornhill, N.F. Detecting Faults in Fermentation Processes. *Computing and Control Engineering Journal*. July, p.187-192. 1990.
- 1.3. Pirt, S.J. The theory of a fed-batch culture with reference to penicillin fermentation. *Journal of Applied Chemistry and Biotechnology*. Vol. 24. p. 415-424. 1974.

- 1.4. Calam, C.T. and D.W. Russell. Microbial aspects of fermentation process development. *Journal of Chemistry and Biotechnology*. Vol. 23. p. 225-237. 1973.
- 1.5. Meer, R. Rv de and F. Valkema. Nederlandse bedrijvigheid in de biotechnologie. *Biotech in Nederland*. Vol. 23. p. 100-102. 1985. *(In Dutch)*
- 1.6. Yamashita, S. C. Munro. Fermentation Processes. *J. Society Instrumentation and Control Engineering*. Vol. 6(10). p.735-740. 1978.
- 1.7. Yamashita, S. M. Hisoshi and J. Inagaki. 1969. Automatic control and optimization of fermentation process - glutamic acid. *Fermentation Advances*. Ed: D. Perlman. Academic Press, New York. p. 441-463. 1969.
- 1.8. Greyson, P. Computer control of batch fermentation. *Process Biochemistry*. Vol. 4, No. 3. p. 43-44. 1969.
- 1.9. Nyiri, L.K. Applications of computer in biochemical engineering. *Advanced Biochemical Engineering*. Vol. 2. p. 49-95. 1972.
- 1.10. Armingier, W.B. Computer applications in fermentation technology. *Biotechnology and Bioengineering Symp No. 9*. 1979.
- 1.11. Nyiri, L.K., R.P. Jefferis and A.E. Humphrey. Application of computers to the analysis and control of microbiological processes. *Biotechnology and Bioengineering Symposium No. 4*. p. 613-628. 1974.
- 1.12. Hampel, W. Applications of micro computers in the study of microbial processes. *Advanced Biochemistry Engineering*. Vol. 13. p.1-33. 1979.
- 1.13. Valero, F., J. Lafuente, M. Pach and C. Sola. Biomass Estimation Using On-line Glucose Monitoring by Flow Injection Analysis. *Applied Biochemistry and Biotechnology*. Vol. 24/25. p. 591-602. 1990.
- 1.14. Cooney, C.L., G.M. O'Conner and F. Sanchez-Riera. An Expert System for Intelligent Supervisory Control of Fermentation Process. *Proceedings of the 8th International Biotechnology Symposium, Paris*. p. 563-575. 1988.
- 1.15. Crabtree, H.G. Observations of the carbohydrate metabolism of tumors. *Biochemical Journal*. Vol. 23, p.536-545. 1929.
- 1.16. Pasteur, M. Influence de l'oxygène sur le développement de la levûre et fermentation alcoolique. *Bulletin de la Societe chimique de Paris*. June, 28. p.79. 1861
- 1.17. Wang, H.Y., C.L. Cooney and D.I.C. Wang. Computer control of Bakers' Yeast production. *Biotechnology and Bioengineering*. Vol. 21. p. 975-995. 1979.

- 1.18. Aiba, S., S. Nagai and Y. Nishizawa. Fed-batch culture of *Saccharomyces cerevisiae*: a perspective of computer control to enhance the productivity in Bakers' Yeast cultivation. *Biotechnology and Bioengineering*. Vol. 18. p. 1001-1016. 1976.
- 1.19. Schugerl, K. Measurement and Bioreactor Control. *Proceedings of the 8th International Biotechnology Symposium, Paris*. p.547-562. 1988.
- 1.20. Fuchs, R., D.Y. Ryu and A.E. Humphrey. Effect of surface aeration on scale-up procedures for fermentation processes. *Ind. Eng. Chem. Process Des Develop.* Vol. 10, No. 2. p.190-196. 1971.
- 1.21. Flynn, D.S. and M.D. Lilly. A Method for the Control of the Dissolved Oxygen Tension in Microbial Cultures. *Biotechnology and Bioengineering*. Vol. IV. p. 515-531. 1967.
- 1.22. Fuchs, R. and D.I.C. Wang. Simple System for Controlling Dissolved Oxygen Concentration in Laboratory Fermenter. *Biotechnology and Bioengineering*. Vol. XVI. p. 1529-1536. 1974.
- 1.23. Lengyel, L. and L. Nyiri. An automatic aeration control system for biosynthetic processes. *Biotechnology and Bioengineering*. Vol. VII. p. 91-100. 1965.
- 1.24. Fukuda, H., T. Shiotani, W. Okada and H. Morikawa. A new culture method of Bakers' Yeast to remove growth-inhibitory substances. *J Ferment Technol.* Vol. 56, No. 4. p.356-360. 1978.
- 1.25. Siegel, S.D. and E.L. Gaden. *Biotechnology and Bioengineering*. Vol. IV. p. 345-354. 1962.
- 1.26. Yano, T., T. Kobayashi and S. Shimizu. Control system of dissolved oxygen concentration employing a microcomputer. *J. Ferment. Technol.* Vol. 59, No.4. p. 295-301. 1981.
- 1.27. Yano, T., T. Kobayashi and S. Shimizu. Fed-Batch Culture of Methanol-Utilizing Bacterium with DO-Stat. *Journal of Fermentation Technology*. Vol. 56, No4. p. 416-420. 1978.
- 1.28. Yano, T., H. Mori, T. Kobayashi and S. Shimizu. Control System for dissolved oxygen concentration in aerobic cultivation. *Journal of Fermentation Technology*. Vol. 57. p.91-98. 1978.
- 1.29. Kobayashi, T., T. Yano and S. Shimizu. Automatic control of dissolved oxygen concentration with microcomputer. *Advances in Biotechnology*. Vol. 1: Scientific and Engineering Principles. Ed: M. Moo-Young. Pergammon Press. p. 413-417. 1981.

- 1.30. Archibald, F. Cost Effective Dissolved Oxygen Monitor-Controller for Continuous Culture. *Biotechnology and Bioengineering*. Vol. 21. p. 1553-1559. 1979.
- 1.31. McInnis, B.C., C.Y. Liz and P.B. Butler. Adaptive Microcomputer Dissolved Oxygen Control for Wastewater Treatment. *IFAC Identification and System Parameter Estimation*. p. 789-793. 1979.
- 1.32. Olsson, G. and O. Hansson. Stochastic modelling and computer control of a full scale waste water treatment plant. Report 7636(C). Department of Automatic Control, Lund Institute, Lund, Sweden. 1976.
- 1.33. Tetley, B. and A. Ulf. Autotuning and Gain Scheduling for Process Control. *Sattcontrol*.
- 1.34. Åström, K.J. and T. Hagglund. Automatic tuning of simple regulators on phase and amplitude margins. *Automatica*. Vol. 20. o. 645-651. 1984.
- 1.35. Hang, C.C., C.C. Lim and S.H. Soon. A new PID auto-tuner design based on correlation technique. *Proceedings of the 2nd Multinational Instrumentation Conference*. China, 1986.
- 1.36. Balchen, J.G. and B. Lie. An adaptive controller based upon continuous estimation of closed loop frequency response. *Proceedings of the 2nd IFAC workshop on Adaptive systems in control and signal processing*. p. 31-36. 1986.
- 1.37. Radke, F. and R. Isermann. A parameter adaptive PID controller with step-wise parameter optimization. *Automatica*. Vol. 23. p. 449-457. 1987.
- 1.38. Bristol, E.H. Pattern recognition: an alternative to parameter identification in adaptive control. *Automatica*. Vol. 13. p. 197-202. 1977.
- 1.39. Wang H.Y., C.L. Cooney and D. I. C. Wang. Computer control of Bakers' Yeast production. *Biotechnology & Bioengineering*. Vol. XXI. p. 975-995. 1979.
- 1.40. Axelson J.P., C.F. Mandenius, O. Holst, P. Hagender and B. Mattiasson. Experience in using an ethanol sensor to control molasses feed-rates in Bakers' Yeast production. *Bioprocess Engineering*. Vol. 3. p. 1-9. 1988.
- 1.41. Dairaku, K., E. Izumoto, H. Morikawa, S. Shioya and T. Takamatsu. An advanced micro-computer coupled control system in a Bakers' Yeast fed-batch culture using a tubing method. *Journal of Fermentation Technology*. Vol. 61, No. 2. p. 189-196. 1983.

- 1.42. Artin, J., A.B. Corripio and C.L. Smith. How to select controller modes and tuning parameters from simple process models. I.S.A. Transactions. Vol. 15. p. 314-319. 1976.
- 1.43. Jones, A.H. and B. Porter. Design of adaptive digital set-point tracking PI controllers incorporating recursive step-change matrix identifiers for gas turbines. Proceedings AIAA Guidance, Navigation and Control Conference, Williamsburg, USA. p.18-20. 1986.
- 1.44. Litt, A. An expert system to perform on-line controller tuning. IEEE Control Systems. p.18-23. April. 1991.
- 1.45. Andreiev, N. A new dimension: A self-tuning controller that continually optimises PID constants. Control Engineering. August. p. 84-85. 1981.
- 1.46. Tan, S. A combined PID and neural control scheme for nonlinear dynamical systems. Proceedings of the Singapore International Conference on Intelligent Control and Instrumentation. p. 377-383. 1992.
- 1.47. Lim, K.W. and C.C. Hang. Performance Studies of an Adaptive PID Controller. Proceedings of the 4th Yale Workshop on Applications of Adaptive Systems Theory, U.S.A. May. p. 30-35. 1985.

CHAPTER 2.

MATERIALS AND EQUIPMENT EMPLOYED.

2.1. INTRODUCTION.

The need to improve the efficiency and productivity of fermentation processes has gained increased importance over the last decade. A major problem in the optimization of fermentation processes is that important process variables, such as concentrations of cell mass and substrate, cannot easily be measured directly on-line making process optimization difficult. Thus, the problem becomes one of using directly such on-line measurements as are available, for example temperature, dissolved oxygen concentration and pH, in conjunction with estimation techniques to arrive at values for process variables such as growth rate and biomass concentration. These factors have resulted in the development of high quality instrumentation, including steam sterilizable probes for measuring temperature or pH. These probes have a long life guarantee and require very little maintenance other than routine calibration. The laboratory scale fermentation plant used for the work has employed a variety of these types of probes, and each will be described briefly in this chapter. Since the project relates to the control of dissolved oxygen concentration, which is a critical factor in a fermentation processes, a more detailed description of the dissolved oxygen probe and the input air flow control system will be given.

A variety of computer software packages have been used including computer aided design programs, programming environments and a fermentation supervisory process control program (MENTOR). The MENTOR software can be executed on either a stand alone computer or on a network of computers. In this project a stand alone configuration was employed (section 2.2.1.).

Previously, fermentation processes were controlled using specially designed microprocessor systems, such as ACCOS-2 from APV International. Invariably these systems were limited in use by a lack of adequate sequential and feedback control capabilities, additionally floating point arithmetic was not readily

available. The current work has not suffered from these drawbacks since modern personal computers have been employed for process control during on-line experiments as well as for all off-line simulation and design work. This chapter will describe both the computers and the software packages utilised in realising the proposed automatic tuning procedure.

2.2. EQUIPMENT REQUIREMENTS.

The hardware used for the work includes computer systems, a fermentation vessel and its associated probes, sensors and instrumentation (Figure 2.1). Each will be described in this section.

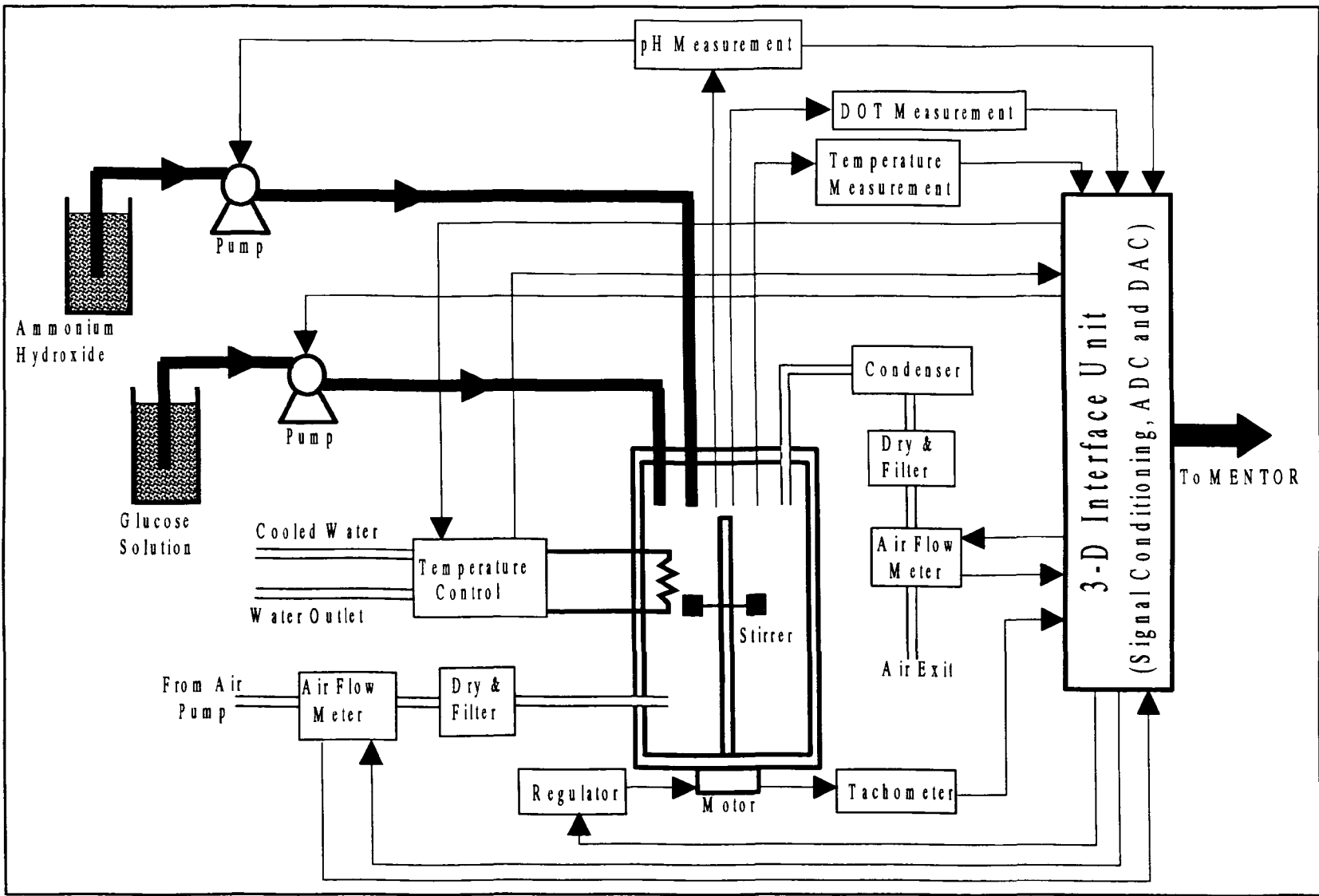
2.2.1. Microprocessor System and Peripherals.

The modern personal computer (PC) has proved to be beneficial in nearly all areas of working life, ranging from teaching and stock control, to cartography and secretarial work. Nowhere has the PC found a more ideally suited operating environment than in the process control industry. Since its introduction in 1981 the PC has become a world-wide standard, spawning numerous computer programs written by established software houses.

The standardization of the PC, with its inherent architecture and memory specification, has allowed the electronics industry in general to mass-produce a variety of plug-in printed circuit cards that encompass a diversity of roles, including serial & parallel communication, analog-to-digital convertors and digital-to-analog convertors. The PC permits the use, with an appropriate programming language, of floating point arithmetic, multi-dimensional arrays and variable passing procedures all performed at high computational speed. This is in contrast to previous dedicated process control computers which had few, if any, of these features. It is for these reasons that the personal computer was chosen as the microprocessor system for the research work presented.

Two personal computers were used in the project; one for the execution of the process control software (the master computer), while the other was primarily used for the tandem execution of the automatic tuning procedure software (the slave computer) as well as being used for controller development and simulation

Figure 2.1 Laboratory Scale Fermentation Plant.



work. The master computer system comprised an IBM-AT personal computer with a 12 MHz, 80286, 16-bit microprocessor. The slave computer consisted of an Amstrad PC2086 personal computer with an 8 MHz, 8086, 8-bit microprocessor in conjunction with an 8 MHz 8087 maths co-processor. The configuration of the computers and associated peripherals is shown in Figure 2.2. The controlling software running on the master computer performed communication with the fermentation equipment using an interface unit - the 3D-Interface - via one of the RS-232 serial data links, the second serial port was used to allow data transfer to be realised with the automatic tuning procedure being executed in parallel on the slave computer.

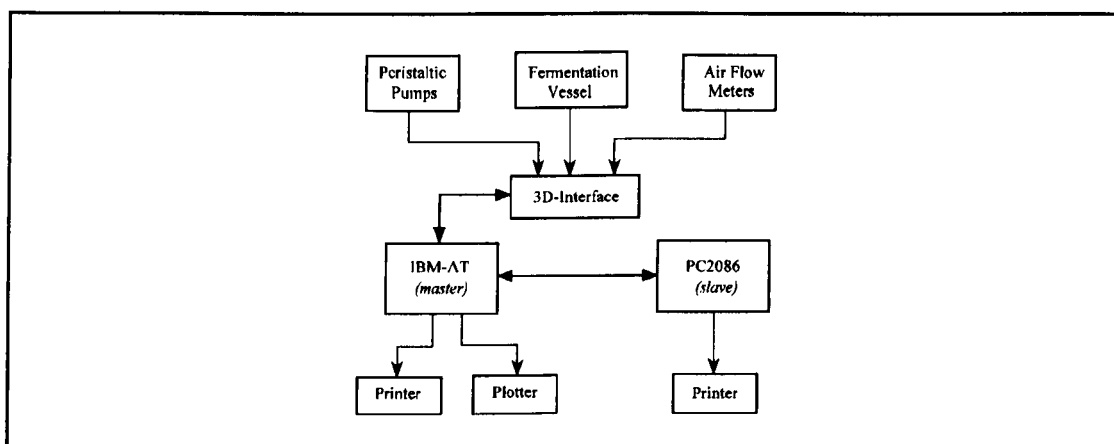


Figure 2.2 Computer controlled fermentation process.

2.2.2. Laboratory Scale Fermentation Vessel.

All on-line experiments were conducted using a 20 litre Biolaffite laboratory scale fermentation vessel (nominal working capacity of 15 litres). The vessel is made from highly polished stainless steel to ensure ease of sterilization and thus reduce contamination of the fermentation medium. The vessel is mounted on a four-wheeled support unit, that also houses the heavy duty 1.25 HP agitation drive motor. The removable headplate is fitted with a membrane protected vessel pressure gauge and an outlet air condensing unit. Around the base of the vessel are located a sterilisable inoculation connector and ports to allow probes to be inserted directly into the broth (Figure 2.3). Sterilisation is performed in-situ using an industrial steam generator, capable of producing steam at 120°C with a pressure up to 3 bar. The agitation system is capable of providing speeds up to 1000 r.p.m., which is transduced into an analog signal of 4-20 mA.

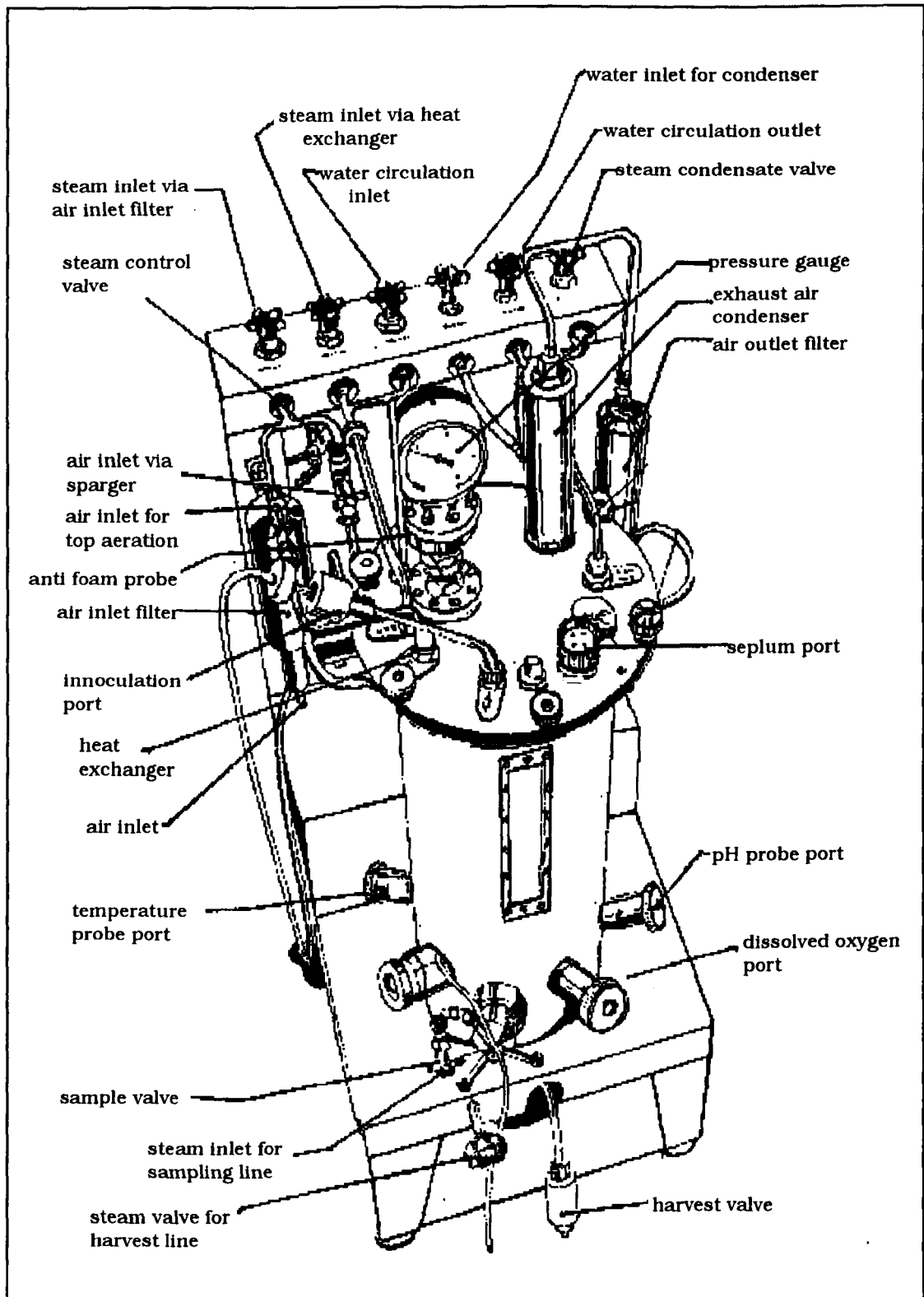


Figure 2.3 Biolafitte Fermentation Vessel.

2.2.3. Sensors and Probes.

The fermentation vessel was equipped with a selection of probes and sensors with associated instrumentation. All instrumentation modules (cards) were housed in a standard rack unit. The cards carry connections to the power supply, control modules, sensors and modules interconnections; these interconnections are made via the backplate of the rack unit. The power supply unit was capable of producing $\pm 15\text{V d.c.}$, -5V d.c. or 24V a.c. , this serviced the power requirements of all the instrumentation cards.

2.2.3.a. Dissolved Oxygen Measurement.

The measurement of the level of dissolved oxygen concentration was performed using an Ingold oxygen sensor, which has been designed for industrial applications; it operates as a polarographic device by determining the partial pressure ($p\text{O}_2$) of the oxygen dissolved in the medium. Automatic compensation for the temperature dependence of the membrane permeability is accomplished by a thermistor built into the sensor. The measurement signal of 4 to 20 mA is fed to the amplifier circuit through a special low-noise cable. The amplifier processes the signal and displays the dissolved oxygen level in percentage of air saturation - with a range of 0% to 100% - to a resolution of 0.1%. The amplifier unit for the probe included two potentiometers for calibration; one for adjustment of the zero reading in saturation nitrogen ($100\% \text{N}_2 = 0\% \text{O}_2$), and the second potentiometer provided gain adjustment.

The Ingold sensor used has been designed to have a small diameter platinum cathode and a double membrane. Both of these features reduce the effect of flow dependence, which is defined as the difference observed between stagnant and agitated solutions [2.1]. The flow dependence must be as low as possible as to minimize error caused by either a change in stirrer speed or an increase in solution viscosity. The sensor is placed in one of the ports at the base of the fermentation vessel to maximize the measurement of dissolved oxygen concentration while minimizing the effect of air bubble interference such as occurs during a rapid change in stirrer speed. All parts of the sensor which come into direct contact with the fermentation medium are made of stainless steel, this allows for in-situ steam-sterilization. Prior to on-line experimentation,

the dynamics of the oxygen sensor were determined from a series of transient responses to step changes in the input. Further details are given in Appendix A. The time constant for the sensor was determined as 60 seconds.

2.2.3.b. Input Air Flow Control.

In order to maintain viable cells, there must be an adequate supply of nutrients and oxygen. The supply of oxygen must be provided such that it exceeds the uptake capacity of the cells so that the broth shows a non-zero oxygen partial pressure preferably approaching saturation [2.2]. Brookes thermal mass flowmeters were used to monitor the input and output air flow rates. The flowmeter operation principle is based on the thermodynamic properties of gases, that is the relationship between the mass flow and heat capacity of a gas (Figure 2.4). With zero flow each temperature element has equal heat reaching it, providing that a constant pressure is maintained. As the flow increases, the flowstream carries heat away from the upstream temperature element (T1), and an increasing amount towards the downstream element (T2). An increasing temperature difference develops between the two elements that is proportional to the volume of gas flowing; that is, the mass flow rate. A bridge circuit interprets the temperature difference and a differential amplifier generates a normalized 0 to 10V d.c. output signal proportional to the mass flow rate. The flowmeters have a working range of 0 to 20 l/min which corresponds to a reading of 0 to 100% (0 to 10V), with a control accuracy of $\pm 0.1\%$.

The flowmeters were connected to a dual channel power supply, read-out and control unit which has been designed to power the flow controllers (Figure 2.5). This unit allows the flow meters to be controlled either manually by a potentiometer or remotely from a computer. The percentage flowrate is indicated by a 3½-digit LED display. The flowmeters were controlled from the master computer via a digital-to-analog convertor, the calibration chart may be seen in Figure 2.6. The calibration holds true for both flow rate as an input and an output value. Oxygen was supplied to the broth by way of pumped air on the assumption that air is 20.9% oxygen.

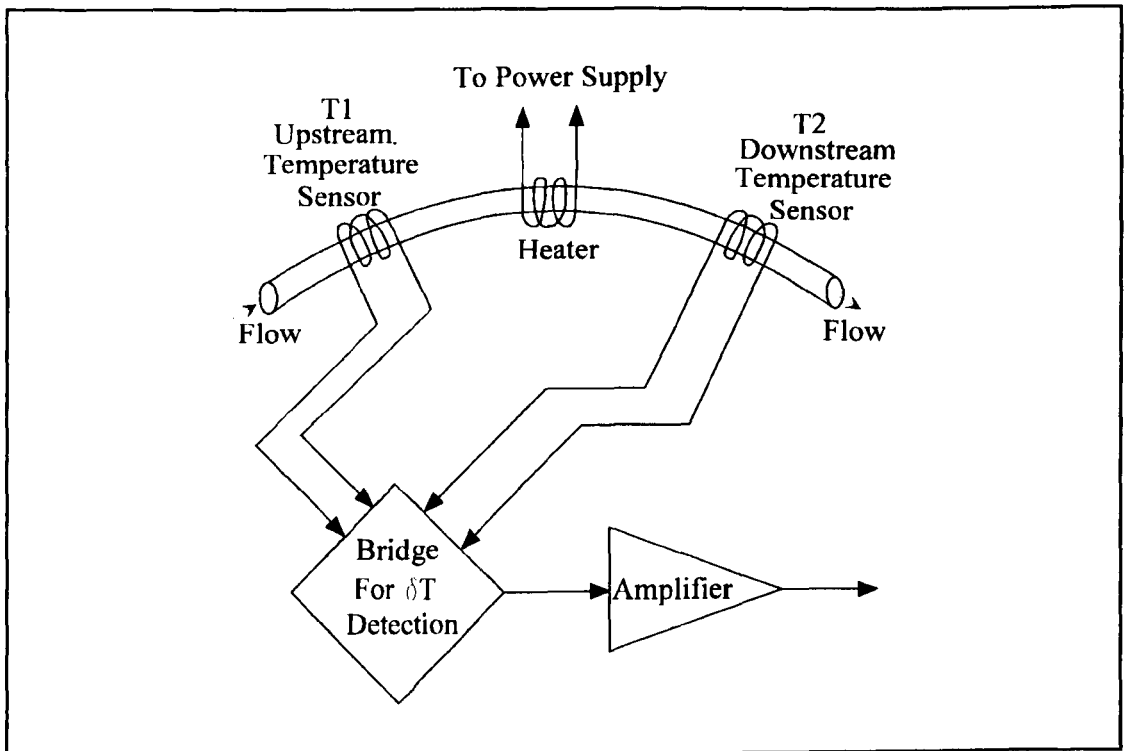


Figure 2.4 Flowsensor Operational Diagram.

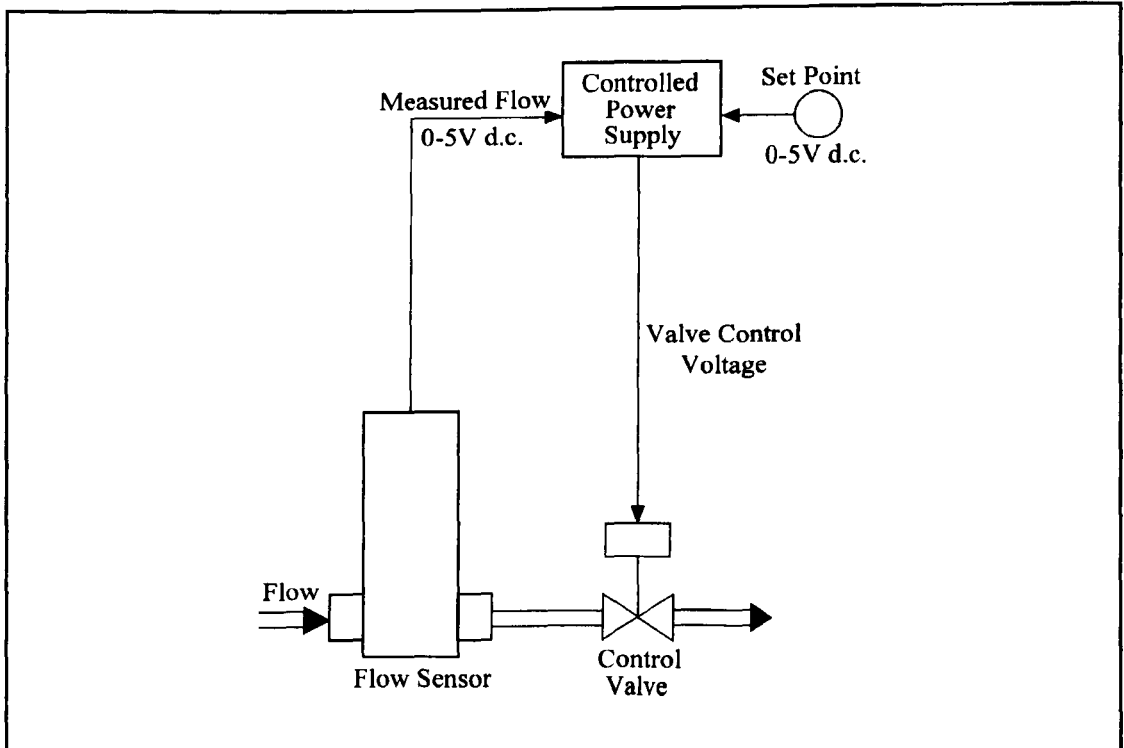


Figure 2.5 Mass Flow Control System.

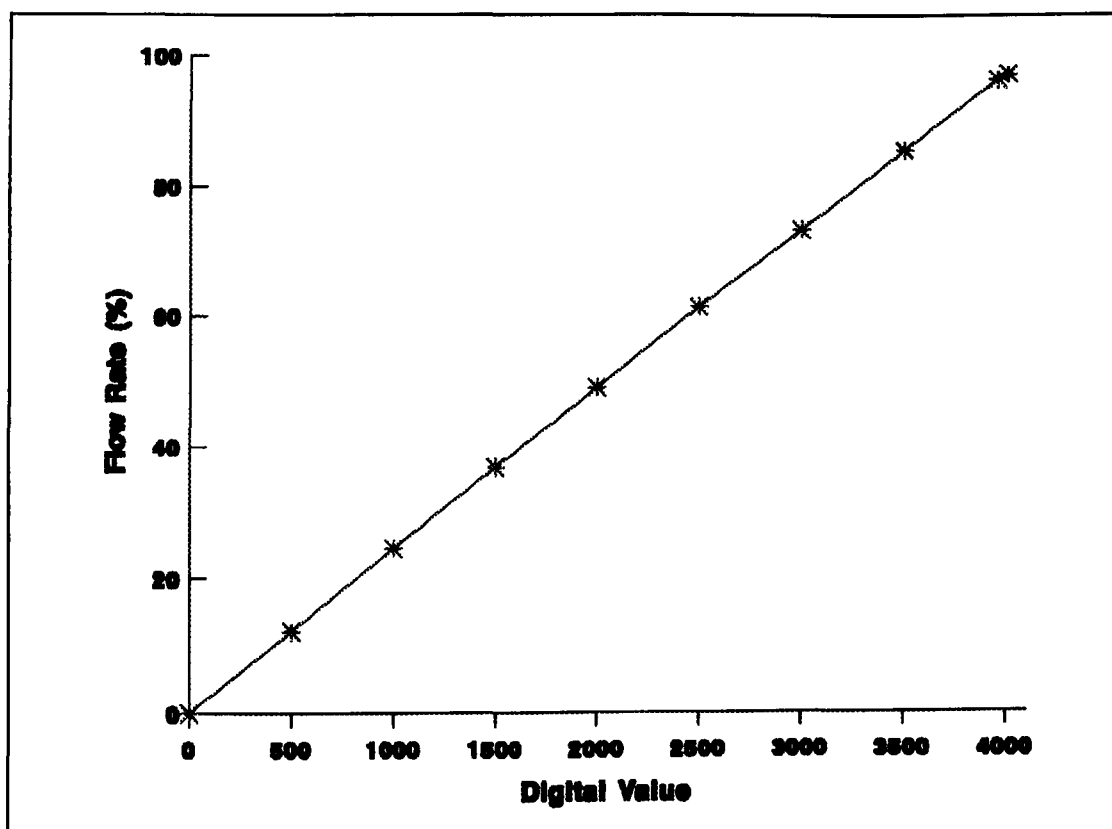


Figure 2.6 Mass Flowmeter Calibration Chart.

2.2.3.c. Temperature Measurement and Control.

A 2-wire platinum resistance temperature probe (Ingold), with appropriate commercial circuitry, mounted in the fermentation vessel provided an electrical signal of 4 to 20 mA for a working temperature range of 0 to 130°C. The analog signal was connected to an amplifier unit which was used to produce an accurate digital display of the broth temperature with a resolution of 0.1°C. The signal was also presented as an output to the temperature controller which, using a two-way proportional gain, gave a control of $\pm 0.2^\circ\text{C}$. The two-way action of 'heating' and 'cooling' allowed an accurate temperature control performance. The heated/cooled water was pumped through a heating element located in the centre of the fermentation vessel.

2.2.3.d. pH Measurement and Control.

The Biolafitte pH measurement and control system has been designed specifically for industrial fermentation applications. The system comprises two complementary modules; the first is an amplifier indicator for the measurement

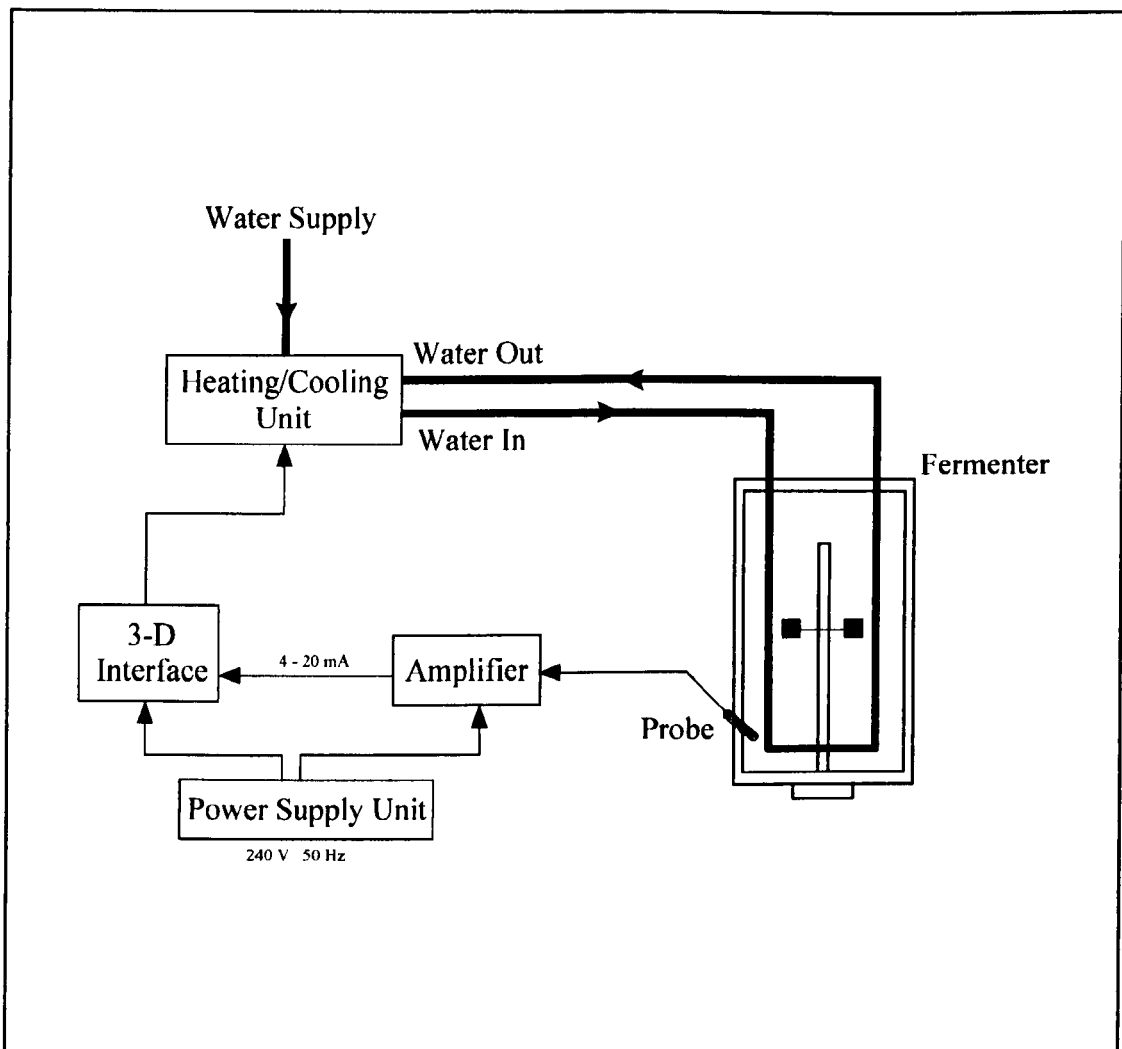


Figure 2.7 Temperature Control Loop.

of the broth acidity via a dedicated pH probe. The second module maintains the pH at a predetermined value by addition into the broth of acid or alkali in liquid form. The amplifier module is capable of measuring pH in the range of 2 to 12 pH, producing an output signal in the range of 4 to 20 mA. An Ingold combined pH probe was used, which had a manual temperature compensation potentiometer for 0 to 100°C. Additionally the probe calibration could be corrected for ageing to a maximum of 1.3 pH. As the fermentation of *S. cerevisiae* progresses, the broth becomes more acidic, thus an aqueous solution of 70% ammonium hydroxide (NH_4OH) was pumped into the broth to maintain the pH at the required set point level during on-line experimentation. The calibration of the pH probe was performed using the two buffer method, with pH values of 4 and 7 used as the standards.

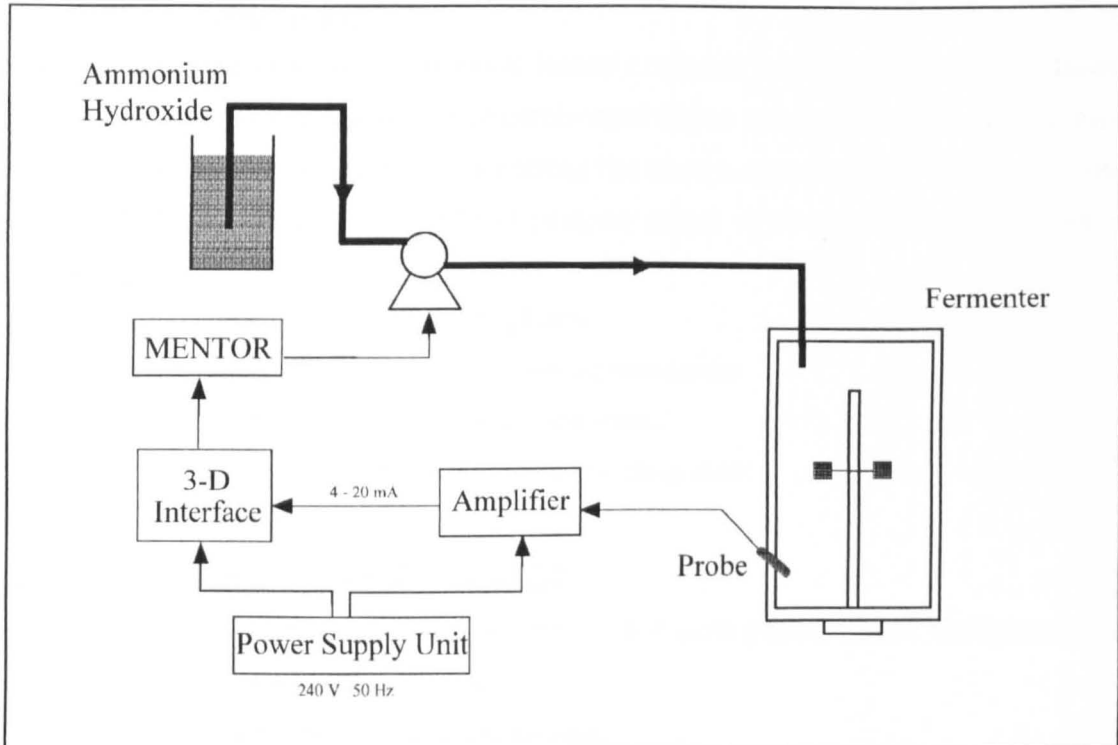


Figure 2.8 pH Control Loop.

2.2.3.e. Foam Control.

During a fermentation of *S. cerevisiae* a foam will develop on the surface of the broth liquid. This foam restricts the oxygen transfer rate of the broth and thus is undesirable. The detection of foam formation on the broth surface was achieved using an adjustable resistivity probe. Once foam was detected an anti-foam agent, polypropylene glycol, was manually pumped into the vessel, using a syringe, until the foam dropped to an acceptable level.

2.2.3.f. Feed Pumps.

Two Watson-Marlow peristaltic pumps were used for the controlled addition of glucose substrate and ammonium hydroxide. The pumps can provide both automatic and manual speed control, the former is achieved by an external voltage of 0 to 10V d.c. For the experiments performed, speed control was accomplished by the voltage input being provided by the master computer via the 3D-Interface unit. The rate of liquid flow is proportional to the bore size of the silicon tube and the rotational speed.

2.2.4. 3D-Interface Unit.

The 3D-Interface is a microprocessor based modular interface system. It allows for remote data acquisition and control capabilities using analog-to-digital and digital-to-analog convertors, transmitting the data to the master computer along an RS-232 serial link. A variety of plug-in cards were used during the work including:

- ▶ 8/16 channel analog multiplexer
- ▶ 4-channel 12-bit digital-to-analog convertor
- ▶ 12-bit fast analog-to-digital convertor
- ▶ 8 channel relay (or optoisolator) control unit

2.3. COMPUTER SOFTWARE UTILISED.

The computer software used during the work encompasses three main areas:

- ▶ Fermentation Process Control
- ▶ Computer Aided Controller Design
- ▶ Programming Environment

2.3.1. Fermentation Control Software (MENTOR).

The software package used to control the laboratory scale fermentation vessel and associated peripherals is MENTOR produced by Life Science Laboratories [2.3]. MENTOR is claimed to provide a complete data acquisition and process control environment, and has been designed to meet the specific needs of the biotechnologist. The MENTOR software provides facilities including Data Logging and Process Control. Once loaded, MENTOR will display the option 'menu': for the process operator this is the heart of the MENTOR system since it is from here that all the modules are invoked, and it is to this screen that the user is returned when exiting from a program module.

2.3.1.a. Data Logging.

MENTOR allows the simultaneous logging and storage of a range of process variables, such as temperature, pH and dissolved oxygen concentration, for up to twenty plants. Additionally, the status of process equipment, such as valves, motors and pumps, may be logged and stored. The status of the equipment is recorded either as a digital input from a device or a digital output to a device on

the plant. MENTOR incorporates a module to archive and retrieve logged data, to and from either a floppy disk or another computer via the RS-232 port.

Process data is obtained from the plant, by sequentially interrogating the inputs from the 3D-Interface. This interface is located between the sensors and the master computer (Figure 2.2). MENTOR includes a program for the sequential scanning of the sensor signals, in a predetermined pattern, by reference to a real time clock. In preliminary scanning cycles the values read from the interface are compared with any predefined limit values entered by the user, that is the set point high/low and alarm high/low values. Deviation from these values may result in alarm displays and printouts as specified by the user. In the final scanning cycle of a sequence, preselection of a logging option enables sensor readings to be permanently recorded in a data file. Logging is available at a predetermined time interval (the log rate) for each measurable process variable and for the status of process equipment; logged data is available for display.

On-line overview displays of the status of each process cycle are available: included are plant mimic diagrams which actively display the value of selected process variables and the current status of process equipment for a specified plant; also available is an analog overview which continuously displays as a histogram, the current values of process variables and their respective alarm and set point limits.

2.3.1.b. Process Control.

MENTOR provides facilities for Direct Digital Control, Supervisory Control and for Sequence Control operations. A sequence consists of a series of operations which are implemented in a defined order during a process cycle. A specific software routine enables the user to create and modify sequences by defining the required operations and their order in the sequence. Simple and conditional operations and their appropriate time intervals may thus be introduced into the process cycle. Applications of sequence control include sterilisation cycles, cleaning cycles, filling, inoculation, emptying and sampling.

Under Supervisory Control, process variables are controlled by analog control loops. Sensors are interfaced directly with the computer enabling values to be measured and if required, logged by the computer. MENTOR compares the inputs from the plant, with the desired set point values and if the process readings do not fall within the prescribed limits an alarm may be actuated. The control loops are maintained via a local controller whose function is to accept signals from the sensors or amplifiers, compare them with the desired set point value of the parameter, sent from the computer, and decide how much corrective action is to be taken. The output from the controller is sent to a suitable actuator which can affect the conditions on the plant, so that the parameter is brought back towards its desired value. The modes of control are limited to a conventional controller, that is one having proportional gain, integral action and derivative action.

The set point values are defined by the user as either a single value or a profile to be followed throughout the course of a fermentation. In the case of a profiled set point, updated set point values are sent to the controller during a run. Proportional, Integral and Derivative terms may be entered for Supervisory Control, either to allow a switch to Direct Digital Control during a process, or to enable calculation of an appropriate set point on the basis of the value of the process variable. Thus the computer may also vary the set point depending on the input received from the plant.

For Direct Digital Control, process variables are directly controlled by a module within MENTOR. Sensors are interfaced directly with the computer and the actuators, pumps, valves etc. are controlled directly through the program; a local controller unit is not required. When monitoring control loops, MENTOR is programmed to scan the inputs and compare them with the set point values previously defined and programmed by the user. If the process readings do not fall within the prescribed limits an alarm or a device on the plant may be actuated. Proportional, Integral and Derivative terms may be entered for each control loop.

2.3.2. Computer Aided Design Software.

The primary computer aided design program used was ACSL (Advanced Continuous Simulation Language [2.4]), which is a simulation language for evaluating the performance of continuous systems described by time dependent non-linear differential equations or transfer functions, and is a language based on FORTRAN. Various integration algorithms are available such as Runge-Kutta; also ACSL incorporates Laplace functions for control system analysis including complex transfer functions, Delay and Zero Order Hold, as well as input functions such as step, sine, pulse and gaussian. During the user's run-time session the eigenvalues and eigenvectors can also be obtained.

An ACSL simulation comprises two sections: the model definition and the run-time commands. The model definition involves specifying the continuous system under consideration in terms of ACSL statements. The model is then analyzed by instructions interpreted during the run-time command section. The advantage of this two tier system is that once a model has been defined, it may be stored and analyzed over and over again by different run-time commands since all variables in the model definition may be displayed or plotted, while any constant or parameter may be changed before a simulation run.

2.3.3. Custom Written Software (QuickBASIC).

The personal computer systems chosen for the work can be programmed in either a low-level or high-level language. The problems of writing code in assembly language are well known, thus it was decided to use one of the many high-level programming environments available for the PC.

The high-level programming language chosen for the work was Microsoft QuickBASIC [2.5] which provides a powerful development tool for professional users. The major reason for choosing QuickBASIC was its compatibility with the language used to program MENTOR, thus allowing incorporation into future issues of MENTOR.

2.4. CHEMICAL COMPOUNDS.

Since two distinct experiment types were performed - Bakers' Yeast fermentations and sodium sulphite tests - different chemicals were used for each. The following sections (2.4.1 & 2.4.2) describe the particular compounds and concentrations used.

2.4.1. Fermentation Experiments.

For the on-line fermentation work a commercial strain of *S. cerevisiae* was used, namely Fermipan from Gist-Brocades in The Netherlands. This is a freeze dried yeast provided in a vacuum pack to ensure a long shelf-life. The initial yeast concentration for the experiments was 8 g.l⁻¹. In addition, the initial broth included the chemicals listed in Table 2.1.

Table 2.1 Initial fermenter contents.

Compound	Formula	Concentration (mol.l ⁻¹)
Glucose (initial broth charge)	C ₆ H ₁₂ O ₆	2.77 x 10 ⁻³
Magnesium sulphate heptahydrate	MgSO ₄ ·7H ₂ O	2.02 x 10 ⁻³
Sodium chloride	NaCl	8.55 x 10 ⁻³
di-potassium hydrogen orthophosphate	K ₂ HPO ₄	5.74 x 10 ⁻³
Potassium dihydrogen orthophosphate	KH ₂ PO ₄	0.01
Ammonium sulphate	(NH ₄) ₂ SO ₄	0.04

For both types of fermentation a total of 632g of glucose was used as the substrate feed, for an 8 litre broth volume. For batch fermentations this was added in total at the start, while for fed-batch fermentations the glucose was mixed with water to produce a 30% weight/volume concentration and the solution added over the fermentation period. The control of pH was achieved by the addition of 70% ammonium hydroxide (NH₃OH).

2.4.2. Sodium sulphite Experiments.

For the experimental work involving sodium sulphite, the concentrations listed in Table 2.1 were used in 1l of water. These were pumped directly into the vessel containing only water.

Table 2.2 Sodium sulphite chemicals.

Chemical	Formula	Concentration (mol.l ⁻¹)
Sodium sulphite	Na ₂ .SO ₃	0.5
Copper sulphate pentahydrate	CuSO ₄ .5H ₂ O	2.26 x 10 ⁻³

2.5. DISCUSSION.

The computer hardware and software described in this chapter proved invaluable in completing the work. More advanced software packages are continuously being produced, however they can only help in improving current methodologies; the packages currently available are more than adequate in assisting with computer aided controller design. The fermentation equipment used during the work comprised some of the most modern available, therefore the overall control performance of the process was an improvement over previous fermentation systems used in the Department. However, there is still a lack of probes for accurate on-line monitoring of process variables, such as an active biomass sensor or a probe to indicate the level of glucose substrate.

2.6. REFERENCES.

- 2.1. Dissolved oxygen probe manual. Ingold Ltd. 1988.
- 2.2. Schugerl, K. Measurement and bioreactor control. 8th International Biotechnology Symposium. Vol. 1. p. 547-562. 1988.
- 2.3. MENTOR 3.0 Manual, Life Science Laboratories Ltd., U. K. 1990.
- 2.4. Advanced Continuous Simulation Language (ACSL) Users Guide, Mitchell and Gauthier, U.S.A. 1988.
- 2.5. Microsoft QuickBASIC version 4.0 Reference Manual, Microsoft. 1988.

CHAPTER 3.

AUTOMATIC TUNING PROCEDURE: THEORY AND IMPLEMENTATION.

3.1. INTRODUCTION.

Today, the majority of industrial controllers are based on the standard PID-controller. Engineers and process operators are familiar with using and tuning them, and often have experience for the effect each parameter has on the process response [3.1]. In the 1940's the PID controller was implemented using pneumatic components; new controllers were developed as analogue electronic technology progressed, from transistors to integrated circuits. Owing to the rapid development of computers, analogue PID-controllers are increasingly being replaced by small computer based systems, thus making it possible to introduce more advanced algorithms onto process control loops.

Basic PID controllers may have their tuning parameters set to values which are optimal for a particular process working point. If the operating conditions change, for instance owing to a load disturbance or a change in ambient conditions, then the controller parameters should be retuned. This is often both a difficult and time consuming job, and frequently ignored. Self-tuning controllers can perform this task on-line and consequently save time for operators and improve the response of the process. There are numerous examples where ordinary self-tuning controllers have improved process control [3.2]. The controllers are typically based on minimum variance or pole placement designs [3.3 & 3.4] although there is a rather large difference in complexity between the PID-algorithm and these self-tuning controller algorithms. The complexity of a self-tuning controller is dependent on the order of the system model used, but not on how difficult the process is to control. Thus it can be concluded that there is a need for simple self-tuning controllers which are capable of handling high order systems and which benefit from retaining the PID structure. Wittenmark *et al* [3.5] presented a self-tuning PID-controller based on pole placement design; however the controller model was

always of second order regardless of the process order. Experiments showed that the controller worked well if the process contained no time delay, and if the process behaviour could be approximated by a second order model.

Kuo *et al* [3.6] presented a model-based algorithm to obtain a controller in either PI or PID form. In 1975 MacGregor *et al* [3.7] modelled a process using a discrete transfer function while the noise disturbance was modelled by an autoregressive-integrated-moving-average model. Åström and Haggund [3.8] presented a self-tuning PID controller based on a second order model with pole-placement. The common disadvantage of these methods is that they require structural knowledge of the process, such as process order and dead time. This limitation can cause problems if the design specification is to produce a generalized controller for a wide variety of systems. Since the earliest developments in automatic control, it has been known that knowledge about the system is seldom available *a priori* to assist in controller design [3.9]. The tuning method described here is based on process parameter estimation and algebraic calculations of the critical gain and ultimate period of the process, where only a small excitation of the input signal is required for the identification procedure.

Since the frequency response approach is such a powerful tool for the design of controllers for linear systems, it was inevitable that an effort would be made to extend the approach to nonlinear systems. This did in fact take place in several countries simultaneously, resulting in the describing function technique. The describing function method can be considered the forerunner of what may be referred to as quasilinear techniques, where a nonlinear element is replaced by a linear gain approximation. The value of the approximated linear gain is dependent upon the criterion chosen for the definition of the best approximation, the magnitude and type (i.e. sinusoidal, random etc.) of input signal and the shape of the nonlinear characteristic. If a nonlinearity is introduced into a closed-loop system, as in Figure 3.1, the signals from the nonlinear element can oscillate with constant amplitude and frequency. By measuring the amplitude and frequency of the oscillation, it is possible to determine the position on the Nyquist diagram of $G(j\omega)$, for that frequency. This knowledge provides the basis for the automatic tuning procedure discussed in this chapter.

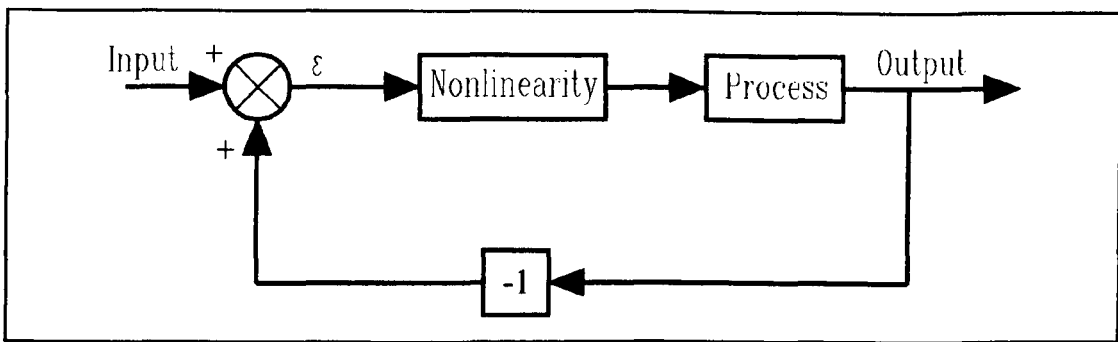


Figure 3.1 Closed-loop system including a nonlinear element.

The important techniques in adaptive control are automatic tuning, gain scheduling and continuous adaptation. When these techniques were originally developed, the objective was to continuously change the controller parameters during the process run-time to maintain optimum performance. In comparison, automatic tuning or single-shot tuning offers a simplified version of adaptive control. The user needs to have *a priori* information before using many adaptive control techniques, with typical knowledge required including ideal sampling period, algorithm forgetting factor, process time constant and controller complexity. To obtain most of this information required considerable effort on the part of the process instrumentation engineer. In order to use the Ziegler-Nichols closed loop tuning method (section 3.3.1), it is necessary to determine the critical gain and ultimate period which applies when a system just continuously oscillates, in closed-loop, with proportional control only. These parameters can be determined on-line by using a self-oscillating adaptive control loop (SOACL) (Figure 3.2). The objective of the adaptive control loop is to obtain a limit cycle from which the ultimate period will be established. The SOACL thus automatically provides the parameters required for the Ziegler-Nichols design rules, while its implementation becomes very simple. However, the system response can sometimes become too oscillatory or even unstable.

The PID tuner described in this thesis was inspired by Åström [3.10, 3.11, 3.12, 3.13 & 3.14] and by the original work of Schuck [3.15], who developed an adaptive controller which maintained a constant gain margin in a system, by using a nonlinearity as an essential element of the controller. The principle of the automatic tuner is to change over from PID control to the tuning procedure, which employs a binary output nonlinearity to induce oscillations in the

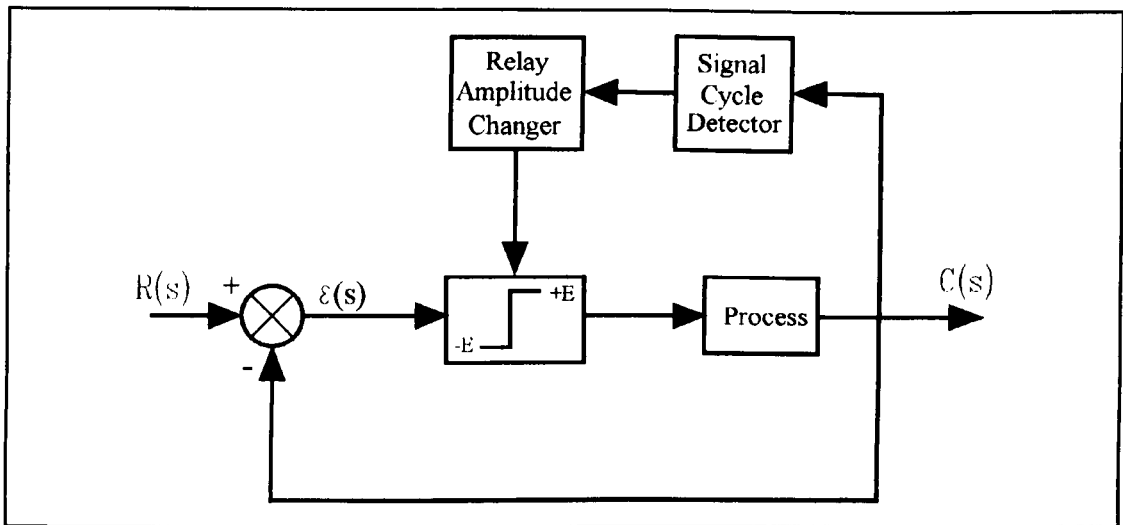


Figure 3.2 Self-oscillating adaptive control loop.

controlled variable. From the characteristics of the oscillatory response, a series of calculations are made to determine appropriate controller tuning parameters to meet some predetermined design criteria. A useful design parameter is the phase margin which is mostly chosen empirically between 30° and 60° [3.16]. Having found the controller settings, the tuning procedure is completed, the values are passed to the PID controller and then process control is returned to the PID controller.

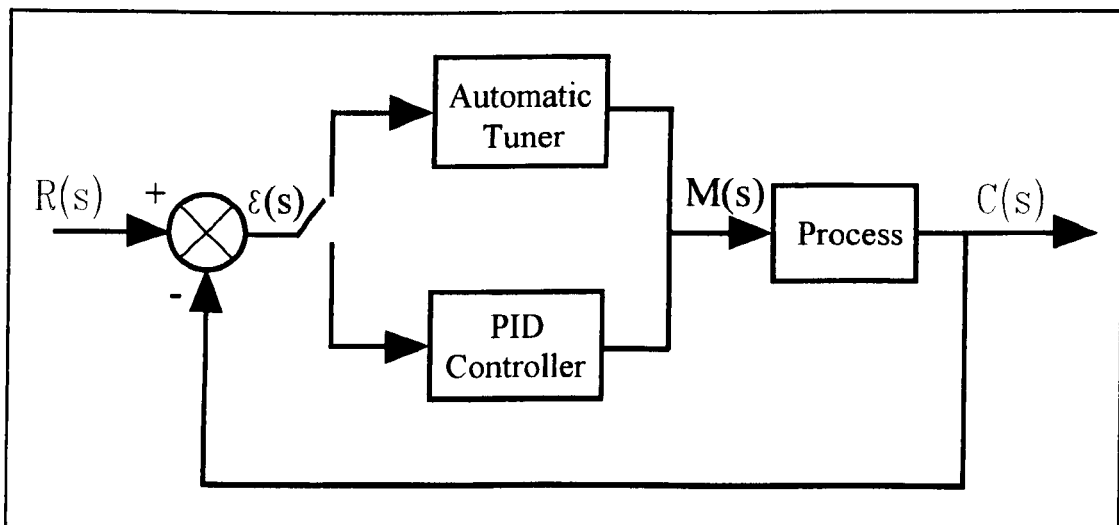


Figure 3.3 The principle of the PID-tuner.

3.2. THE THREE TERM REGULATOR

Many control problems may be solved by the use of a Proportional plus Integral plus Derivative controller, where the PID controller algorithm may be represented by the transfer function

$$\frac{M(s)}{\epsilon(s)} = K_p \left(1 + \frac{1}{T_i s} + T_d s \right) \quad (3.1)$$

where K_p represents the proportional gain, T_i is the integral action (reset time) and T_d is the derivative action (rate time), and $\epsilon(s)$ represents the difference between the set point signal, $R(s)$, and the process output signal, $C(s)$

$$\epsilon(s) = R(s) - C(s) \quad (3.2)$$

As a continuous algorithm, the PID controller has several forms. However the widely accepted or 'textbook' version is

$$M(t) = K_p \left[\epsilon(t) + \frac{1}{T_i} \int \epsilon(t) dt + T_d \frac{d\epsilon(t)}{dt} \right] \quad (3.3)$$

Correctly, this equation should be referred to as the 'ideal noninteracting form'. From equation (3.3) it will be seen that the values of the integral action and derivative action may both be changed independently without affecting the other two terms. The digital (sampled data) form of algorithm (3.3) is referred to as the positional form of the PID, where the integral becomes a 'summation' while the derivative becomes a 'finite difference'; for example

$$y_n = K_p \left(\epsilon_n + \frac{1}{T_i} \sum_{i=1}^n (\epsilon_i + \epsilon_{i-1}) \frac{\tau_s}{2} + T_d \frac{(\epsilon_n - \epsilon_{n-1})}{\tau_s} \right) \quad (3.4)$$

where τ_s is the sample time. The digital three term controller allows independent tuning of each term which can be an advantage for the control of nonlinear processes [3.17 & 3.18].

3.3. MANUAL TUNING PROCEDURES.

If a mathematical model of a process can be determined then it is possible to apply a variety of design techniques to determine a set of controller parameters to achieve the required design specification. If, however, the process is so complex that a model cannot be derived, then it is not possible to follow

analytical approaches to design a PID controller. Instead, an experimental approach must be employed for controller tuning.

There are a number of manual techniques for determining controller tuning parameters. Two of the popular methods were proposed by Ziegler and Nichols [3.19 & 3.20], and are known as the 'open loop' and 'closed loop' tuning methods. The open loop method requires a step input to be applied to the open loop system. This method is empirically known to give poor results, since the determination of the response curve characteristic can be prone to experimental error. Also the effect of an integrator produces a response which increases towards infinity, thus the point of inflection of the curve cannot be found; however an approximation is often accepted. The second method requires the process to be placed under closed-loop proportional control, as described in section 3.3.1.

The process-reaction curve method of Cohen and Coon [3.21] attempts to model the process as a first-order lag plus dead-time, by analysing the open-loop response to a step change in the input. As far as fermentation processes are concerned, the drawback of this method is that it requires open-loop operation and is limited to low-order processes. A modification to the Ziegler-Nichols closed loop tuning method was proposed by Aikman [3.22] after frequency response studies, based on the determination of the proportional gain required to produce a damped oscillation with a subsidence ratio of 3.5:1.

The open-loop tuning methods are difficult to apply to fermentation systems, firstly because the process needs to be under some form of control for it to respond, and secondly for some fermentations the response time would be in hours and thus very time consuming for the operator. The reaction curve method is probably the easiest way to estimate controller parameters for linear processes. This is not true for nonlinear processes such as the control of dissolved oxygen concentration in fermentations. The open-loop response of the controlled variable to a step increase in the manipulated variable is different to that for a step decrease. These differences are primarily caused by the different mechanisms for oxygen absorption (physical phenomenon) and consumption

(biological phenomenon). Further, the process gain and time constant are functions of fermentation age. Thus controller parameters have to be found on-line during the fermentation process.

3.3.1. Closed-Loop Tuning Method.

The fundamental principle of the Ziegler-Nichols closed-loop method is the determination of the critical stability condition for a given process when under proportional control. This requires the identification of the point where the Nyquist curve of the open-loop system intersects the negative real axis. The controller is set to provide proportional control only, with the integral and derivative actions inoperative (usually meaning $T_i = \infty$ and $T_d = 0$). The proportional gain is set to the minimum value possible, from which it is progressively increased in small increments until the controlled process variable responds with a continuous oscillation at fixed amplitude. The proportional gain at which these oscillations occur corresponds to the maximum value for limiting stability and is known as the 'critical gain', K_c . The oscillation period is referred to as the 'ultimate period', T_u . The controller tuning parameters recommended by Ziegler & Nichols are based on these experimentally determined values, and are designed to produce a controlled variable response with a subsidence ratio of approximately 4:1, with an acceptable degree of overshoot. The values of the parameters K_p , T_i and T_d should be set according to the formulae shown in Table 3.1. If the controlled variable does not exhibit sustained oscillations for any value of gain, then this particular method cannot be applied.

Table 3.1 Ziegler-Nichols Recommended Parameter Settings.

Controller Configuration	K_p	T_i	T_d
P	$0.5 K_c$	∞	0
P+I	$0.45 K_c$	$0.833 T_u$	0
P+I+D	$0.6 K_c$	$0.5 T_u$	$0.125 T_u$

Åström [3.23] has suggested that the Ziegler-Nichols closed loop tuning method is designed to produce a phase margin of approximately 25° at the critical

frequency; however the proportional gain is then reduced to 0.662 times smaller:

For 25° phase margin

$$K_p = 0.906 K_c \quad T_i = 0.5 T_u \quad T_d = 0.125 T_u$$

From Ziegler-Nichols

$$K_p = 0.6 K_c \quad T_i = 0.5 T_u \quad T_d = 0.125 T_u$$

Using the Ziegler-Nichols closed-loop method produces a PID controller given by

$$M(s) = 0.6K_c \left(1 + \frac{1}{0.5T_u s} + 0.125T_u s \right)$$

therefore

$$M(s) = 0.075K_c T_u \frac{\left(s + \frac{4}{T_u} \right)^2}{s} \quad (3.5)$$

Thus the controller has a pole at the origin and double zero at

$$s = \frac{-4}{T_u}$$

A drawback of the Ziegler-Nichols closed loop or ultimate sensitivity method is that the amplitude of the induced oscillations on the output variable may exceed process safety limits, since the system must be taken to the limit of stability. Another disadvantage of a Ziegler-Nichols tuned system is that it varies significantly with process dead-time. As far as the Nyquist diagram is concerned, the Ziegler-Nichols closed-loop tuning method is established on the knowledge of the location of the point, A, where the $G(j\omega)$ -loci crosses the negative real axis. The critical period, T_u , is given by $T_u = 2\pi/\omega_c$, where ω_c is the critical frequency (rad.s^{-1}).

3.3.2. Phase Margin and Gain Margin.

The gain and phase margins of a control system are a measure of the closeness of the Nyquist polar plot to the $-1+j0$ point. Hence these margins may be used as a controller design criteria. The phase margin is defined as the amount of additional phase lag, at the gain crossover frequency, which is required to bring the system to the verge of instability. The gain crossover frequency is the frequency at which the magnitude of the open-loop transfer function is unity.

The phase margin of a system, ϕ_m , is given by 180° plus the phase angle, δ , of the open-loop transfer function at the gain crossover frequency, that is

$$\phi_m = 180^\circ + \delta \quad (3.6)$$

The gain margin is defined as the reciprocal of the magnitude of the open-loop transfer function at the frequency, when the phase angle is -180° . If the phase crossover frequency, ω_1 (Figure 3.4), is the frequency at which the phase angle of the open-loop transfer function is -180° , then the gain margin, G_M , is given by

$$G_M = \frac{1}{|G(j\omega_1)|} \quad (3.7)$$

It is more usual to refer to the gain margin in decibels

$$G_M \text{ dB} = 20 \log G_M = 20 \log |G(j\omega_1)| \quad (3.8)$$

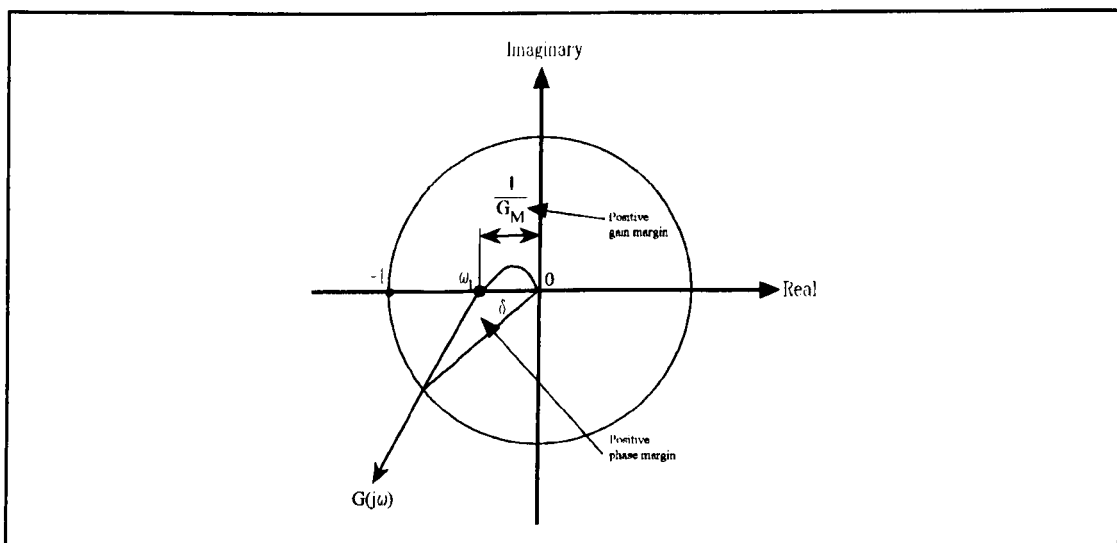


Figure 3.4 Gain margin and phase margin.

The gain and phase margins, as measures of process stability, are only valid for open-loop stable systems. Also, either the gain margin alone or the phase margin alone do not provide sufficient indication of the relative stability; both need to be determined as a measure of relative stability. For a minimum phase system the gain and phase margins must both be positive for system stability; negative margins are an indication of instability. A large gain or phase margin indicates a very stable system but with a very slow response. A highly oscillatory system is indicated by a gain margin close to unity or a phase margin close to zero.

For a satisfactory degree of relative stability, the phase margin should be in the range 30-60°, while the gain margin should be at least 6dB [3.16]. In most practical systems, a good phase margin automatically guarantees a good gain margin, and *vice versa*. For process control systems a decay ratio of ¼ ($\zeta=0.21$) is considered acceptable, where this type of response corresponds to $G_M=2$ and $\phi_m=40^\circ$. In contrast, servo systems require a much less oscillatory response because of potential damage to equipment. Typically a peak overshoot of less than 20° is required which corresponds to $G_M \geq 5$ and $\phi_m \approx 50^\circ$ [3.24]. A correlation between phase margin, ϕ_m , and damping ratio, ζ , is given by [3.25]

$$\phi_m = \tan^{-1} \left(2\zeta \sqrt{\frac{1}{\sqrt{4\zeta^4 + 1} - 2\zeta^2}} \right) \quad (3.9)$$

with an acceptable linear approximation, for the range $0 \leq \zeta < 0.7$, given by

$$\zeta = 0.01 \phi_m \quad (3.10)$$

where ϕ_m is in degrees.

3.3.3. Phase Margin Design.

If a specific point on the Nyquist diagram is known for a controlled process, then it is possible to move that point to some arbitrary location in the complex plane by adjusting the values of proportional, integral and derivative gains. This idea may be used to develop a controller to meet specific design criteria. For example, if the point is moved onto the negative real axis then a given gain margin may be attained, whereas for a prescribed phase margin the point has to be moved onto the unit circle. Figure 3.5 illustrates how a point, P, may be moved in the direction of $G(j\omega)$, $G(j\omega)/j\omega$ and $j\omega G(j\omega)$ by changing the values of K_p , T_i and T_d respectively.

If the point, B, where the Nyquist locus of $G(j\omega)$ intersects the negative real axis is known, then the argument of the transfer function at B is

$$\arg \left(1 + \frac{1}{j\omega_c T_i} + j\omega_c T_d \right) - 180^\circ \quad (3.11)$$

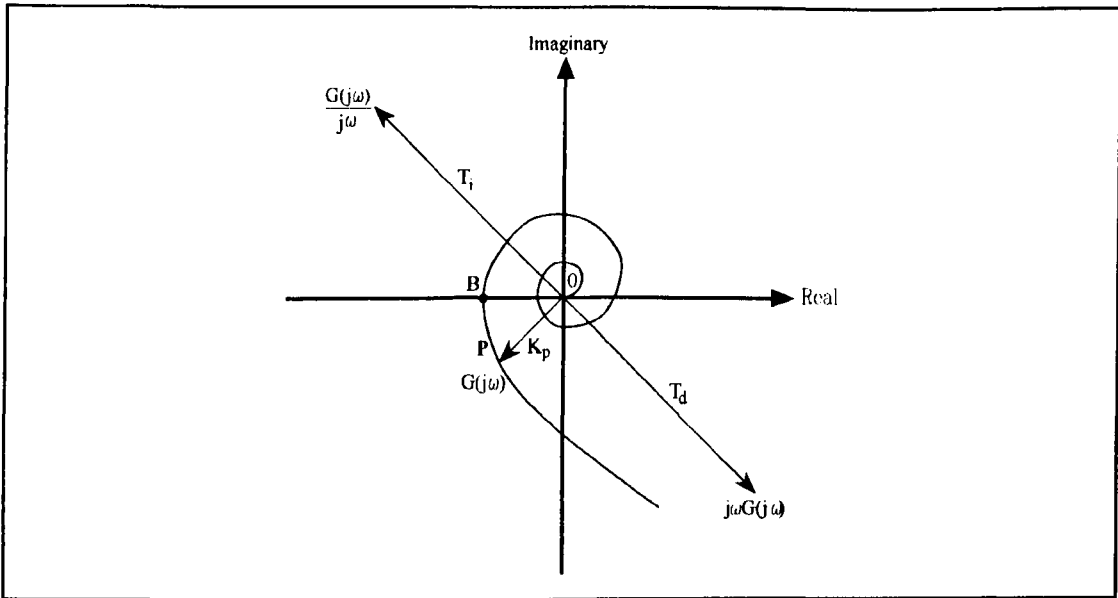


Figure 3.5 Nyquist diagram for phase and gain margin design.

If the required phase margin is ϕ_m then the argument is $\phi_m - 180^\circ$ and the following condition is obtained

$$\omega_c T_d - \frac{1}{\omega_c T_i} = \tan \phi_m \quad (3.12)$$

Numerous values of T_d and T_i satisfy this condition, with one possibility being a constant ratio between T_i and T_d , such as

$$T_i = \alpha T_d \quad (3.13)$$

A value of $\alpha=4$ is widely used. Substituting this value into equation (3.12) produces a second order equation with the solution

$$T_d = \frac{\tan \phi_m + \sqrt{\frac{4}{\alpha} + \tan^2 \phi_m}}{2\omega_c} \quad (3.14)$$

Further calculations show that the loop transfer function has unity gain at B, if the regulator gain is chosen as

$$K_p = \frac{\cos \phi_m}{|G(j\omega_c)|} = K_c \cos \phi_m \quad (3.15)$$

where K_c is the critical gain of the process. The design rules of equations (3.11) to (3.15) can be used to provide the tuning values for different phase margins (Table 3.2).

Table 3.2 Phase-margin-design rules for a PID controller.

ϕ_m	K_p	T_i	T_d
30°	0.87 K_c	0.55 T_u	0.14 T_u
45°	0.71 K_c	0.77 T_u	0.20 T_u
60°	0.50 K_c	1.22 T_u	0.30 T_u
Ziegler-Nichols	0.6 K_c	0.5 T_u	0.125 T_u

As an example consider the process

$$G(s) = \frac{1}{(s+1)(s+2)(s+3)} \quad (3.16)$$

which has a critical gain of $K_c=60.0$ and an ultimate period of $T_u=1.88$ units. (Note: Since equation (3.16) is a generalized transfer function, no specific time units can be referred to. Hence the time units of T_i and T_d are the same as for T_u .) The corresponding tuning parameters to Table 3.2 are presented in Table 3.3.

Table 3.3 Tuning parameters for $G(s)$.

ϕ_m	K_p	T_i	T_d
30° (GPID1)	52.2	1.04	0.26
45° (GPID2)	42.6	1.44	0.37
60° (GPID3)	30.0	2.29	0.56
Ziegler-Nichols (GZN)	36.0	0.94	0.24

Using the above rules, the process of equation (3.16) was simulated under closed-loop PID control. The phase margins obtained from the simulated tuned controlled process were 29.76°, 45.25° and 59.99° respectively. Figure 3.6 illustrates both the Nyquist diagram and the transient responses for the closed-loop PID controlled process.

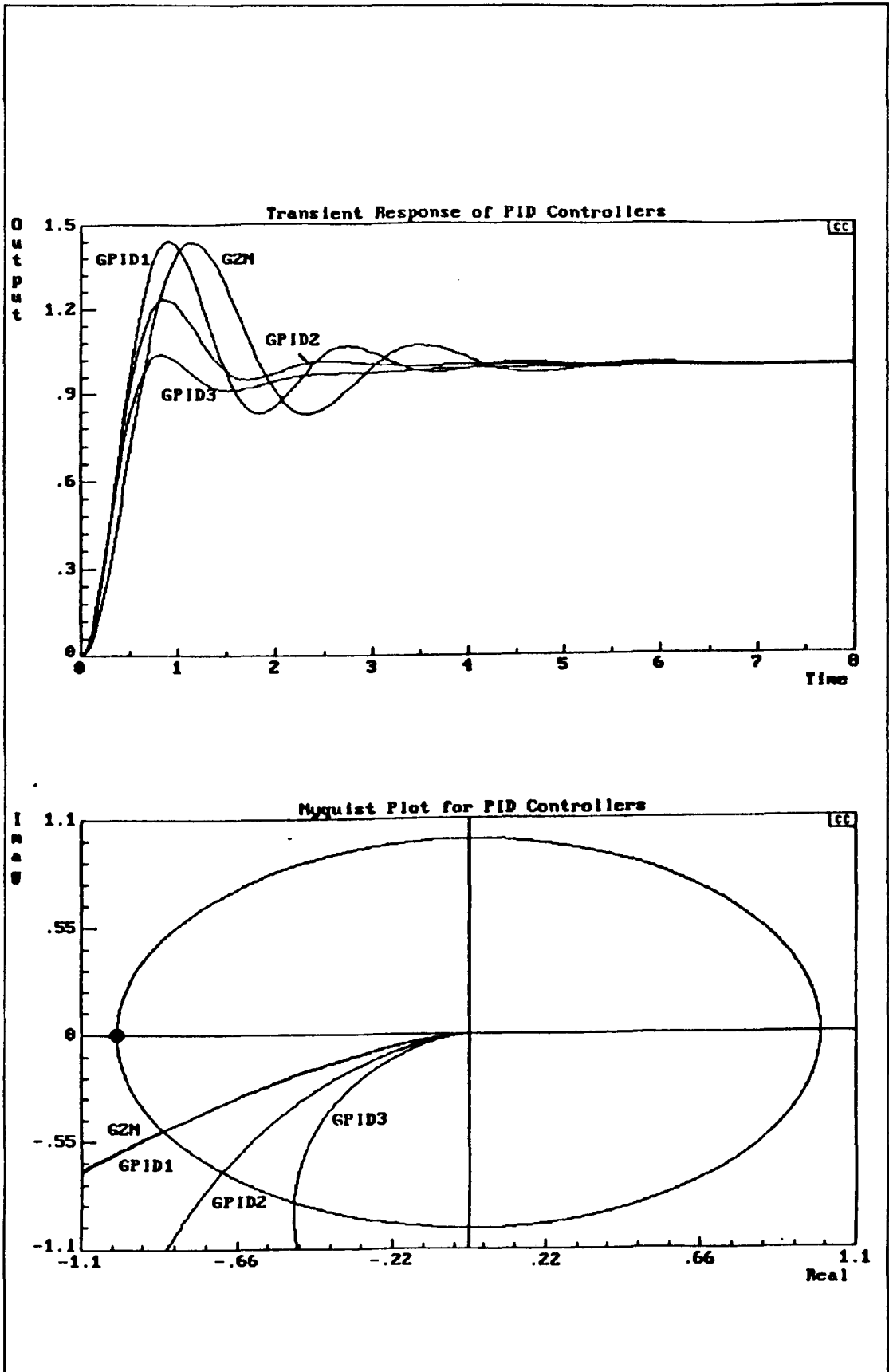


Figure 3.6 Phase-margin-designed PID controllers for process of equation (3.16).

3.3.4. Gain Margin Design.

Once the point of critical stability is known, the controller may also be designed to attain a desired gain margin, for example by choosing

$$K_p = \frac{K_c}{G_m} \quad (3.17)$$

where G_m is the desired gain margin, K_c the critical gain and K_p the required controller gain. If the process requires the addition of integral and derivative action, where the frequency response of a PID controller is given by

$$M(j\omega) = K_p \left(1 + \frac{1}{j\omega T_i} (1 + \omega^2 T_i T_d) \right) \quad (3.18)$$

then it can be shown that a controller with a gain given by equation (3.18) has the relationship

$$T_d = \frac{1}{\omega_c^2 T_i} \quad (3.19)$$

Thus the value of the integral time may be chosen arbitrarily and the derivative time then given by equation (3.19), for the PID controller to provide the required gain margin.

The above rules were used to design PID controllers to obtain gain margins of 2, 5 and 8 for the process given by equation (3.16). The controller parameters calculated are shown in Table 3.4 with the resultant Nyquist loci and closed-loop transient response shown in Figure 3.7. For comparison, a Ziegler-Nichols tuned PID controller is also represented. The gain margins achieved were 1.99, 4.98 and 7.99 respectively from a process with an initial gain margin of 60.0.

Table 3.4 Tuning parameters for gain margin design.

G_m	K_p	T_i	T_d
2 (GM3)	30.0	20.0	0.008
5 (GM1)	12.0	2.0	0.045
8 (GM2)	7.5	5.0	0.018

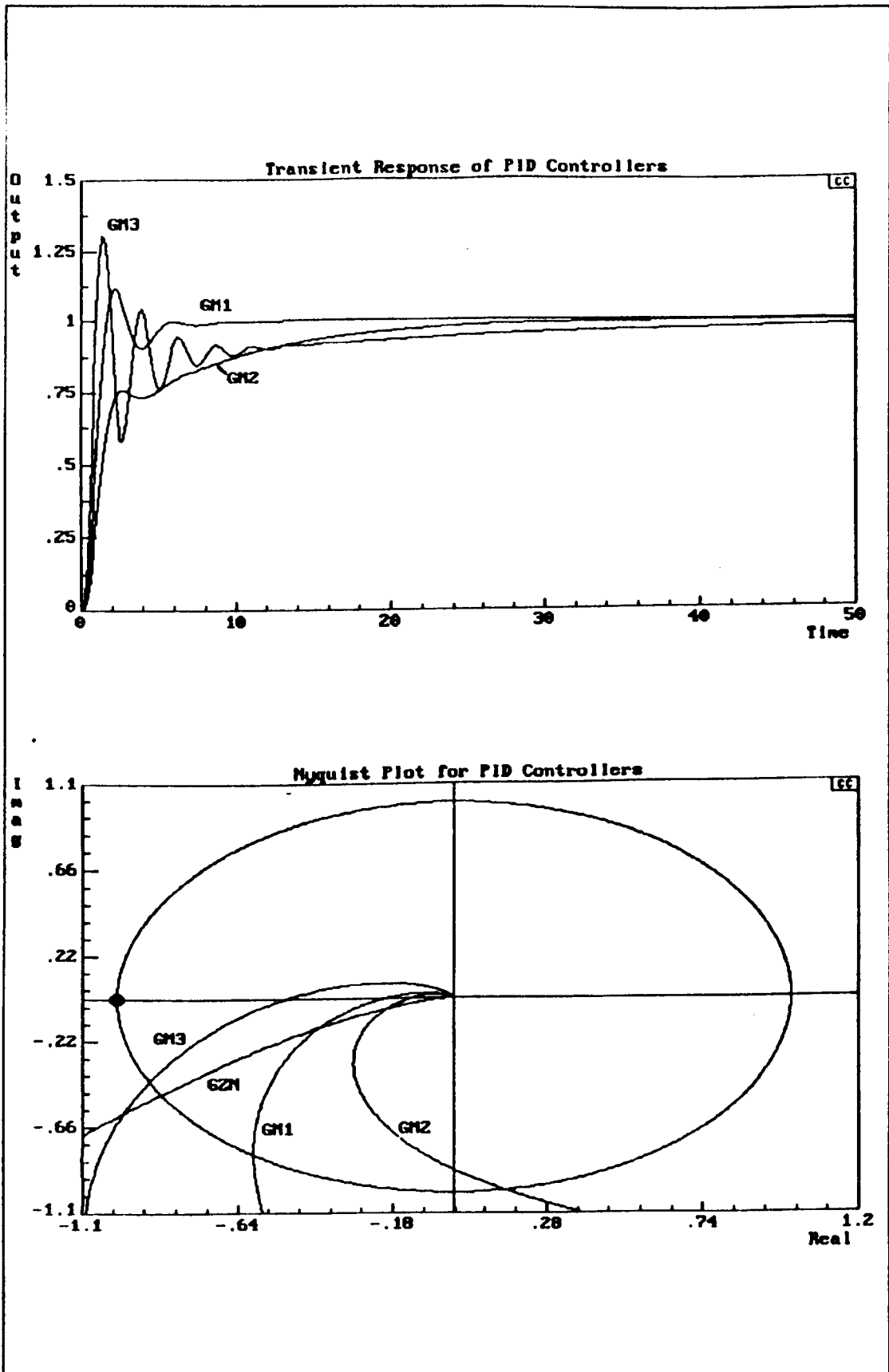


Figure 3.7 Gain-margin-designed PID controllers for process of equation (3.16).

3.4. RELAY CONTROL.

Relay control systems are widely used in various technological areas because they are simpler than other types of control systems, and often have better dynamic properties. They have been widely applied, for example, in stationary control of industrial processes and the control of mobile objects such as spacecraft. Owing to their principle of operation, relays are highly nonlinear and as such cannot be directly analyzed by established linear techniques. However, because the output of the relay is essentially independent of its input then it is possible to study them by using relatively simple methods.

3.4.1. Limit Cycles.

A limit cycle is an oscillation occurring in a process which may contain both linear and nonlinear elements. The limit cycle oscillations may not be strictly sinusoidal however they will have a repeated cycle, and can be considered as either stable or unstable. For an unstable limit cycle the oscillations are not sustained, and there is a tendency for the system to move away from the critical point. Thus, only stable limit cycles are observable in practice, and the describing function technique can be used to predict these oscillations. For the limit cycle analysis to be performed, the higher harmonics generated by the nonlinearity must be filtered out by the process, $G(j\omega)$. It must also be assumed that the poles and zeros of $G(j\omega)$ lie in the left half plane. The describing function analysis of limit cycles has been given a rigorous mathematical treatment by Miller and Michel [3.26]. The Loeb criterion may be used to predict the stability properties of limit cycles, although it can yield incorrect results.

3.4.2. Describing Function Technique.

Single loop feedback systems are often tested for stability using the describing function method [3.27 & 3.28], which can determine the behaviour of a wider class of systems than is possible by the phase-plane method. To discuss the basic idea underlying these techniques, consider the block diagram of a unity feedback nonlinear system (Figure 3.8), where block $G(j\omega)$ represents a linear system, and N represents the nonlinear element.

The closed loop transfer function of such a system is given by

$$\frac{C(j\omega)}{R(j\omega)} = \frac{N G(j\omega)}{1 + N G(j\omega)} \quad (3.20)$$

If the condition

$$G(j\omega) = \frac{-1}{N} \quad (3.21)$$

is met, the output will exhibit a limit cycle. This corresponds to the condition where the $G(j\omega)$ -locus passes through the critical $(-1+j0)$ point in conventional linear frequency response analysis [3.29]. The widest use of describing functions is in stability investigations and the prediction of limit cycles in feedback systems. Consider the system shown in Figure 3.8, where the nonlinearity, N , has been replaced by its describing function, $N(a,\omega)$. The system having thus been linearized, its characteristic equation can be written as

$$1 + G(j\omega)N(a,\omega) = 0 \quad (3.22)$$

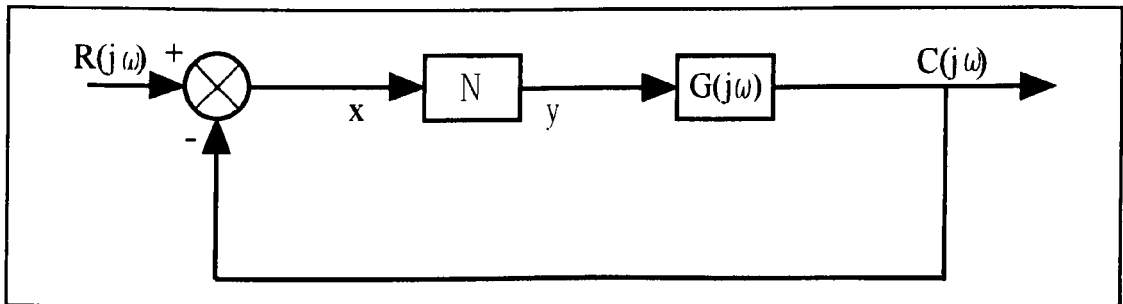


Figure 3.8 Block diagram representing a nonlinear system.

The solution of equation (3.22) is a particular kind of first order approximation to the actual oscillatory behaviour of the system. Sometimes it is essential to include higher order harmonics because the errors introduced in taking only the fundamental frequency are large enough to prevent the describing function method from providing a solution [3.30], but in most cases the fundamental component solution is adequate; often the process acts as a low-pass filter, attenuating higher frequency components.

According to the Nyquist stability criterion, a system will exhibit sustained oscillations, called a limit cycle, when

$$G(j\omega)N(a,\omega) = -1 \quad (3.23)$$

This condition implies that the plot of $G(j\omega)N(a,\omega)$ passes through the critical point of -1. The describing function technique has thus helped in extending the Nyquist stability criterion to nonlinear systems. This extension is completely heuristic and has no mathematical basis. It is, however, a powerful tool because it is often applicable. The condition of equation (3.23) can be written in the modified form

$$G(j\omega) = \frac{-1}{N(a,\omega)} \quad (3.24)$$

This condition differs from equation (3.23) in that the frequency response of the linear part $G(j\omega)$ is plotted, while the critical point -1 becomes the critical locus of $-1/N(a,\omega)$. The negative real axis of the Nyquist diagram coincides with the describing function of a pure relay. For purely linear systems the Nyquist criteria requires that the $G(j\omega)$ -locus does not enclose the -1 point for closed-loop stability. As far as nonlinear systems are concerned, the extended Nyquist criteria states that if the $-1/N(a,\omega)$ -locus lies inside the $G(j\omega)$ -locus (as the $G(j\omega)$ -locus is traversed in the direction of increasing frequency) then the closed-loop system is unstable. Conversely, if the $-1/N(a,\omega)$ -locus lies outside the $G(j\omega)$ -locus then the system is stable. The intersections of the $G(j\omega)$ plot with the critical locus determine the limit cycle amplitude and frequency.

For most processes, the output oscillation will approach a sinusoidal waveform while the input to the process (i.e. the output from a relay nonlinearity) will be a square wave (Figure 3.9). The reason for the sinusoidal appearance of the limit cycle response for a square wave input is that usually, the linear transfer function, $G(j\omega)$, acts as a low pass filter, reducing the higher harmonics and leaving the fundamental component as the preponderant contribution in the output signal. The dominance of the fundamental component in the output signal provides the basis of the describing function method. It should be noted that the process input and output are out of phase, owing to the lag introduced by the process. Also the oscillation amplitude is proportional to the amplitude of the nonlinearity. The values of the amplitude and frequency of the limit cycle indicated by the intersection of the $-1/N(a,\omega)$ -locus and the $G(j\omega)$ -locus are approximate values. Classically the describing function technique is applicable only to systems with a single nonlinear element where the output is periodic in

response to a sinusoidal input. Nonlinear systems are approximated to a linear part and a nonlinear part with the system-nonlinearity being combined with the nonlinear element (relay) before the describing function technique is applied.

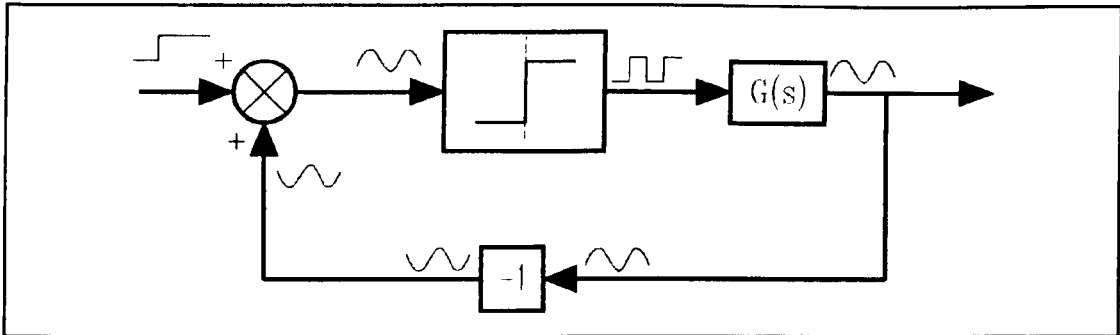


Figure 3.9 Generalized form of signals at each system component.

Assuming that the input, x , to the nonlinear element is sinusoidal

$$x = a \sin \omega t \quad (3.25)$$

then the output of the nonlinear element will be a nonsinusoidal periodic function which may be expressed in terms of a Fourier series as follows:

$$y = A_0 + \sum_{n=1}^{\infty} A_n \sin n \omega t + \sum_{n=1}^{\infty} B_n \cos n \omega t \quad (3.26)$$

It is important to note that in writing the above expression, it has been assumed that the nonlinearity does not generate subharmonics. Furthermore, if the nonlinearity is assumed to be symmetrical, the average value of y is zero, and the output is then given by

$$y = \sum_{n=1}^{\infty} (A_n \cos n \omega t + B_n \sin n \omega t) \quad (3.27)$$

In the absence of an external set point, that is $R(j\omega)=0$, the output of the nonlinearity is fed back to its input through the linear element $G(j\omega)$. If $G(j\omega)$ has low-pass characteristics¹, which is usually the case in control systems, it can be assumed that all the harmonics of y are filtered out in the feedback process (or have small amplitudes compared to the fundamental frequency amplitude) such that the input $x(t)$ to the nonlinear element N is mainly contributed by the

¹ Filtering characteristics of the linear part of a nonlinear system improve as the order of the system goes up.

fundamental component of y , $x(t)$ remains sinusoidal. Under such conditions the harmonic content of y may be disregarded² to give:

$$y_1 = A_1 \cos \omega t + B_1 \sin \omega t \quad (3.28)$$

or

$$y_1 = Y_1 \sin(\omega t + \phi_1) \quad (3.29)$$

where ϕ_1 is the phase shift of the fundamental harmonic component of the output with respect to the input; and the coefficients A_1 and B_1 of the Fourier series are given by

$$A_1 = \frac{1}{\pi} \int_0^{2\pi} y_1 \cos \omega t \, d(\omega t) \quad (3.30)$$

$$B_1 = \frac{1}{\pi} \int_0^{2\pi} y_1 \sin \omega t \, d(\omega t) \quad (3.31)$$

This procedure heuristically linearizes the nonlinearity, since for a sinusoidal input, only a sinusoidal output of the same frequency is now assumed to be produced. Under the above assumption, the nonlinearity can be replaced by a describing function $N(a, \omega)$ which is defined to be the complex valued ratio of the fundamental harmonic component of the output to the input [3.33]:

$$N(a, \omega) = \frac{Y_1}{a} \angle \phi_1 \quad (3.32)$$

where 'a' is the amplitude of the input sinusoid, Y_1 the amplitude of the fundamental harmonic component of the output:

$$Y_1 = \sqrt{A_1^2 + B_1^2} \quad (3.33)$$

and

$$\phi_1 = \tan^{-1} \left(\frac{B_1}{A_1} \right) \quad (3.34)$$

If the first harmonic is not dominant, then additional filtering of the signal will be necessary [3.34]. From Figure 3.8, it is observed that it is easier to handle a

² The effect of neglecting the harmonics has been studied by various authors [3.31 & 3.32].

nonlinear system when the nonlinearity is replaced by its describing function, since linear frequency domain techniques can now be applied. It is important to remember that this simplicity has been achieved at the cost of certain limitations, the foremost being the assumption that the linear element in the system has low-pass characteristics. Because of such limitations, the describing function method is primarily used for stability analysis and is not directly applied to controller design. Furthermore, although the describing function technique is a frequency domain approach, no general correlation is possible between time and frequency responses.

3.4.3. Stability Analysis using Describing Functions.

Consider a simple frequency-invariant describing function where the locus of $-1/N(a,\omega)$ is a curve in the complex plane as shown in Figure 3.10. Let the $G(j\omega)$ plot be superimposed on the $-1/N(a,\omega)$ locus, assuming that the system under investigation is open-loop stable.

The values of 'a' for which the $-1/N(a,\omega)$ -locus is enclosed by the $G(j\omega)$ -plot (i.e. the $-1/N(a,\omega)$ -locus lies in the region to the right of an observer traversing the $G(j\omega)$ -plot in the direction of increasing positive frequencies), correspond to unstable conditions. Similarly, the values of 'a' for which the $-1/N(a,\omega)$ -locus is not enclosed by the $G(j\omega)$ -plot (i.e. the $-1/N(a,\omega)$ -locus lies in the region to the left of an observer traversing the $G(j\omega)$ -plot in the direction of increasing positive frequencies), correspond to stable conditions. The $-1/N(a,\omega)$ -locus and $G(j\omega)$ -plot intersect at the point $(\omega=\omega_2, a=a_2)$ which corresponds to the condition of limit cycle (self-sustained oscillation). The system is unstable for $a < a_2$ and is stable for $a > a_2$.

The stability of the limit cycle can be judged by the perturbation technique. Suppose the system is originally operating at point A (Figure 3.10) under the state of a limit cycle. Assume that a slight perturbation is given to the system so that the input to the nonlinear element increases to a_3 , i.e. the operating point is shifted to B. Since B is in the range of stable operation, the amplitude of input to the nonlinear element progressively decreases and hence the operating point moves back towards A. Similarly, a perturbation which decreases the amplitude

of input to the nonlinearity shifts the operating point to C which lies in the range of unstable operation. The input amplitude now progressively increases and the operating point again returns to A. Therefore the system has a stable limit cycle at A.

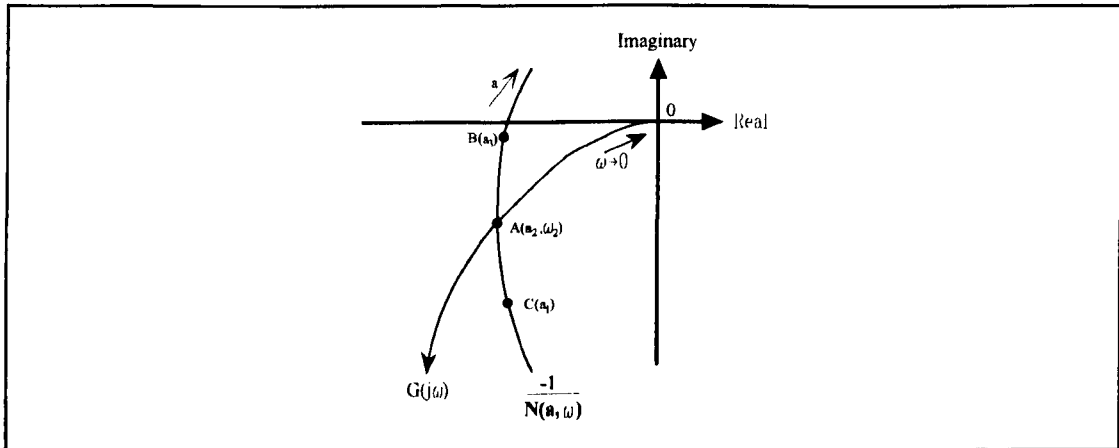


Figure 3.10 Prediction and stability of limit cycle.

For systems having frequency dependent describing functions³, the method of stability analysis is essentially the same except that $-1/N(a, \omega)$ has infinitely many loci with one for each value of ω . The limit cycles, if any, are determined by the intersections of $-1/N(a, \omega)$ -loci and $G(j\omega)$ -plot. Only such intersections qualify for a limit cycle for which the $1/N(a, \omega)$ -loci and $G(j\omega)$ -plot have a common value of ω . If an intersection point belongs to different values of ω for $G(j\omega)$ -plot and $1/N(a, \omega)$ -loci, it does not contribute a solution to equation (3.24) and hence does not determine a limit cycle. The criterion for stability is that the $-1/N(a)$ -locus is not enclosed by the $G(j\omega)$ -locus, thus there is no limit cycle at steady state. Although the describing function is useful in stability prediction it provides little information on the transient response of a system. When the nonlinearity is a nonlinear element with hysteresis, the oscillation at an intersection is stable if and only if the function $\angle G(j\omega)$ is decreasing at this point. For example, in the case shown in Figure 3.11, it is possible to get a stable oscillation with amplitude and frequency corresponding to either intersection 'a' or 'c', but not any corresponding to 'b'.

³ Frequency dependent describing functions occur for elements which are described by nonlinear differential equations.

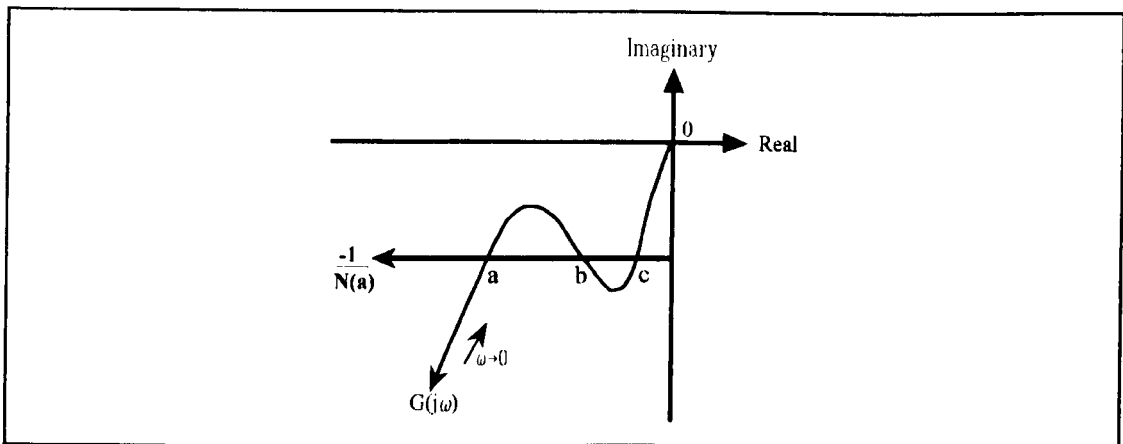


Figure 3.11 Example of a frequency response curve $G(j\omega)$ and the negative inverse describing function $-1/N(a,\omega)$.

3.5. DEVELOPMENT OF THE AUTOMATIC TUNER.

3.5.1. Choice of Nonlinear Element.

During the simulation studies several relay types were investigated within the automatic tuning procedure, with processes represented by various transfer functions (discussed in detail in Chapter 5). It is from these results that a relay with hysteresis was chosen for the tuning procedure, since it makes it possible to classify a wider range of processes than can be identified by an ordinary relay. Additionally, a relay with hysteresis is less susceptible to the influence of measurement noise (Figure 3.12). With even a small amount of noise an ideal nonlinearity would be switched 'on/off' continuously; however the introduction of hysteresis helps to reduce the switching effect the noise has on the nonlinearity. This is highlighted in Figure 3.13 where 'N' represents a random input signal, Y1 & Y2 illustrate the output from an ideal nonlinearity and a nonlinear element with hysteresis.

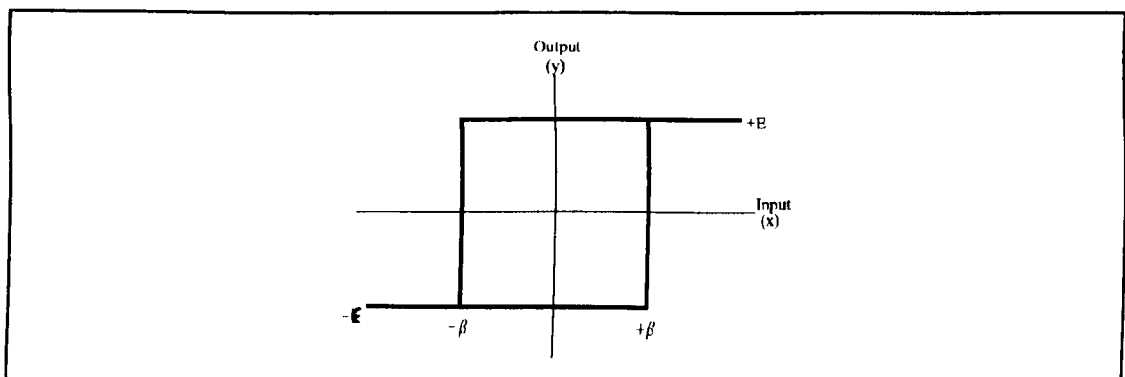


Figure 3.12 Nonlinear element with hysteresis.

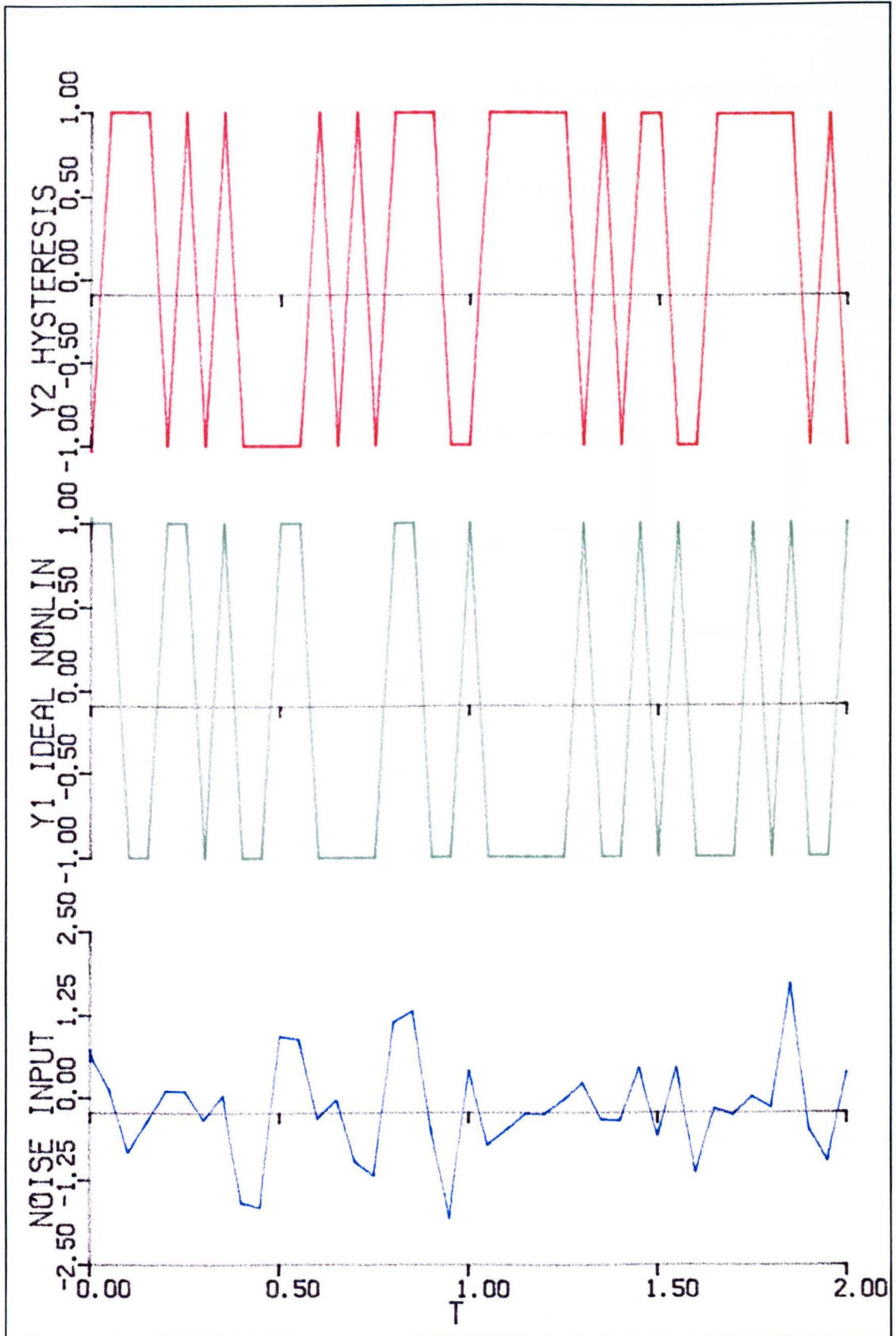


Figure 3.13 Comparison of nonlinearity outputs.

3.5.2. Analysis of the Describing Function of a Nonlinear Element with Hysteresis.

Consider the characteristics of a nonlinear element with hysteresis (Figure 3.14) with an input signal of

$$x = a \sin t \quad \text{for } t \in [0, T] \quad (3.35)$$

where T is the oscillation period.

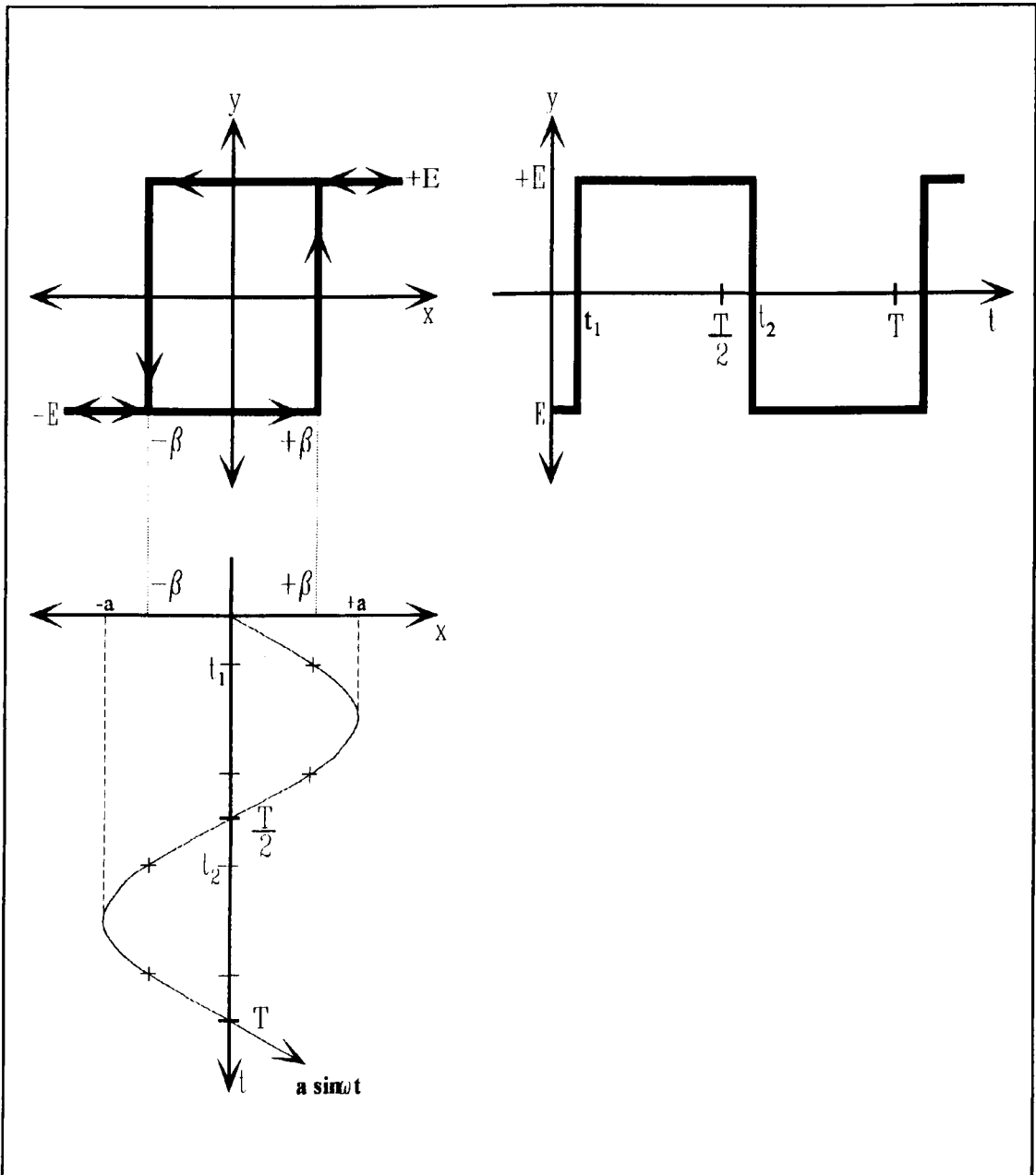


Figure 3.14 Input-output characteristics for a nonlinear element with hysteresis.

It can be seen that the switching points occur at

$$t_1 = \sin^{-1}\left(\frac{\beta}{a}\right) \quad \text{and} \quad t_2 = \sin^{-1}\left(\frac{-\beta}{a}\right) \quad (3.36)$$

where β is the hysteresis width. Making an equality between $t \in [0, T]$ and $u \in [0, 2\pi]$, then the output may be described by

$$\begin{aligned} y(u) = & -E \quad \text{for } 0 < u < \sin^{-1}\left(\frac{\beta}{a}\right) \\ & +E \quad \text{for } \sin^{-1}\left(\frac{\beta}{a}\right) < u < \sin^{-1}\left(\frac{-\beta}{a}\right) \\ & -E \quad \text{for } \sin^{-1}\left(\frac{-\beta}{a}\right) < u < 2\pi \end{aligned} \quad (3.37)$$

where

$$u = \frac{2\pi T}{t} \quad (3.38)$$

The Fourier series for the output signal, $y(u)$, is given by equation (3.28), where

$$A_1 = \frac{1}{\pi} \int_0^{2\pi} y(u) \cos u \, du \quad (3.39)$$

Hence

$$A_1 = \frac{-4E\beta}{\pi a} \quad (3.40)$$

The second coefficient, B_1 , can be found from

$$B_1 = \frac{1}{\pi} \int_0^{2\pi} y(u) \sin u \, du \quad (3.41)$$

$$\therefore B_1 = \frac{E}{\pi} \left[2 \cos \left[\sin^{-1} \left(\frac{\beta}{a} \right) \right] - 2 \cos \left[\sin^{-1} \left(\frac{-\beta}{a} \right) \right] \right] \quad (3.42)$$

But

$$\cos x = \sqrt{1 - \sin^2 x} \quad (3.43)$$

Hence

$$B_1 = \frac{4E}{\pi a} \sqrt{1 - \frac{\beta^2}{a^2}} \quad (3.44)$$

Thus the Fourier series is given by

$$y(\mu) = \frac{-4E\beta}{\pi a} \sin \mu + \frac{4E}{\pi a} \sqrt{1 - \frac{\beta^2}{a^2}} \cos \mu \quad (3.45)$$

and the describing function is given by

$$N(a, \omega) = \frac{4E}{\pi a} \left[-\beta + j \sqrt{1 - \frac{\beta^2}{a^2}} \right] \quad (3.46)$$

$$N(a, \omega) = \frac{4E}{\pi a} \angle -\sin^{-1} \left(\frac{\beta}{a} \right) \quad (3.47)$$

On a Nyquist diagram this represents a straight line parallel to the real axis in the complex plane. It is therefore possible to choose a point on the Nyquist curve and hence determine the values of E and β . A variety of nonlinearities are shown on page 65, whose describing functions can be derived in a similar manner, as shown in Table 3.5 [3.35].

Since the describing function for the nonlinear element with hysteresis, is independent of frequency, ω , then the describing function can be referred to simply as $N(a)$. It will also be seen that the phase shift, $\theta(a)$, is independent of frequency and decreases with amplitude. Since it is a memory type nonlinearity (that is, the output is dependent upon the history of input), $N(a)$ has both magnitude and phase.

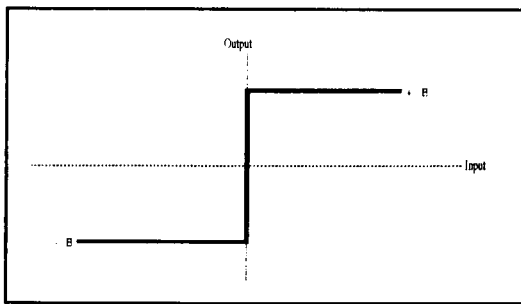


Figure 3.15 Ideal nonlinearity.

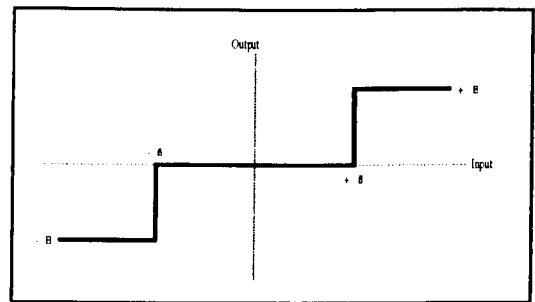


Figure 3.16 Nonlinearity with dead-band.

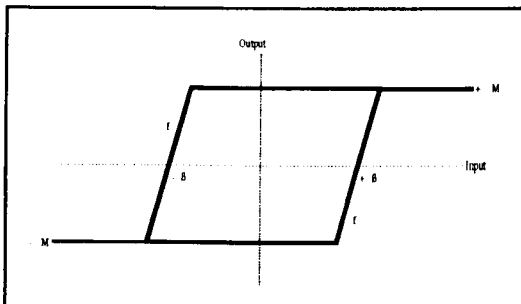


Figure 3.17 Saturation nonlinearity element with hysteresis.

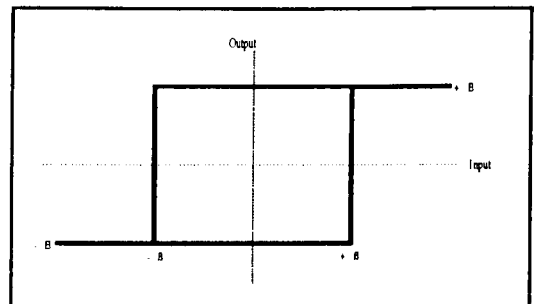


Figure 3.18 Nonlinear element with hysteresis.

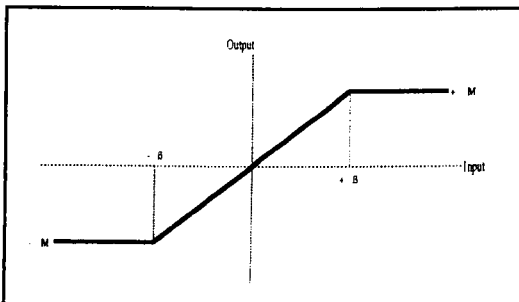


Figure 3.19 Saturation nonlinearity.

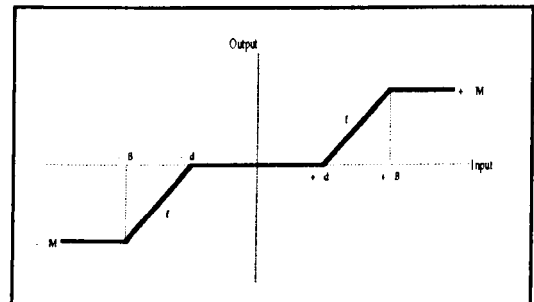


Figure 3.20 Saturation nonlinearity with dead-band.

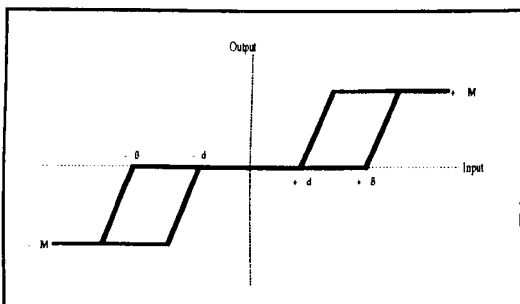


Figure 3.21 Saturation nonlinearity with dead-band and hysteresis.

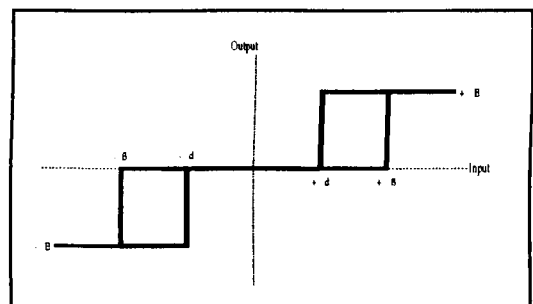


Figure 3.22 Nonlinearity with dead-band and hysteresis.

Table 3.5 Describing functions for various nonlinearities.

Nonlinearity Type	Real part of N(a)	Imaginary part of N(a)
Figure 3.17	$0 \text{ for } \frac{a}{\beta} \leq 1$ $\frac{K}{2} \left[1 - N_s \left(\frac{\frac{a}{\beta}}{2 - \frac{a}{\beta}} \right) \right] \text{ for } 1 < \frac{a}{\beta} \leq \frac{E}{\beta}$ $\frac{K}{2} \left[N_s \left(\frac{a}{E} \right) - N_s \left(\frac{\frac{a}{\beta}}{2 - \frac{E}{\beta}} \right) \right] \text{ for } A \geq E$	$0 \text{ for } A \leq \beta$ $\frac{4K\beta(\beta - A)}{\pi A^2} \text{ for } \beta \leq A \leq E$ $\frac{4K\beta(\beta - E)}{\pi A^2} \text{ for } A \geq E$
Figure 3.18	$0 \text{ for } a \leq \beta$ $\frac{4E}{\pi a} \sqrt{1 - \left(\frac{\beta}{a} \right)^2} \text{ for } a > \beta$	$0 \text{ for } a < \beta$ $\frac{-4\beta E}{\pi a^2} \text{ for } a > \beta$
Figure 3.19	$E \text{ for } \frac{a}{\beta} \leq 1$ $EN_s \left(\frac{a}{\beta} \right) \text{ for } \frac{a}{\beta} \geq 1$	0 0
Figure 3.20	$0 \text{ for } \frac{a}{\beta} \leq 1$ $K \left[1 - N_s \left(\frac{a}{\beta} \right) \right] \text{ for } \frac{a}{\beta} \geq 1$	0 0

3.5.3. Analysis of a System Containing a Nonlinear Element with Hysteresis.

Consider a third order transfer function, shown in Figure 3.23, given by

$$G(s) = \frac{10}{(1+s)(1+\frac{s}{4})(1+\frac{s}{8})} \quad (3.48)$$

If the input is not zero, that is $R(s) \neq 0$, then a d.c. or bias signal may exist at the input to the nonlinearity, since $G(s)$ in this example has a finite gain of 10 at zero frequency.

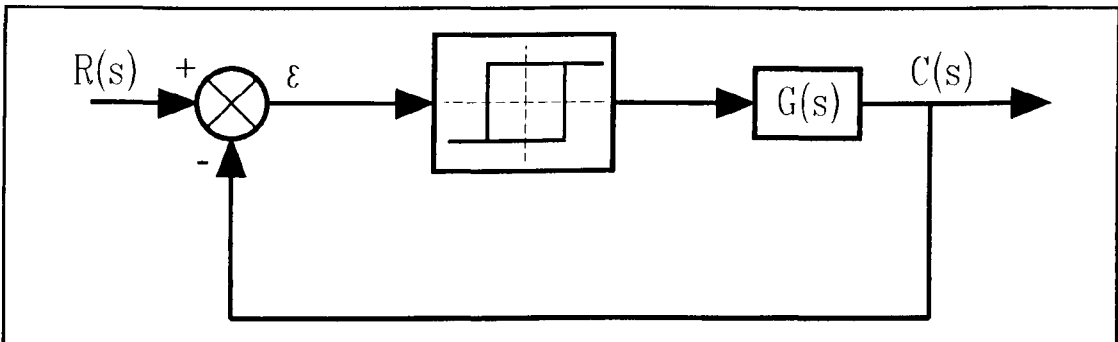


Figure 3.23 Block diagram for process of section 3.5.3.

The describing function, $N(a)$, for a nonlinear element with hysteresis with zero bias is given by

$$N(a) = \left(\frac{4E}{a\pi}\right) e^{-j\theta} \quad \text{for } a > \beta \quad (3.49)$$

where $\theta = \sin^{-1}(\beta/a)$. This gives

$$\frac{-1}{N(a)} = \frac{-a\pi}{4E} e^{j\theta} = \frac{-a\pi}{4E} (\cos\theta + j\sin\theta) = \frac{-\pi}{4E} \sqrt{(a^2 - \beta^2)} - j\frac{\pi\beta}{4E} \quad (3.50)$$

The imaginary part of $-1/N(a)$ is independent of the nonlinearity amplitude, a , so that the locus is a straight line parallel to the real axis of the Nyquist diagram. The assumed loci of $G(j\omega)$ and $-1/N(a)$ are sketched in Figure 3.24, and intersect at a single point. The solution is a stable oscillation as the $G(j\omega)$ locus is crossed by the describing function for increasing amplitude.

In this particular case, since the $-1/N(a)$ locus is a straight line, an exact solution for the values of 'a' and ' ω ' at the point of intersection is easily calculated for a chosen β/E ratio.

$$G(s) = \frac{10}{(1+s)(1+\frac{s}{4})(1+\frac{s}{8})} = \frac{320}{(s+1)(s+4)(s+8)} \quad (3.51)$$

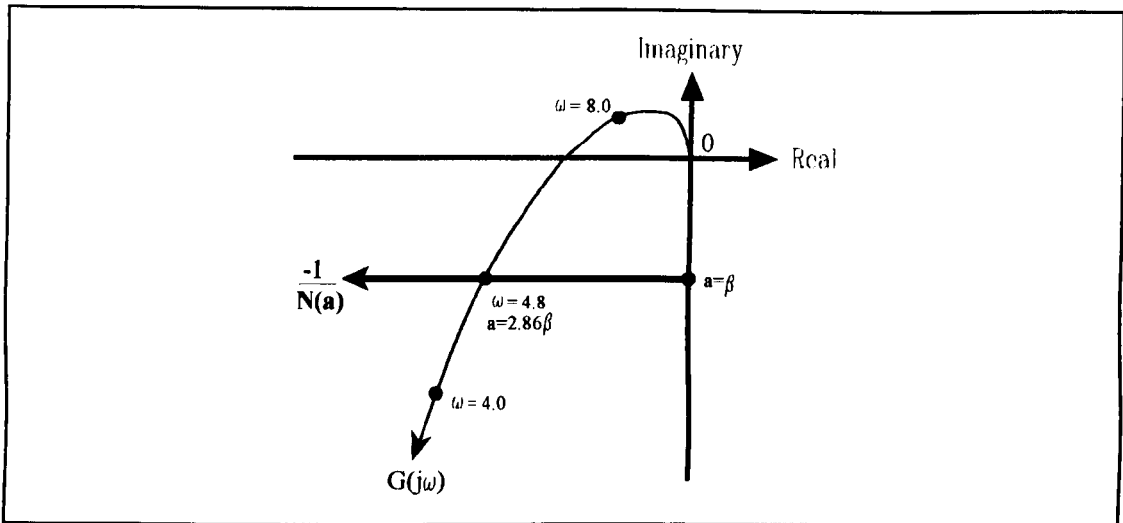


Figure 3.24 Nyquist diagram for equation (3.48) and the describing function.

substituting $s=j\omega$ produces

$$G(j\omega) = \frac{320(32 - 13\omega^2 - j\omega(44 - \omega^2))}{(1 + \omega^2)(16 + \omega^2)(64 + \omega^2)} \quad (3.52)$$

The loci intersect where the imaginary parts of $G(j\omega)$ and $N(a)$ are equal, that is

$$\text{Im} |G(j\omega)| = \frac{\pi \beta}{4E} \quad (3.53)$$

Taking $\beta/E=0.5$, for example, gives

$$\frac{320\omega(44 - \omega^2)}{(1 + \omega^2)(16 + \omega^2)(64 + \omega^2)} = \frac{\pi}{8} \quad (3.54)$$

The solution to equation (3.54) has only one real value, thus $\omega=4.8$ rads/sec. The oscillation amplitude, a , at the input to the nonlinearity is given by equating the real parts of $G(j\omega)$ and $N(a)$:

$$\frac{\pi(a^2 - \beta^2)^{\frac{1}{2}}}{4E} = \frac{320(13\omega^2 - 32)}{(1 + \omega^2)(16 + \omega^2)(64 + \omega^2)} \quad (3.55)$$

with $\omega=4.8$, then

$$a = 1.43E \text{ or } 2.86\beta \quad (3.56)$$

Thus the oscillation amplitude is dependent upon the characteristics of the nonlinear element with hysteresis.

3.6. IMPLEMENTATION OF THE AUTOMATIC TUNING PROCEDURE.

The theory described previously can be applied to the on-line tuning of a three term controller, designed to meet some specification such as a phase margin. The inclusion of the nonlinearity within the feedback path induced an oscillatory response on the process output, this oscillation has to be monitored to determine the frequency and amplitude of the oscillation.

If 'E' is the amplitude of the nonlinearity output and 'a' the corresponding amplitude of the first harmonic of the process variable output, then a Fourier series expansion gives the process output amplitude [3.36]

$$a = \frac{4E}{\pi} \quad (3.57)$$

with a limit cycle frequency of

$$\omega_c = \frac{2\pi}{t_c} \quad (3.58)$$

while the following condition is obtained for the feedback loop

$$G\left(j\frac{2\pi}{t_c}\right) = -\frac{\pi a}{4E} \quad (3.59)$$

This result may also be found from the describing function approximation which describes the nonlinearity as

$$N(a) = -\frac{4E}{\pi a} \quad (3.60)$$

The above expressions are only approximations to the describing function of the nonlinear element, however exact conditions have been derived by Hamel [3.37] and Tsypkin [3.38]. It is relatively easy to control the oscillation amplitude of the system output, because it depends directly on the nonlinearity output amplitude, $\pm E$; thus the procedure is easy to automate. It should be noted that the technique automatically generates a process input signal with a significant frequency component at ω_c ; this ensures that the critical point may be determined accurately. It should be remembered that the values of oscillation period and amplitude are only as accurate as the algorithm used to calculate them.

3.6.1. Estimation of Process Response Amplitude and Frequency.

An essential part of the estimation of the process transfer function is the determination of the frequency and the amplitude of the output. This is a familiar problem, with several well known solutions. The choice of identification method is a weighting between the demand for a simple algorithm which requires a small amount of computer memory, and the need for a fast and precise algorithm.

3.6.1.a. Amplitude Estimation.

The simplest way to estimate the amplitude of a sinusoidal function, varying about a mean value, is to compare all the measured values and allow the one with the greatest magnitude to determine the peak, while the lowest magnitude identifies a trough. The difference between the maximum and minimum thus determines twice the amplitude. This estimation method is very easy to implement because it is based on counting and comparison only. However, this method is sensitive to noise disturbance and does not use the information provided by all the measurements except the ones with the greatest and smallest magnitudes. If the algorithm is required for a computer with limited memory available, it may be a good practical choice.

An alternative solution is provided by using recursive least squares identification, where the function

$$\sum (y(t) - A_s \sin \omega t - A_c \cos \omega t)^2 \quad (3.61)$$

is minimised with respect to A_s and A_c . The amplitude is then determined from

$$a = \sqrt{A_s^2 + A_c^2} \quad (3.62)$$

The procedure requires an estimate of the oscillation frequency, ω , the frequency estimation routine must operate for a short time before the initiation of the amplitude estimation procedure. The estimate of 'a' will oscillate with frequency ω but should have a correct value when $\omega t = n\pi$, $n=1,2,\dots$, [3.34]. Since all the measurements are used to estimate the amplitude, the method is less sensitive to disturbances than the peak detection method. On the other hand, it requires more computer memory. Another difference between the two amplitude

estimation methods is that the first estimates the true amplitude of the output, while the second estimates the amplitude of the fundamental component. If the process $G(j\omega)$ is an ideal low-pass filter, there will be no difference. However, since in practice the higher frequencies form a disturbance on the amplitude then a difference will exist between the two estimation methods.

3.6.1.b. Frequency Estimation.

The simplest method of frequency estimation, if the output has a zero mean value, is the zero crossing method, whereby the time between each zero crossings of the output provides an approximation of the oscillation period, and thus of the frequency. The method is simple to implement and therefore favourable in small computers. The method can be enhanced by the additional use of peaks and troughs. If the output has a d.c. bias, that is a non-zero mean, then the mean value must also be determined.

The oscillation period may also be estimated based on the observation that a sinusoidal signal with period T satisfies the linear difference equation

$$y(t) - \theta y(t-\tau) + y(t-2\tau) = 0 \quad (3.63)$$

where τ is the sampling period, y is the signal amplitude and θ is given by

$$\theta = 2 \cos\left(\frac{2\pi\tau}{T}\right) \quad (3.64)$$

The period can be obtained by estimating the variable θ in equation (3.64) by least squares and computing an estimate of T from

$$\hat{T} = \frac{2\pi\tau}{\cos^{-1}\left(\frac{\theta}{2}\right)} \quad (3.65)$$

The signal may have a non-zero mean, hence it should be high-pass filtered prior to estimation. Alternatively θ_1 and θ_2 could be estimated from the model

$$y(t) - \theta_1 y(t-\tau) + y(t-2\tau) + \theta_2 = 0 \quad (3.66)$$

Once the period T has been found, then the amplitude can be obtained from solving the least squares

$$\sum_{k=1}^N [y(k\tau) - \theta_1 \sin \omega k\tau - \theta_2 \cos \omega k\tau - \theta_3]^2 \quad (3.67)$$

where

$$\omega = \frac{2\pi}{T} \quad (3.68)$$

while the estimate of the amplitude is given by

$$a = \sqrt{\theta_1^2 + \theta_2^2} \quad (3.69)$$

It is also possible to estimate the frequency using recursive least squares identification. Here the function

$$\sum (y(t) - 2\cos(\hat{\omega}\tau)y(t-\tau) + y(t-2\tau))^2 \quad (3.70)$$

is minimized with respect to $\hat{\omega}$, where τ is the sampling period and $\hat{\omega}$ is the estimate of the frequency ω . This method is superior to the first, if the identification time is short. As time increases, it is dependent on the type of noise which method is the best. A number of frequency estimation methods are compared by Lindgren in [3.39]. The estimation of the oscillation period can be problematic in the presence of noise. However averaging over several periods of oscillation can make the estimation procedure less sensitive to noise disturbance, but is slower to implement.

3.6.1.c. Practical Implementation.

For a process which has a nonsymmetrical oscillation waveform (Figure 3.25), such as the one for dissolved oxygen concentration in a Bakers' Yeast fermentation, the estimation of the amplitude and oscillation period is difficult, and can be compounded by the addition of measurement noise. The methods chosen should also require the minimum amount of computer memory, and should execute in the shortest time. For these reasons the methods chosen for this work were the minimum-maximum and zero-crossing methods previously described.

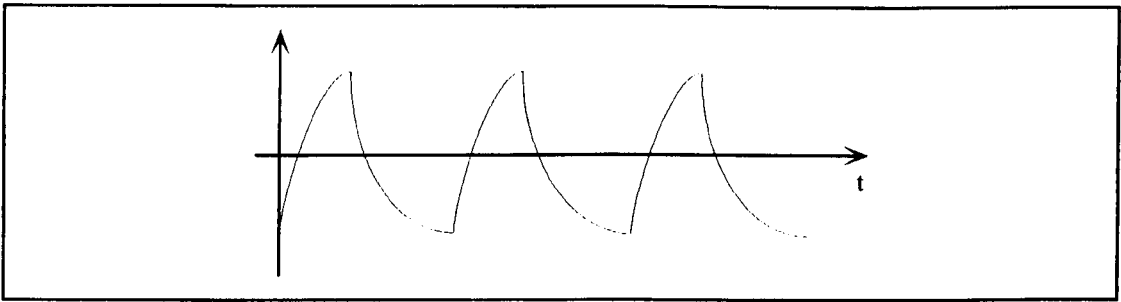


Figure 3.25 Nonsymmetrical oscillation waveform.

3.7. TUNING RULES.

In the development and implementation of the automatic tuner, a nonlinear element is introduced to the control loop to make the system oscillate. By estimating the amplitude and frequency of the oscillation it is possible to determine certain process properties. From these characteristics it is possible to calculate a set of PID tuning parameters to meet a desired phase margin design criteria. Once the tuning phase is complete, the proportional gain is reintroduced to the system where the gain from the automatic tuner, K_A , is given by

$$K_A = \frac{4E}{\pi a} \quad (3.71)$$

where E is the nonlinearity amplitude and ' a ' is the amplitude of the process oscillation. This value of gain is the critical gain of the process under the restrictions imposed by the nonlinearity. Thus the Ziegler-Nichols gain, K_z , is equivalent to the automatic tuner gain

$$K_A = K_z$$

Equating K_A and the Ziegler-Nichols tuning equations gives:

For P control only

$$\frac{2E}{\pi a} \quad (3.72)$$

For P+I control only

$$\frac{4E}{2.2\pi a} \quad (3.73)$$

For P+I+D control

$$\frac{4E}{1.7\pi a} \quad (3.74)$$

The integral action is also introduced to the process as

$$T_i = \frac{T}{2\pi\nu} \quad (3.75)$$

where T is the final estimated oscillation period, and the constant, ν , is usually chosen between 0.1 and 0.2 [3.40]. Before introducing the integral action, the system will have a specific phase margin, ϕ , while the design objective is to achieve a specified phase margin of ϕ_m . When the integral part is reintroduced into the controller, the phase margin will decrease by an amount ϕ_i . From (3.75) it is concluded that

$$\phi_i = 90^\circ - \arctan\left(\frac{2\pi T_i}{T}\right) = \arctan(\nu) \quad (3.76)$$

Thus ν is used for phase margin correction. The tuning rule therefore requires the adjustment of the controller gain, K_p , such that the phase margin for $K_p G(j\omega)$ becomes $(\phi_m + \phi_i)$, and then the integral term is introduced. If K_p is chosen in this way, and T_i given by (3.75) is introduced afterwards, the system will obtain the desired phase margin ϕ_m .

The inclusion of derivative action follows a similar principle to the Ziegler-Nichols rules, that is

$$T_d = 0.125 T_n = \frac{T}{2.6\pi} \quad (3.77)$$

The tuning rules for P, P+I and P+I+D controllers can be summarized as shown in Table 3.6.

Table 3.6 Automatic Tuner Parameter Settings.

Controller Configuration	K_p	T_i	T_d
P	$2E/\pi A$	∞	0
P+I	$4E/2.2\pi A$	$T/2\nu\pi$	0
P+I+D	$4E/1.7\pi A$	$T/6.3\nu\pi$	$T/2.6\pi$

The system will oscillate during the tuning phase, where practical considerations of the particular process being controlled dictate the amplitude that can be

tolerated during the tuning phase. It is possible to influence the amplitude, by specifying a maximum amplitude A^* , which is the amplitude corresponding to the correct gain K . If noise is present, a large A^* will improve the tuning procedure, since the signal to noise ratio then becomes large. The adjustment of the gain K_p will be deduced from the amplitude estimates. When both the characteristics and the position of the nonlinear element with hysteresis are determined, the tuning procedure can be initiated. As mentioned previously, the goal is to adjust the gain, K , so that the $KG(j\omega)$ curve goes through the point 'P' as in Figure 3.28. One useful method is to use the two latest measurements of $KG(j\omega)$, and approximate the $KG(j\omega)$ curve by a straight line going through these points. The new value of K can then be chosen by the Regula-Falsi method, so that the new gain is given by

$$K_{n+1} = K_n - (A_n - A^*) \frac{K_n - K_{n-1}}{A_n - A_{n-1}} \quad (3.78)$$

Here A_n and A_{n-1} are the two latest estimated amplitudes of the output signal, y .

The output from the nonlinear element with hysteresis is a square wave. The describing function technique requires that no zero-order harmonic is present; that is, the time when the output is at $+E$ is as long as the time it is $-E$. Real processes, however, normally operate around some d.c. level, which has to be considered during the tuning phase. Let u_{ref} denote the input to the process $G(j\omega)$ which gives the desired output y_{ref} . Then the output will be free from the zero-order harmonic only if the nonlinear element with hysteresis is specified as in Figure 3.26. The reference control signal u_{ref} must be estimated before the adjustment of the gain, K_p , starts. This can be achieved, for example, by measuring the times T_+ and T_- , defined in Figure 3.27, for the output from the nonlinearity.

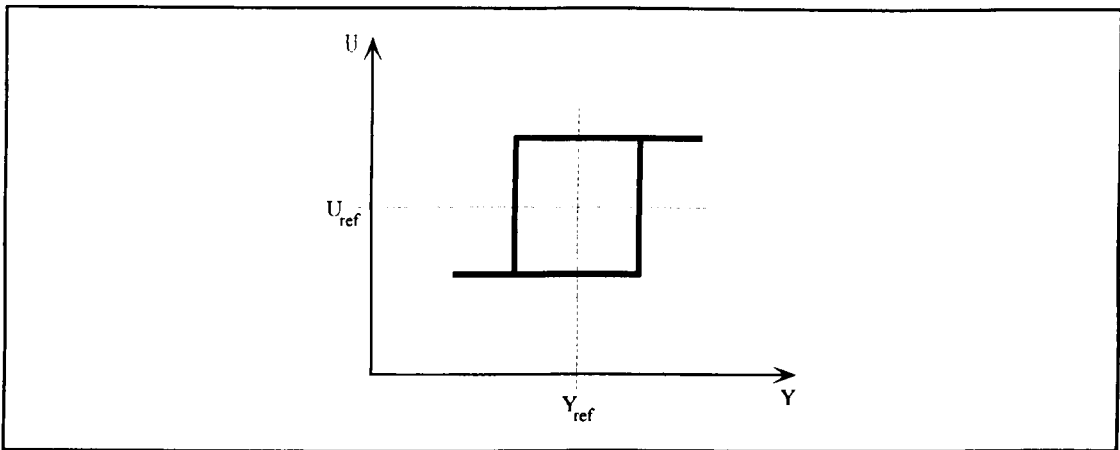


Figure 3.26 Correct position of the nonlinear element with hysteresis.

Introducing $P(t)$ as

$$P(t) = \frac{T_-(t)}{T_+(t)} \tag{3.79}$$

u_{ref} can now be estimated using the Regula-Falsi method

$$u_{ref}(t+1) = u_{ref}(t) - (P(t) - 1) \frac{u_{ref}(t) - u_{ref}(t-1)}{P(t) - P(t-1)} \tag{3.80}$$

When the controller gain, K_p , is introduced in the loop, then u_{ref} must be changed to u_{ref}/K_p .

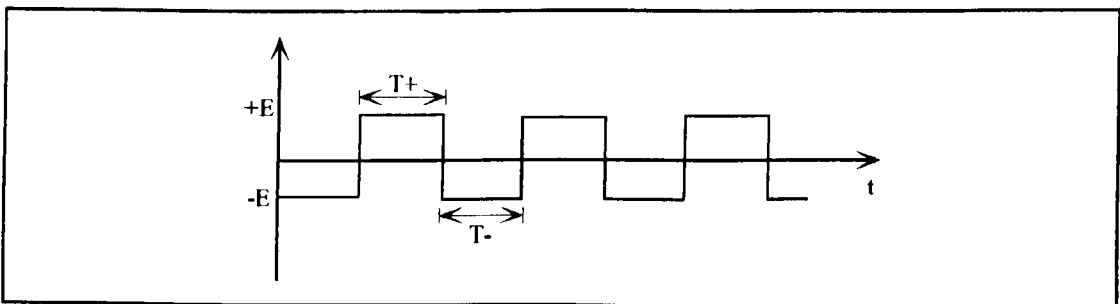


Figure 3.27 Output from the nonlinear element with hysteresis.

3.7.1. Using the Nonlinear Element with Hysteresis.

The gain, K , is to be adjusted so that the $KG(j\omega)$ curve goes through the point 'P' in Figure 3.28. To make it possible to decide when this point is reached, the $-1/N(a)$ curve must also go through this point.

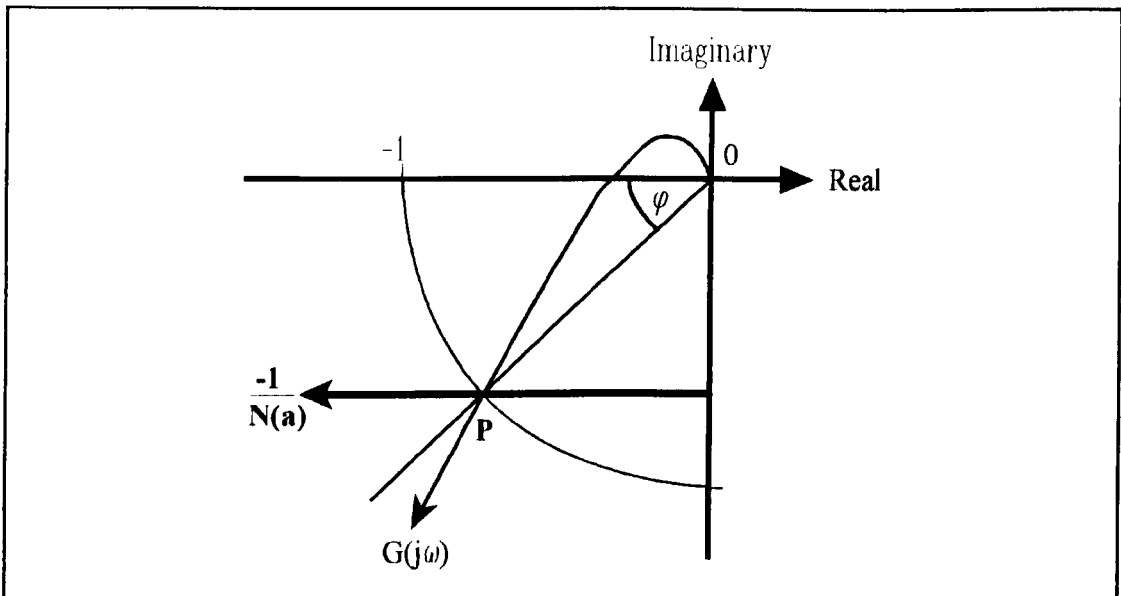


Figure 3.28 Location of the $-1/N(a)$ and $G(j\omega)$ -loci.

Suppose, that the desired amplitude of the output signal at point 'P' is A^* , then

$$\frac{-1}{N(A^*)} = \frac{-\pi A^*}{4E} = -1 \quad (3.81)$$

Hence

$$E = \frac{\pi A^*}{4} \quad (3.82)$$

and β is determined from

$$\phi_m + \phi_i = \arcsin\left(\frac{\beta}{A^*}\right) \quad (3.83)$$

Therefore

$$\beta = A^* \sin(\phi_m + \phi_i) \quad (3.84)$$

The characteristics of the nonlinear element with hysteresis are thus given by the desired phase margin, the relation between T_1 and τ and by the desired amplitude of the output signal.

3.7.1.a. Criteria for Ending the Tuning Phase.

Once the oscillation amplitude is approximately equal to the maximum amplitude, A^* , then the tuning procedure is stopped and the nonlinear element removed. In the practical implementation, the tuning procedure may also be

designed such that the detection of three consecutive amplitudes, which are approximately equal, will stop the procedure. The complete tuning rule can be summarized by the following scheme:

1. Calculate E and β from equation (3.82) and (3.83)
2. Insert the nonlinear element with hysteresis and remove the PID controller.
3. Let (3.80) be performed until an acceptable estimate of u_{ref} is obtained.
4. Measure the output during an oscillation period, and estimate the frequency and the amplitude of the oscillation.
5. If measured amplitude is close to the maximum amplitude, A' , do step 7.
6. Adjust the gain K according to (3.78). Change the reference control signal to u_{ref}/K , and go to step 4.
7. Calculate the tuning parameters according to the equations in Table 3.8.
8. Pass the tuning parameters to the PID controller.
9. Remove the nonlinear element with hysteresis.
10. Place the process under PID control.

3.8. DISCUSSION.

The stability of the nonlinear system can be investigated using any of the conventional linear techniques with the nonlinearity replaced by an amplitude dependent gain, known as its describing function $N(a, \omega)$. These methods include the use of the Routh criterion, Nyquist diagrams, Nichols chart and several others. When the frequency response locus, $G(j\omega)$, and the negative reciprocal of the describing function, $-1/N(a)$, are plotted on a Nyquist diagram any intersection will be a solution of equation (3.24). The amplitude of the oscillation 'a' and its frequency ' ω ' can then be read from the $-1/N(a)$ and $G(j\omega)$ loci as shown in Figure 3.10. The oscillation may be stable or unstable as noted for limit cycles of second order systems, where in this context quasi-stable cases are classified as unstable. If no intersection of the loci $G(j\omega)$ and the $-1/N(a)$ exists, the stability of the system is assessed using the normal Nyquist criterion with respect to any point on the $-1/N(a)$ locus rather than the point $(-1, 0)$. It should however be remembered that the describing function method is an approximate technique and a 'near miss' of the $-1/N(a)$ and $G(j\omega)$ loci may in fact be a 'hit' as far as the actual system is concerned.

The basic principle behind the automatic tuning procedure is that many processes will exhibit limit cycle behaviour if a nonlinearity is placed in the feedback loop [3.41, 3.42 & 3.43]. From these limit cycles it is possible to determine properties of the controlled process which can then be used to develop a set of tuning parameters to meet some design criteria, such as a specified phase margin. The nonlinearity method is based on the observation that a system with a phase lag of at least π , will normally oscillate with a frequency of ω_s when placed under the control of a nonlinear element.

It should be pointed out that an absolute set of tuning parameters for a general optimum process performance does not exist. For a given process and controller, the transient response of the system will depend upon the type of disturbance experienced by the system. Even a load disturbance will produce different responses depending upon whether the disturbance is in the supply or demand. Finally, the duration (momentary or sustained) of the disturbance will produce varying results. Various criteria have been proposed in an attempt to define the optimum response curve; however, no one criteria is universally accepted.

It is known that adaptive controllers which use parametric models, such as model algorithmic control (MAC), can provide results with large errors if the model order does not agree with the plant order [3.44 & 3.45]. For industrial applications, perturbations affect the plant model structure more often than the measurable variables, that is a change in model order is more likely than an alteration of the gain. One of the widely used adaptive control methods relies on the explicit identification of process parameters and the estimation of the corresponding state variables. The information gathered is then used in the determination of a feedback signal which achieves some design criteria. However a drawback in the method can occur if the model size has to be reduced, owing to computer memory restrictions.

The automatic tuning procedure does not operate continuously, as do other self-tuning controllers. Instead it is executed either when requested by an operator, or on a periodic time base. This can be a drawback if something suddenly happens to the process. However process operators often prefer to

have the decision to retune or not. A partial solution to this is to have the automatic tuning procedure activated when a sustained and significant deviation is detected in the controlled variable. A drawback of this is the precise definition of the initiation conditions. The advantage of an automated-tuning controller, such as this proposed automatic tuning procedure, is that it permits an inexperienced operator to retune a process.

3.9. REFERENCES.

- 3.1. Atherton, D. Nonlinear control engineering. Von-Nostrand Reinhold. 1975.
- 3.2. Åström, K.J. Adaption, Auto-Tuning and Smart Controls. International symposium advanced process supervision and real-time knowledge based control. p. 1276-1281. November, 1988.
- 3.3. Åström, K.J. and B. Wittenmark. Self-Tuning controllers based on pole-zero placement. IEE Proceedings. Vol. 127(D), No.3. p.120-130. 1980.
- 3.4. Hagglund, T. and K.J. Åström. Automatic Tuning of PID Controllers Based on Dominant Pole Design. IFAC Adaptive Control of Chemical Processes. p. 205-210. 1985.
- 3.5. Wittenmark, B., P. Hagander and I. Gustavsson. STUPID - Implementation of a self-tuning PID controller. Department of Automatic Control, Lund Institute of Technology, Lund, Sweden. Report CODEN: LUFTD2/(TFRT-7201)/(1980). 1980.
- 3.6. Kuo, C.C., A.B. Corripio and C.L. Smith. Digital control algorithms. Control systems. October. 1973.
- 3.7. MacGregor, J.F., J.D. Wright and H.N. Hong. Optimal tuning of digital PID controller using dynamic-stochastic methods. IEC Process Des Dev. Vol. 14. p. 4. 1975.
- 3.8. Åström K.J. and T. Hagglund. Automatic tuning of simple regulators for phase and amplitude margin specifications. IFAC workshop on Adaptive Systems in control and signal processing. San Francisco, USA. p. 271-276. 1983.
- 3.9. Åström, K.J. and T. Hagglund. Automatic Tuning of PID Controllers. Instrument Society of America. Research Triangle Park, NC, USA. 1988.

- 3.10. Åström, K.J. and T. Hagglund. Automatic Tuning of Simple Regulators. Proceedings IFAC 9th World Congress. p. 1867-1872. 1984.
- 3.11. Åström, K.J. More STUPID. Department of Automatic Control, Lund Institute of Technology, Lund, Sweden. Report CODEN: LUFTD2/(TFRT-7214)/1-005/(1981). 1981.
- 3.12. Hang, C.C. and K.J. Åström. Practical Aspects of PID Auto-Tuning Based on Relay Feedback. Proceedings IFAC Symposium on Adaptive Control of Chemical Processes. Copenhagen, Denmark. p. 153-158. 1988.
- 3.13. Hagglund, T. and K.J. Åström. Method and an Approach in Tuning a PID Regulator. United States Patent No. 4549123. 1985.
- 3.14. Åström, K.J. Theory and Applications of Adaptive Control. IFAC World Congress, Kyoto, Japan. Invited Plenary Lecture. p. 727-748. 1981.
- 3.15. Schuck, O.H. Honeywell's history and philosophy in the adaptive control field. Technical Report, Wright Air Development Centre, Wright-Patterson Air Force Base, Ohio, U.S.A. January, 1959.
- 3.16. Ogata, K. Modern control engineering. Prentice-Hall International. 1990.
- 3.17. Giusti, A.L., R.E. Otta and T.J. Williams. Direct digital computer control. Control Engineering. June. 1962.
- 3.18. Skaggs, W.L. Practical aspects and results of DDC. Paper presented at the workshop on 'The use of digital computers in Process Control', Louisiana State University. March, 1966.
- 3.19. Ziegler, J.G. and N.B. Nichols. Optimum settings for automatic controllers. Transactions of the American Society of Mechanical Engineers. November. p. 759-767. 1942.
- 3.20. Ziegler, J.G. and N.B. Nichols. Process lags in automatic-control circuits. Transactions of the American Society of Mechanical Engineers. July. p. 433-444. 1943.
- 3.21. Cohen, G.H. and G.A. Coon. Theoretical investigations of retarded control. Transactions of the American Society of Mechanical Engineers. Vol. 75. p. 827. 1953.
- 3.22. Aikman, A.R. The frequency response approach to automatic control problems. Transactions of Instrument Technology. Vol. 3. p. 2-16. 1951.

- 3.23. Åström, K.J. Ziegler-Nichols Auto Tuners. Department of Automatic Control, Lund Institute of Technology, Lund, Sweden. Report CODEN: LUTDF2/(TFRT-3067)/0-025/1982. 1982.
- 3.24. Golte, J. and A. Vermer. Control systems design and simulation. McGraw-Hill. 1991.
- 3.25. Nagrath, I.J. and M. Gopal. Control systems engineering. John Wiley & Sons, Eastern Limited. India. 1975.
- 3.26. Miller, R.K. and A.N. Michel. On limit cycles of feedback systems which contain a hysteresis nonlinearity. Proceedings of the 23rd IEEE Conference on decision and control. Las Vegas, USA. Vol. 3. p. 1306-1311. 1984.
- 3.27. Gelb, A. and W.E. van de Velde. Multiple input describing functions and nonlinear system design. McGraw Hill. 1968.
- 3.28. Grensted, P.E.W. Frequency response methods applied to nonlinear systems. Process Control Engineering. Vol. 1, p. 105-139. 1962.
- 3.29. Hsu, J.C. and A.U. Meyer. Modern control principles and applications. McGraw Hill. 1968.
- 3.30. Mees A.I. The describing function matrix. Journal of the Institute Of Mathematics and its Applications. Vol. 10, p. 49-67. 1972.
- 3.31. Bergen A.R. and R.L. Franks. Justification of the describing function method. SIAM Journal of control. Vol. 9, p. 568-589. 1971.
- 3.32. Kudremicz, J. Theorems on the existence of periodic vibrations. Proc IFAC. Warsaw. section 4, 1, p. 46-60. 1969.
- 3.33. Graham, D. and D. McRuer. Spectral moment oscillation by means of level crossings. Biometrika. Vol. 61. p. 401-418. 1961.
- 3.34. Åström, K.J. Lectures on System Identification. Chapter 3: Frequency Response Analysis. Department of Automatic Control, Lund Institute of Technology, Lund, Sweden. Report CODEN: LUTFD2/(TFRT-7504)/0-095/(1975). 1975.
- 3.35. Mohler, R.R. Nonlinear systems: Volume 1 - Dynamics and control. Prentice-Hall, USA. 1991.
- 3.36. Åström, K.J. and T. Hagglund. A frequency domain method for automatic tuning of simple feedback loops. Proceedings 23rd IEEE Conference on Decision and Control. Las Vegas, USA. p. 299-304. 1984.

- 3.37. Hamel, B. Contribution à l'étude mathématique des systèmes de réglage par tout-ou-rien. C.E.M.V. Service Technique Aéronautique. Vol. 17. 1949.
- 3.38. Tsytkin, J.A. Theorie des relais systeme der automatischen regelung. R. Oldenburg, Munich. 1958.
- 3.39. Lindgren, G. Spectral moment estimation by means of level crossings. Biometrika. Vol. 61. p. 401-418. 1974.
- 3.40. Åström, K.J. and T. Hagglund. Automatic tuning of simple regulators with specifications on phase and amplitude margins. Automatica. Vol.20, No.5. p. 645-651. 1984.
- 3.41. Hagglund, T. A PID Tuner Based on Phase Margin Specification. Department of Automatic Control, Lund Institute of Technology, Lund, Sweden. Report CODEN: LUFTD2/(TFRT-7224)/0-020/(1981). 1981.
- 3.42. Hang, C.C. and K.J. Åström. Refinements of the Ziegler-Nichols Tuning Formula for PID Auto-Tuners. Instrument Society of America. Paper No. 88-1542. p. 1021-1030. 1988.
- 3.43. Åström, K.J. Ziegler-Nichols Auto-Tuners. Department of Automatic Control, Lund Institute of Technology, Lund, Sweden. Report CODEN: LUFTD2/(TFRT-3176)/1-025/(1982). 1982.
- 3.44. Rouhani, R. and R.K. Mehra. Model algorithmic control (MAC): Basic theoretical properties. Automatica. Vol. 8, No. 4. p. 401-414. 1982.
- 3.45. Åström, K.J. Interactions Between Excitation and Unmodeled Dynamics in Adaptive Control. Proceedings 23rd IEEE Conference on Decision and Control. Las Vegas, USA. p. 1276-1281. December, 1984.

CHAPTER 4.

MATHEMATICAL MODELS OF FERMENTATION PROCESSES.

4.1. INTRODUCTION.

The two mathematical models, used for simulation work, representing a fed-batch fermentation of Bakers' Yeast (Model I) and a batch Bakers' Yeast fermentation with ethanol production (Model II) are presented in this chapter. Each model will be discussed in detail and, for the equations given, simulation results will be presented for an open-loop fermentation lasting 7½ hours. A generalized discussion on dissolved oxygen in fermentation broth and its use by growing cells will be presented.

The models used in this work are based on mass balances and stoichiometric equations. The first model relates the case of an open-loop fed-batch fermentation with an exponential feed rate to sustain optimal growth; the second model presents a more complex representation of a fermentation by incorporating the production of ethanol as a by-product. Both models are valid only for an increasing growth phase.

4.2. CELL GROWTH.

The rate of cell division, and therefore biomass production, varies according to a characteristic sequence (Figure 4.1) which comprises seven distinct phases. These are:

- | | |
|---|---------------------------|
| a | Activation phase |
| b | Lag phase |
| c | Exponential growth phase |
| d | Deceleration growth phase |
| e | Stationary phase |
| f | Increasing death rate |
| g | Exponential death rate |

In the activation phase (a) the microorganisms are coming out of dormancy. The lag phase (b) is a period of accelerated cell growth to critical size prior to cell division, and can often be reduced by increasing the inoculum size and

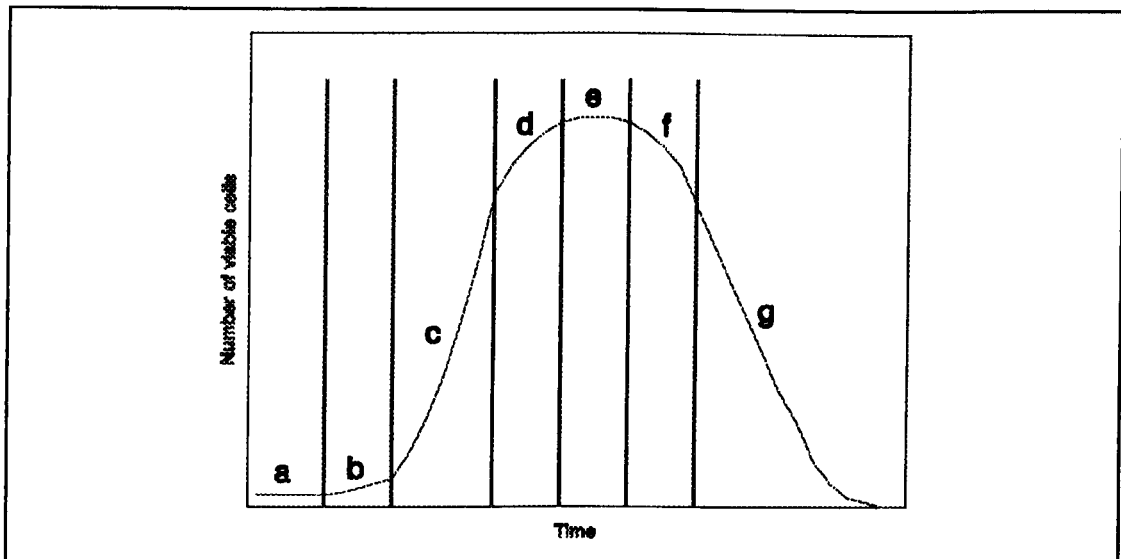


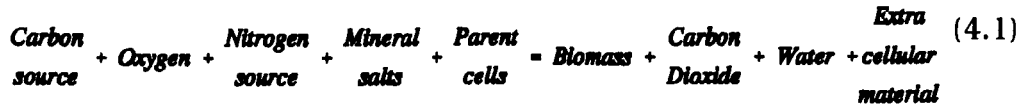
Figure 4.1 Microorganism growth phases.

optimizing the physical conditions within the fermenter. For commercial processes, the duration of the fermentation contributes to the cost of the final product, thus a minimal lag phase is desirable. It is during the exponential growth phase (c) that cell division, described earlier, is at a maximum. Hence this phase represents the normal growth period during which the cell concentration increases exponentially with time. After the exponential cell population growth there is a period of deceleration of the rate of population increase (d). The Carbon and Nitrogen nutrient sources are being depleted while growth inhibitory toxic waste products are building up, for example ethanol. The stationary phase, (e), marks a condition of equilibrium between the number of cells dying and the number of newly formed cells and although the total number of cells remains constant, the number of viable cells may drop. During this period the cells are respiring their own internal structures as food and hence beginning to autolyse, so the death rate of cells starts increasing leading to (f). Eventually the number of cells dying increases until there is an exponential death rate (g).

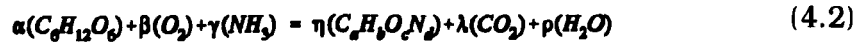
It has been observed that during a batch fermentation, the first stage produces ethanol. The second stage is invoked once all the glucose has been consumed, and involves the oxidation of the produced ethanol. Thus the high initial glucose concentration represses the oxidative pathway. Furukawa *et al* [4.1] have

reported typical specific growth rates of $\mu=0.4$ and 0.2hr^{-1} for the first and second phases, with biomass yields of 0.15 and 0.5 g cells/g glucose. The effect of glucose on the metabolic pathway is known as the Glucose Effect or the Crabtree Effect [4.2]. The lack of oxygen is known to inhibit the fermentation pathway according to the Pasteur Effect [4.3]; the observed effects being decreases in substrate consumption and carbon dioxide production rates. In the presence of a high concentration of glucose, the Crabtree Effect overrides the Pasteur Effect, while the fermentative pathway will dominate if both oxygen and glucose have high concentrations (Figure 4.2).

The basic equation for the aerobic growth of yeast can be written as



This may be described in stoichiometric terms as



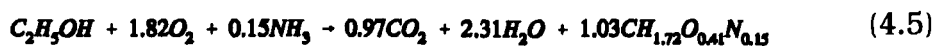
where $\alpha, \beta, \gamma, \eta, \lambda$ and ρ represent stoichiometric constants; $C_aH_bO_cN_d$ is a generalized cell unit where a,b,c and d vary according to the molecular composition of the microorganism being grown. Consequently the values of the molecular constants will determine the stoichiometric constants. A typical equation for *S. cerevisiae* fed-batch growth on glucose substrate is given by [4.4]



A batch fermentation has two growth phases: growth on glucose followed by growth on ethanol. A typical equation for the first phase is



while for growth on ethanol substrate it is



During a fermentation the sugar is provided as a glucose solution which is fed incrementally to the process for a fed-batch process; while it is fed wholly at the start for a batch process. The oxygen is obtained from air which is pumped into

the broth during the fermentation. A stirrer is used to break-up the air bubbles thereby allowing the oxygen to dissolve so that it can be more easily utilised by the yeast. The supply of ammonia is primarily used to control the pH level in the broth but it is also used in yeast growth as a source of nitrogen. Broth components must be in solution before they are available to a microorganism and oxygen is approximately 6000 times less soluble in water than glucose. Thus it is not possible to provide a microbial culture with all the oxygen needed for the complete respiration of the glucose (or any other carbon based substrate) in one addition. Therefore, a microbial culture must be continuously supplied with oxygen during growth at a rate sufficient to satisfy the organism's demand.

It can be shown from equations (4.4) and (4.5) that for a batch fermentation of *S. cerevisiae*, 7.89 moles of oxygen are needed to produce 1.0 mole of cells for growth on glucose, whereas growth on ethanol requires 1.76 moles of oxygen to produce 1.0 mole of cells; this represents a significant reduction in the consumption of oxygen during diauxic growth.

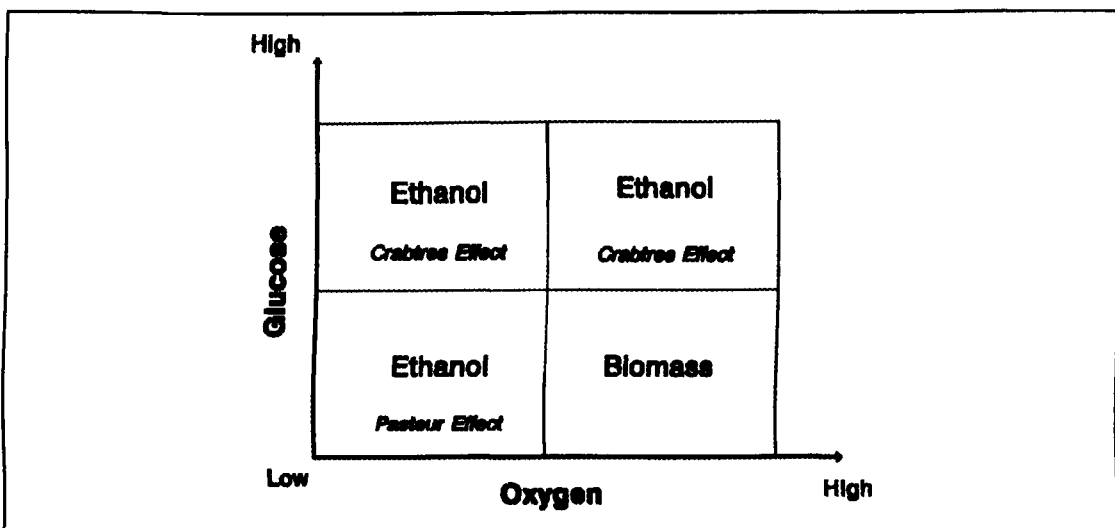


Figure 4.2 Influence of low and high levels of Glucose and Oxygen.

4.3. DISSOLVED OXYGEN IN THE FERMENTER.

The major problem of supplying oxygen to fermentation processes is that it has a low solubility coefficient, and biomass production requires large amounts of dissolved gas. For an active yeast fermentation with an oxygen uptake rate of $2 \text{ mg.m}^{-3}.\text{s}^{-1}$ and one cubic metre of culture broth containing 8 mg of oxygen, the

oxygen would last only 4 seconds.

The method of providing oxygen for a fermenting microorganism involves bringing oxygen in contact with the broth liquid, allowing the gas to dissolve and then transferring the dissolved oxygen from the liquid to the microorganism. To allow brisk transfer, a large contact area between the gas and the liquid is required, additionally the dissolved oxygen must be evenly distributed throughout the culture medium. To facilitate both these requirements, the oxygen supply is aerated into the vessel while the medium is agitated.

4.3.1. Oxygen Transfer Rate.

The oxygen transfer rate, OTR, is the rate at which oxygen is transferred from the gas to the liquid, that is from the input air bubbles to the broth medium:

$$OTR = K_L \cdot a_{gl} \cdot \Delta C \quad (4.6)$$

where a_{gl} is the gas-liquid interfacial area and K_L is the mass-transfer coefficient. The specific gas-liquid interfacial area per unit volume is given by

$$a_{gl} = \frac{A_B}{V} = \frac{6\epsilon}{d_b(1-\epsilon)} \quad (4.7)$$

where A_B is the total area of all the gas bubbles (m^2), V is the total broth volume (m^3), d_b is the average bubble diameter (m) and ϵ is the gas hold up:

$$\epsilon = \frac{V_G}{V_L + V_G} \quad (4.8)$$

where V_G is the volume of the gas in the broth (m^3) and V_L is the volume of the liquid of the broth (m^3). In practice it is difficult to separate between K_L and a_{gl} , thus a single parameter is usually referred to, K_{La} . Thus equation (4.6) may be rewritten as

$$OTR = K_{La}(C^* - C_L) \quad (4.9)$$

where C^* is the saturation concentration of dissolved oxygen, C_L the dissolved oxygen concentration and K_{La} the volumetric oxygen transfer coefficient. The value of C^* is almost constant since the most common source of oxygen is air, and oxygen solubility varies only slightly with the composition of the broth [4.5],

with a typical value being 7 mg of oxygen per litre of water. Both C' and C_L are temperature dependent, this is discussed further in section 4.3.4. From equation (4.9) it will be seen that OTR is increased by increasing K_{La} and C' and by decreasing C_L . The oxygen concentration in the broth, C_L , is important since at low levels aerobic cell growth may be inhibited; while high levels of C_L (close to the value of C') can impair the oxygen transfer rate. Aeration is usually provided by an input air flow rate of 1 litre per minute per litre volume of broth, and a predetermined stirrer speed (typically 600 rpm for a 5 litre fermentation vessel).

4.3.2. Oxygen Uptake Rate.

The oxygen transfer rate affects the oxygen uptake rate, OUR, which is a measure of the rate at which the cells utilise the available dissolved oxygen for growth, that is

$$OUR = f(O_{2in} - O_{2out}) \quad (4.10)$$

where f is the gas flow rate, while O_{2in} and O_{2out} are the oxygen concentrations in the inlet and outlet gases respectively. The OUR, and hence the OTR, are said to be growth limiting factors for the process. As the total number of cells increases, the demand for oxygen will increase and hence the OUR will also increase. Thus, the OTR must maintain the dissolved oxygen concentration at a sufficiently high level to prevent growth limitation. If the dissolved oxygen concentration drops below a certain level, then cell growth ceases and the glucose substrate is utilised to form ethanol. This is known as the Pasteur Effect. The volumetric oxygen uptake rate is given by

$$OUR = \frac{\mu X}{Y_{O_2}} \quad (4.11)$$

where μ is the specific rate of cell growth and Y_{O_2} is the yield coefficient of cells with respect to oxygen. This equation is based on the assumption that the temperature, pressure and flow rates of the input and output gases to the fermenter are constant.

The oxygen transfer rate, OTR, is usually controlled by the gas-liquid interfacial area, a , which is a function of the specific power input, P_i/V , and can thus be controlled by either the stirrer speed and/or the input air flow rate. A correlation between OTR and agitator (or impeller) tip speed has been shown by Steel and Maxon [4.6] to be

$$OTR = \text{constant} \times (\pi \cdot N \cdot D_i)^{1.6} \quad (4.12)$$

where N is the impeller rotational speed and D_i is the diameter of the impeller.

4.3.3. Volumetric Oxygen Transfer Coefficient.

The volumetric oxygen transfer coefficient, K_{La} , is a function of vessel temperature, the broth materials, the velocity of the gas through the liquid, v_s , and the speed of agitation. At constant temperature, the relationship is

$$K_{La} = R \left(\frac{P_i}{V} \right)^x (v_s)^y \quad (4.13)$$

where R is the empirical coefficient characteristic of the fermenter, V the broth volume, P_i the power input per unit volume of liquid, while x and y are empirical exponents with values less than 1.0 [4.7]. Thus the value of K_{La} may be increased by increasing the power input, however the change in K_{La} is proportionally less than the change in input power. The power factor, L_{O_2} , with respect to oxygen consumption is related to the OTR by

$$L_{O_2} = \frac{P_i}{V \cdot OTR} \quad (4.14)$$

where V is the broth volume (m^3) and P_i is the power input to the fermenter. In fermenters with both gas sparging and agitation, K_{La} may be increased by either raising the superficial gas velocity or the input power. However with y typically being greater than x (in equation (4.13)), then it is more economical to increase the superficial gas velocity, v_s , by increasing the input air flow rate. This steady increase in K_{La} , owing to an increase in v_s , continues until bubble coalescence causes a reduction in the gas-liquid interfacial area by increasing the average bubble size. Schugerl *et al* [4.8] expressed this as

$$K_{La} = 0.0023 \left(\frac{v_s}{d_b} \right)^{1.58} \quad (4.15)$$

where d_b is the mean bubble diameter. If x and y are assumed to be 0.6 and 0.75 respectively, this corresponds well with equation (4.13). The volumetric oxygen transfer rate can be determined by the ratio of OUR and OTR.

$$K_L = \frac{OUR}{OTR} \quad (4.16)$$

4.3.4. Oxygen Partial Pressure.

The electrode current developed at the cathode of the Ingold oxygen sensor (section 2.2.3.a), depends on the oxygen partial pressure and not the oxygen solubility in the solution being measured. That is, for a defined solution the oxygen concentration in air-saturated water, C_L , is proportional to the partial pressure of oxygen in the gaseous phase [4.9] as given by Henry's Law

$$C_L = \frac{pO_2}{H} \quad (4.17)$$

where Henry's constant, H , has a value of 0.026 at 25°C. The effect of temperature on the solubility of oxygen in water is given by

$$C_L = 14.16 - 0.394.T + 7.714 \times 10^{-3}.T^2 - 6.46 \times 10^{-5}.T^3 \quad (\text{mg.l}^{-1}) \quad (4.18)$$

Despite the decrease of oxygen solubility in water with increasing temperature, C_L is also dependent on the nature and concentration of other substances dissolved in the broth medium. The average value of dissolved oxygen concentration in a fermentation media is 5-6 $\text{mg}_{\text{O}_2} \cdot \text{l}^{-1}$ at 30°C. Although oxygen dissolves more easily at lower temperatures, the benefit is offset by a corresponding fall in the mass transfer coefficient, K_{La} [4.10].

$$\frac{(K_{La})_{T^\circ\text{C}}}{(K_{La})_{20^\circ\text{C}}} = 0.53 \left(\frac{T}{20} \right) + 0.47 \quad (4.19)$$

4.3.5. Factors affecting K_{La} values in fermentation vessels.

A number of factors have been demonstrated to affect the volumetric oxygen transfer coefficient, K_{La} , in a fermentation vessel. Such factors include the input air-flow rate, the degree of agitation, the rheological properties of the culture broth and the presence of anti-foam agents. If the scale of operation of a fermentation is increased it is important that the optimum K_{La} found on the small scale is employed in the larger scale vessel.

4.3.5.a. Effect of air-flow rate on K_{La} .

The input air-flow rate has a relatively small effect on K_{La} values in conventional agitated systems. The range of air-flow rates employed rarely fall outside the range 0.5 to 1.5 volumes of air per volume of medium per minute.

4.3.5.b. Effect of the degree of agitation on K_{La} .

The degree of agitation has been demonstrated to have a profound effect on the oxygen transfer efficiency of an agitated fermenter. Barks [4.11] claimed that agitation assisted oxygen transfer in the following ways:

1. Agitation delays the escape of air bubbles from the liquid,
2. Agitation prevents coalescence of air bubbles,
3. Agitation increases the area available for oxygen transfer by dispersing the air in the culture fluid in the form of small bubbles.

4.4. FED-BATCH FERMENTATION (MODEL I).

Presented is a simple mathematical model of a Bakers' Yeast fermentation, which covers the case for aerobic growth without excess glucose addition in a fed-batch fermentation.

4.4.1. Cell Growth Rate.

In an active and growing population of organisms, provided with an unlimited supply of nutrients; the rate of increase of cell mass concentration is dependant on the number of cells already present. The equation for rate of cell growth can be defined from a balance equation, that is

$$\text{Rate of Growth} = \text{Biomass Entering} - \text{Biomass Leaving} + \text{Growth} \quad (4.20)$$

For fed-batch and batch fermentations biomass is neither added nor removed. If all the requirements for biomass growth are satisfied, then during an infinitely small time (dt) one expects the increase in biomass (dX) to be proportional to the amount (X) present and to the interval; that is

$$\frac{dX}{dt} = \mu X \quad (4.21)$$

where X is the concentration of biomass and μ is the specific growth rate of the biomass. This first order differential equation has the following solution, giving

an exponentially increasing cell concentration.

$$X = X_0 e^{\mu t} \quad (4.22)$$

This equation describes constant exponential or logarithmic cell growth (phase c of Figure 4.1).

A significant parameter to be considered in the fermentation is the biomass doubling time, T_2 . This is the time taken for the cell concentration, X , to increase to $2X$. The relationship between T_2 and μ can be determined from

$$T_2 = \frac{\ln(2)}{\mu} \quad (4.23)$$

Assuming that $\mu = 0.19 \text{ hr}^{-1}$ [4.12], then $T_2 = 3.64 \text{ hr}$, that is a doubling time of 3 hours 38 minutes. Thus a fermentation lasting $7\frac{1}{4}$ hours allows two doublings of the cell mass, or a quadrupling of the initial cell mass concentration. The increase in cell mass concentration during the fermentation period is shown in Figure 4.3.

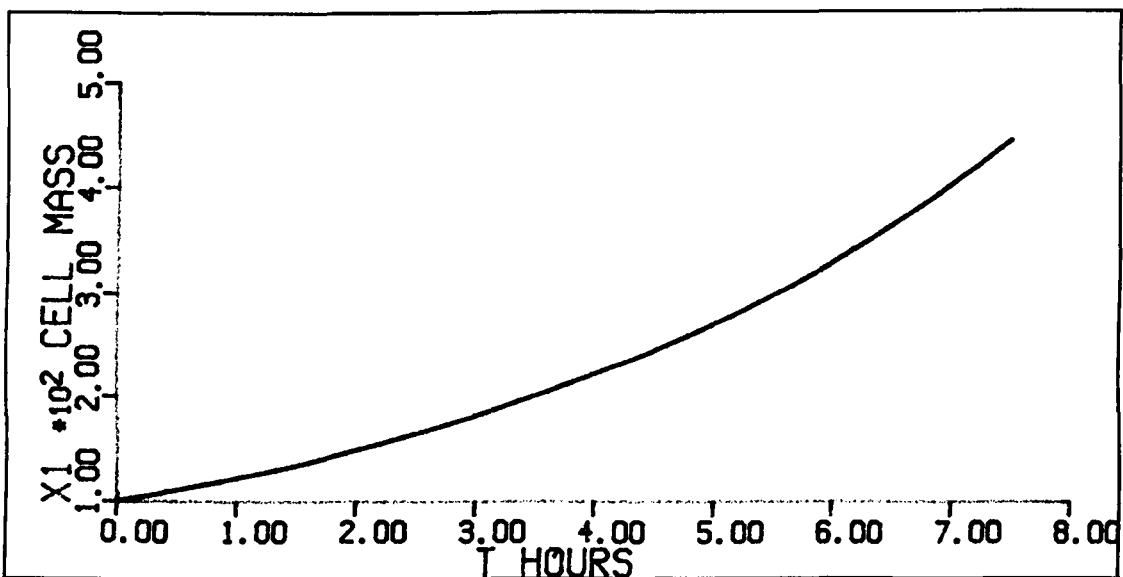


Figure 4.3 Cell mass concentration.

4.4.2. Specific Growth Rate.

The value of specific growth rate, μ , may be determined experimentally by plotting $\ln(X)$ against 't' which will give a straight line of slope $\mu \text{ h}^{-1}$ for constant μ . However, careful measurement of biomass reveals that μ is not a constant for batch cultures; the relationship depends upon the available substrate

concentration, S , and may be represented by the Monod relationship [4.13].

$$\mu = \frac{\mu_{\max} S}{K_s + S} \quad (4.24)$$

where μ_{\max} is the maximum rate of growth of the biomass, S is the concentration of the substrate and K_s is the saturation coefficient characteristic of the organisms. That is, K_s corresponds to the affinity of the organism for growth on the sugar substrate and is also known as the Monod constant, whose magnitude represents the value of S when [4.14]

$$\mu = \frac{\mu_{\max}}{2} \quad (4.25)$$

For *Saccharomyces cerevisiae* growth on a glucose substrate the Monod constant has a typical value of 25 mg.l⁻¹. As the culture consumes the substrate, the concentration, S , decreases until it reaches a value approximately equal to K_s , from which point the culture growth decreases significantly until the stationary phase (e in Figure 4.1) is attained. It should be noted that for any yeast fermentation, while the specific growth rate, μ , reaches a maximum value, the actual cell growth increases with an increasing population. This produces an exponential increase in cell mass with time which continues until the available substrate concentration has been reduced to a minimum.

4.4.3. Glucose Feed Rate.

For fed-batch processes, a nutrient solution (such as glucose) must be delivered to the process for the fermentation period. The rate of feed can be varied according to the process, it may be constant or follow some preset pattern, such as a ramp, exponential or pulse function. The culture's demand for glucose increases as more cells grow. If this demand is not met then the growth will be inhibited owing to the lack of nutrient and thus the process will no longer operate efficiently.

On the other hand, if the feed rate is greater than the demand, the cells will convert the excess nutrient into alcohol; this is known as the Crabtree Effect. The alcohol produced as a by-product can be utilised as a nutrient in the event

of a lack of glucose substrate, however the process should be avoided since it reduces the efficiency of the fermentation process.

The demand for glucose changes constantly depending upon the concentration of cells, their growth rate and the cell yield on the nutrient substrate (Y_{xs}). Assuming the yeast is initially active and ready to start the exponential growth phase, the biomass requires a corresponding exponential glucose feed pattern to maintain optimal growth, that is

$$U = X_0 e^{\mu t} \quad (4.26)$$

where U is the glucose feed rate ($\text{g}\cdot\text{hr}^{-1}$), X_0 is the initial biomass concentration (g) and μ the specific growth rate of the yeast (hr^{-1}). Given that the cell yield on a glucose substrate is Y_{xs} grams of cells per gram of substrate, the required glucose feed for optimum cell growth is

$$\text{Optimum Feed} = \frac{1}{Y_{xs}} \cdot \frac{dX}{dt} \quad (4.27)$$

Combining equations (4.21), (4.22), (4.26) and (4.27) results in

$$U = \frac{\mu X_0}{Y_{xs}} e^{\mu t} \quad (4.28)$$

For *S. cerevisiae*, $\mu=0.19 \text{ hr}^{-1}$ and $Y_{xs}=0.5$; with an initial cell concentration of $10 \text{ g}\cdot\text{l}^{-1}$ dry weight and an 8 litre broth, then $X_0=80 \text{ g}$. Thus

$$U = 30.4 e^{\mu t} \quad (4.29)$$

The glucose feed is added to the broth in a distilled water solution; with the concentration quite high at 30%, that is $S_{\text{glin}}=0.3 \text{ g}\cdot\text{l}^{-3}$; hence the fluid added to the broth is

$$F = \frac{U}{S_{\text{glin}} \cdot 1000} = \frac{U}{300} \text{ l}\cdot\text{hr}^{-1} \quad (4.30)$$

while the change in broth volume is given by

$$\frac{dV}{dt} = F \quad (4.31)$$

4.4.4. Substrate Concentration.

For a fed-batch fermentation, the substrate concentration equation can be developed using mass balance, which produces the equation

$$\frac{dS}{dt} = S_{in} F - \frac{\mu X}{Y_{xs}} \tag{4.32}$$

where S_{in} is the substrate feed concentration, F is the rate of feed and Y_{xs} is the yield of cells on a glucose substrate. The change in substrate concentration during a fed-batch fermentation may be seen in Figure 4.4.

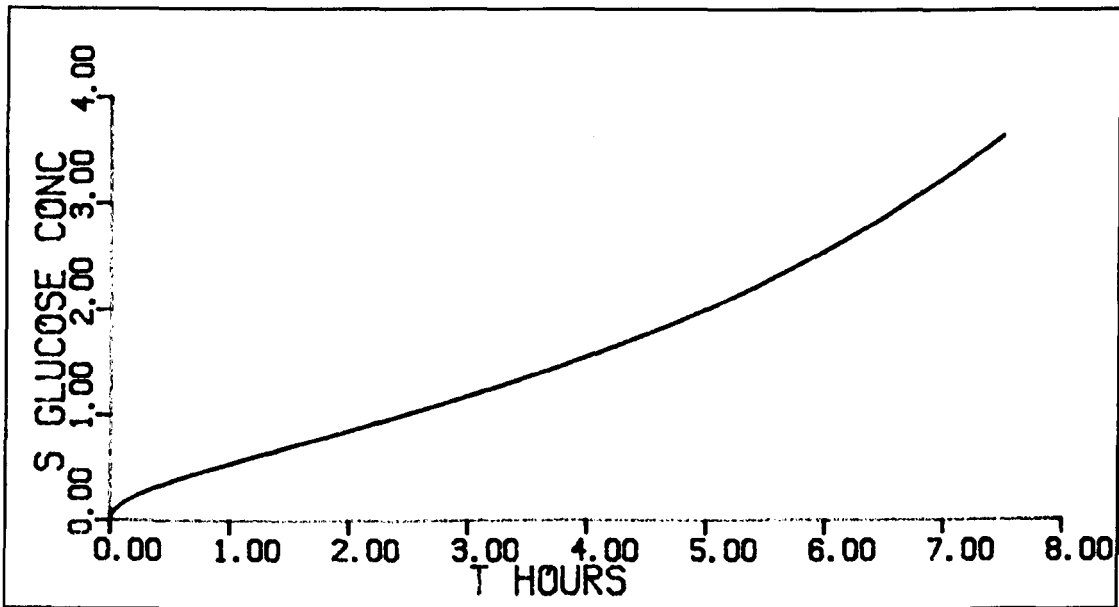


Figure 4.4 Substrate concentration.

4.4.5. Dissolved Oxygen Concentration.

During a fermentation, oxygen is consumed during cell growth and is dissolved into the broth via aeration and agitation. Using mass balance techniques, the rate of change in dissolved oxygen concentration, C_L , can be expressed as

$$\begin{matrix} \text{Rate of change} \\ \text{of } C_L \end{matrix} = \begin{matrix} \text{Rate of Oxygen} \\ \text{Entering System} \end{matrix} - \begin{matrix} \text{Rate of Oxygen} \\ \text{Leaving System} \end{matrix} \tag{4.33}$$

However, the dissolved oxygen removed from the system is the oxygen consumed by the cells, which is referred to as the oxygen uptake rate, OUR. Thus

$$\frac{dC_L}{dt} = K_L a (C^* - C_L) - OUR \tag{4.34}$$

however

$$OUR = \frac{\mu X}{Y_{O_2}} \quad (4.35)$$

where Y_{O_2} is the cell yield on oxygen, therefore

$$\frac{dC_L}{dt} = K_{La}(C^* - C_L) - \frac{\mu X}{Y_{O_2}} \quad (4.36)$$

where C^* is the saturation oxygen concentration in equilibrium (Figure 4.5), and K_{La} is the volumetric oxygen transfer coefficient of the system. The value of dissolved oxygen at saturation can be defined either before or after inoculation.

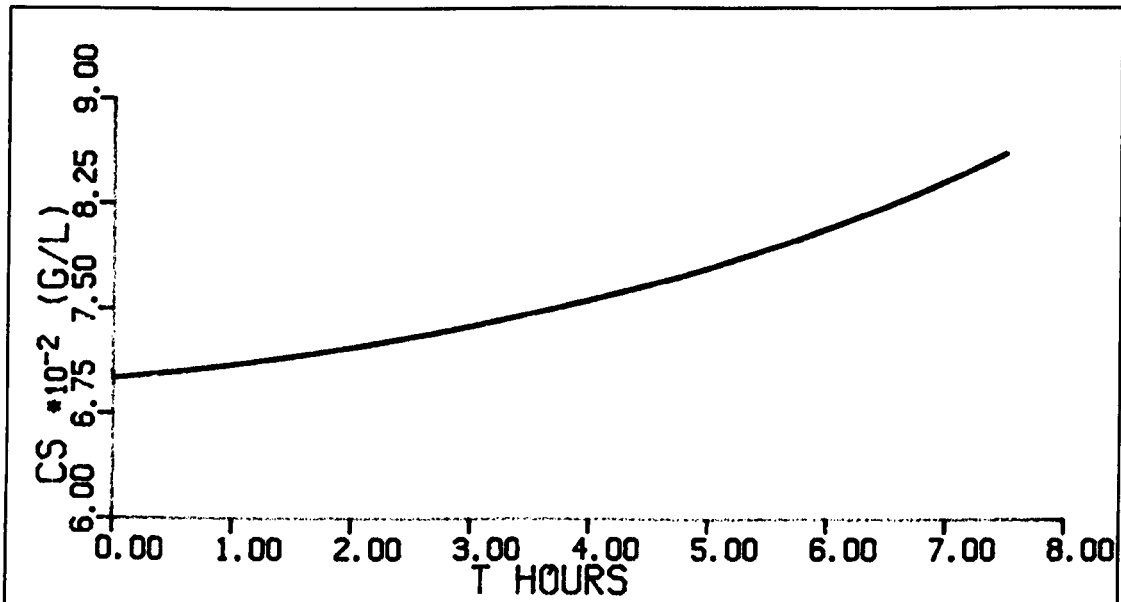


Figure 4.5 Saturation oxygen concentration.

4.5. OXYGEN DEMAND FOR GROWTH.

During a complete fermentation period, the cells require a supply of oxygen dissolved in the broth; this is true for all phases of growth. The greatest demand for oxygen occurs during the exponential growth phase (Figure 1.1) and may be determined from the oxygen uptake rate:

$$Demand = OUR = \frac{\mu X}{Y_{O_2}} \quad (4.37)$$

Equating (4.9) and (4.37), and solving for the specific growth rate, μ , gives

$$\mu = \frac{Y_{O_2}}{X} K_{Ls} (C^* - C_L) \quad (4.38)$$

However, from (4.21),

$$\mu = \frac{1}{X} \frac{dX}{dt} \quad (4.39)$$

Thus

$$\frac{dX}{dt} = Y_{O_2} K_{Ls} (C^* - C_L) \quad (4.40)$$

From this equation it can be seen that the growth of microorganisms under oxygen limitation is a linear function of the driving force for oxygen transfer, namely $(C^* - C_L)$

4.6. GROWTH YIELD.

At the end of the fermentation the growth yield coefficient, Y_G , expresses the amount of cells produced during the fermentation period. The nett growth yield is given by

$$Y_G = \frac{\text{Cell Mass Produced}}{\text{Mass of Sugar Utilised}} \quad (4.41)$$

4.7. BATCH FERMENTATION (MODEL II).

The second mathematical model used during the work, describes a fermentation which includes the production of ethanol in the presence of a high concentration of glucose substrate. This phenomenon is known as the Crabtree Effect, and can occur even if the dissolved oxygen concentration is sufficient for cell growth. A batch fermentation has the complete glucose feed supplied to the broth at the inoculation stage. The cells consume the glucose as the primary growth nutrient, however, once the glucose substrate has almost been exhausted, the cells continue to grow by utilizing the ethanol, previously produced, as the nutrient source.

The production of ethanol by a fermentative process is a common biochemical process, used primarily in the brewing industry. The formation of ethanol causes

a reduction in the yield of cells on a glucose substrate, additionally a high concentration of ethanol has an adverse effect on the quality of the cells produced. The model used here describes both the production and consumption of ethanol to provide a more realistic representation of a yeast fermentation. Okada *et al* [4.15] suggested that ethanol is produced when the substrate concentration was greater than 0.28 g.l⁻¹, while consumption of the ethanol occurs at substrate concentrations less than 0.28 g.l⁻¹.

4.7.1. Cell Mass Concentration.

Under aerobic conditions, the batch fermentation growth characteristic of Bakers' Yeast on a glucose substrate is dependent upon the concentration of the substrate. Above a critical concentration level the process is fermentative even in the presence of excess oxygen. In a batch fermentation of yeast on glucose, the growth characteristic has two phases, owing to the initial high concentration of glucose followed by an extremely low glucose concentration (Figure 4.6). Cell growth during a fermentation is normally given by equation (4.21), which may also be written as

$$\frac{d(VX)}{dt} = \mu VX \quad (4.42)$$

However, once the broth substrate concentration falls below the critical level, then the previously produced ethanol is consumed as the growth nutrient. Cell growth during this period is given by

$$\frac{d(VX)}{dt} = Y_{xe} v_e VX \quad (4.43)$$

where v_e is the specific rate of ethanol consumption and Y_{xe} is the yield of cells on the ethanol substrate. Thus the overall equation for cell growth can be obtained by combining equations (4.42) and (4.43) to give

$$\frac{d(VX)}{dt} = \mu VX + Y_{xe} v_e VX \quad (4.44)$$

This equation requires modification to ensure that cell growth on ethanol is only accounted when the glucose substrate concentration (S) is below the critical value, therefore the following logical operators are used here and throughout the model.

$$\begin{aligned} \text{IF } S > 0.28 \text{ THEN } a_1=0 \text{ AND } a_2=1 \\ \text{IF } S \leq 0.28 \text{ THEN } a_1=1 \text{ AND } a_2=0 \end{aligned}$$

The cell growth equation may now be written as:

$$\frac{d(VX)}{dt} = a_2 \mu VX + a_1 Y_{\text{m}} v_r VX \quad (4.45)$$

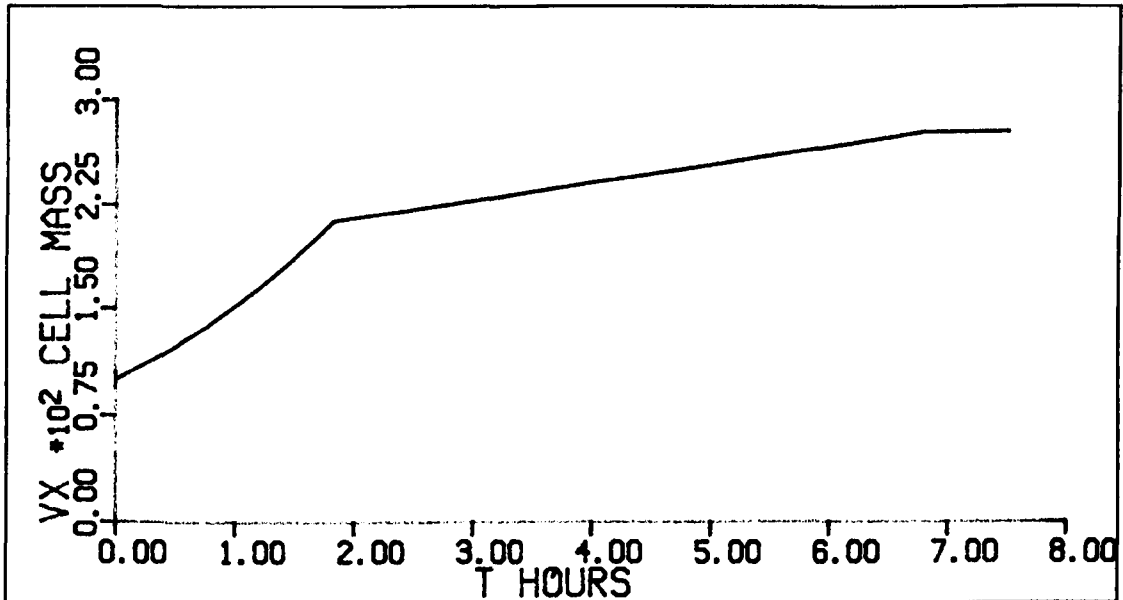


Figure 4.6 Cell mass concentration.

4.7.2. Substrate Concentration.

During a batch fermentation, the glucose substrate is used for

- biomass production
- ethanol formation
- cell maintenance energy

Hence the rate of substrate consumption can be given by

$$\frac{d(VS)}{dt} = - \left(\frac{\mu VX}{Y_{\text{m}}} + m_t VX + \frac{\pi_r VX}{Y_{\text{m}}} \right) \quad (4.46)$$

where π_r , Y_{m} , m_t and Y_{cs} are the specific ethanol production rate, growth yield of cells on a glucose substrate, maintenance coefficient of yeast and yield of ethanol on a glucose substrate, respectively. This assumes that all the available glucose substrate will be consumed for cell growth, maintenance of metabolism and ethanol production.

This equation applies only to a batch fermentation, where glucose substrate and ethanol are neither added nor removed. In contrast, for a fed-batch

fermentation the equation becomes

$$\frac{d(VS)}{dt} = FS_m - \frac{\mu VX}{Y_m} - m_t VX - \frac{a_2 \pi_e VX}{Y_m} \quad (4.47)$$

where F is the rate of substrate feed and S_m is the concentration of the feed. Obviously to simulate a batch fermentation, both F and S_m would be zero. The profile of the glucose substrate concentration during a batch fermentation is shown in Figure 4.7.

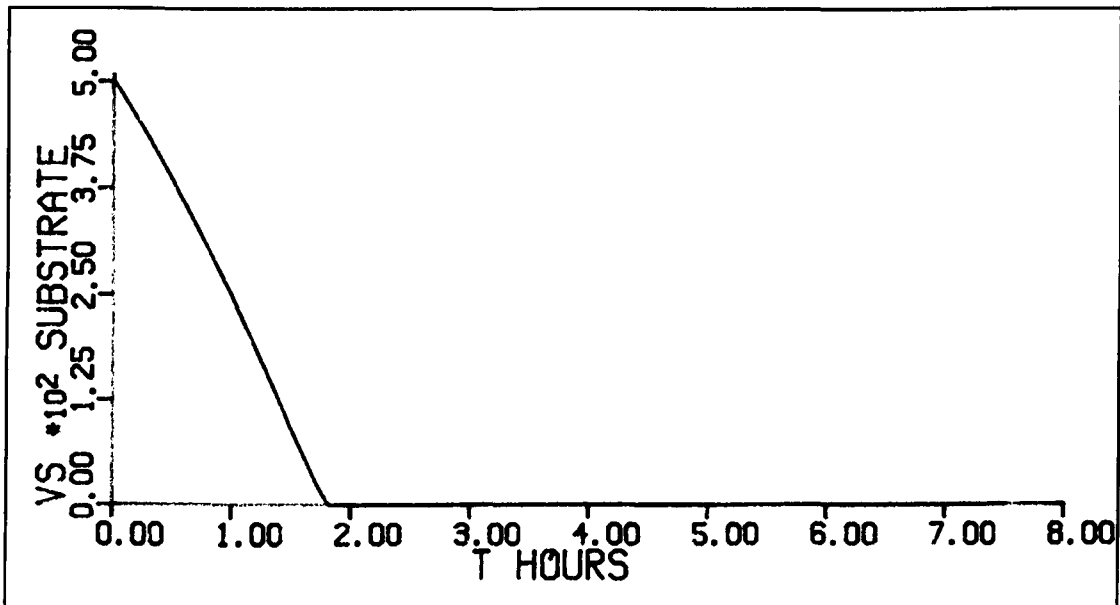


Figure 4.7 Glucose substrate concentration.

4.7.3. Ethanol Concentration.

During a batch fermentation, ethanol is initially formed while the concentration of glucose substrate is high. Once this concentration falls below the critical level of 0.28 g.l⁻¹, the ethanol is consumed as the growth nutrient.

The concentration of the ethanol is thus given by

$$\frac{d(VC_e)}{dt} = a_2 \pi_e VX - a_1 v_e VX \quad (4.48)$$

where C_e is the concentration of ethanol, π_e is the rate of ethanol production and v_e is the consumption rate of ethanol. As the fermentation proceeds the ethanol concentration increases until the glucose substrate falls below 0.28 g.l⁻¹ (Figure 4.8).

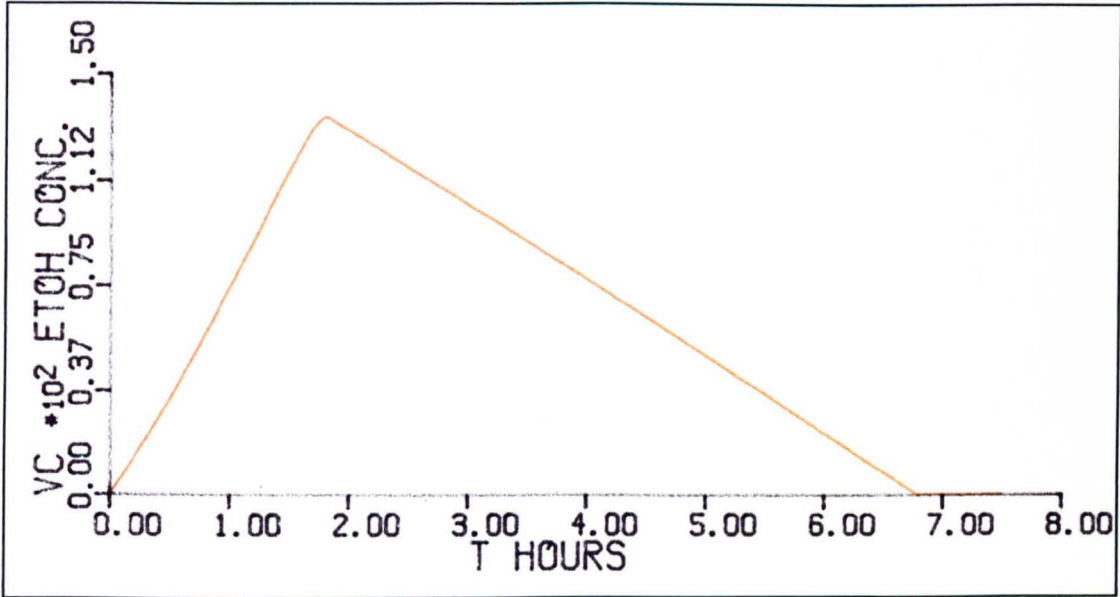


Figure 4.8 Ethanol concentration.

4.7.3.a. Specific Ethanol Production Rate, π_e .

Through experimentation, Okada *et al* [4.15] discovered that the production rate of ethanol, π_e , has a linear relationship to the natural logarithm of the available glucose substrate concentration:

$$\pi_e = 0.155 + 0.123 \log_e(S) \quad (4.49)$$

From Figure 4.9 it will be seen that ethanol production decreases with the depletion of the glucose substrate, eventually reaching its minimum of zero.

4.7.3.b. Specific Ethanol Consumption Rate, v_e .

Okada *et al* also developed an empirical relationship between the available glucose substrate concentration and the consumption rate of ethanol:

$$v_e = 0.138 - 0.062P + \frac{0.0028}{(S-0.28)} \quad (4.50)$$

where P is the concentration of growth inhibitory substances.

4.7.4. Growth Inhibitory Substances.

The rate of formation of growth inhibitory substances follows a pattern similar to that of cell growth (section 4.7.1). That is

$$\frac{d(VP)}{dt} = k_1 VX + k_2 \mu VX \quad (4.51)$$

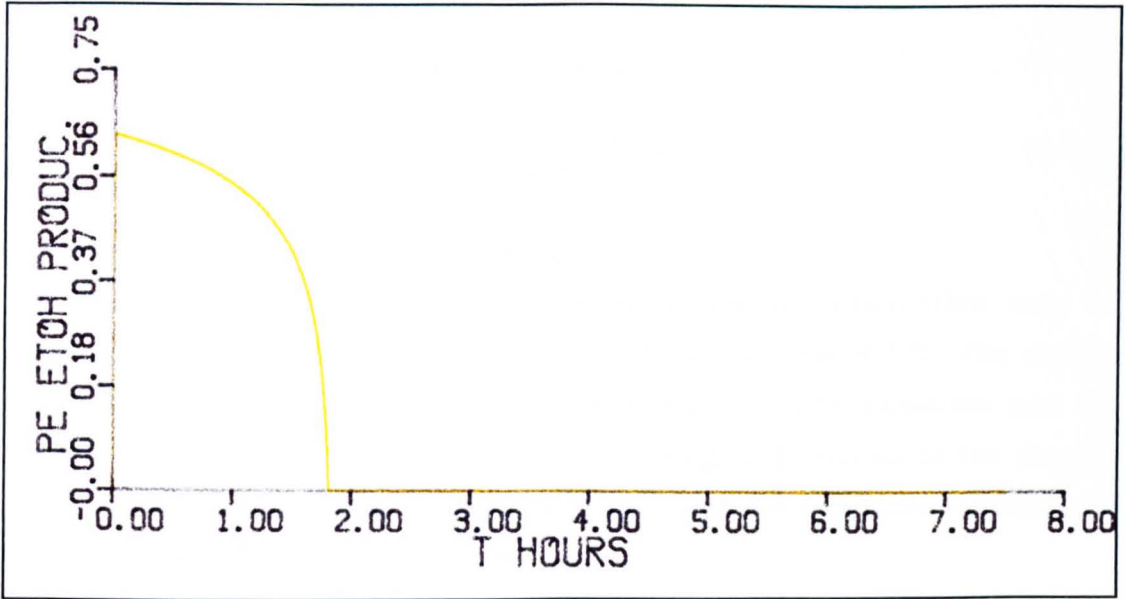


Figure 4.9 Ethanol production rate, π_e .

where k_1 and k_2 are microorganism explicit constants. For a *S. cerevisiae* fermentation these typically have values of 0.0023 l/g-cell.hr and 0.007 l/g-cell respectively [4.16]. A typical growth pattern of inhibitory substances may be seen in Figure 4.10.

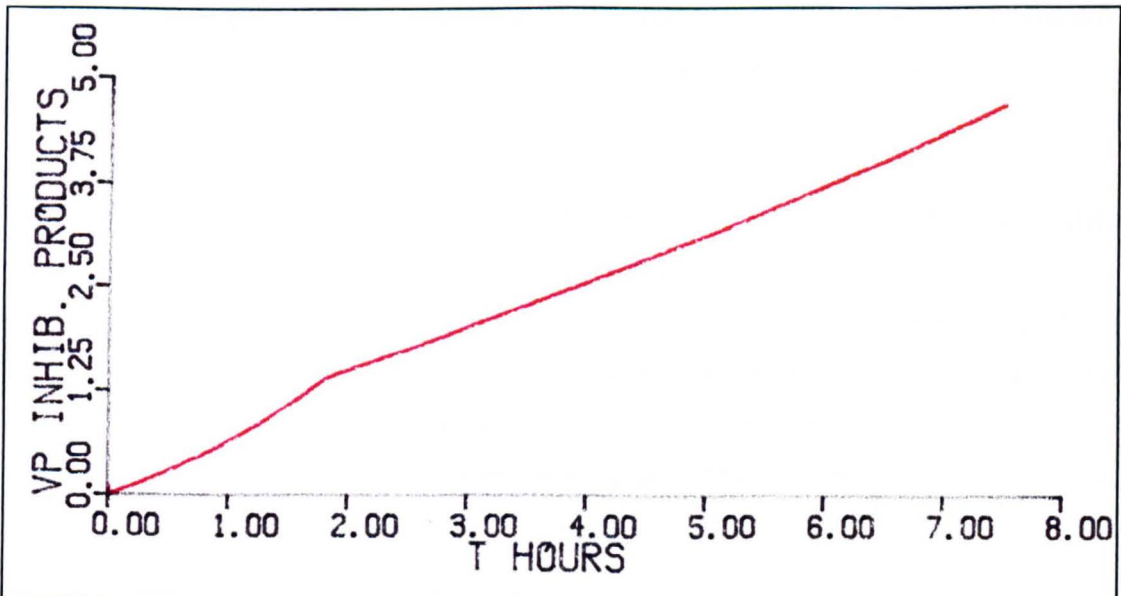


Figure 4.10 Concentration of growth inhibitory substances.

4.7.5. Specific growth rate.

The specific growth rate can be expressed as

$$\mu = \frac{\mu_{\max} S}{(1+P^2)(K_s+S)} \quad (4.52)$$

4.7.6. Dissolved Oxygen Concentration.

The dissolved oxygen concentration during a batch fermentation may be developed in a manner similar to that described in section 4.4.5. The oxygen uptake rate, OUR, is still a function of the cell mass concentration and the oxygen required by the cells to reproduce during both phases of the diauxic growth. For the first phase, the cell yield on oxygen (for a glucose substrate) is Y_{O_2} , while for growth on ethanol is Y_{eO} .

$$\frac{dC_L}{dt} = K_{La}(C^* - C_L) - \mu VX \left(\frac{a_2}{Y_{O_2}} + \frac{a_1}{Y_{eO}} \right) \quad (4.53)$$

The cell mass demand for oxygen during a batch fermentation comprises two phases (Figure 1.2). The first phase imposes a heavy demand for oxygen whilst the cell mass is increasing exponentially with a high yield factor on the glucose substrate. The second phase has a significantly lower oxygen demand since the cells may obtain part of their oxygen requirement from the consumed ethanol. Additionally, cell yield on ethanol is significantly lower than on glucose.

4.7.7. Glucose Feed Rate.

This second fermentation model can be used to represent both batch and fed-batch processes. In a fed-batch process, the equations for glucose substrate feed rate, total sugar added and broth volume increase are equations (4.28), ? and (4.31) respectively. If the second model is used to represent a batch fermentation then $U=0$, leading to $F=0$ and $T_s=0$, and the increase in broth volume is also zero. For the work presented here, this model is used only in the batch fermentation configuration.

4.8. DISCUSSION.

The above equations describe the development of the two mathematical models used during the simulation work of the investigation (Chapter 5). A summary of the model equations used are shown in Table 4.1 for the simple model (Model I)

and Table 4.2 for model II, while the values of the model constants are given in Table 4.3. The models are widely accepted as accurate representations of batch and fed-batch fermentations. However they are limited by the values of the constants employed during the simulation. For each microorganism and nutrient substrate, there is a different set of values for the constants, examples of these are shown in Table 4.4.

Even for a well known organism such as *S. cerevisiae*, a number of values have been recorded. Yousefpour [4.17] quoted values for specific growth rate as diverse as 0.18, 0.183, 0.2 and 0.21 hr^{-1} for the maximum specific growth rate. For a batch fermentation, Hill and Robinson [4.18] found that the yield of ethanol per gram of glucose was 0.456, while the maximum specific growth rate was 0.476 h^{-1} . Additionally their work showed that the yield of biomass per gram of glucose has a linear reduction from a value of 0.099, once the concentration of ethanol reached 40.9 g.l^{-1} . Figure 4.11 and Figure 4.12 demonstrate the difference in the simulated responses of a batch fermentation for maximum specific growth rates of 0.2 hr^{-1} and 0.42 hr^{-1} .

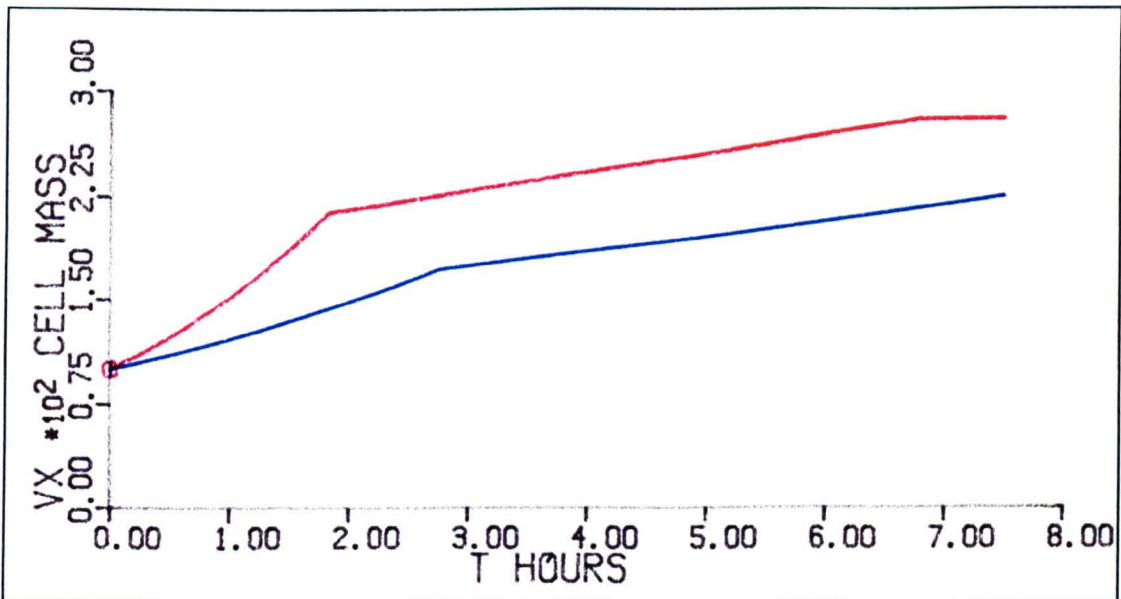


Figure 4.11 Cell mass concentration for two values of μ_{\max} .

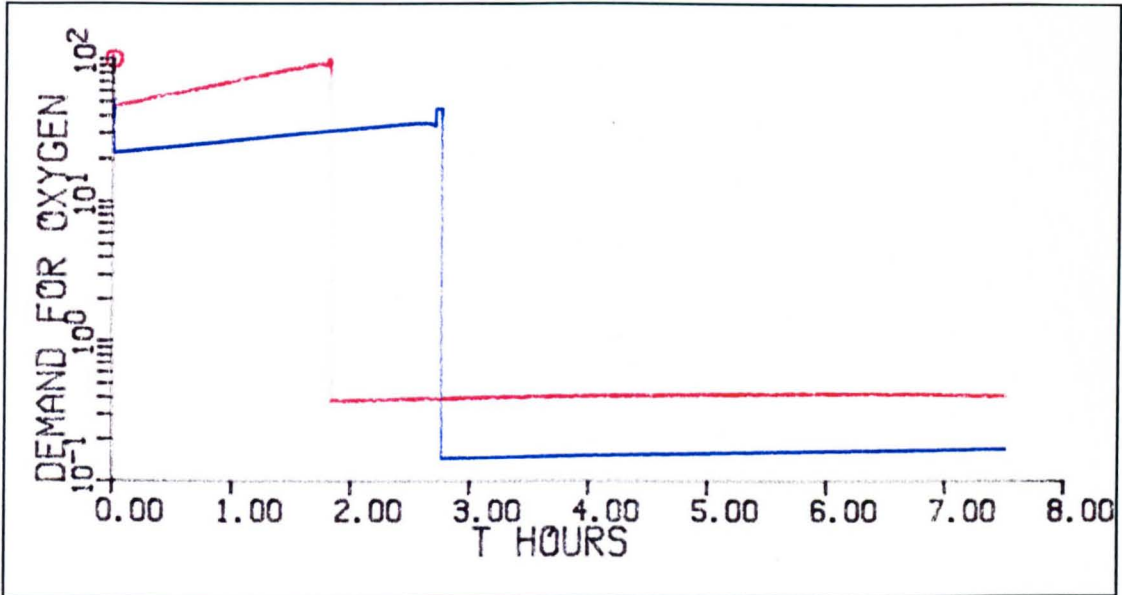


Figure 4.12 Oxygen demand for two values of μ_{\max} .

Table 4.1 Equations used for Model I.

$$\frac{dX}{dt} = \mu X$$

$$\frac{dV}{dt} = F$$

$$\frac{dT_s}{dt} = U$$

$$\frac{dS}{dt} = S_{in}F - \frac{\mu X}{Y_{xs}}$$

$$\frac{dC_L}{dt} = K_{La}(C^* - C_L) - \frac{\mu X}{Y_{O_2}}$$

$$F = \frac{U}{300}$$

$$\mu = \frac{\mu_{\max} S}{K_s + S}$$

Table 4.2 Equations used for Model II.

$$\frac{d(VX)}{dt} = a_2 \mu VX + a_1 Y_{xe} v_e VX$$

$$d(VS) = FS_e - \frac{\mu VX}{Y_{xs}} - m_1 VX - \frac{a_2 \pi_e VX}{Y_{oe}}$$

$$\frac{d(VC_p)}{dt} = a_2 \pi_e VX - a_1 v_e VX$$

$$\frac{d(VP)}{dt} = K_1 VX + K_2 \mu VX$$

$$\pi_e = 0.155 + 0.123 \log_e(S)$$

$$v_e = 0.138 - 0.062P + \frac{0.0028}{(S - 0.28)}$$

$$\mu = \frac{\mu_{max} S}{(1 + P^2)(K_s + S)}$$

$$\frac{dC_L}{dt} = K_L(C^* - C_L) - \mu VX \left(\frac{a_2}{Y_{oe}} + \frac{a_1}{Y_{xe}} \right)$$

Table 4.3 Model constant values used for simulations.

Constant	Model I	Model II
μ_{max}	0.19 hr ⁻¹	0.42 hr ⁻¹
S_{in}	300.0 g.l ⁻¹	----
K_s	0.003 g-substrate/l	0.025 g-substrate/l
m_1	----	0.03 g-substrate/g-cell.hr
k_1	----	0.0023 l/g-cell.hr
k_2	----	0.007 l/g-cell
Y_{o_2}	0.91 g-cell/g-oxygen	0.91 g-cell/g-oxygen
Y_{xs}	0.5 g-cell/g-substrate	0.5 g-cell/g-substrate
Y_{xe}	----	0.48 g-cell/g-EtOH
Y_{eo}	----	0.00009377 g-EtOH/g-oxygen
Y_{es}	----	0.51 g-EtOH/g-substrate

Table 4.4 Saturation constant, K_s , for growth of organisms on diverse substrates.

Oranism (genus)	Substrate	K_s (mg.l ⁻¹)
<i>Saccharomyces</i>	glucose	25.0
<i>Klebstella</i>	carbon dioxide	0.4
<i>Klebstella</i>	sulphite ions	2.7
<i>Escherichia</i>	glucose	4.0
<i>Escherichia</i>	lactose	20.0

4.9. REFERENCES.

- 4.1. Furukawa, F. E. Heinzle and I.J. Dunn. Influence of oxygen on the growth of *Saccharomyces cerevisiae* in continuous culture. *Biotechnology and Bioengineering*. Vol. XXV. pp. 2293-2317. 1983.
- 4.2. Crabtree, H.G. Observations of the carbohydrate metabolism of tumors. *Biochemical Journal*. Vol. 23, p.536-545. 1929.
- 4.3. Pasteur, M. Influence de l'oxygène sur le développement de la levûre et fermentation alcoolique. *Bulletin de la Societe chimique de Paris*. June, 28, p.79. 1861.
- 4.4. Battley, E.H. Growth-reaction equation for *Saccharomyces cerevisiae*. *Physiologia Plantarum*. vol. 13, p.192-203. 1960.
- 4.5. Truesdale, G.A., A.L. Downing and G.F Lowden. *Journal of Applied Chemistry*. Vol. 5, p.53-57. 1955.
- 4.6. Steel, R and W.D. Maxon. Some effects of turbine size on Novobiocin fermentations. *Biotechnology and Bioengineering*. Vol. IV, p.231-240. 1962.
- 4.7. Winkler, M.A. *Biological treatment of Waste-Water*. Kalstead Press. 1981.
- 4.8. Schugerl, K., J. Lucke and U. Oels. Bubble column bioreactors. *Advanced Biochemical Engineering*. Eds: T.K. Ghose, A. Flechter and N. Blakebrough. Springer-Verlag. Vol.7, p.1-84. 1977.
- 4.9. Pirt, S.J. *Principles of Cell and Microbial Cultivation*. Blackwell Scientific Publications. 1975.
- 4.10. Smith, J.M., K. van't Riet and J.C. Middleton. Scale-up of agitated gas-liquid reactors for mass transfer. *Preprints of 2nd European Conference on Mixing*. Cambridge, UK, p.51-66. 1977.

- 4.11. Barks, G.T. Aeration of moulds and streptomycetes culture fluids. Topics in enzyme and fermentation. Biotechnology, vol. 1, p.72-110. Ed. A. Wiseman. Ellis Horwood. 1977.
- 4.12. Dochain, D. Multivariable adaptive control of nonlinear completely mixed bioreactors. Advances in adaptive control. p. 308-313. 1991.
- 4.13. Monod, J. Recherche sur la croissance des cultures bactériennes. Herman, Paris, 1942.
- 4.14. Suktasch, D.A. and A. Dziengel. Biotechnology: A Handbook of practical formulae. Longman Scientific and Technical Press. Hong Kong. 1987.
- 4.15. Okada, W., H. Fukada and H. Morikawa. Kinetic expressions of ethanol production rate and ethanol consumption rate in Bakers' Yeast cultivation. Journal of Fermentation Technology. Vol. 59, No. 2. p.103-109. 1981.
- 4.16. Fukuda, H., S. Shiotani, W. Okada and H. Morikawa. A new culture method of Bakers' Yeast to remove growth-inhibiting substrates. Journal of Fermentation Technology. Vol. 56, No. 4. p.354-360. 1978.
- 4.17. Yousefpour, P. On-line adaptive control of a multivariable fermentation process. Ph.D. Thesis. Liverpool Polytechnic, United Kingdom. 1982.
- 4.18. Hill, G.A. and C.W. Robinson. A modified ghose model for batch cultures of *Saccharomyces cerevisiae* at high ethanol concentrations. Chemical Engineering Journal. Vol. 44. p.B69-B80. 1990.

CHAPTER 5.

SIMULATION OF THE AUTOMATIC TUNING PROCEDURE.

5.1. INTRODUCTION.

The chapter describes the validation of the automatic tuning procedure through simulation tests. A series of off-line simulation tests were performed to investigate and develop the automatic tuner prior to on-line application. Furthermore, it was necessary to ascertain the feasibility, and suitability, of applying the auto tuning PID controller on-line during batch and fed-batch fermentations of Bakers' Yeast. Initially an assortment of simulations were performed to investigate the operational concepts of the tuning procedure; these were carried out using transfer functions, chosen to represent a variety of process types and orders, with a third-order type 2 system being the highest order. The choice of transfer function was purely arbitrary since the objective was to test the operation of the tuning procedure and not to simulate a particular system.

On completion of the initial simulation work, the tuning procedure was applied to mathematical models of batch and fed-batch Bakers' Yeast fermentations. The fed-batch process was represented by Model I (the simple model outlined in Chapter 4), while Model II (given in Chapter 4) portrayed the more complex dissolved oxygen concentration dynamics in a batch fermentation involving ethanol production and consumption.

The simulation of a physical system using a mathematical model is a standard technique used for the design and evaluation of a controller. The simulation language used, has been produced to assist in modelling systems described by time dependent, nonlinear differential equations and/or transfer functions. The use of the continuous and discrete properties of ACSL allow the inclusion of time-related events, such as a sudden loss of an input signal for '*n-minutes*' occurring after '*x-minutes*' to represent a process disturbance. Assuming that both the system model and its simulation representation are accurate and

reliable, then the major advantages of computer simulation can be summarized as follows [5.1]:

- 1) Simulation results can be obtained at a lower cost than real experimentation.
- 2) Trials of processes under consideration can be achieved faster.
- 3) System performance can be examined under a range of conceivable conditions.
- 4) Future systems, currently in a conceptual stage, may be examined and appropriate decisions made.
- 5) Computer modelling and simulation is often the only practical or safe method of analysing and evaluating a system.
- 6) Hypothetical situations can be accomplished even when the condition is currently unrealizable in the real world.

The work presented in this chapter illustrates some of the simulation work covered during the investigation stages of the automatic tuning procedure, and highlights that the work performed encompasses the above statements.

In this chapter, the 'rationale' behind the decision to use the hysteresis nonlinearity as the forcing function within the tuning procedure will be presented. The preliminary simulation tests using a variety of transfer functions with individual characteristics will also be presented. The Chapter will continue with a description of the results of including noise disturbance into the process simulation. The shape of the nonlinear element has an effect on the process response and hence on the calculation of the tuning parameters. The Regula-Falsi method can be used to modify the characteristic of the hysteresis nonlinearity, thereby improving parameter determination; results obtained will be presented and described. The Chapter will conclude with the results showing the outcome of applying the automatic tuning procedure to simulations of Bakers' Yeast fermentations in both batch and fed-batch mode.

5.2. CHOICE OF NONLINEAR ELEMENT.

A variety of nonlinearities which are central to the technique were investigated to determine which displayed the most suitable characteristics. The purpose of the nonlinearity is to induce oscillations on the process output, therefore only

elements which had no 'linear' part should be used, that is only bi-state or tri-state nonlinearities could be investigated. Hence from the eight nonlinear elements presented in Chapter 3, only four were applicable:

- ★ Ideal nonlinearity (pure relay)
- ★ Nonlinearity with dead-band
- ★ Nonlinearity with hysteresis
- ★ Nonlinearity with dead-band and hysteresis

To determine which of the nonlinear elements offered the best characteristics to induce continuous oscillations, each of the nonlinear elements was incorporated within the feed-forward path of a feedback system (Figure 5.1). To obtain an overall impression of the nonlinear performance, the processes investigated included representations of first, second and third-order systems (Table 5.1).

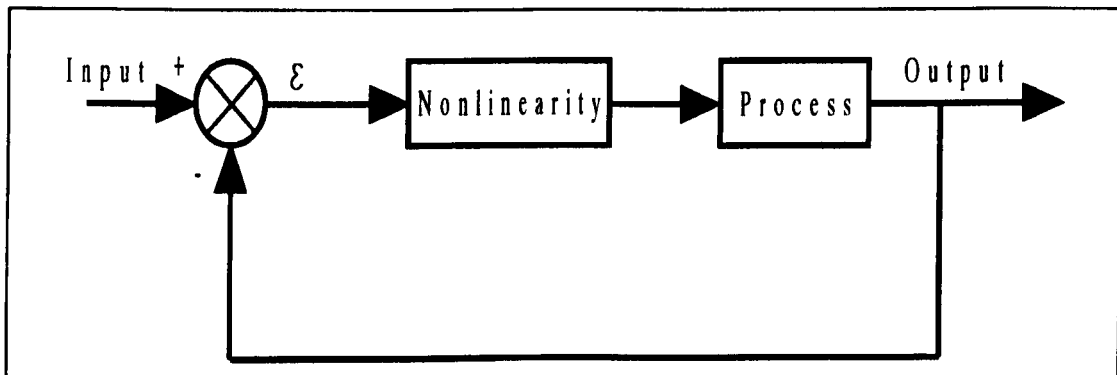


Figure 5.1 Simple control system.

The particular transfer functions were chosen with arbitrary values of time constants. The range of process order and type was chosen to attempt to encompass a realistic range of systems. These choices were made on the basis that in including the nonlinear element, the process response is dominated by the type and order. That is, the gain of the system primarily affects the oscillation amplitude value, while the time constants affect the rise-time and oscillation period of the processes.

Table 5.1 Transfer functions used for nonlinear element tests.

System	Order	Type	System	Order	Type
$\frac{1}{s+1}$	1	0	$\frac{1}{(s+1)(s+1)(s+1)}$	3	0
$\frac{1}{(s+1)(s+1)}$	2	0	$\frac{1}{s(s+1)(s+1)}$	3	1
$\frac{1}{s(s+1)}$	2	1	$\frac{1}{s^2(s+1)}$	3	2

The simulation environment, ACSL, included a function to represent a pure on-off nonlinearity:

$$y = \text{FCNSW}(\text{input}, \text{lower output}, \text{zero point}, \text{upper output})$$

The 'FCNSW' function performed inaccurately if the 'zero point' output value was made equal to the 'lower output' or the 'upper output', making it a tri-state device. Owing to the problems with 'FCNSW' and since none of the other nonlinearities could be simulated with a similar in-built function, each nonlinear element was expressed as a series of simple logical statements. For example, the ideal nonlinearity statements were of the form:

```

procedural
  output = +E
  IF input < 0.0 THEN output = -E
end

```

The results obtained from the simulation of a number of general processes with a range of nonlinear elements are summarized in Table 5.2. A selection of the simulated responses are shown in Figure 5.2 to Figure 5.7. These highlight some of the responses obtained during the investigations, such as increasing oscillations (Figure 5.7), decreasing oscillations (Figure 5.4), noisy oscillations (Figure 5.2) and ideal oscillations, that is a limit cycle (Figure 5.3, Figure 5.5 and Figure 5.6). Each result illustrates the process output; the set-point, and the process input (that is the nonlinearity output).

Table 5.2 Summary of Nonlinearity Simulation Tests.

Nonlinearity	Process					
	First-order Type 0	Second-order Type 0	Second-order Type 1	Third-order Type 0	Third-order Type 1	Third-order Type 2
Ideal	N	↓	↓	✓	✓	↑ Figure 5.7
Dead band	N	✓ Figure 5.3	↓	✓	✓	↑
Hysteresis	N Figure 5.2	✓	✓	✓ Figure 5.5	✓	↑
Hysteresis with dead band	✓	✓	↓ Figure 5.4	✓	✓ Figure 5.6	↑

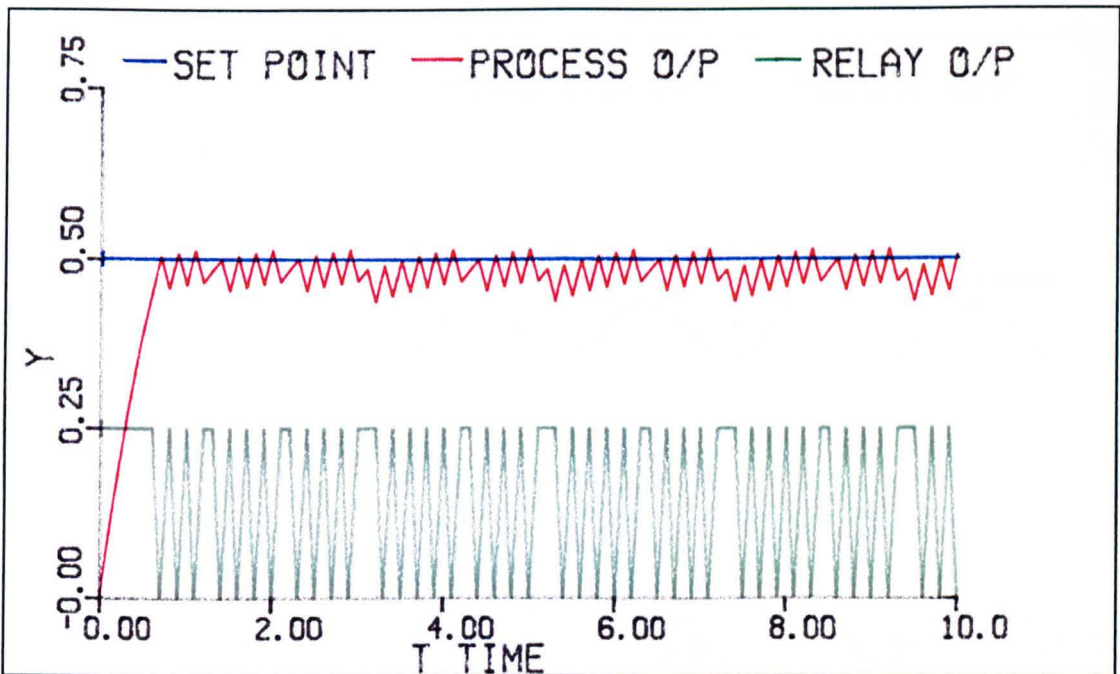
Key:

✓ - Limit cycle oscillations

↓ - Decaying oscillations

↑ - Increasing oscillations

N - Noisy oscillations

**Figure 5.2** Response for first-order type 0 system including nonlinearity with hysteresis.

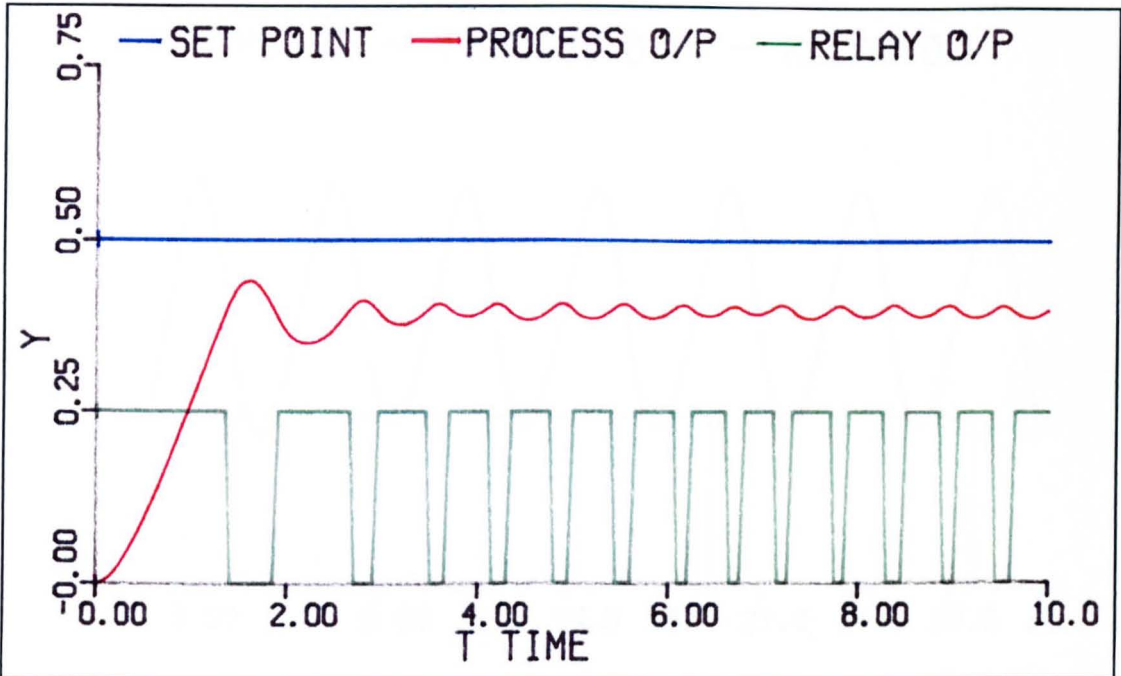


Figure 5.3 Response for second-order type 0 system including nonlinearity with dead-band.

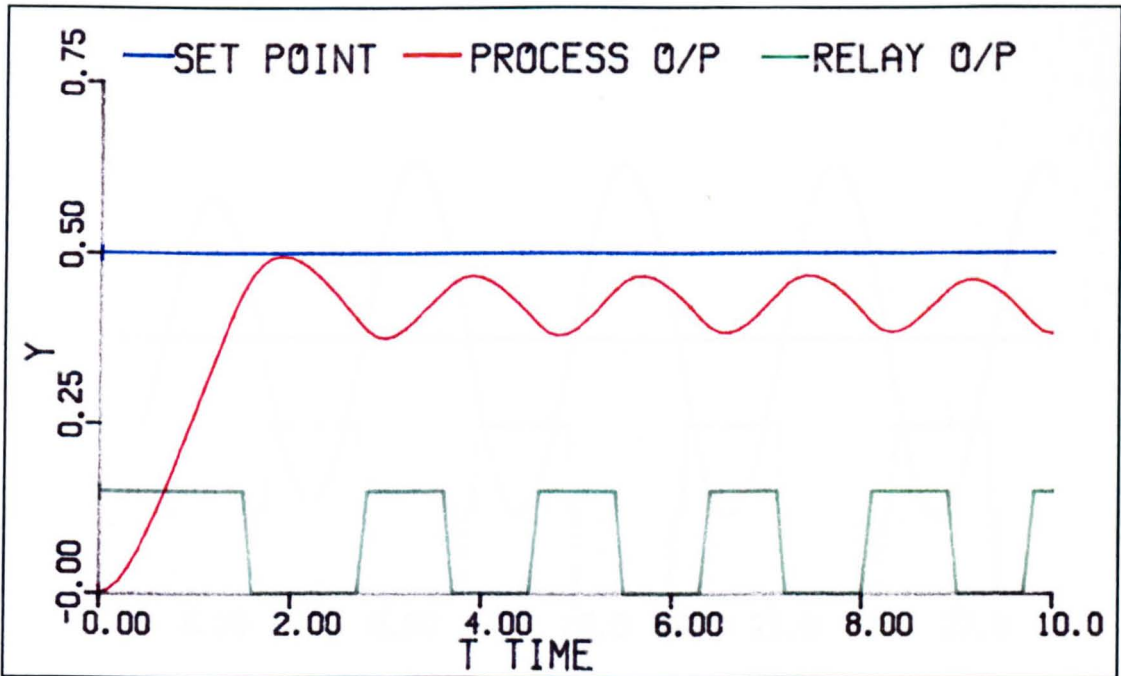


Figure 5.4 Response for second-order type 1 system including nonlinearity with dead-band and hysteresis.

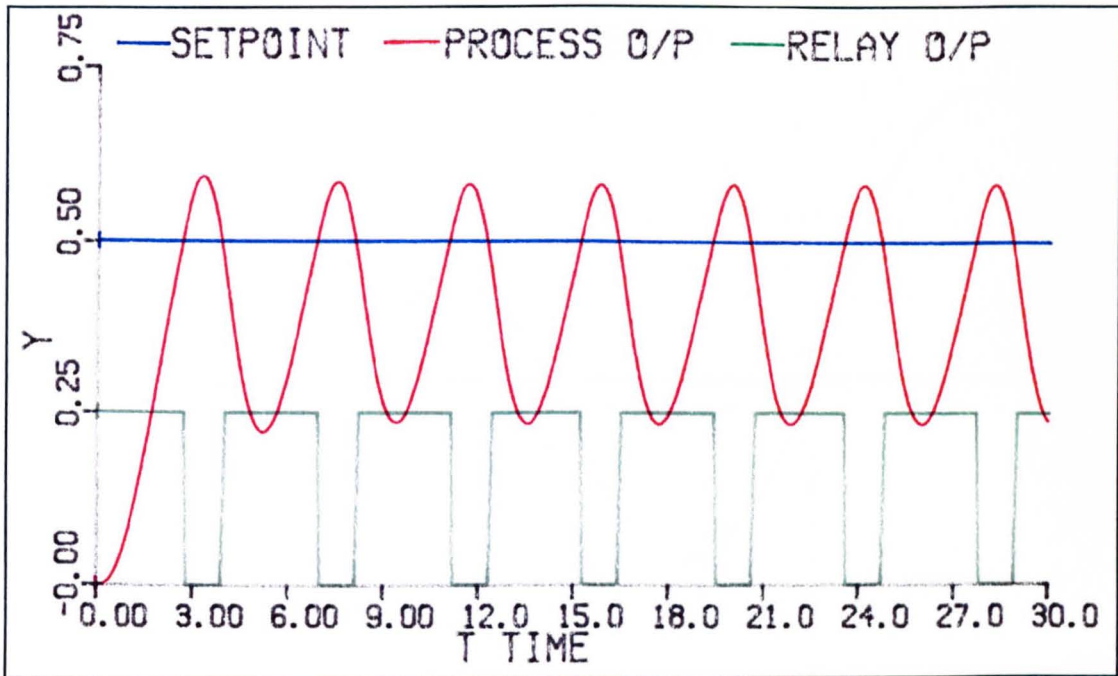


Figure 5.5 Response for third-order type 0 system including nonlinearity with hysteresis.

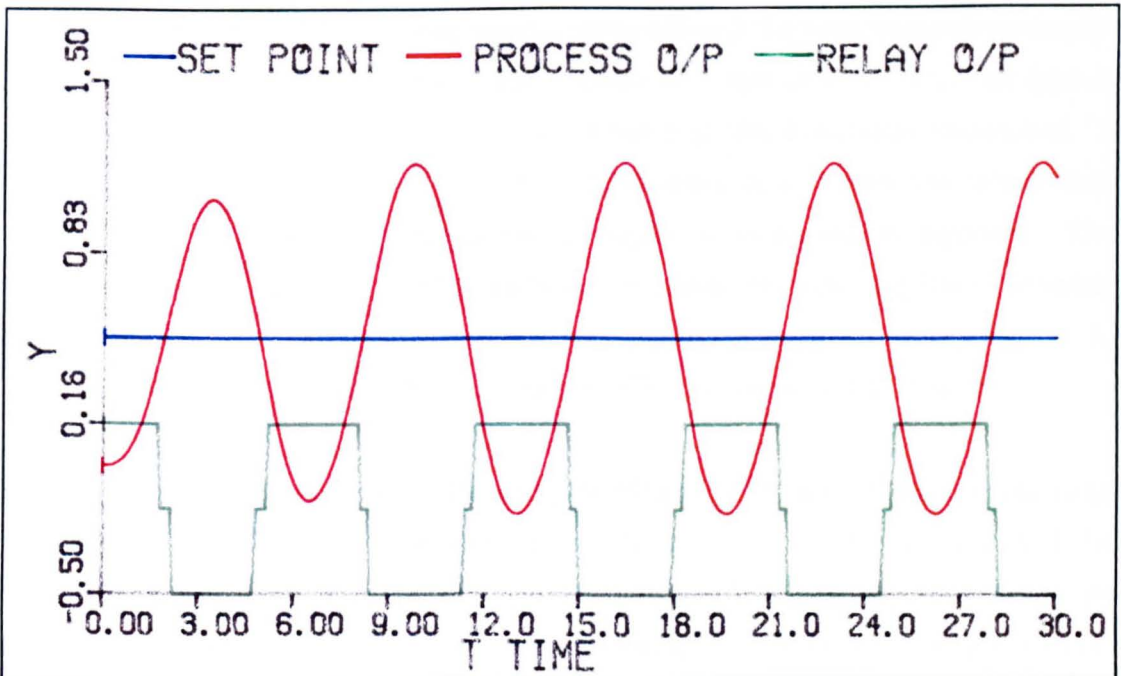


Figure 5.6 Response for third-order type 1 system including nonlinearity with dead-band and hysteresis.

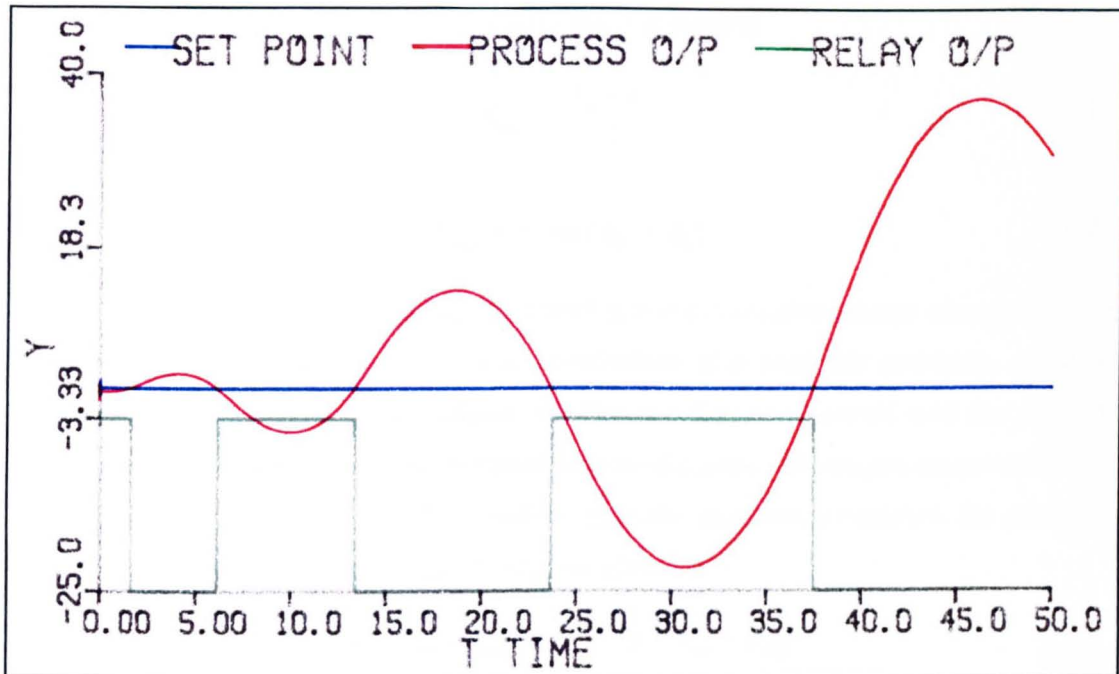


Figure 5.7 Response for third-order type 2 system including ideal nonlinearity.

5.2.1. Advantage of using the Hysteresis Nonlinearity.

The simulation results in Table 5.2 indicate that, over the range of selected transfer functions, the hysteresis nonlinearity offered the best characteristics for the automatic tuning procedure. This nonlinearity induces the required type of oscillations on the output for nearly all of the transfer functions simulated. A notable exception is the output of the third-order type 2 process which has increasing amplitude oscillations for all types of nonlinearity applied. The hysteresis within the nonlinearity provides a means of reducing the chattering effect on the process output if a pure nonlinearity is used (see Chapter 3), thereby providing a means of reducing the effect of measurement noise.

Before installing the automatic tuning procedure within a process control loop, the value of the maximum oscillation amplitude, A' , that the system will be subjected to, must be selected. This value is entered into the computer code as a pseudo-constant, as such it can only be changed by the control engineer and not by a process operator.

When the tuning procedure is initiated on-line, the maximum oscillation amplitude, A' , is used in the calculation of the nonlinearity output amplitude.

$\pm E$, and the hysteresis width, $\pm\beta$, using the equations

$$E_{\text{mag}} = \frac{K_c \pi A^*}{4} \quad (5.1)$$

$$\beta_{\text{mag}} = A^* \sin(\phi_m + \phi_l) \quad (5.2)$$

where ϕ_m is the required phase margin and ϕ_l is a correction phase margin for the inclusion of the nonlinearity. On a simulation of a realistic process, such as fermentation, the input and output for the nonlinear element will be specific manipulated variables, such as air flow rate and dissolved oxygen concentration. Therefore the values of y_{ref} and u_{ref} will be specific positive numbers, for example 600 rpm and 30%, thus $\pm\beta$ and $\pm E$ will be given by

$$\begin{aligned} +\beta &= \beta_{\text{ref}} + \beta_{\text{mag}} & -\beta &= \beta_{\text{ref}} - \beta_{\text{mag}} \\ +E &= E_{\text{ref}} + E_{\text{mag}} & -E &= E_{\text{ref}} - E_{\text{mag}} \end{aligned} \quad (5.3)$$

Thus a degree of flexibility is provided for the characteristics of the hysteresis nonlinearity to be modified in the light of any *a priori* knowledge of the process.

The nonlinearity with hysteresis can be simulated in ACSL by the program statements shown in Listing 5.1. The input to the nonlinearity is the variable 'Error' which is simply applied as a sine wave for test purposes, while the square wave nonlinearity output is given by 'U'.

5.3. IMPLEMENTATION OF THE AUTOMATIC TUNING PROCEDURE.

The integral action of a PID controller is usually represented as the definite integral of the error. This is satisfactory for the continuous domain, however for the discrete domain the integral action is approximated to the summation of the error over time. Similarly, the discrete derivative action may be formed from the difference between successive error values. Thus the common form of the PID in the continuous domain:

$$y = K_p \left(\epsilon + \frac{1}{T_i} \int \epsilon dt + T_d \frac{d\epsilon}{dt} \right) \quad (5.4)$$

Listing 5.1. ACSL coding for hysteresis nonlinearity simulation.

```

Program Hyst3
  Initial
    constant BETA=0.2 , ERROR=0.0 , DIREC=0.0, OLD1=0.0, U=0.0
  End $ ' of Initial '
  Dynamic
    Cinterval Cint = 1
    Constant TSTP = 10.0
  Derivative
    ALGORITHM IALG = 5
    NSTEPS = 1
    MAXTERVAL MAXT = 0.01
    MINTERVAL MINT = 0.01
  PROCEDURAL
    '--- define model equations ---'
    OLD1=ERROR
    ERROR = 2*sin(t)
    DIREC=ERROR-OLD1
    U=1.0
    '--- relay simulation ---'
    IF (ERROR.GE.BETA) U=1.0
    IF (ERROR.LE.-BETA) U=-1.0
    IF (DIREC.GE.0.0.AND.ERROR.GT.-BETA.AND.ERROR.LT.BETA) U=-1.0
    IF(DIREC.LT.0.0.AND.ERROR.LT.BETA.AND.ERROR.GT.-BETA)U=1.0
  END
  '--- define termination ---'
  TERMT(T.GE.TSTP)
  End $ ' of Derivative '
  End $ ' of Dynamic '
  End $ ' of Program '

```

is represented in the discrete domain as

$$y = K_p \left(\epsilon_n + \frac{1}{T_i} \sum_{i=1}^n \epsilon_i + T_d \left(\frac{\epsilon_n - \epsilon_{n-1}}{\Delta t} \right) \right) \quad (5.5)$$

The tuning procedure has been designed to produce controller tuning parameters for this PID algorithm throughout the sampled-data simulations.

Under normal operating conditions, the process would be under PID control, however, during the tuning phase the PID controller is removed from the forward path and the nonlinear element placed within the control loop to induce an oscillatory output (Figure 3.3). The tuning parameters for a PID controller may be chosen to achieve a specified design criteria, for example, Zeigler-Nichols' methods have been designed to produce a 1/4-wave amplitude damped response. In Chapter 3 it was stated that for a phase margin or gain margin design the

$1/4$ -wave damped response corresponds to values of $\phi_1=40^\circ$ and $G_M=2$ dB. For a satisfactory degree of relative process stability, the gain margin should be approximately 6 dB while the phase margin should be in the range 30 - 60° (for a second order dominant process, this corresponds to a damping ratio of 0.3 to 0.6 , given by equation 3.10). Thus it can be suggested that a satisfactory design criteria would be a phase margin of 60° , with a gain margin of no more than 6 dB.

The operation of the tuning procedure can be explained by the flowchart presented in Figure 5.40. The ACSL program initializes the variables and constant values before calculating the nonlinearity characteristics ($\pm E$, $\pm\beta$). The program calculates the output from the process transfer function before determining the error between the process output and the required set point. The process output is compared with the maximum and minimum output values to determine any new values, and are then modified if appropriate. The output from the nonlinear element is determined from the error and its direction of change (that is, increasing or decreasing in value). This nonlinearity output is applied to the process transfer function to eventually produce an oscillatory response, whose amplitude and period are determined.

Since the design rules for the automatic tuning procedure are based on approximate characterizations, then it is reasonable to use approximation techniques for the determination of the amplitude and oscillation period. The amplitude of the oscillation is calculated as the difference between the process output maximum and minimum values (Figure 5.41). To ensure that these values are determined correctly, the initial values of the minimum value and the maximum value are set to 100% and 0% respectively. The period of oscillation is calculated using a composite of the zero-crossing method which was described in Chapter 3 (Figure 5.42). Having calculated the current error and previous error, the program determines if there has been a change in sign, that is a crossing of the zero point. On a positive change (from $\epsilon < 0$ to $\epsilon > 0$), the time elapsed between the last and the current sign change is taken as *Period B* and doubled. In contrast, *Period A* is taken as the time between two consecutive sign changes (from $\epsilon > 0$ to $\epsilon < 0$); as shown in Figure 5.8. The oscillation period value

used is given by

$$\text{Period} = \frac{\text{Period A} + 2 \text{Period B}}{2} \quad (5.6)$$

The detection of peaks and zero crossing points will be subject to errors caused by measurement noise. These errors may be reduced by suitable filtering of the signal.

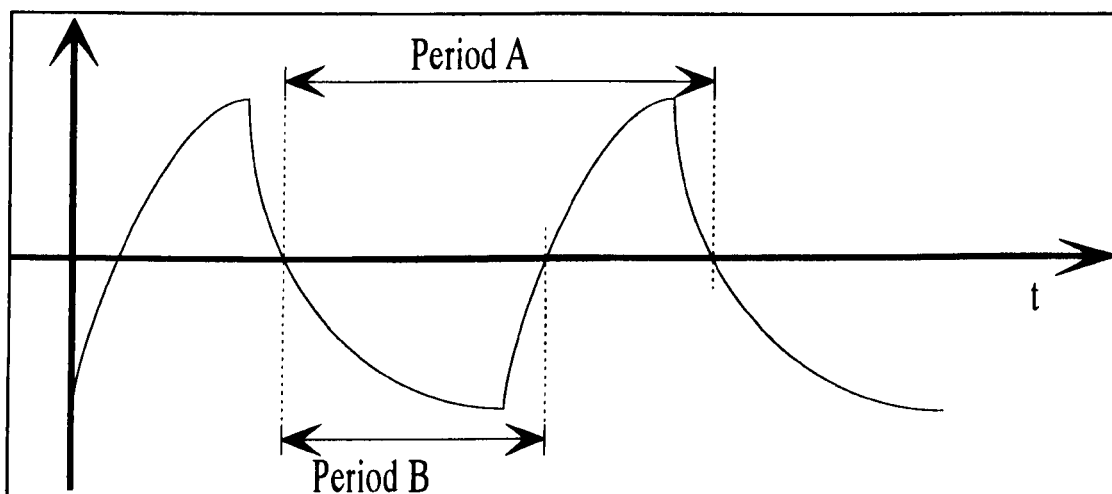


Figure 5.8 Composite period determination.

Figure 5.9 shows the simulated responses of the resulting automatically tuned P, PI and PID controllers. Each plot shows the transient response for a unit step input from zero initial conditions. As expected, the unity feedback controller (Y1) produces an unstable response, while the P, PI and PID controllers stabilize the response. The outcome of the P only system (Y2) is a steady-state offset, which is a characteristic of a proportional controller; this offset is removed when a P+I controller (Y3) is used. The full PID controller response (Y4) shows the typical Zeigler-Nichols $\frac{1}{4}$ -wave amplitude damping response. These results testify that the tuning parameters obtained from the automatic tuning procedure can provide controllers to produce classic Zeigler-Nichols output dynamics.

5.4. ADAPTION OF NONLINEARITY CHARACTERISTICS.

5.4.1. Regula-Falsi.

The overall characteristics of the hysteresis nonlinearity have a direct effect on the PID tuning parameter calculations. The major factor is the nonlinearity output amplitude, $\pm E$, since the hysteresis width is used primarily for noise

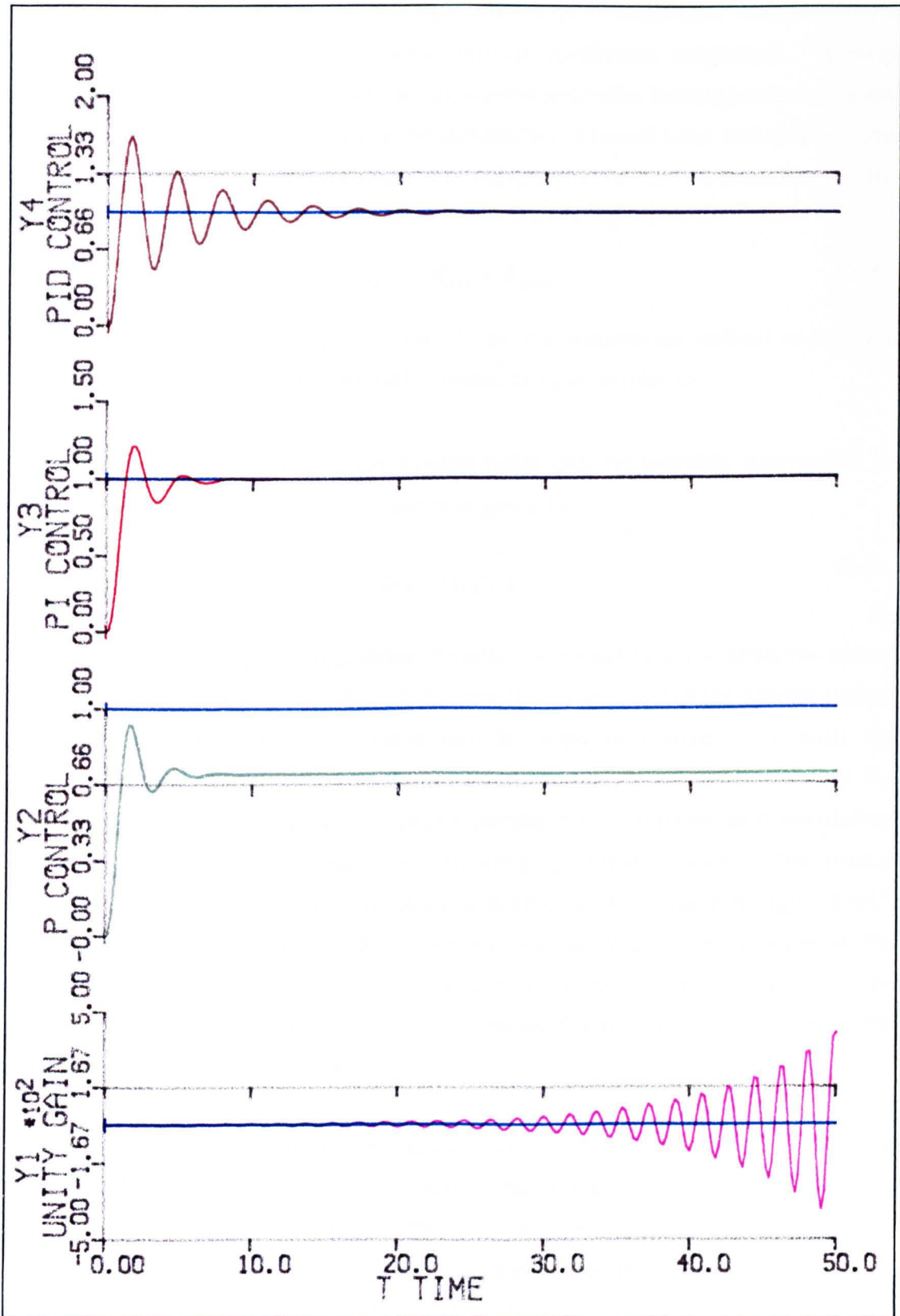


Figure 5.9 Comparison of controller responses.

rejection. An alteration to the nonlinearity output magnitude will produce a corresponding change in the process output oscillation amplitude. A large oscillation amplitude means that the calculated controller tuning parameters will approach those determined by the Zeigler-Nichols Closed-Loop technique. One method of automatically changing the value of E is the application of the Regula-Falsi equation (3.78) to adjust the nonlinearity value by

$$E_{n+1} = K_{n+1} \times E_{(t=0)} \quad (5.7)$$

where K is the multiplication factor, A' is the maximum output oscillation amplitude allowed and A the actual process output amplitude.

The estimation methods and the tuning rules can be suitably illustrated by considering a third-order, type 1 process given by

$$\frac{1}{s(s+1)(s+2)} \quad (5.8)$$

For simplicity both y_{ref} and u_{ref} , defined earlier, were set at zero, while the phase margin was 30° and v in equation (3.76) was 0.1. The effect of the simple tuning procedure on the process response can be seen in Figure 5.10, with the maximum oscillation amplitude, A' , set as 2.0 units. It will be noted that the calculation of both the process output oscillation amplitude and oscillation period takes a relatively short time to attain a steady value. The tuning parameters found in this case produce a system with a phase margin of 61° , which is twice the specified 30° . However, the natural phase margin of the transfer function is 53.14° . It is possible to improve on this by applying the Regula-Falsi equation to increase the process oscillation amplitude towards the specified maximum of 2.0 units.

The result of Figure 5.11 shows that before each change of gain, K, the amplitude and frequency estimations are interrupted. Since the two latest measurements are used in updating K (equation (3.78)), the second change in K is supposed to be efficient, which was found in this and other simulations. The estimated parameters, in the method, do not converge precisely to the true value. The final estimated frequency in this example is 0.61 rads/sec; while the value according

to the Zeigler-Nichols Closed-Loop tuning technique is 0.706 rads/sec. The final amplitude of oscillation of the process output becomes 2.002 units, which is extremely close to the value of A' and a significant improvement over the 1.76 units recorded previously. The resultant phase margin of the system becomes 53.14° , which is the natural phase margin of the system.

5.5. COMPARISON OF CONTROLLER RESPONSES.

The automatic tuning procedure was simulated using the transfer function

$$G(s) = \frac{80}{(s+1)(s+2)(s+4)} \quad (5.9)$$

with a maximum oscillation amplitude of $A' = 1.3$ and a phase margin of $\phi_m = 60.0^\circ$. The constant, ν , was given a value of 0.1 which corresponds to a phase margin of $\phi_1 = 5.71^\circ$, while the nonlinearity characteristics (given by equations (5.1) and (5.2)), were $E=0.765$ and $\beta=1.184$. The simulated results obtained had an oscillation amplitude of 1.968 with a period of 3.019 units, which determines the tuning parameters given in Table 5.3. The Zeigler-Nichols closed-loop tuning method applied to the same process revealed a critical gain of $K_c=0.75$ and an ultimate period of $T_u=3.02$ units.

Table 5.3 Calculated PID tuning parameters.

	K_p	T_i	T_d
P	0.248	--	--
PI	0.225	4.806	--
PID	0.291	1.5268	0.369

The following section will provide summary details on how the tuning procedure has been implemented, how the Regula-Falsi equation has improved the performance of the tuning procedure, and how the performance of both tuning procedure versions compares with established manual tuning techniques. Since the idea of the procedure is to tune a PID controller to some required specification, it is appropriate that the response of an automatically tuned PID be compared with those of manually tuned PID controllers.

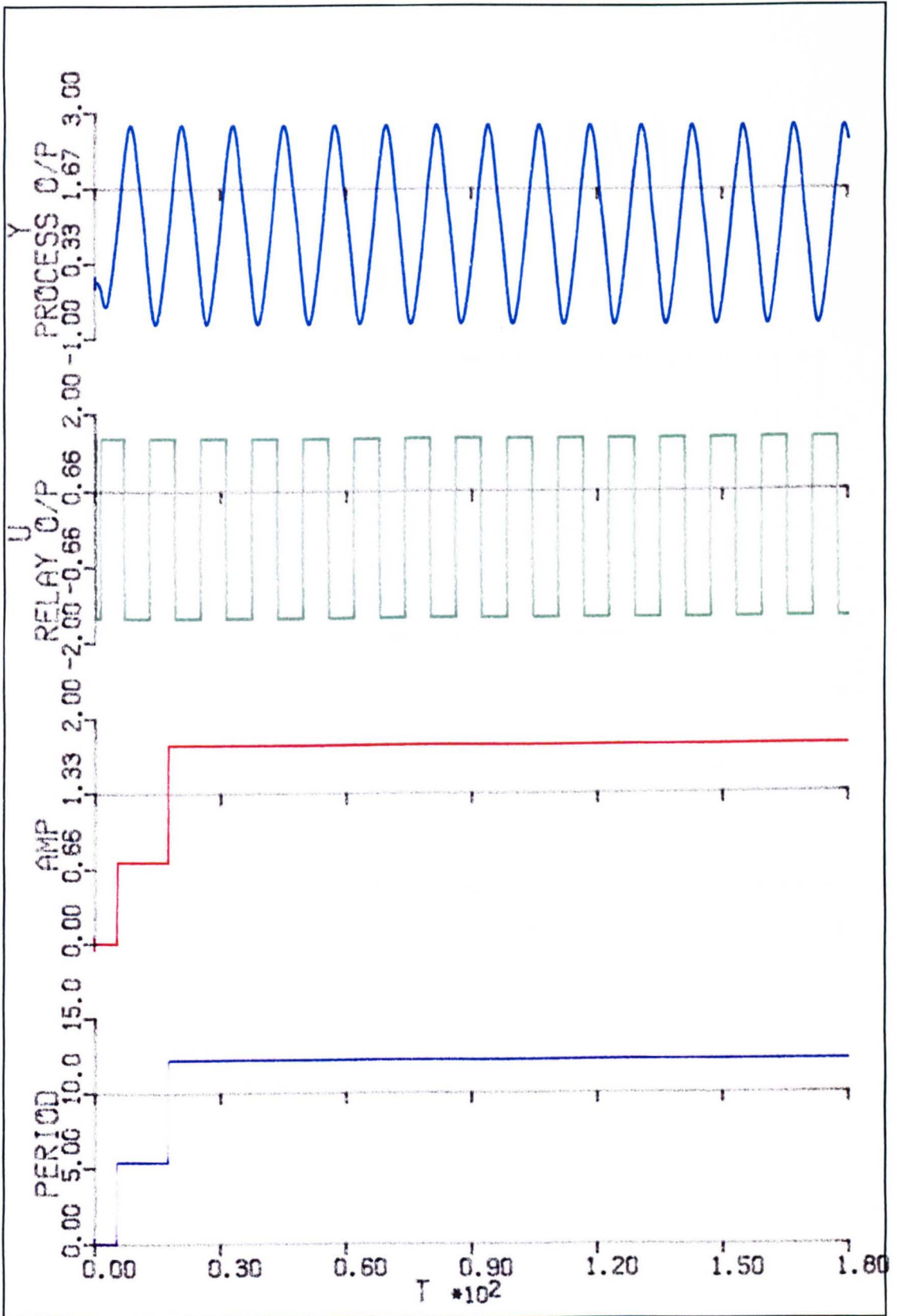


Figure 5.10 Application of the automatic tuning procedure.

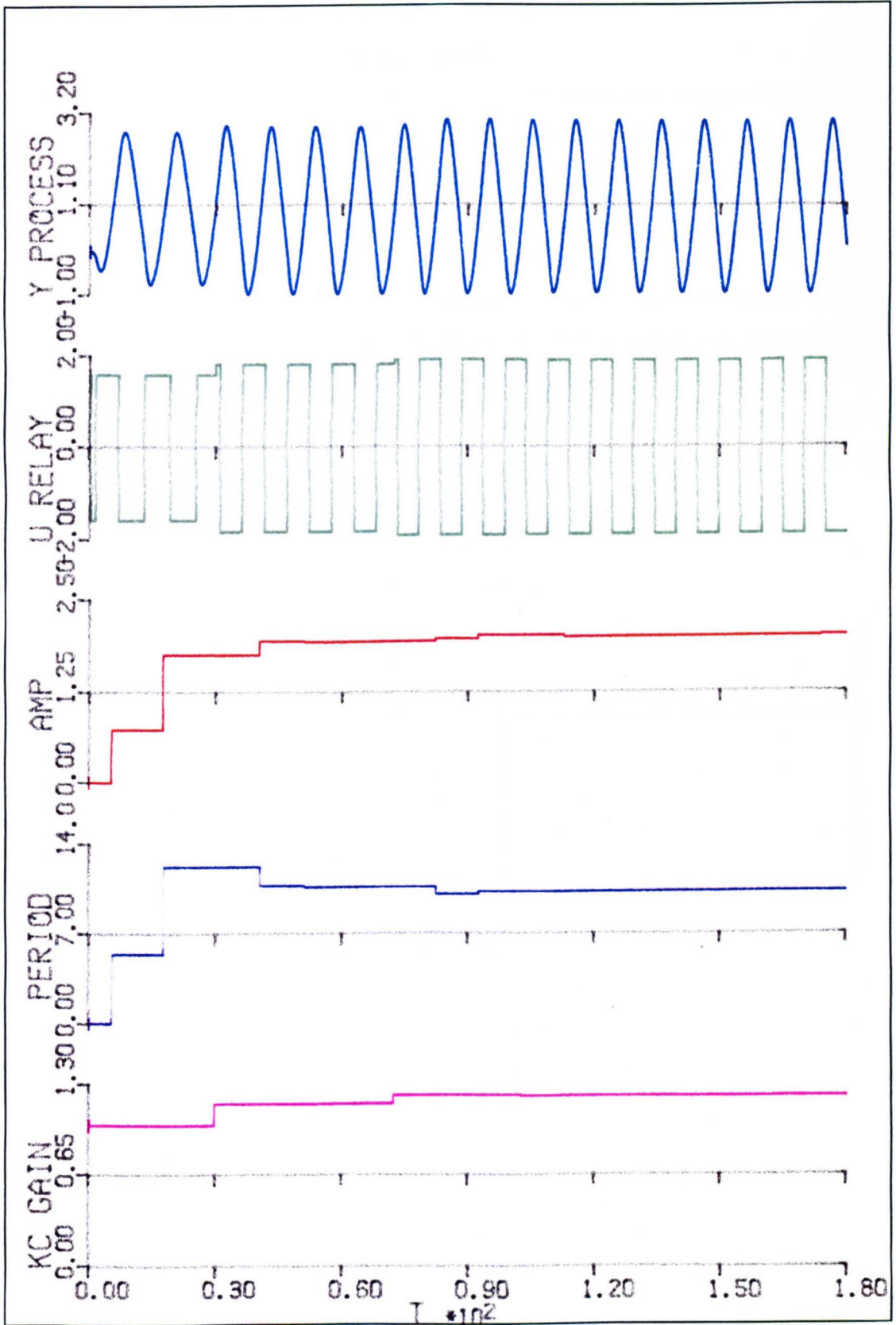


Figure 5.11 Inclusion of Regula-Falsi into the tuning procedure.

5.5.1. Manual Tuning Methods.

5.5.1.a. Ziegler-Nichols Open-Loop Method.

From the open-loop response of equation (5.9) standard Ziegler-Nichols PID tuning parameter values can be determined (Table 5.4). The table also indicates the settling time (T_s), the peak value attained (Y_{peak}) and the resulting process phase margin (ϕ_m).

The PID response conforms to the standard response expected from a Ziegler-Nichols controller: overshoot with amplitude damping before attaining steady-state about the set-point. Since the open-loop method relies on the determination of the point of inflection on the response curve, it is possible to produce a range of PID values dependent upon the gradient taken at the inflection.

Table 5.4 Open-loop response tuning parameters.

	K_p	T_i	T_d	T_{st}	Y_{peak}	ϕ_m
P	0.14	∞	0	— ¹	0.67	106°
PI	0.129	1.10	0	5.8	1.18	50°
PID	1.71	0.67	0.17	9.1	1.39	31°

5.5.1.b. Ziegler-Nichols Closed-Loop Method.

The Ziegler-Nichols closed-loop method was applied to the process (equation (5.9)) and the measured critical gain was $K_c=1.125$ with a natural frequency of $T_u=1.673$. From the values of K_c and T_u the tuning parameters were determined as shown in Table 5.5. Åström has shown that [5.2] that for a phase margin of 25° a slightly different set of tuning parameters should be used (Table 5.5). From the table it will be seen that the phase margin design procedures (25°, 45° & 60°) produce PID controllers which attain the specified phase margins.

¹ No settling time was recorded. The steady-state value was below the set-point.

Table 5.5 Closed-loop response tuning parameters.

	K_p	T_i	T_d	T_{st}	Y_{peak}	ϕ_m
P	0.56	∞	0	— ²	1.32	24°
PI	0.51	1.39	0	17.0	1.67	11°
PID	0.68	0.84	0.21	4.50	1.46	29°
25° PM	1.02	0.84	0.21	4.28	1.52	25°
30° PM	0.98	0.92	0.24	3.37	1.44	30°
45° PM	0.80	1.30	0.34	1.76	1.24	46°
60° PM	0.56	2.05	0.50	2.49	1.05	60°
'Some overshoot'	0.37	0.84	0.56	3.40	1.08	71°
'No overshoot'	0.23	0.84	0.56	4.17	1.11	68°
6 db Gain margin	0.19	1.0	0.07	25.7	1.08	38°

In addition, a modified set of PID parameters has been proposed [5.3] which accommodate options for 'some overshoot' or 'no overshoot' on the process response (Table 5.5). The responses both the 'normal PID' and the '25° phase margin' are shown in Figure 5.12. From the responses it will be seen that the 25° phase margin has a lower peak overshoot although both PID's have approximately the same settling time. The characteristic responses obtained for the 'normal PID', 'no overshoot PID' and 'some overshoot PID' can also be seen in Figure 5.12.

5.5.2. Automatic Tuning Procedure.

The automatic tuner was applied to the process described by equation (5.9), with the results obtained shown in Figure 5.13, for a design criteria of 60° PM. The results highlight the oscillatory process output (Y) to the square-wave input from

² No value recorded.

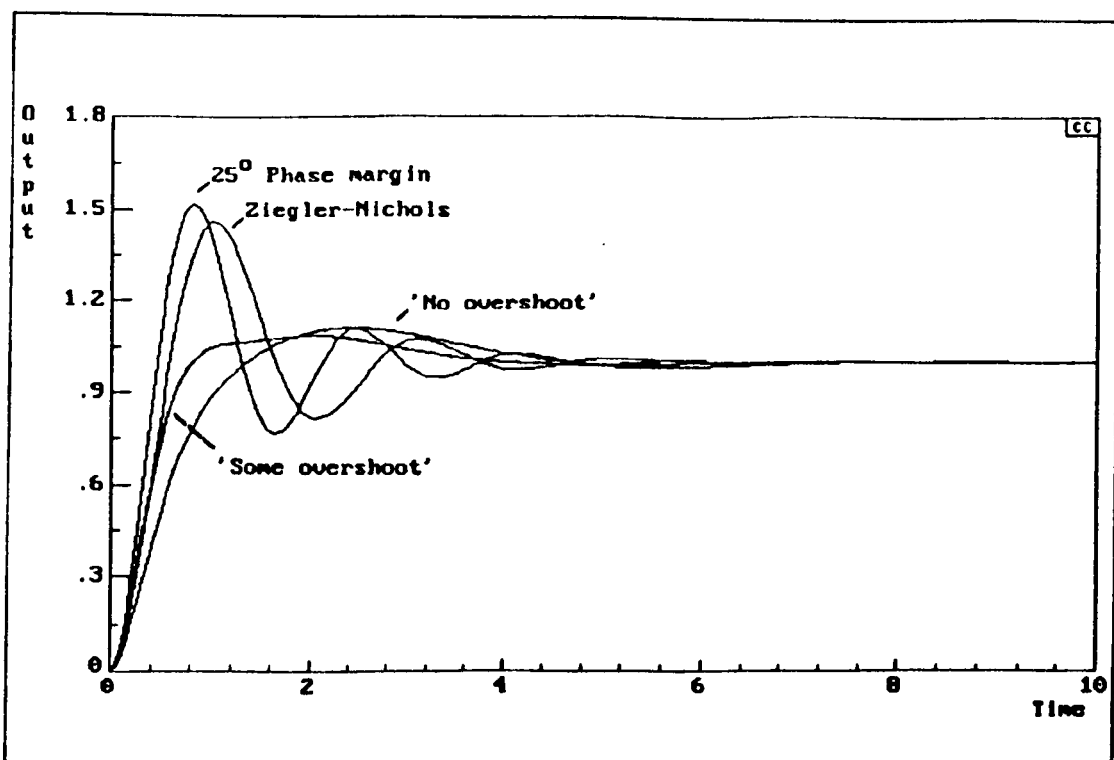


Figure 5.12 Tuned PID controller responses.

the nonlinear element (U), as the oscillations become periodic the amplitude calculation (AMP) settles to a steady value of 2.79 units; similarly the calculation of the oscillation period (PERIOD) steadies at 2.6 units. This particular arrangement provided a set of tuning parameters as shown in Table 5.6.

In this case the auto tuner calculated nonlinearity characteristics were $\pm E=1.021$ and $\pm\beta=1.185$. The response of the resultant tuned PID controller can be seen in Figure 5.14, which also illustrates the response of a closed-loop Ziegler-Nichols tuned PID. The design criteria for the tuning procedure was for a phase margin of 60° , while the attained phase margin was 60.5° , compared to the 28.4° for the Ziegler-Nichols tuned controller.

Table 5.6 Automatic tuning procedure developed tuning parameters (required $\phi_m=60^\circ$).

	K_p	T_i	T_d	T_{st}	Y_{peak}	ϕ_m
P	0.24	∞	0	— ³	0.90	65°
PI	0.22	3.92	0	1.64	1.01	60°
PID	0.29	1.25	0.30	2.78	1.11	59°

5.5.2.a. Modified Tuning Procedure.

As stated earlier, it is possible to modify the characteristics of the nonlinearity with hysteresis on-line by using the Regula-Falsi equation to change the 'gain' of the nonlinearity output. The Regula-Falsi was applied to the automatic tuning procedure for the process given by equation (5.9), with the obtained results shown in Figure 5.15. This modified tuning procedure develops a set of tuning parameters as shown in Table 5.7.

Table 5.7 Automatic tuning procedure PID parameter values.

	K_p	T_i	T_d	T_{st}	Y_{peak}	ϕ_m
P	0.22	∞	0	— ⁴	0.84	73°
PI	0.20	4.25	0	15.85	— ⁴	68°
PID	0.25	1.35	0.33	2.89	1.05	65°

The effect of the Regula-Falsi equation was to change the nonlinearity output values from $\pm E=1.021$ to $\pm E=0.767$, while the oscillation period changed to 3.2 units. The response of the tuned PID controller can be seen in Figure 5.14, with the normal tuning procedure PID for comparison. The Zeigler-Nichols tuned PID

³ No value recorded.

⁴ No value recorded.

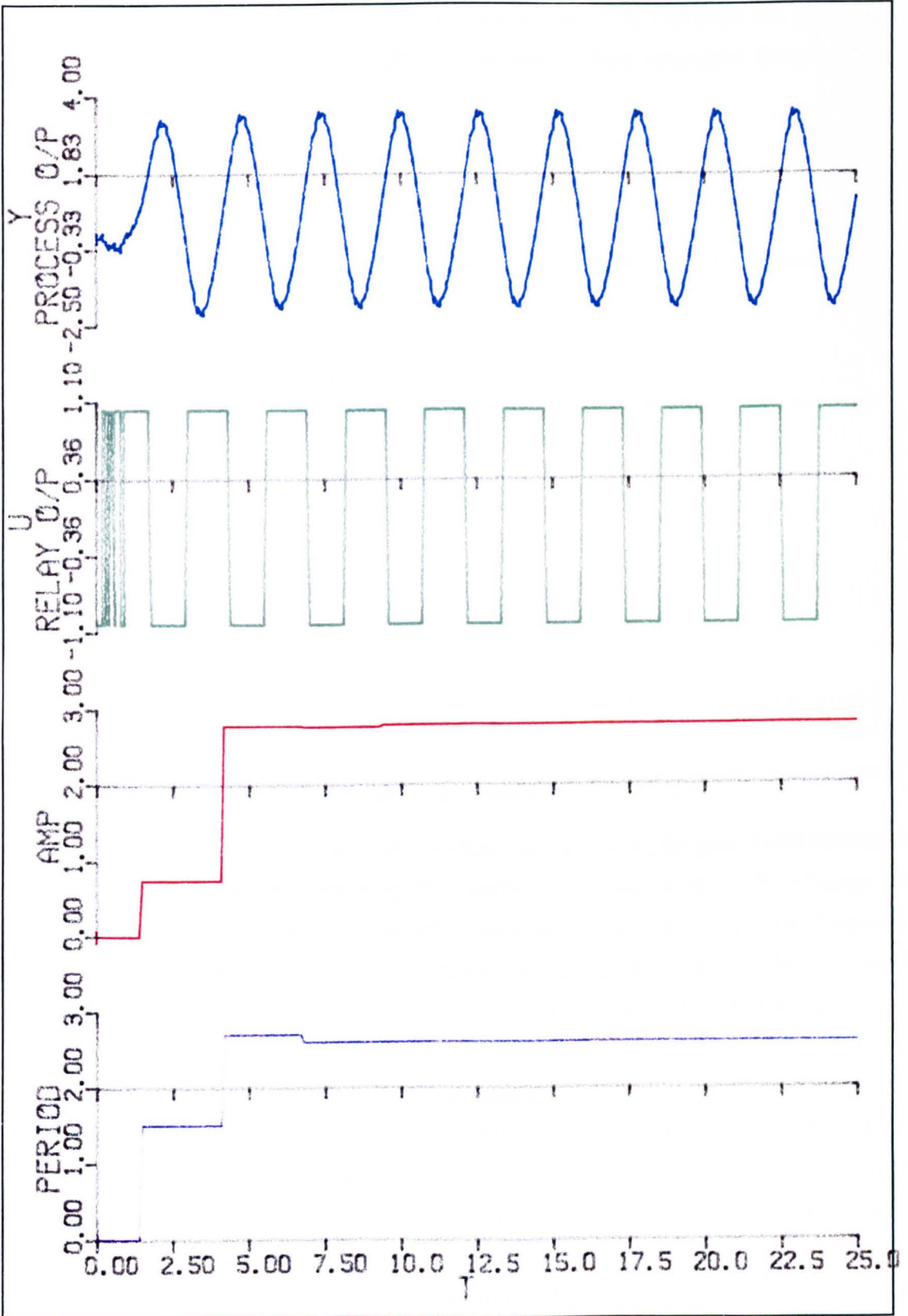


Figure 5.13 Simulation of the tuning operation for equation (5.9).

shows the expected $\frac{1}{4}$ -wave damped response, while the automatically tuned PID has a limited overshoot before attaining steady-state. In contrast the inclusion of the Regula-Falsi produces a PID which has a fast response time and no overshoot.

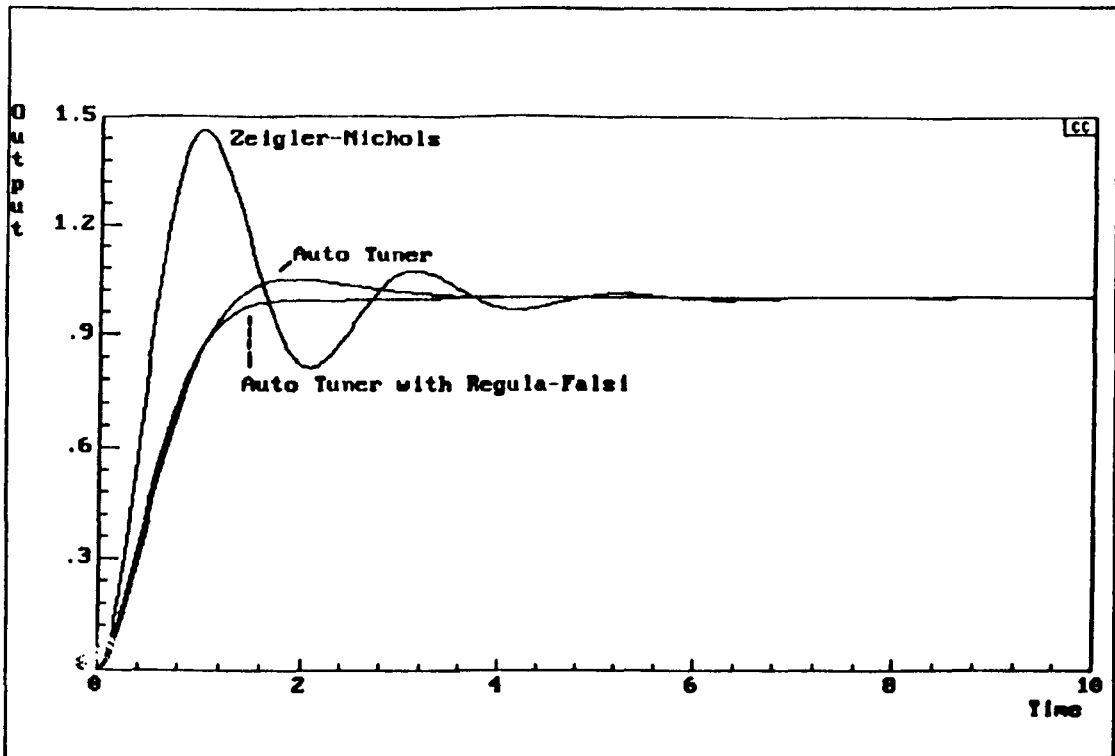


Figure 5.14 Responses of automatically tuned PID controller.

Figure 5.15 clearly shows the change in the 'gain' from the Regula-Falsi equation and the resultant modification to the nonlinearity output (U). The change in nonlinearity output produces a 'rogue' oscillation amplitude calculation, however the tuning procedure includes a check for a number of continuous and approximately equal amplitudes before it terminates the tuning procedure.

5.5.3. Summary of Transfer Function Results.

Figure 5.16 provides a comparison of the phase margins, settling times and peak values obtained from the various PID tuning methods described in the previous sections. Although the automatically tuned PID does not have the ideal response, say a 60° phase margin or minimum overshoot, it does however provide a set of PID tuning parameters after a single attempt with no manual intervention or knowledge of the process model.

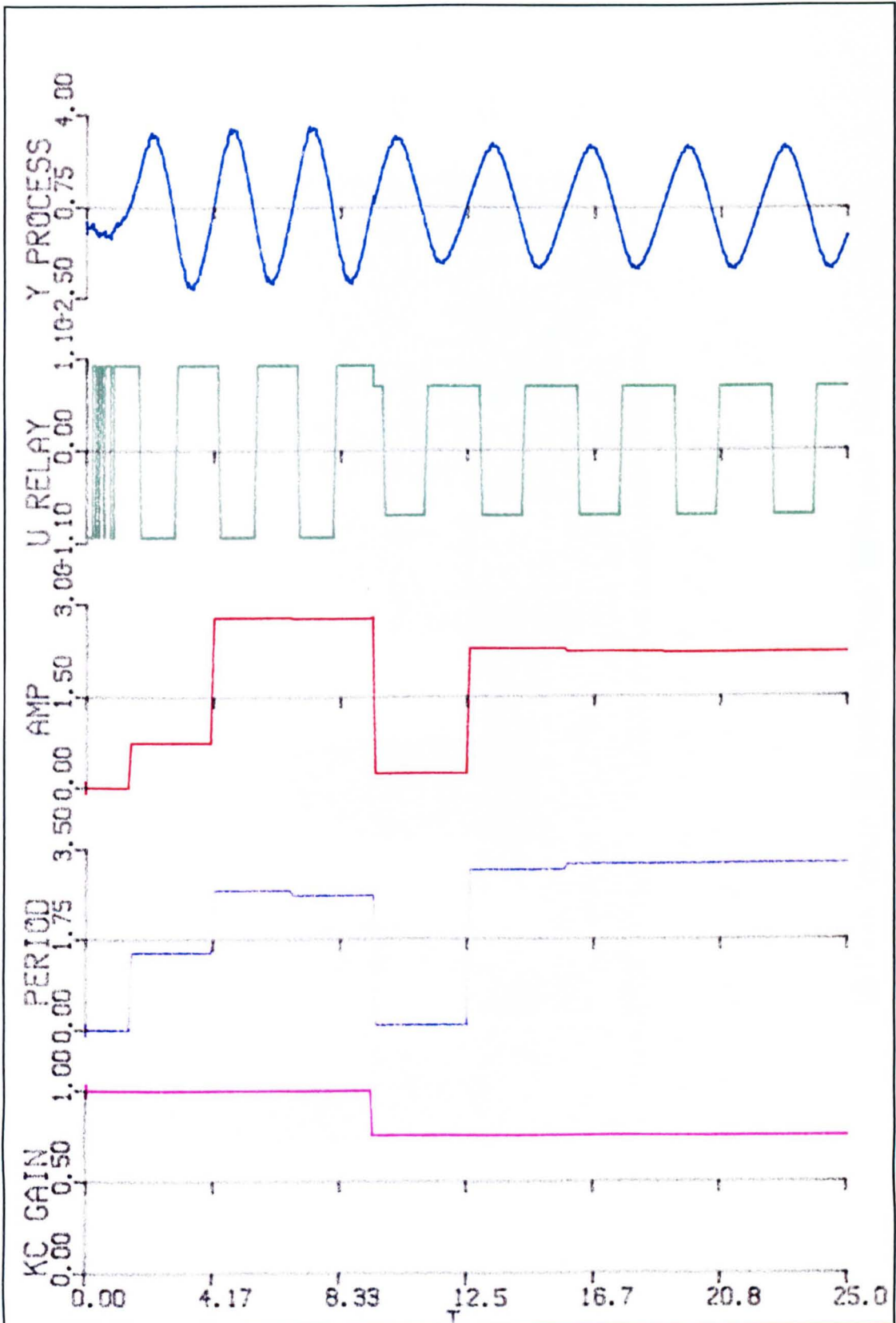


Figure 5.15 Effect of applying Regula-Falsi on tuning procedure transient.

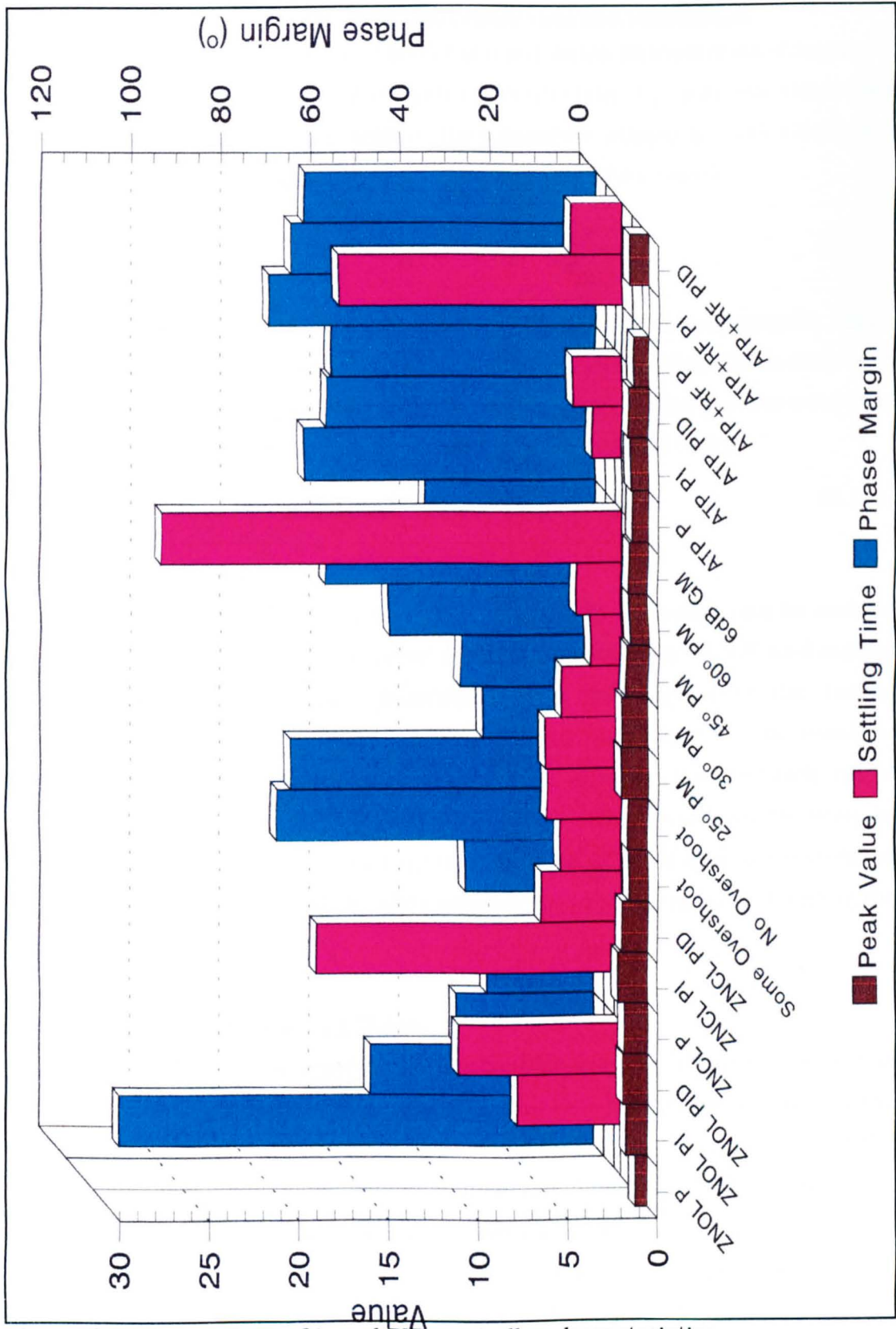


Figure 5.16 Comparison of tuned PID controller characteristics.

5.6. APPLICATION TO A FED-BATCH FERMENTATION (MODEL I).

A simulation of the mathematical model of a fed-batch fermentation (Chapter 4) was performed. The dissolved oxygen concentration, C_L , was the controlled variable and the manipulated variable, the volumetric oxygen transfer coefficient (K_{La}), represented a change in air flow rate and/or stirrer speed:

$$\frac{dC_L}{dt} = K_{La}(C^* - C_L) - \frac{\mu X}{Y_{O_2}} \quad (5.10)$$

where Y_{O_2} is the oxygen yield coefficient for growth on a glucose substrate. Since the model is for a fed-batch fermentation, an exponential feed profile is used with the assumption that 0.5g of yeast is produced for each gram of glucose substrate consumed (taken from $Y_{xs}=0.5$); using equations (4.21) and (4.22)

$$\text{Total Substrate Consumed} = 2X_0(e^{\mu t} - 1) \quad (5.11)$$

5.6.1. Manually Tuned Controller.

The result of many attempts at manually tuning a PI controller can be seen in Figure 5.17, where both the dissolved oxygen concentration (NCLP) and oxygen transfer coefficient (KLA) are illustrated. The final values of the tuning parameters chosen in this case were $K_p=1.5$ and $T_i=3.16 \times 10^{-4}$. The result of applying the same controller tuning parameters, used for the manually tuned process (Figure 5.17), to the fed-batch process with noise can be seen in Figure 5.18. These results show that the inclusion of noise onto the controlled variable provides a more realistic simulation of the process without changing the basic system.

5.6.1.a. Inclusion of Gaussian Noise.

Unlike the on-line measurement of dissolved oxygen concentration, which is notoriously noisy, the previous result represents an ideal situation in that the process simulated has no measurement noise included. Thus for most of the simulations conducted, the process simulation description was modified to accommodate an element of noise. This noise signal was added to the dissolved oxygen value before being compared to the set point value to provide the error signal, and was achieved by using the ACSL Gaussian function:

$$\text{GAUSS}(\mu_p, \sigma_p)$$

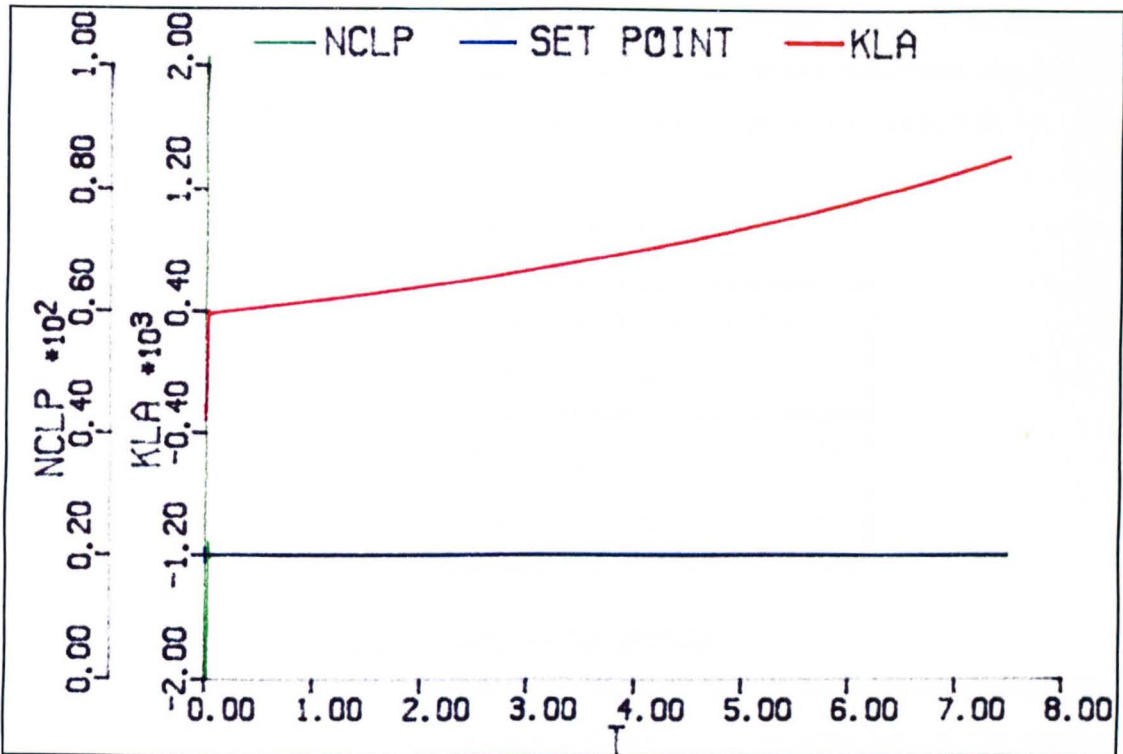


Figure 5.17 Manually tuned PI controller on a fed-batch fermentation.

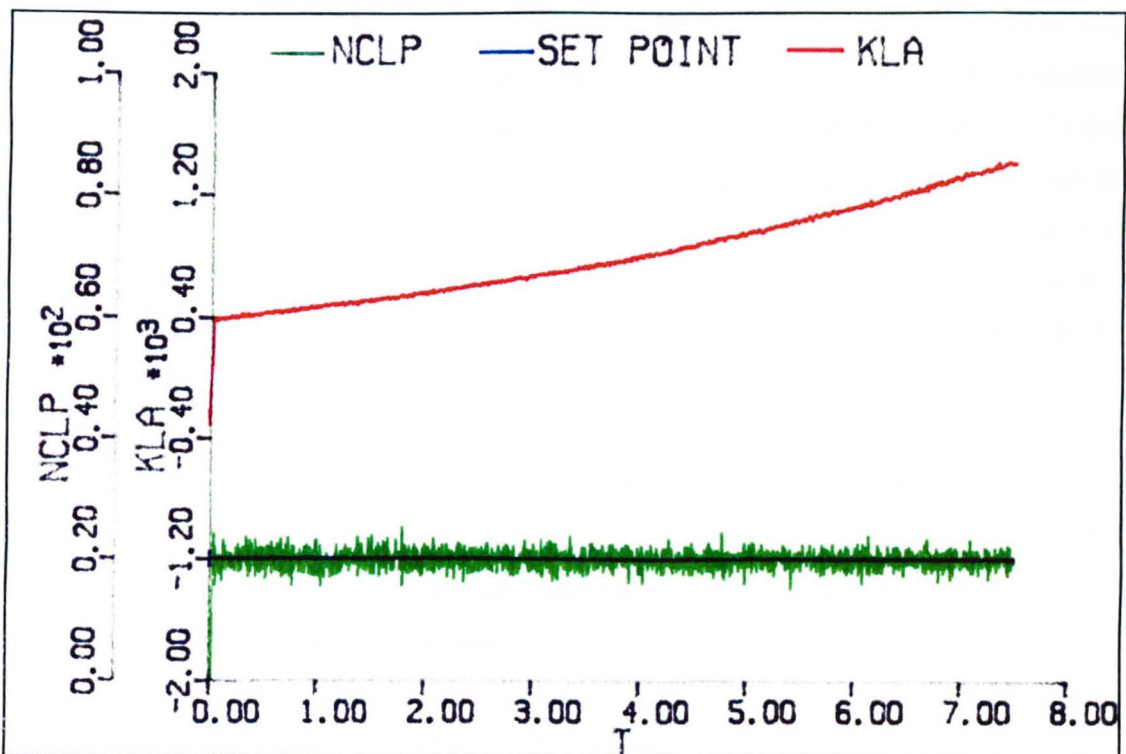


Figure 5.18 Manually tuned controller on process with simulated noise.

where μ_p is the mean of the data and σ_p is the standard deviation. This function provides a normally distributed random noise signal. When analyzed, the output from this function was found to have the properties given in Table 5.8.

Table 5.8 Statistical analysis results for noise data.

Property	Required Value	Actual Value	Error
μ_p	0.0	0.0081	0.8 %
σ_p	1.0	0.9786	2.1 %

5.6.2. Automatic Tuning Procedure: Single Tuning.

The first simulation test of the automatic tuning procedure was on a noise free fed-batch fermentation, where the tuning procedure was activated at the start of the fermentation ($T=0.0$ hours). The results illustrate that the tuning procedure is only active for a relatively short time period (Figure 5.19), and that the controller parameters produced provide a controlled variable performance comparable with the manually tuned process, illustrated earlier. Closer inspection of the operation of the simulated automatic tuning procedure can be seen in Figure 5.20. The plot of the variable NFLAG indicates when the tuner is on ($NFLAG=0.0$) and when it is off, ($NFLAG=1.0$). This approach to the control of the tuning procedure was required owing to the form of the ACSL Boolean-logic statement

IF (*check variable*) THEN '*procedure for true*'

which requires that *check variable* is TRUE. The manipulated variable (KLA) switches between the upper and lower limits causing an oscillation on the controlled variable (NCLP). Once the tuning phase has completed, the tuned PID controller is reapplied to the system.

The tuning procedure applied to dissolved oxygen concentration control during a simulated fed-batch fermentation was also tested with the addition of noise onto the controlled variable (Figure 5.21). The tuning procedure again develops a controller which maintains the oxygen concentration about the set point with

a performance comparable to the manually tuned controller.

Table 5.9 provides a comparison of the different tuning parameters used for the simulation results provided. Clearly the same manually tuned controller was used for both the noiseless and noisy process. Although the same tuning procedure characteristics were used for both the noisy and noiseless systems, different PID parameters were obtained. This can be explained by the calculation of the oscillation amplitude, since the addition of noise will produce a slightly different amplitude and hence alter the parameter calculations.

Table 5.9 Summary of tuning parameters used.

	K_p	T_i	T_d	Process
Figure 5.17	1.5	316×10^{-6}	0.0	No noise. Manual.
Figure 5.18	1.5	316×10^{-6}	0.0	Noise. Manual.
Figure 5.19	5.0	202×10^{-6}	489×10^{-6}	No noise. Tuning procedure.
Figure 5.21	6.53	101×10^{-6}	244×10^{-6}	Noise. Tuning procedure.

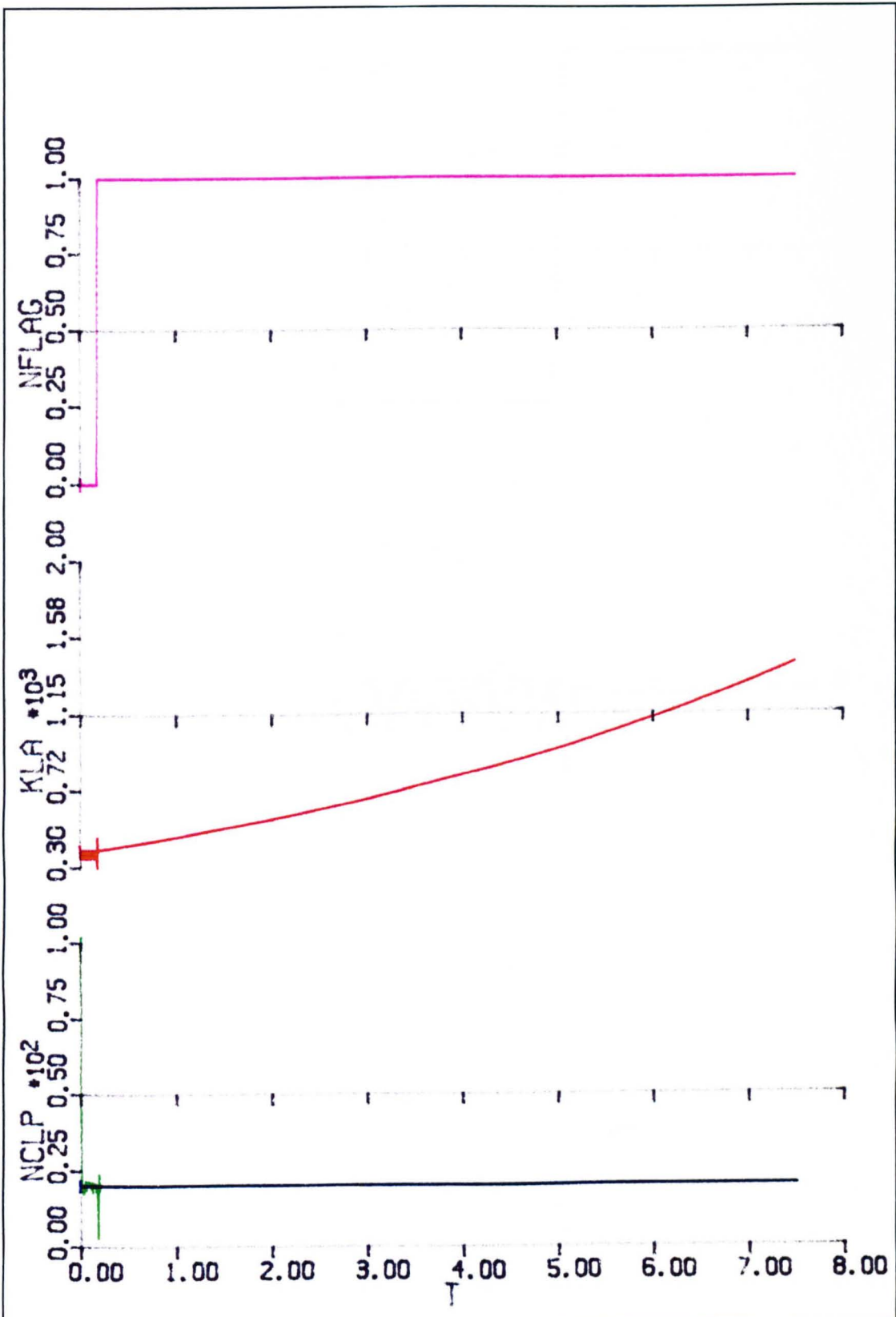


Figure 5.19 Single application of the automatic tuning procedure.

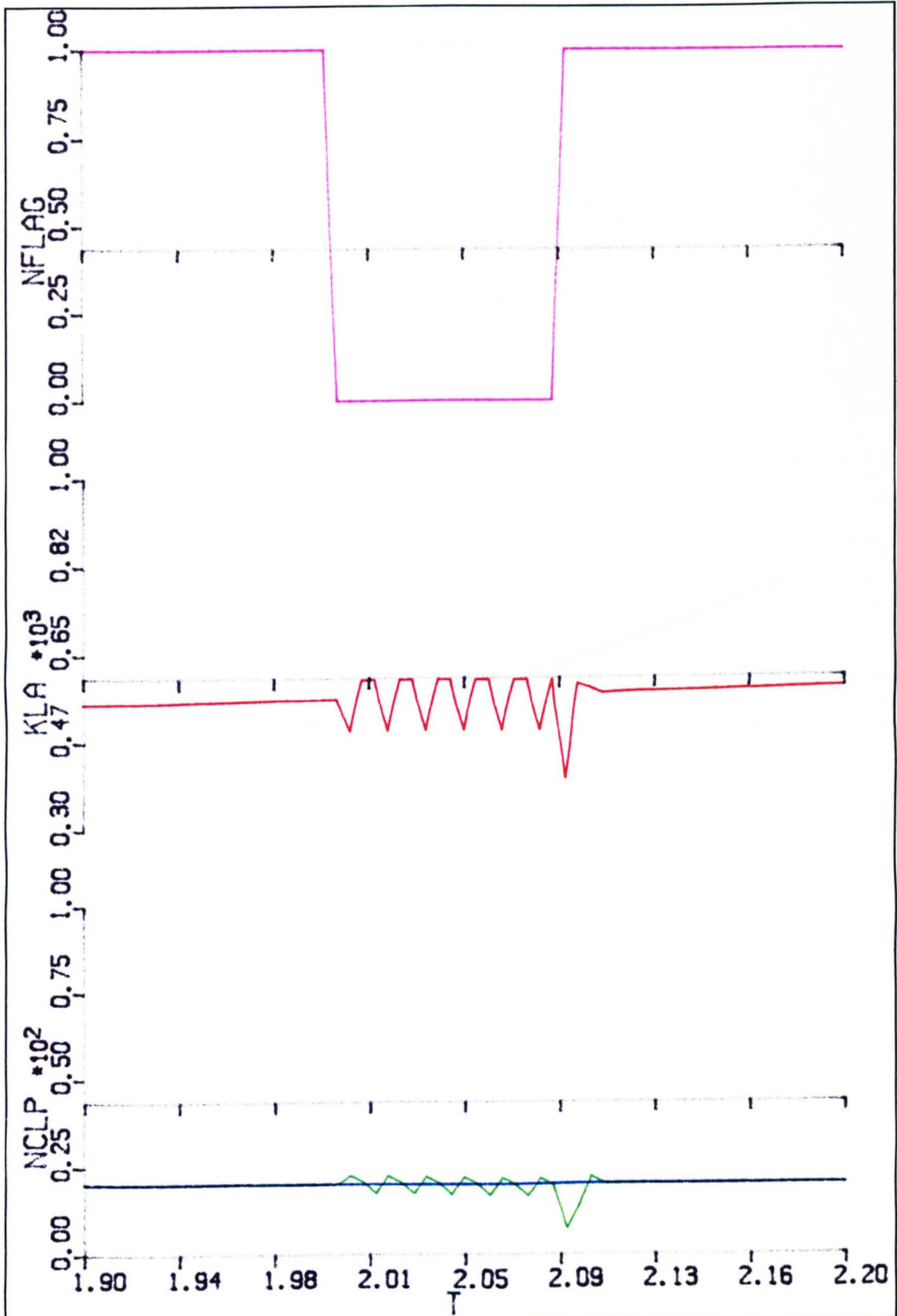


Figure 5.20 Operational view of the automatic tuning procedure.

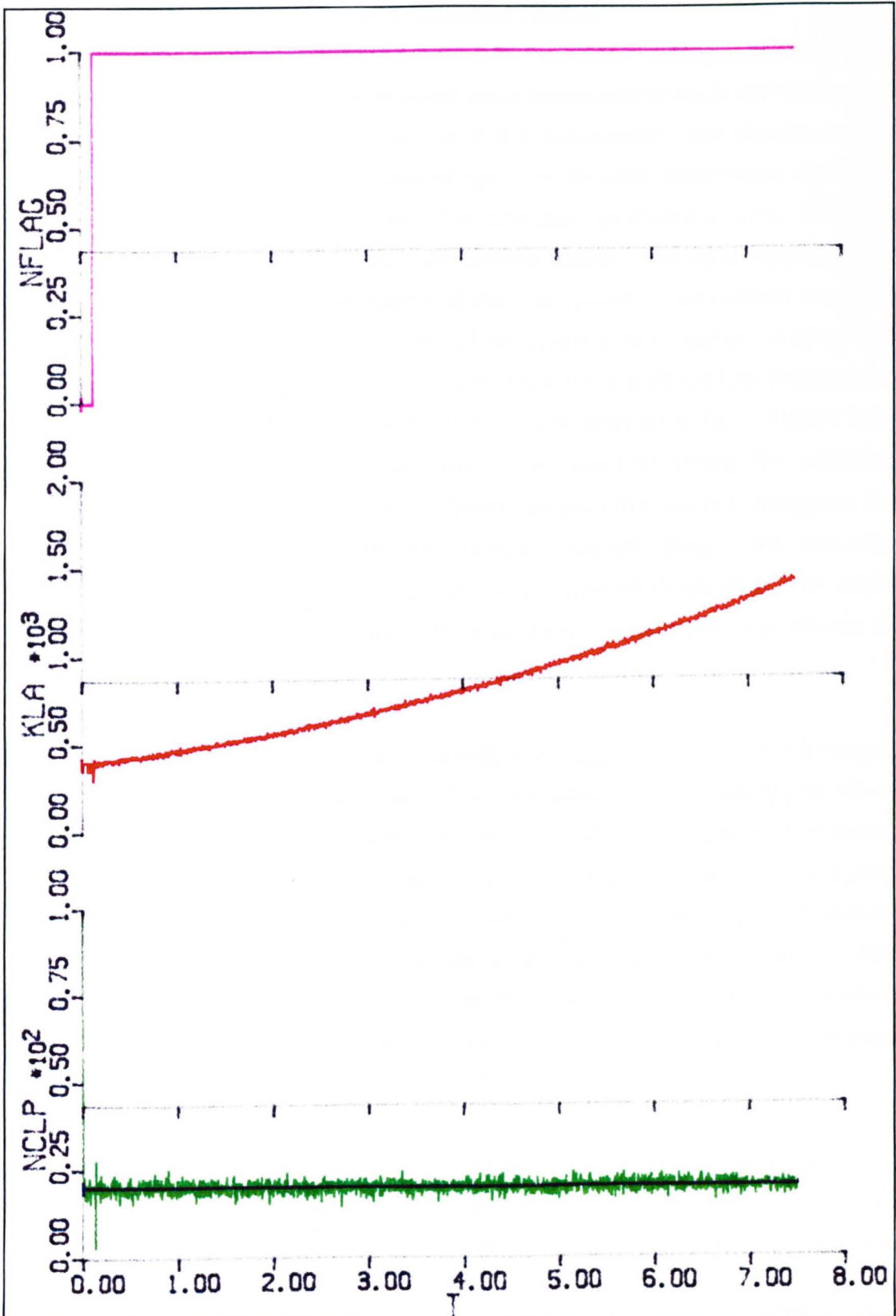


Figure 5.21 Automatically tuned controller on fed-batch process with noise.

5.6.3. Automatic Tuning Procedure: Multiple Tuning.

In these tests a number of activations of the automatic tuning procedure were simulated on the fed-batch fermentation simulation; where each activation was initiated at pre-specific time ($T=0.0, 2.0, 4.0$ & 6.0 hours). The results can be seen in Figure 5.22, where the plot of variable 'NFLAG' illustrates when the tuning procedure was active ($NFLAG=0.0$) and inactive ($NFLAG=1.0$). It will be seen from the result that regulatory control of the dissolved oxygen concentration has been maintained for the duration of the simulation. The system was also simulated with the noise element included, and produced a similar result to that of the noiseless process (Figure 5.23). After each tuning phase has terminated, the tuning parameters remain constant until the next retuning. Figure 5.24 illustrates the derived values of the controller parameters during the noiseless simulation. It is noticeable that the proportional gain increases throughout the simulation period, although the increase is less as the time progresses. Thus the tuning procedure is following the change in the process dynamics. The ACSL program for the tuning procedure with a fed-batch fermentation is shown in Listing 5.2.

5.6.4. Disturbance Tests.

Two disturbances were investigated: firstly a change in the dissolved oxygen concentration set-point and secondly a load disturbance. The tuning procedure was arranged to automatically commence operation whenever there was a change in the set-point (this includes the start of the simulation since the set-point prior to $T=0.0$ is assumed to be 0% while it is 20% at $T=0.0$). The initial dissolved oxygen concentration set-point of 20%, was changed to 45% after 2.0 hours. The result, shown in Figure 5.25, indicates that the procedure is capable of retuning on a change in set-point, which corresponds to a probable change in the process dynamics owing to a change in operating conditions.

The load disturbance was simulated by changing the maximum dissolved oxygen concentration, C' (CS on the graph), for a short time (that is, 0.1 hours). Two disturbances were used, allowing for both an increase and decrease in the maximum dissolved oxygen concentration. Figure 5.26 shows the result of the tuning procedure being activated on the performance of the dissolved oxygen concentration, C_L . This simulation produces a total of three activations of the

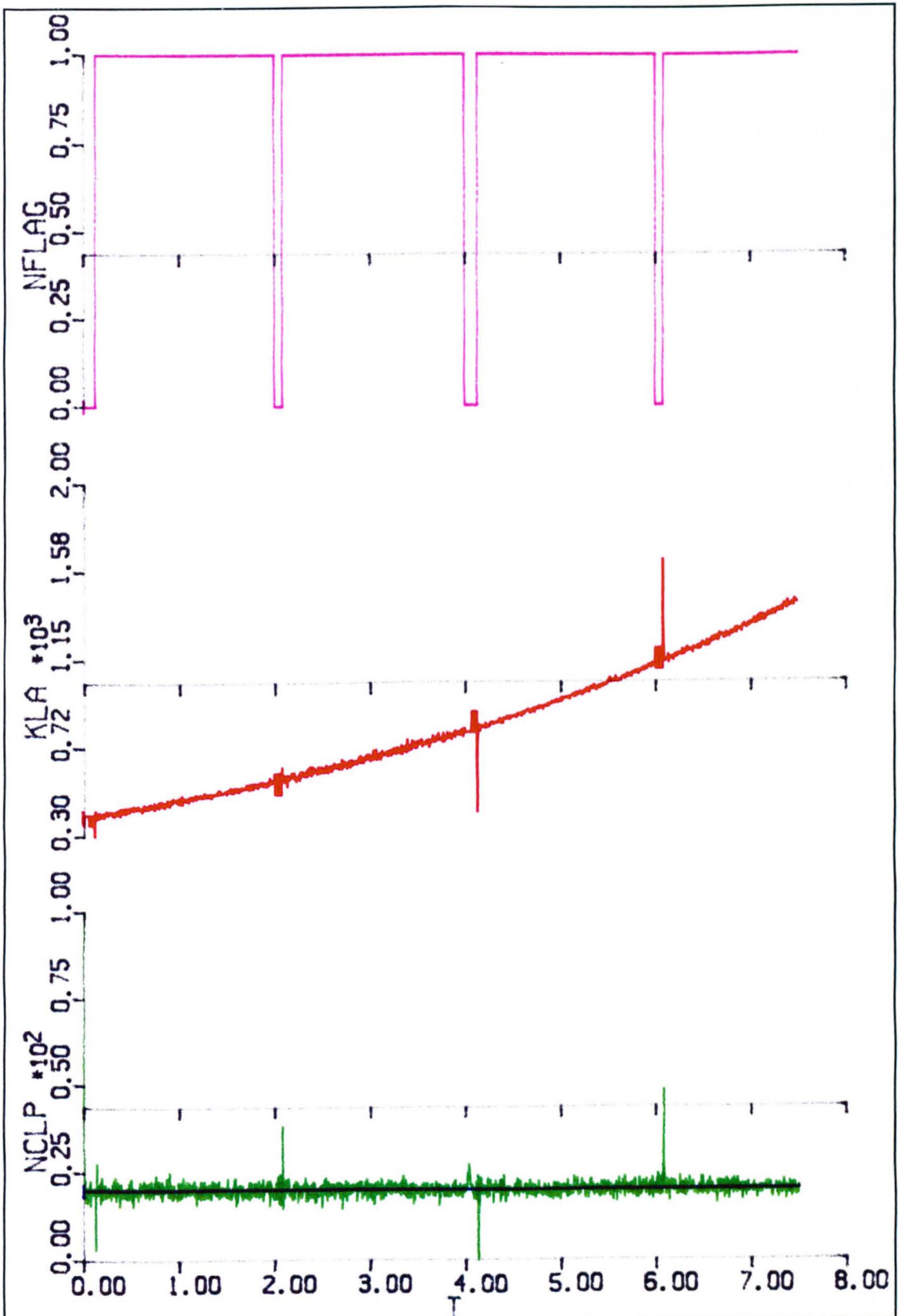


Figure 5.22 Multiple tuned fed-batch process with noise.

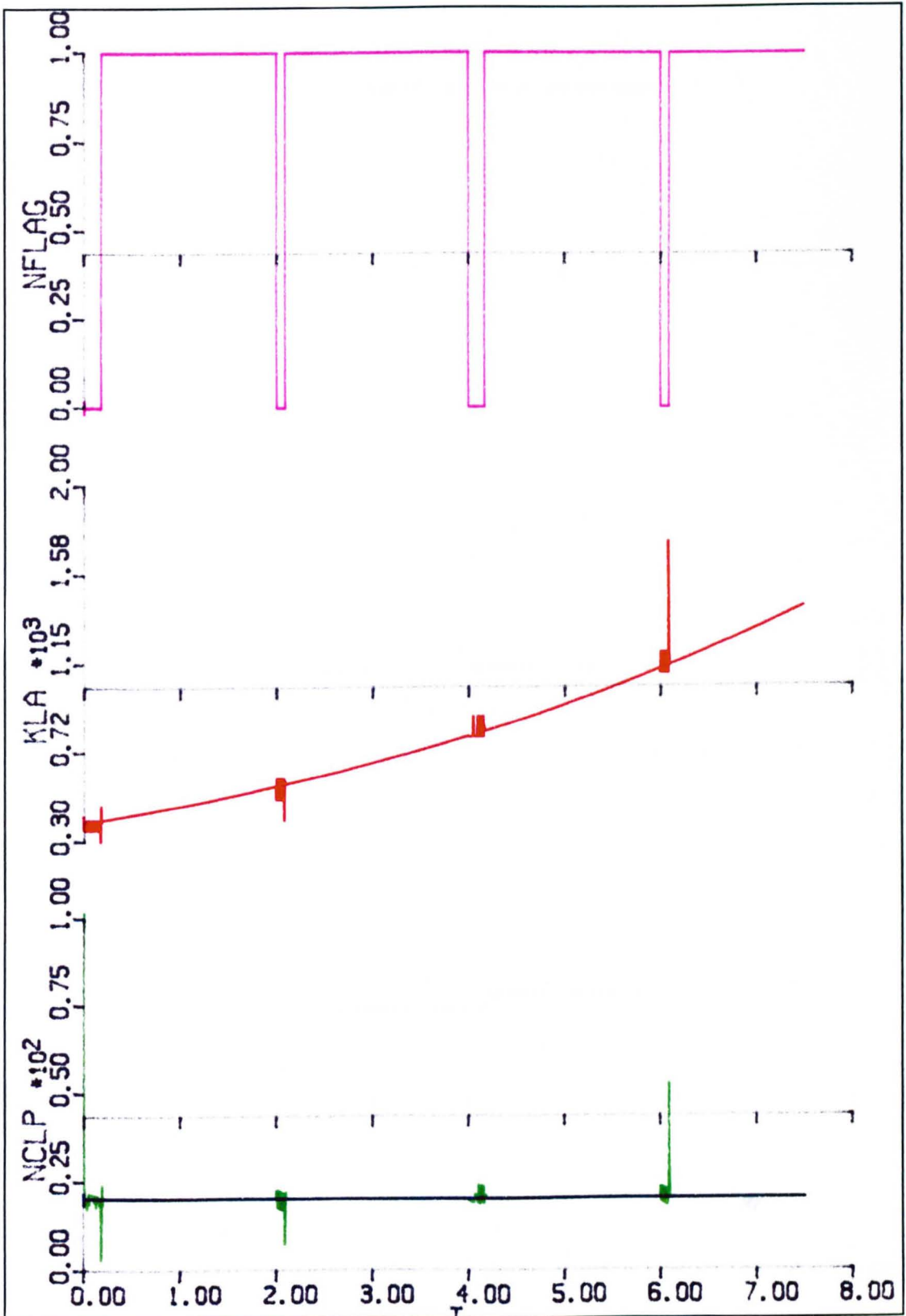


Figure 5.23 Multi-tuning of the automatic tuning procedure on a fed-batch simulation.

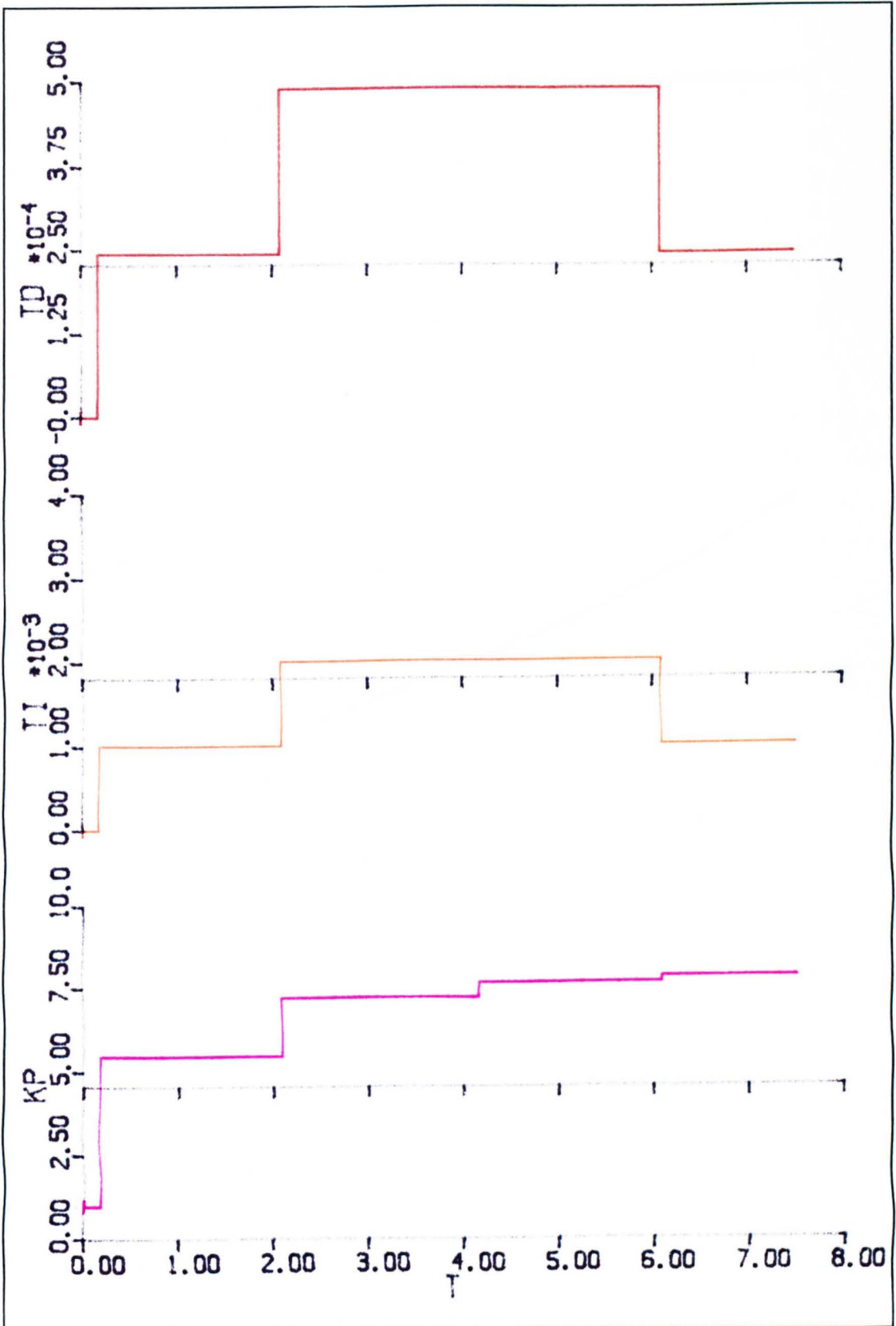


Figure 5.24 Change in PID values.

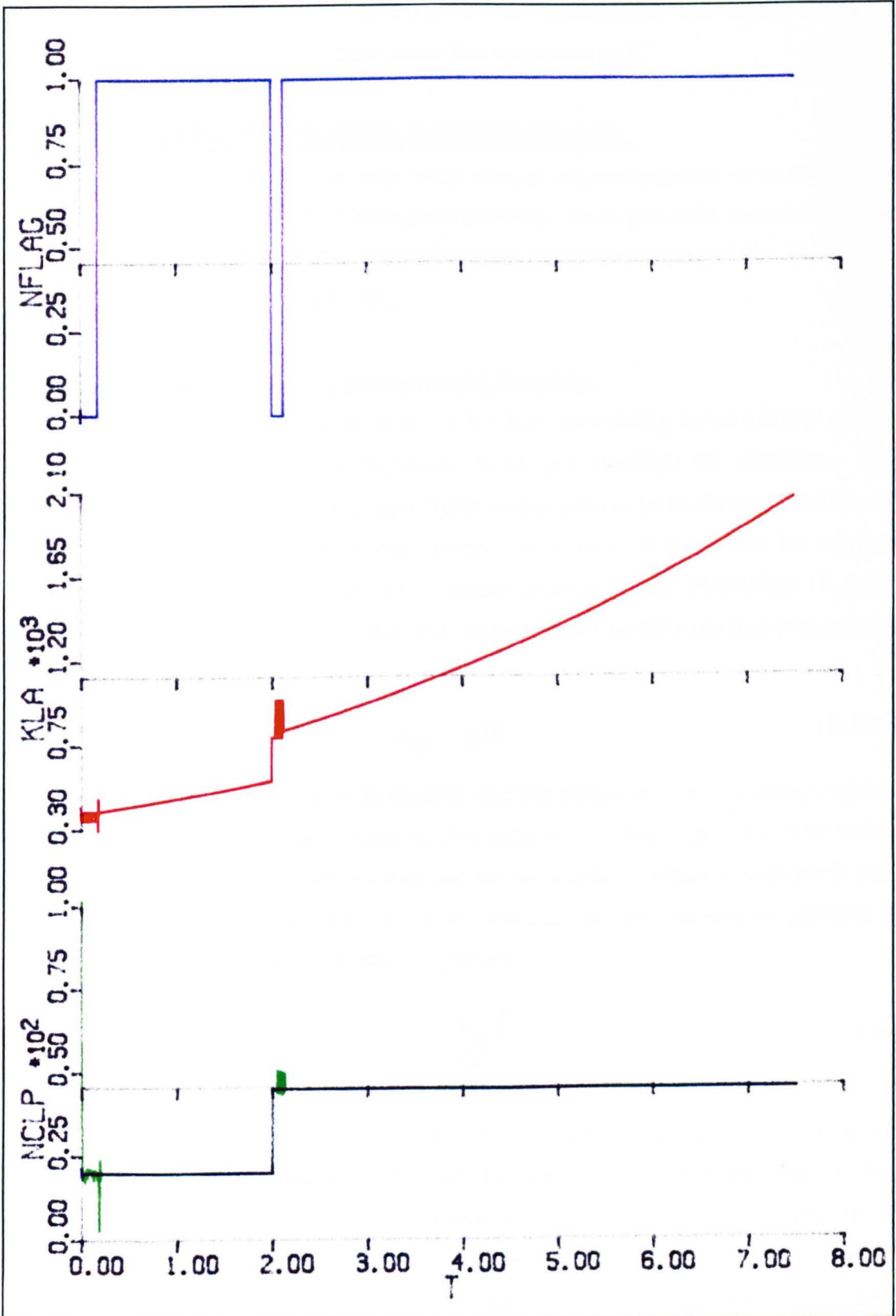


Figure 5.25 Response for a set-point change.

tuning procedure; firstly at the start of the simulation, secondly when C' increases and finally a short time after the decrease in C' .

5.7.ENHANCEMENT OF PROCESS REPRESENTATION.

This fermentation model is a relatively simple representation of a fed-batch process, concentrating on the biological process. It is possible to enhance the model to include some of the variables and characteristics of the fermenter vessel, actuators and transducers.

5.7.1. Use of Stirrer Speed as Manipulated Variable.

Agitation of the fermenter broth is used for both providing a completely mixed broth, and to maintain the air bubbles circulating through the medium. The faster the speed of rotation the longer the bubbles take to pass through the liquid in the fermenter before exiting, and hence more time is available for oxygen transfer or absorption to occur. The overall mass transfer coefficient (K_{La}) for such vessels has been shown [5.4 & 5.5] to be related to the speed of revolution, N , by

$$K_{La} = \gamma\sqrt{N} \quad (5.12)$$

The proportionality constant, γ , is unique to each fermenter vessel design and is dependent upon the size and shape of the baffles used for agitation. The value for γ quoted for the particular vessel used for the on-line experimental work was 64 [5.6]. Equation (5.12) was included within the simulation to provide a representative stirrer speed, N , for the process:

$$N = \left(\frac{K_{La}}{64} \right)^2 \quad (5.13)$$

A typical result can be seen in Figure 5.27, which compares with that of Figure 5.17 showing only K_{La} . It can be seen that the dissolved oxygen concentration response for both versions (K_{La} or stirrer as the manipulated variable) are very similar. There is a decrease in the dissolved oxygen concentration level from $T=5.5$ hours owing to the saturation of the allowed stirrer speed at 1000 rpm. This relationship between K_{La} and N assumes that all

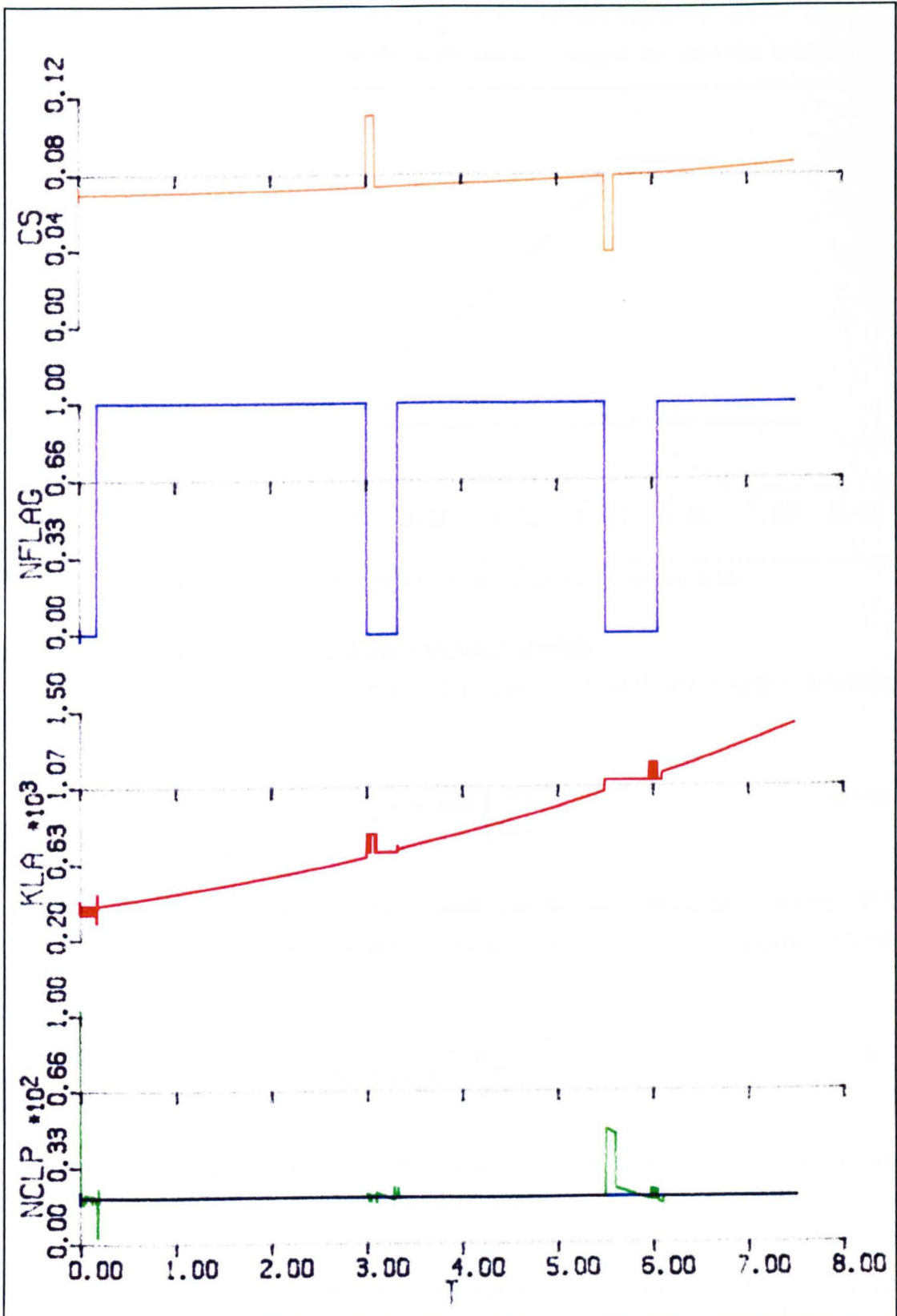


Figure 5.26 Automatic Tuning Procedure applied during load disturbances.

of the oxygen transfer into the broth occurs through agitation alone, however some proportion will occur with the addition of sparged air into the broth.

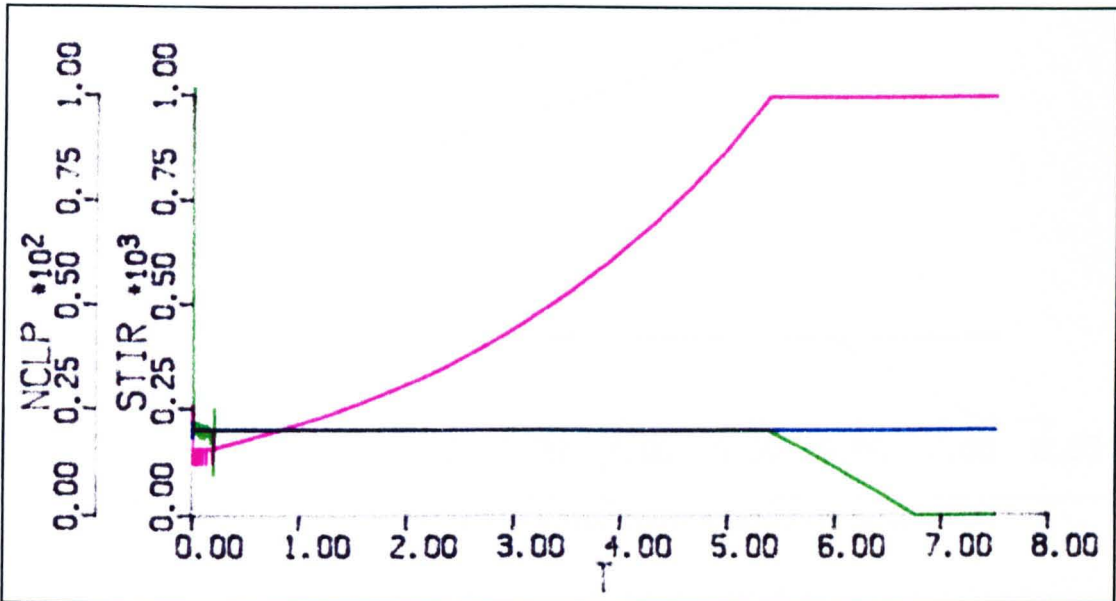


Figure 5.27 Inclusion of stirrer speed as the manipulated variable.

5.7.2. Use of Air Flow Rate as Manipulated Variable.

The relationship between the input air flow rate and the oxygen transfer coefficient can be given by

$$K_{La} = 0.0023 \left(\frac{v_s}{d_b} \right)^{1.58} \quad (5.14)$$

where d_b is the mean bubble diameter and v_s is the superficial gas velocity. If it is assumed that the mean bubble diameter is 0.025 m, then equation (5.14) becomes

$$v_s = 0.025 \left(\frac{K_{La}}{0.0023} \right)^{0.633} \quad (5.15)$$

The result of using the superficial gas velocity as the manipulated variable can be seen in Figure 5.28 (plotted as variable AIR).

As with the K_{La} - N relationship, the K_{La} - v_s relationship assumes complete oxygen transfer occurring through air input alone. In trying to represent an on-line implementation, the volumetric oxygen transfer coefficient, K_{La} , was used as the

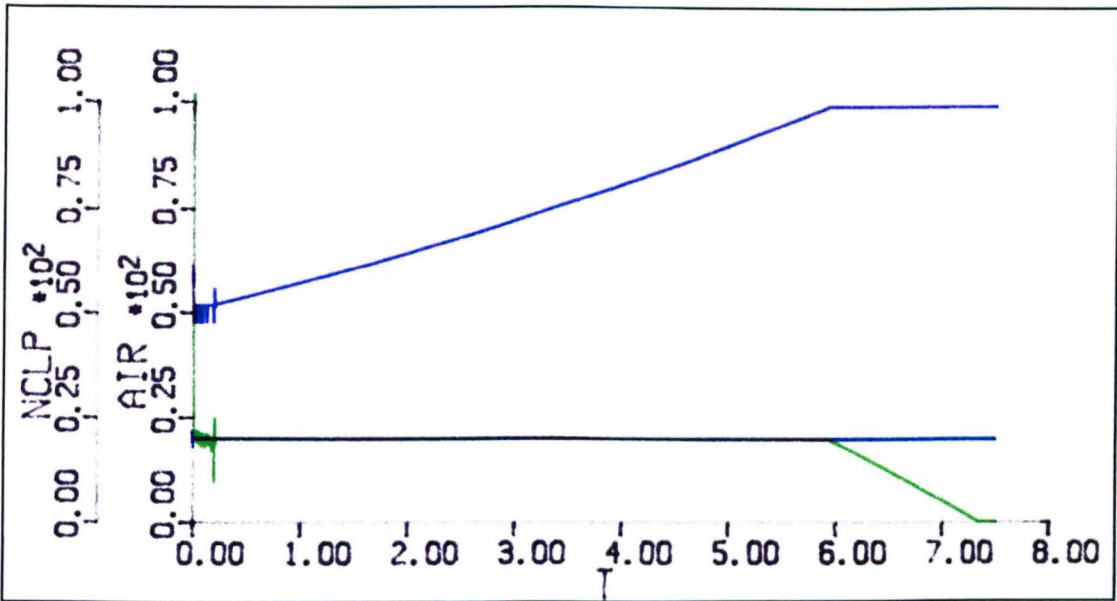


Figure 5.28 Inclusion of gas velocity as the manipulated variable.

manipulated variable. This decision can be justified since some unknown proportion of the oxygen transfer occurs with agitation and the remainder through air input

$$K_{La} = \eta K_{La}^{stirrer} + (1-\eta)K_{La}^{air} \quad (5.16)$$

where the factor η is an unknown and variable quantity.

5.8. APPLICATION TO A BATCH FERMENTATION (MODEL II).

The batch mode fermentation has two distinct growth phases; initially growth on the glucose substrate producing cells and ethanol, followed by reduced cell growth on the produced ethanol. Thus any fixed system used for the control of a fed-batch fermentation will be inadequate for the batch process since a controller used for dissolved oxygen regulation at the start of the fermentation will be inappropriately tuned for the second phase. Thus at least two sets of PID tuning parameters are required for the batch fermentation.

5.8.1. Manual Tuning of the Dissolved Oxygen Loop.

A PI controller was manually tuned for each of the two growth phases simply to maintain set-point regulation, with $K_p=200$, $T_i=0.05$ for the first phase, and $K_p=50$, $T_i=0.01$ for the second; Figure 5.29 also illustrates the concentration of

the glucose substrate to provide an indication of when the change in growth phases occurs.

The response of this configuration was the best that could be obtained by repeated experiment, and is recognised as extremely poor regulation, indicating that standard empirical methods do not succeed. At $T=1.89$ hours the dissolved oxygen level falls to zero; this would result in the death of the Yeast cells and thus the premature termination of the fermentation. The simulation is allowed to continue to provide an indication of the 'typical' response to be expected from the second phase PID controller. In this second phase, the dissolved oxygen level is eventually maintained around the required set-point; however for the first 1.65 hours after the initiation of the second phase controller, there is an extremely high overshoot of the dissolved oxygen level. This overshoot is acceptable from a physiological aspect since microorganisms can grow aerobically as long as the dissolved oxygen level is above a known critical level (see Chapter 4). However, inspection of the manipulated variable (K_{La}) shows that there is an input to the process (for example an air flow rate) which is undesirable from an economic consideration. Hence it can be stated that the simulation of a set of manually determined controller parameters provide an unacceptable control of the concentration of dissolved oxygen during both phases of a batch fermentation. The PID parameters determined by the tuning procedure for each growth phase are shown in Table 5.10. There is a significant difference between the two sets, highlighting the need for a retuning of the controller.

Table 5.10 Derived PID values.

	First Tuning	Second Tuning
K_p	0.374	0.473
T_i	32.34×10^{-3}	16.17×10^{-3}
T_d	7.85×10^{-3}	3.92×10^{-3}

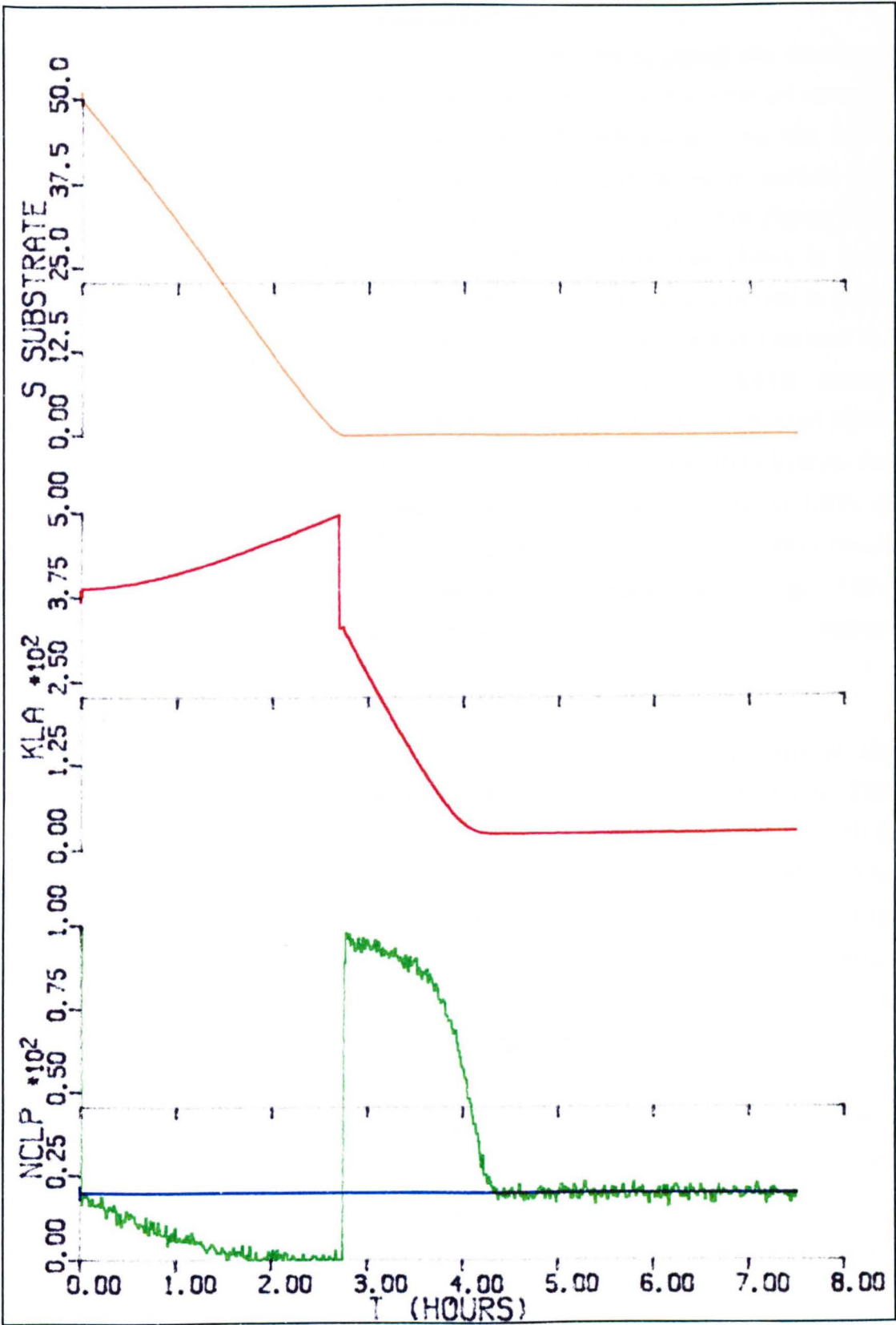


Figure 5.29 Manually tuned PI controller for each phase.

5.8.2. Single Application of the Tuning Procedure.

The difficulty in manual tuning could be overcome by applying the developed tuning procedure. The tuning procedure should be activated at least once for each growth phase, and ideally at the start of each phase. In the initial simulation trials the same nonlinear element characteristics were used in both tuning procedure activations, with the resultant response shown in Figure 5.30. The tuning oscillation disturbance obtained during the first phase is quite noticeable although acceptable for the control loop. The tuning period is much longer than that for a fed-batch process, and once PID control is attained the regulation of the level of dissolved oxygen starts to deteriorate almost immediately. In contrast the same nonlinearity applied during the second phase produces an extremely positive response on the controlled variable; that is, the level of dissolved oxygen concentration becomes saturated at almost 100% at which it remains and the tuning procedure fails to stop tuning. This result provides an indication that the automatic tuning procedure can be applied to a batch fermentation with a small degree of success however it is obvious that an improved response is required.

The first improvement which can be achieved is the adjustment of the characteristics of the nonlinearity used for the second growth phase tuning. This was accomplished by changing the characteristics from $\pm\beta=1.0\%$, $\pm E=10.0$, $U_{ref}=0.0\%$ and $y_{ref}=30.0$, to $\pm\beta=1.0\%$, $\pm E=50.0$, $U_{ref}=0.0\%$ and $y_{ref}=400.0$. The result of the application of this system can be seen in Figure 5.31. For this configuration the induced oscillations are less severe during the second tuning, although there is still a significant delay of 1.4 hours between the reintroduction of the PID and the attainment of set-point regulation.

This only leaves the problem with tuning the first growth phase, which is when the Yeast is in a highly active state growing on glucose and hence absorbing high levels of dissolved oxygen. Close investigation of the nonlinearity characteristic for the first tuning provides no solution for the first phase; since under all combinations the introduction of the tuned PID produces a response which eventually leads to a dissolved oxygen level of 0%, when only one application of the tuning procedure is made.

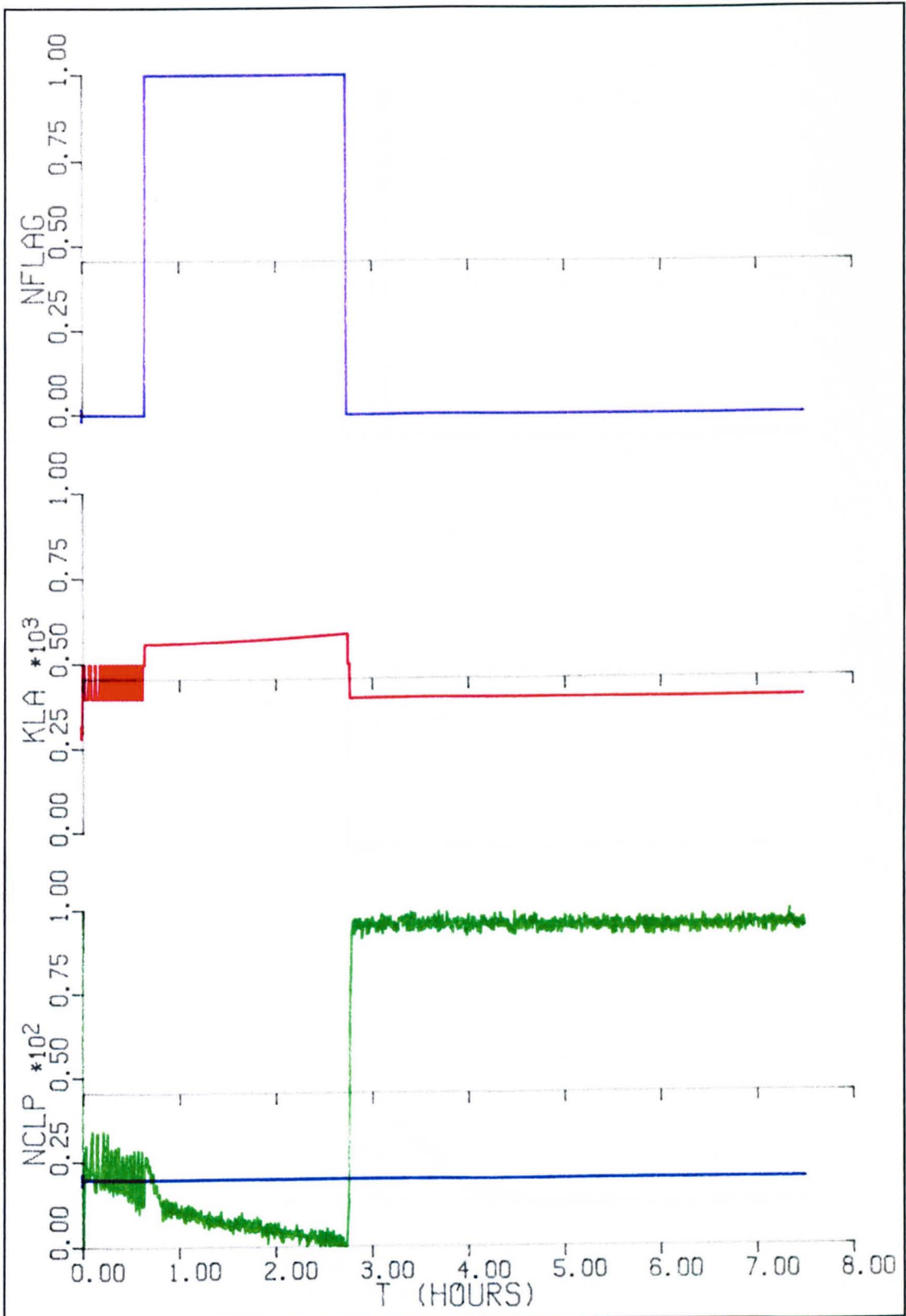


Figure 5.30 Same nonlinear element applied for both growth phases (including noise).

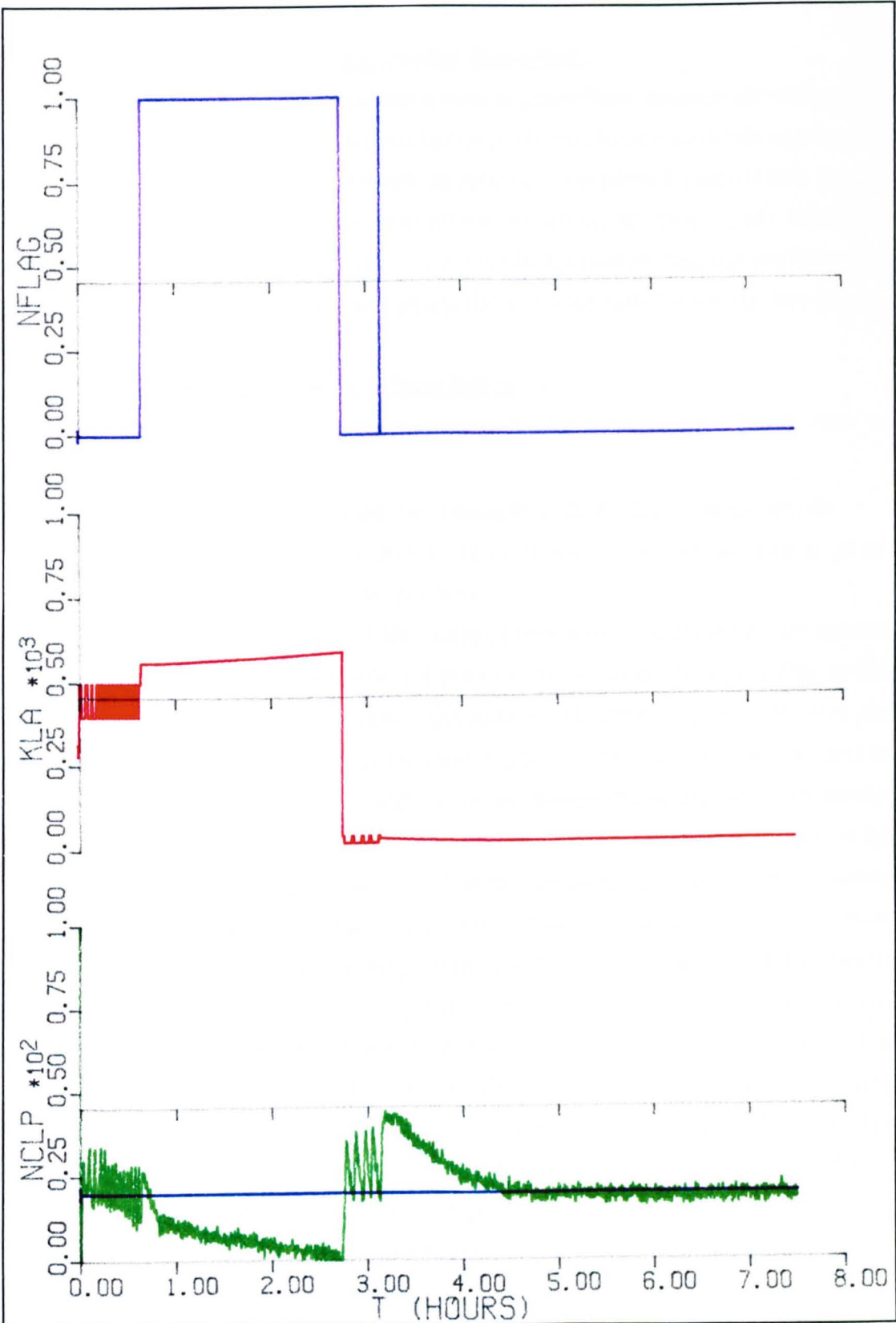


Figure 5.31 Modified nonlinearity for second tuner application.

5.8.3. Multiple Application of the Tuning Procedure.

The single application of the automatic tuning procedure, to each growth phase, does not provide a complete solution to the problem, hence multiple application of the tuning procedure is necessary during the complete fermentation period. This can be accomplished, in simulation at least, in two ways: firstly by activating the tuner on a time basis; or secondly by monitoring the performance of a process variable and retuning when the variable falls below the set-point.

5.8.3.a. Multiple Application on a Time Basis.

The activation of the automatic tuning procedure on a time basis can be performed by either:

- a) Use of a periodic time base, for example $T=0, 1, 2, \dots, n$ hours, or
- b) Use of a set of specific times defined with the use of any *a priori* knowledge available for the process.

The problem with using (a) is that the tuning procedure may have just completed prior to the change over to the second growth phase, thus the controller action would be unsuitable for the process dynamics. However, option (b) does not provide a general solution since it requires *a priori* knowledge which may not be available, or if available might be inappropriate owing to a degree of uncertainty; for example the change from growth phase 1 to phase 2 may occur between 3.0 and 4.5 hours depending upon the batch composition. Since the tuning procedure is only undergoing simulation trials option (b) offers the more appropriate solution. This arrangement has been simulated and the result provided in Figure 5.32, where the particular system had the tuning procedure activated at the arbitrary times of $T=0.0, 1.45, 2.71, 4.19$ and 6.19 hours. The change in value of the PID parameters after each application of the tuning procedure can be seen in Figure 5.33. There is little change in T_i and T_d after the second tuning, while K_p has a dramatic increase. During the ethanol consumption phase, K_p decreases only slightly, unlike the significant changes in T_i and T_d . These results show that there is a need for the automatic tuning procedure during a batch fermentation.

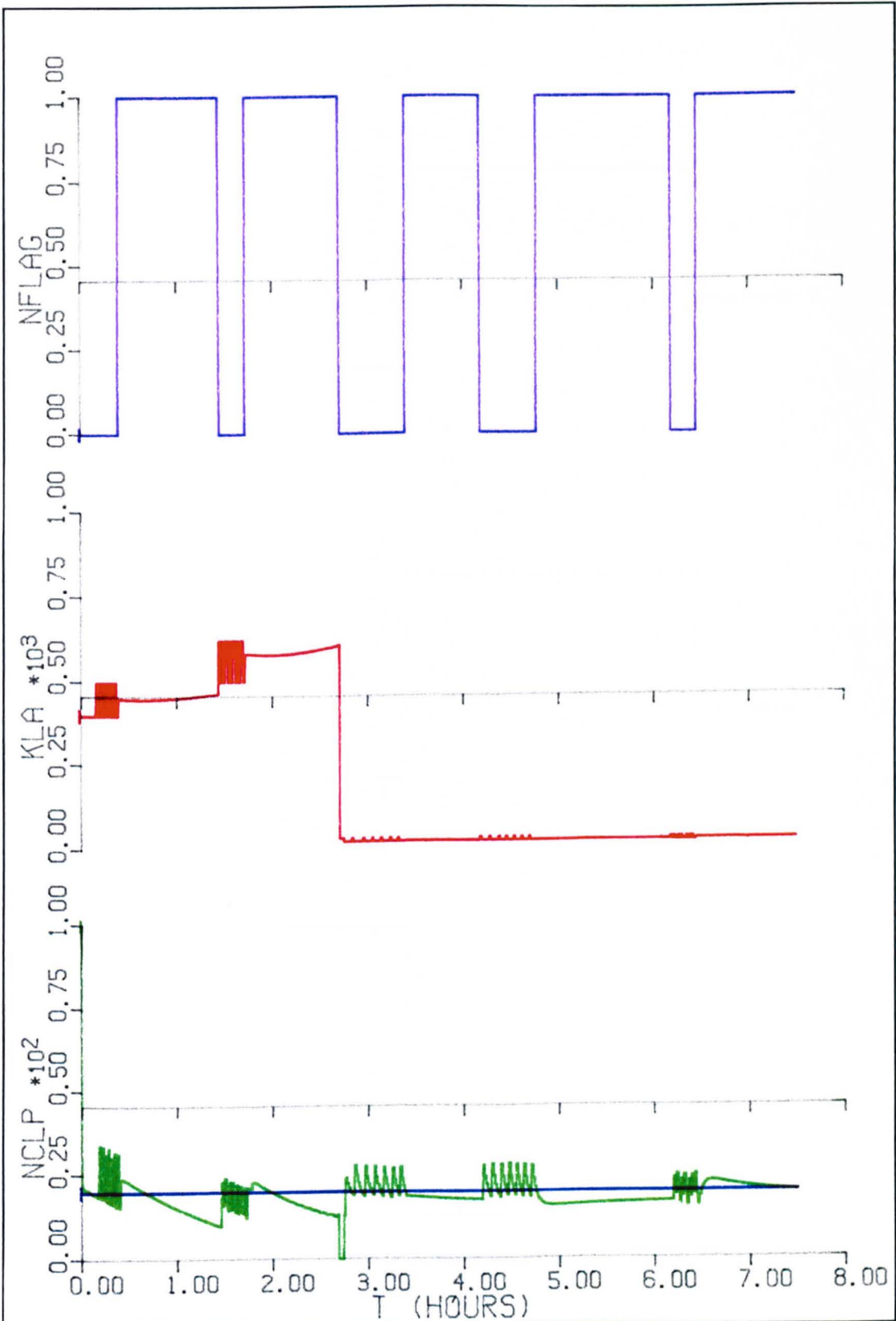


Figure 5.32 Specific time retuning of a batch fermentation (no noise).

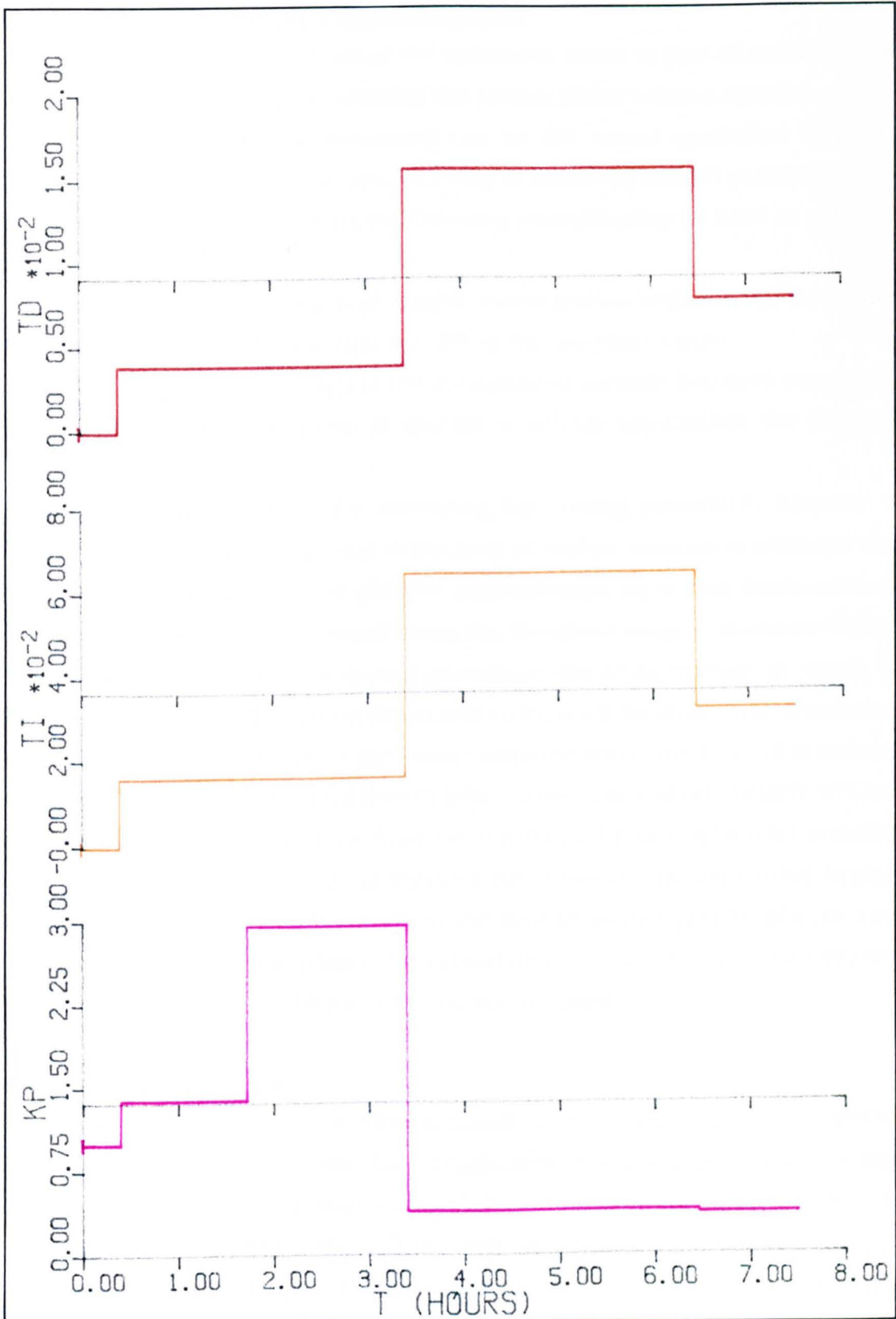


Figure 5.33 Change in PID value during a batch fermentation.

5.8.3.b. Multi-tuning on Process Performance.

An attractive option for activating the automatic tuner is that of monitoring a specific process variable and starting the tuning phase when a specific criteria is achieved. The variable monitored can be the actual controlled variable, manipulated variable or some other directly or indirectly related variable. Thus for the process considered here, the following examples may be used as possible scenarios:

- a) when the level of dissolved oxygen concentration begins to fall below the set point level; for example by 10% of the set-point value.
- b) when the rate of change of the manipulated variable becomes excessive.
- c) when the concentration of glucose substrate approaches the limiting factor of 0.28 g/l.

This last example is ideal for activating the tuning procedure; however a drawback of this type of concept is the lack of on-line sensors to measure the important variables such as glucose concentration in a real fermentation. Investigative tests were performed using the dissolved oxygen concentration as the activating trigger for the tuning procedure; the ACSL coding for which is given in Listing 5.3.. The result illustrated in Figure 5.34 shows the simulation of a number of activations of the tuner: initiated when the level of dissolved oxygen falls below the set point level of 20%. Observation of the variable NFLAG indicates that the tuner is active from $T=0.0$ to $T=1.55$ hours, which is excessive when compared to Figure 5.31 or Figure 5.32. However, the only other tuning occurs shortly before the change from the first to second growth phases and continues into the second phase. This simulation included the use of a different set of nonlinearity characteristics for the second phase.

5.8.4. Disturbance Tests.

As with the simulation of the fed-batch model, the batch model was subjected to a set of disturbance tests. The first of these step changes was a change in the dissolved oxygen concentration set-point, from an initial value of 20% to 45% and then down to 15%. Throughout this simulation the automatic tuning procedure was started when the value of the dissolved oxygen concentration fell below the set-point value by 10%. The result obtained is shown in Figure 5.35.

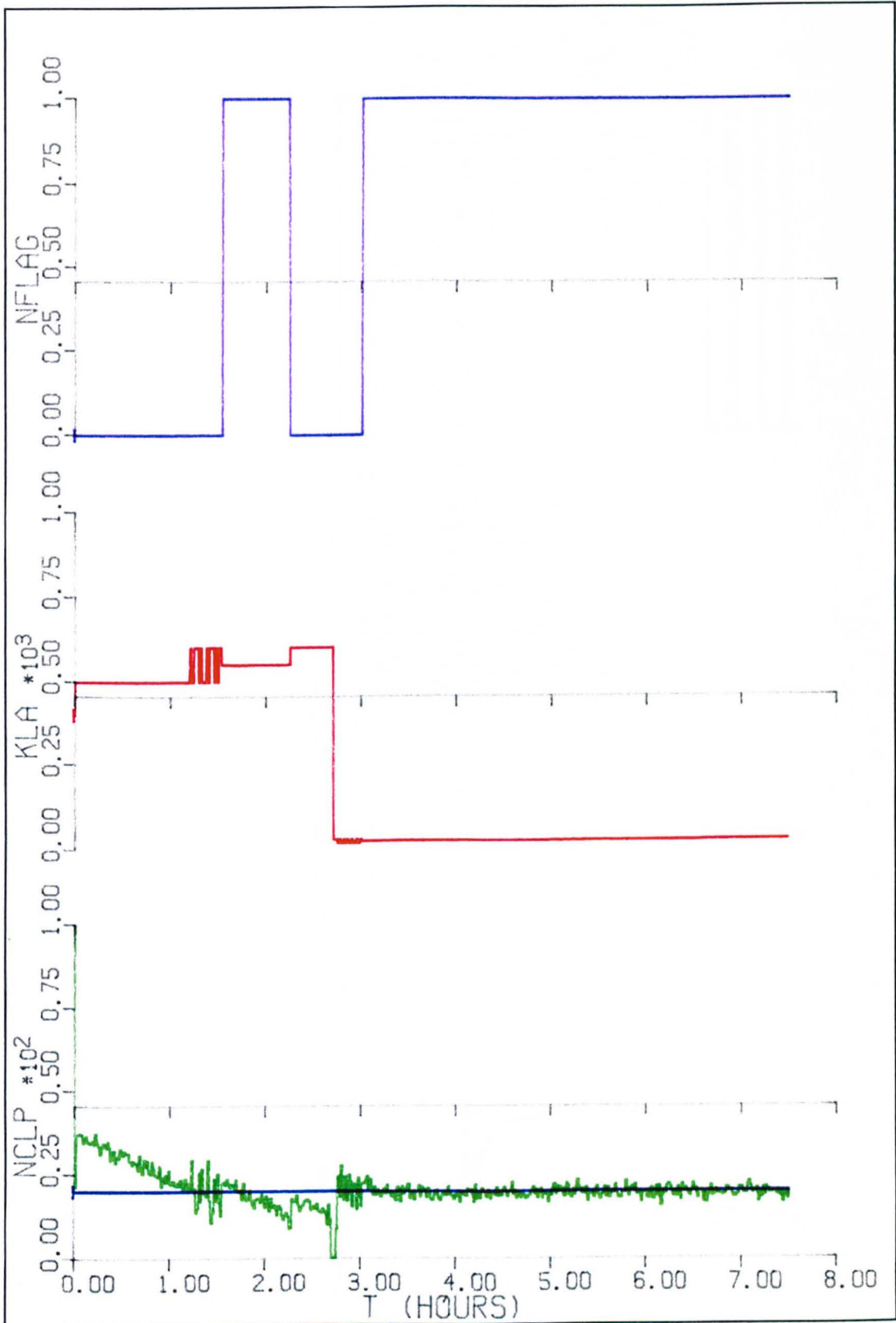


Figure 5.34 Multiple tuning on the dissolved oxygen concentration performance.

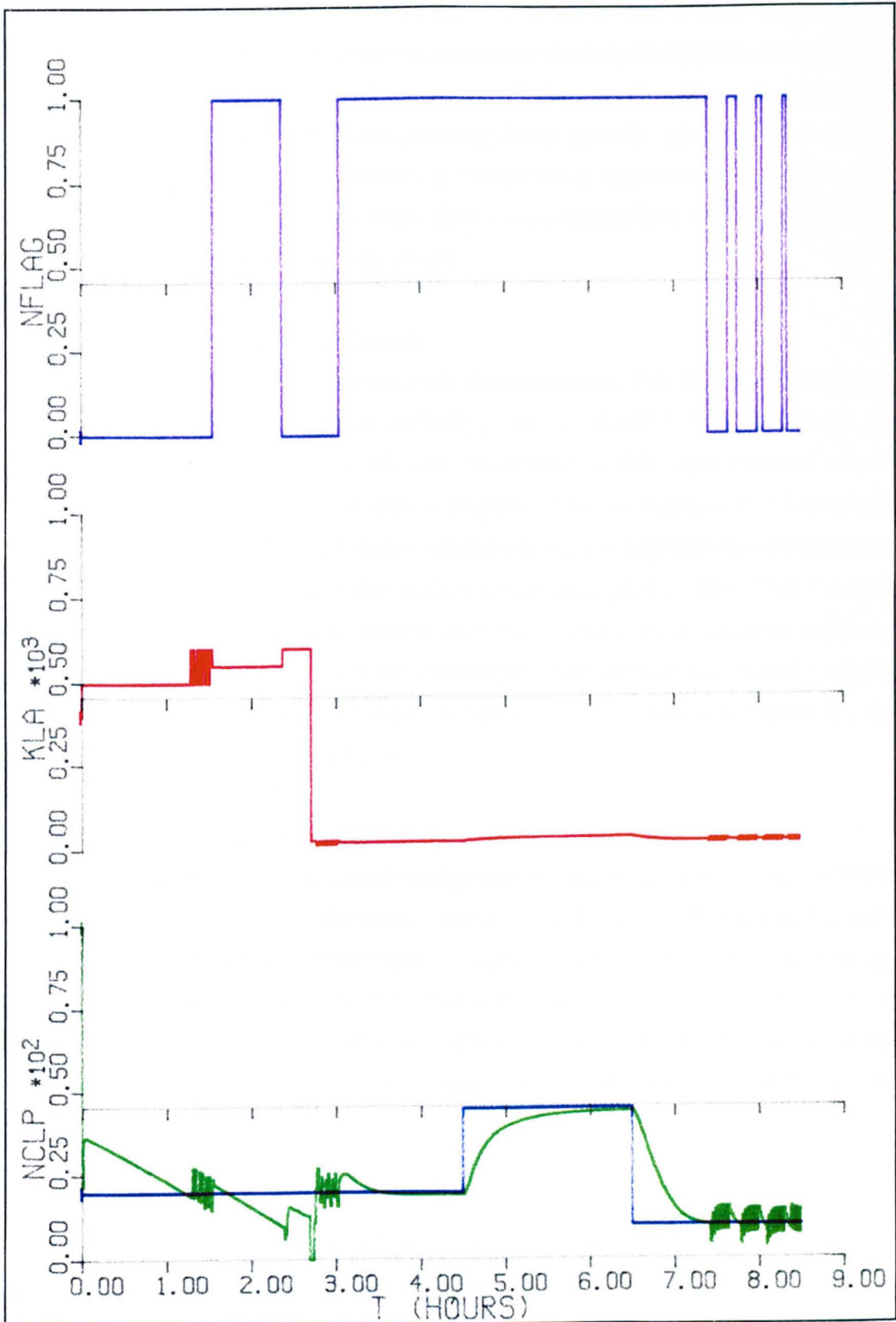


Figure 5.35 Automatic Tuning Procedure applied during set-point changes.

The second type of process disturbance simulated was a load disturbance; achieved by changing the value of the maximum dissolved oxygen concentration, C^* . Both an increase and a decrease in C^* were used, with each simulation having a short-time disturbance during each growth phase. The results displayed in Figure 5.36 and Figure 5.37 illustrate that the automatic tuning procedure can retune the PID controller to accommodate either type of load disturbance during either growth phase.

5.8.5. Multi-tuning on Stirrer Speed.

As with the simulation of a fed-batch fermentation, the batch fermentation simulation can be enhanced by including the application of agitation as the manipulated variable (equation (5.13)). The result of this improvement can be seen in Figure 5.38, which includes a number of tuner applications (on a time basis). This result has an adequate dissolved oxygen regulation performance, however the manipulated variable during the second phase (after $T=2.7$ hours) falls to an extremely low value (stirrer=0.6 rpm), which for a real process is an unacceptable rate of agitation if the fermenter broth is to be adequately mixed. Industrial applications often maintain a constant stirrer speed and alter K_{La} by adjusting only the input air flow rate.

5.8.6. Multi-tuning using Air Flow Rate.

The result of using the air flow rate as the manipulated variable (Figure 5.39) is similar to that obtained for the stirrer speed. An obvious difference is the lack of an overshoot in the dissolved oxygen response which occurs after the change from the tuning procedure to the PID controller. This is clearly seen by contrasting the two responses at $T=3.0$ hours. The primary reason for this is the effect that air flow rate has on the dissolved oxygen concentration compared to the effect from the stirrer speed.

5.9. DISCUSSION.

The results provided in this Chapter do not represent all the simulation scenarios which could be simulated *in toto*. However they do provide a broad spectrum of major problems the automatic tuning procedure might encounter when applied to a real process. Since the main criteria for the work is to present

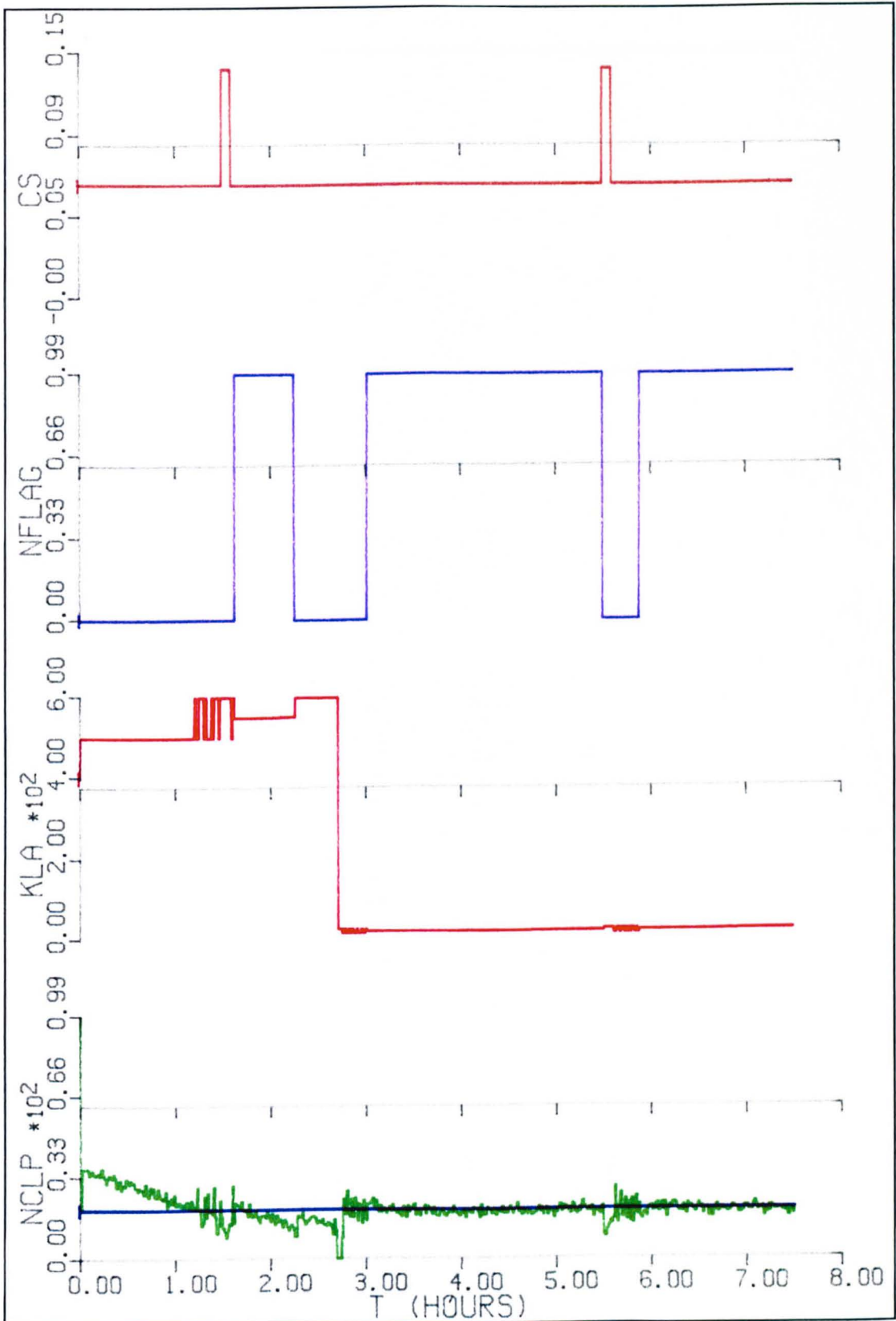


Figure 5.36 Positive load disturbance test.

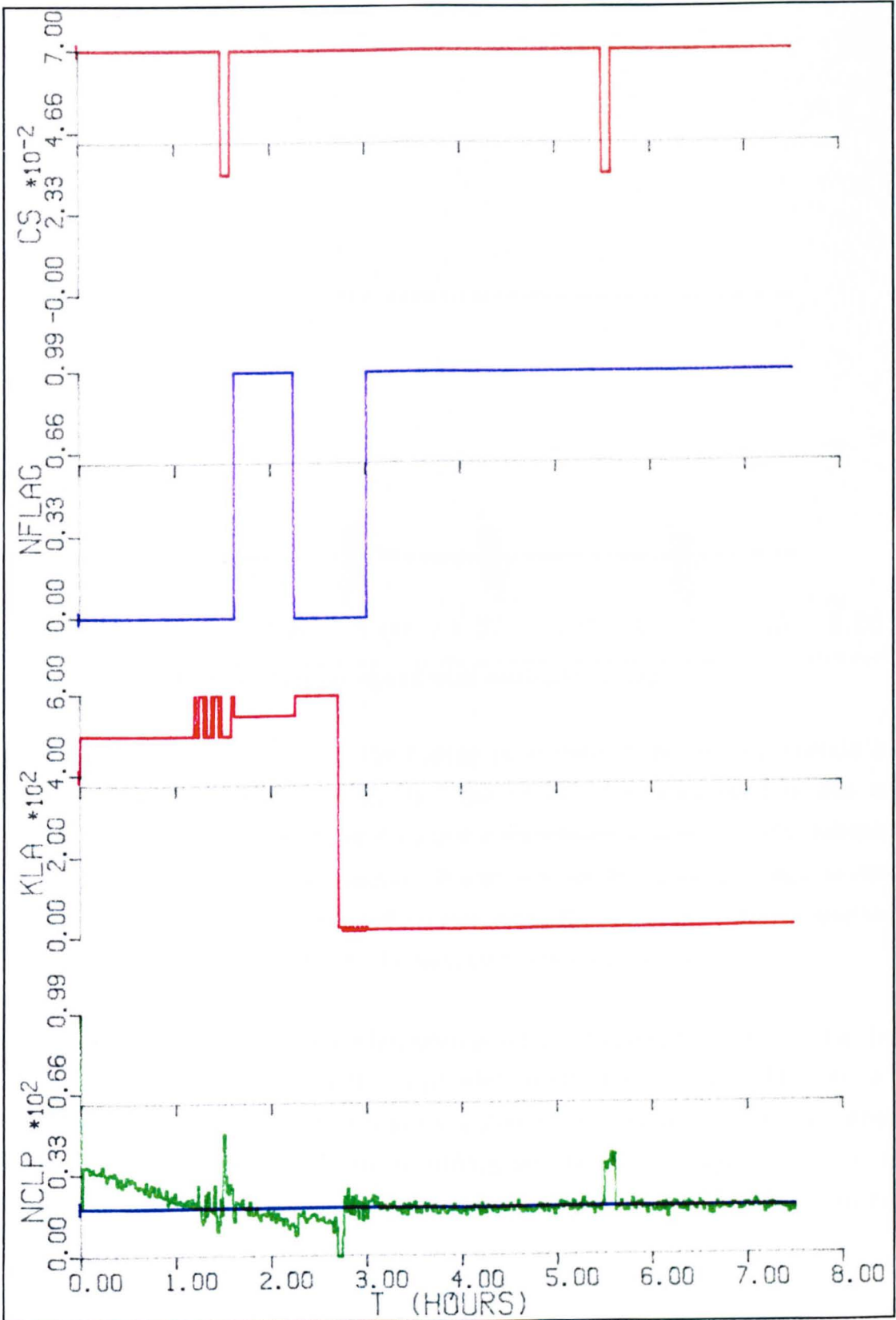


Figure 5.37 Negative load disturbance test.

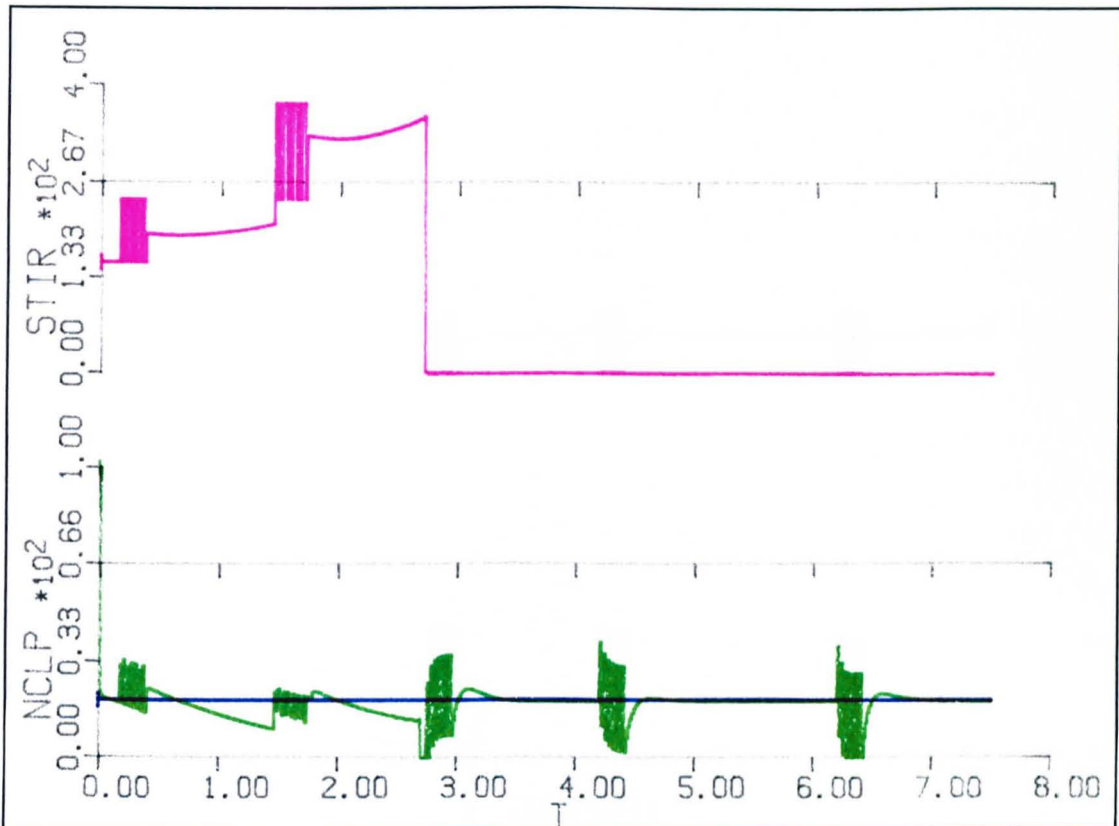


Figure 5.38 Inclusion of stirrer speed with multiple tuning.

the on-line implementation of the tuning procedure, it is not appropriate to continue simulations *in perpetuum*. The result of a simulation is not as beneficial as it might initially seem; since a simulation can only really indicate when a system will not work on-line. If a system works in simulation it is *non sequitur* to surmise that it will work on-line; since the accuracy of the simulation is in relation to the accuracy of the mathematical model used.

The automatic tuning procedure has been developed to provide assistance for the Control Engineer in determining controller tuning parameters. The results presented in this Chapter show that the automatic tuning procedure is capable of determining a set of controller tuning parameters that will produce a controlled response which is an improvement over the favoured manual tuning techniques.

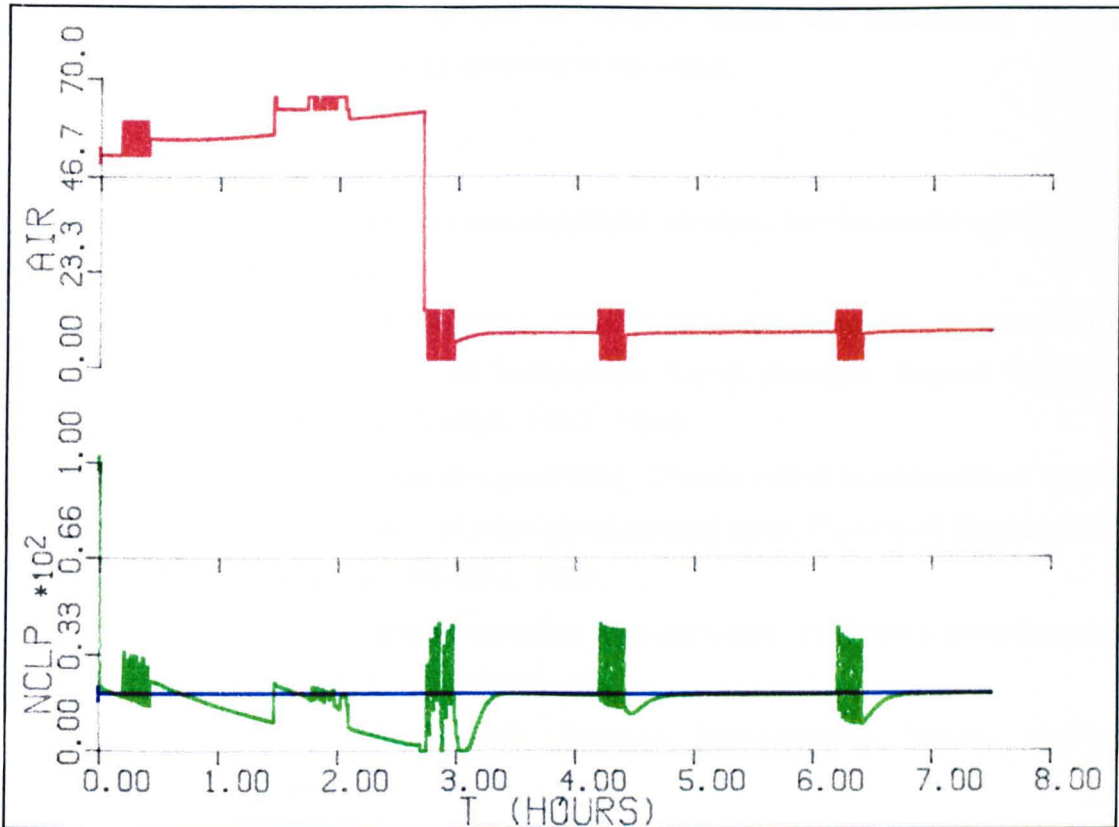


Figure 5.39 Inclusion of air flow rate as the manipulated variable.

The automatic tuning procedure presented has several advantages over other automated tuning methods:

1. No *a priori* knowledge of the process time constants or delays is required. The operation of the tuning procedure automatically results in a sustained oscillation close to the critical frequency of the process. The only parameters which have to be chosen by the operator, are the values of the nonlinearity output ($\pm E$) and the hysteresis width ($\pm\beta$), although these can be determined from the maximum oscillation amplitude, A^* , and the required phase margin, ϕ_m .
2. Since the tuning procedure is a closed-loop test, the process will not drift away from the set point. The process is maintained around a localized linear region, where an approximate transfer function model of the process can be obtained. Thus the tuning procedure works because nonlinear processes can be linearised about a set-point.
3. Accurate information about the process is obtained from the important critical frequency; that is, near a phase margin of -180° . However the

critical frequency need not be known since the automatic tuning procedure is designed to determine its value.

5.10. REFERENCES.

- 5.1. G. Jackson. Software for control systems design. Mechanical engineering. July. 1990. p.44-45.
- 5.2. Åström, K.J. Zeigler-Nichols Auto Tuners. Department of Automatic Control, Lund Institute of Technology, Lund, Sweden. Report CODEN: LUTDF2/(TFRT-3067)/0-025/1982. 1982.
- 5.3. Ogata, K. Modern control engineering. Prentice-Hall International. 1990.
- 5.4. Rushton, J.H. The use of pilot plant mixing data. Chemical Engineering Progress, Vol. 47. p. 467-472. 1951.
- 5.5. Richards, J.W. Studies in aeration and agitation. Processes in Industrial Microbiology, Vol. 3, p.143-148. 1961.
- 5.6. *Private correspondance*. Life Science Laboratories, Luton, United Kingdom. 1990.

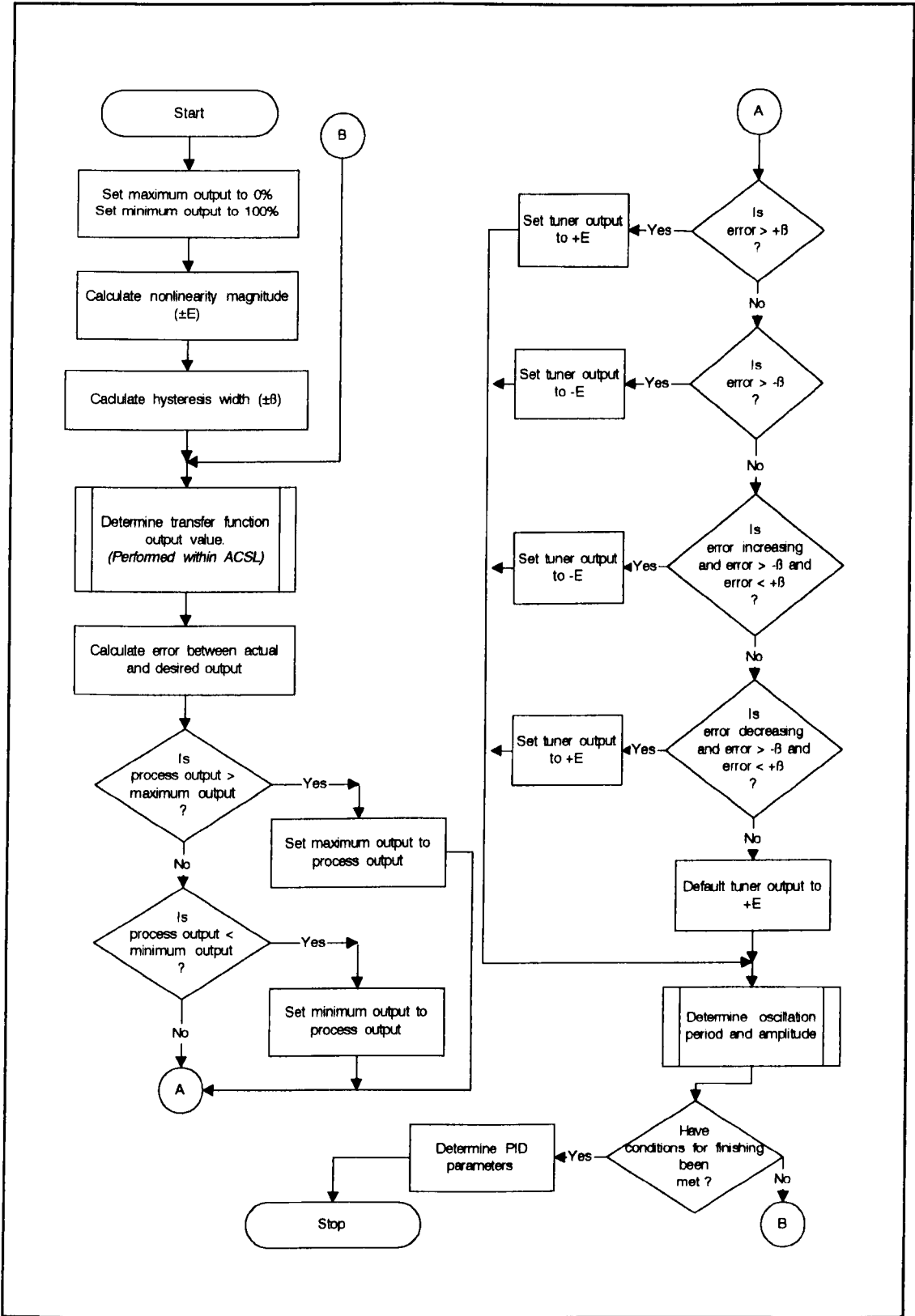


Figure 5.40 Flowchart for simulated automatic tuning procedure on generalized transfer functions.

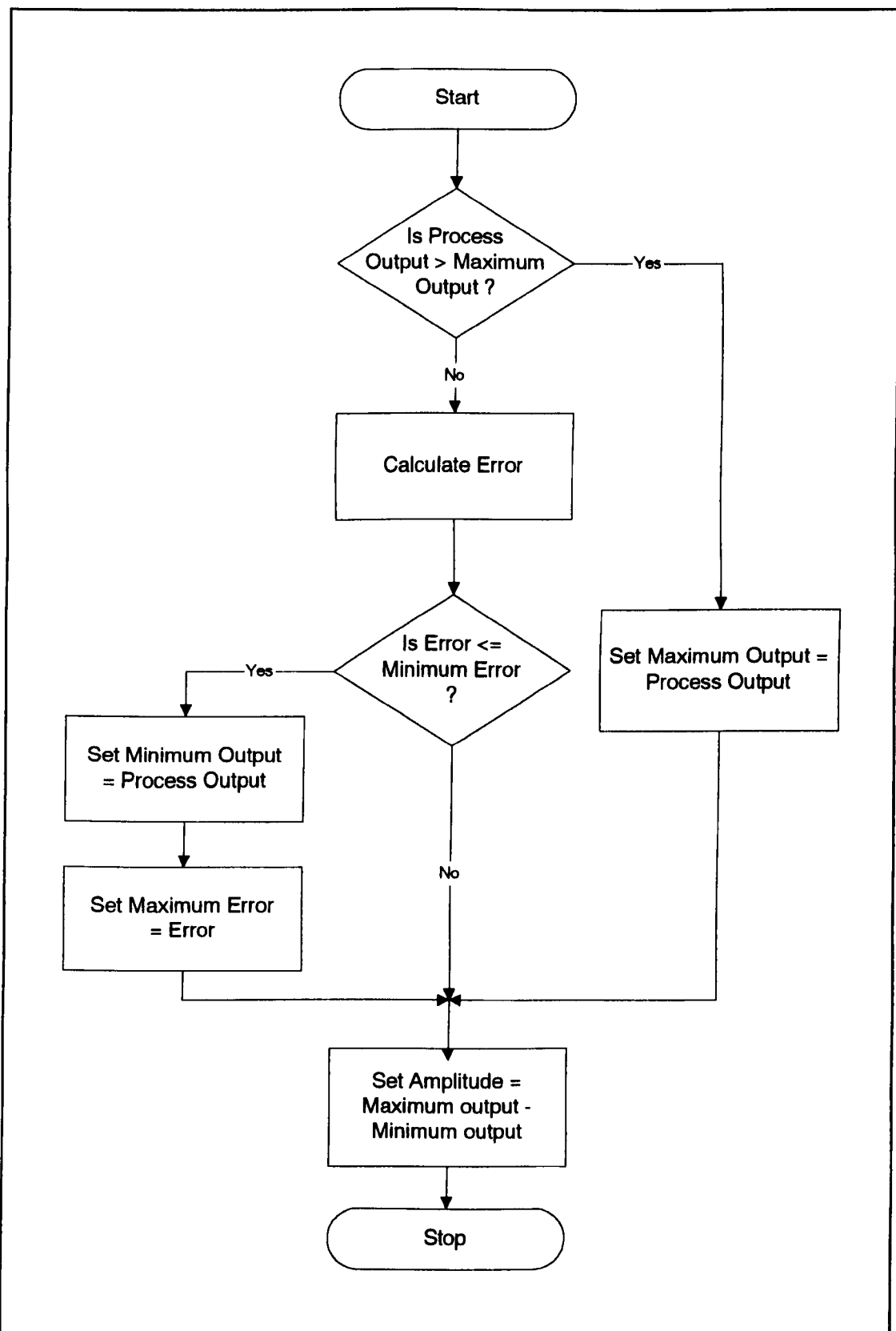


Figure 5.41 Flowchart for the determination of the oscillation amplitude.

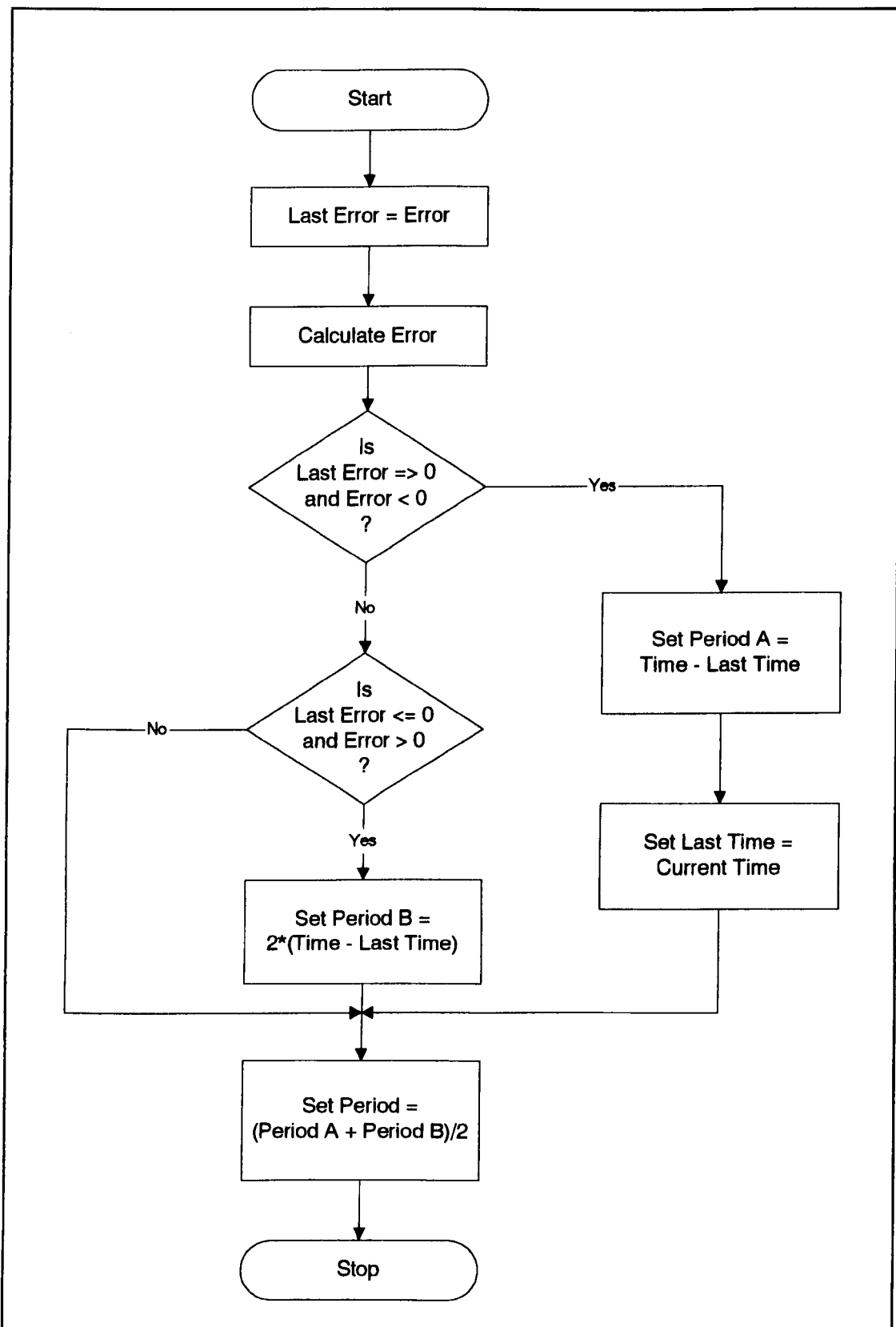


Figure 5.42 Flowchart for the determination of the oscillation period.

Listing 5.2. ACSL code for multiple auto tuning on a fed-batch fermentation.

```

Program Baker_ml
Initial
constant timer=0.0, llims=60,
lamp=0.0, leror1=0.0, eror1=0.0,
koj=40, high=500.0, low=350.0,
pcent=20.0, beta=1.0, direc=0.0,
leror=0.0, eror=0.0, pi=3.14159,
vu=0.1, clpmin=100.0, clpmax=0.0,
amp=0.0, oldk=500.0, period=0.0,
lastt=0.0, pcent=20.0, eror=0.0,
mu=0.254, yxs=0.5, ks=0.003,
mumax=0.2, f=0.0, u=12.0,
sgln=300.0, yo2=0.91, gpl=0.007,
cl=0.07, cs=0.0, clsp=0.0, clp=0.0,
ti=1.0, kp=1.0, td=0.0, tot=0.0,
leror=0.0, mr=392.46, nclp=0.0,
ncl=0.0, gas=1.0, noise=0.0,
std=0.001, count=0
logical nflag
    constant nflag=.FALSE.
End $ 'of initial'
Dynamic
    cinterval cint=0.005
    constant tstp=0.5
Derivative
    algorithm ialg=5
    nsteps nstp=1
    mininterval mint=0.005
    maxterval maxt=0.005
constant x1init=100.0, tsinit=0.0,
vinit=10.0, clinit=0.07, pinit=0.0,
sinit=0.01
    if (s.lt.0.0) s=0.0
    f=u/300
    mu=(mumax*s)/(ks+s)
    x1=integ(mu*x1,x1init)
    s=integ(sgln*f-(mu*x1)/yxs,sinit)
    v=integ(f,vinit)
    ts=integ(u,tsinit)
    cs=gpl*v
cl=integ((kla*(cs-cl))-((1/yo2)*mu*x1),c
linit)
    if (cl.lt.0.0) cl=0.0
    clp=100*(cl/cs)
    clsp=(pcent/100)*cs
    u=40*exp(mu*t)
    if (clp.ge.clpmax) clpmax=clp
    if (clp.le.clpmin) clpmin=clp
procedural
if (t.eq.2.0)
nflag=.FALSE.:low=500:high=600
if (t.eq.4.0) nflag=.FALSE.:
low=800:high=900
if (t.eq.6.0)
nflag=.FALSE.:low=1100:high=1200
end
End $ 'of derivative'
Discrete
    interval tsamp=0.01
procedural
    noise=gas*GAUSS(0.0,std)
    ncl=cl+noise
    if (ncl.lt.0.0) ncl=0.0
    nclp=100*(ncl/cs)
    timer=timer+t
    iff(timer.lt.sample) go to jjm2
    timer=0.0
    if (nflag) go to jjmp1
    leror=eror : eror=pcent-nclp
    direc=eror-leror : oldk=kla:kla=low
        if (eror.ge.beta) kla=high
        if (eror.lt.-beta) kla=low
    if (direc.ge.0.0 .and. eror.ge.-beta
.and. eror.lt.beta) kla=low
    if (direc.lt.0.0 .and. eror.lt.beta .and.
eror.gt.-beta) kla=high
        if (kla.eq.oldk) go to jmp2
    lamp=amp : amp=clpmax-clpmin
    clpmax=0.0 : clpmin=100.0
    period=2*(t-lastt) : lastt=t
    if (lamp.eq.amp) go to jjj
        count=count+1
    jjj..continue
    if (count.lt.lims) go to jmp2
    nflag=.TRUE. : count=0
        kp=(4*(high-low)/2)/(1.7*pi*amp)
        ti=period/(6.3*pi*vu)
        td=period/(2.6*pi)
    jjmp1..continue
    leror1=eror1 : eror1=clsp-ncl
    tot=tot+eror1
    kla=(kp*eror1)+((kp/ti)*tot)+(kp*td*(ler
or1-eror1)/tsamp)
    if (kla.lt.mr) kla=mr
    jmp2..continue
    jjm2..continue
end $ 'of procedural'
End $ ' of discete'
    call logd(.TRUE.)
    termt(t.ge.tstp)
End $ 'of dynamic'
End $ 'of program'

```

Listing 5.3. ACSL Code for batch fermentation with automatic tuning procedure.

```

Program M2BTAT_2
Initial
constant demand=0.0, eyo2=0.0000091,
vu=0.1, amp=0.0, oldk=500.0, period=0.0,
lastt=0.0, pcent=20.0, sample=0.016,
timer=0.0, lims=15, lamp=0.0, leror1=0.0,
eror1=0.0, count=0, high=500.0, v=10
low=400.0, mr=450.0, beta=1.0,
direc=0.0, leror=0.0, eror=0.0, kla=400.0,
pi=3.14159, ti=0.0, kp=1.0, td=0.0,
tot=0.0, s=0.0000001, gas=0.0, noise=0.0,
std=0.001, two8=0.28, mu=0.154,
yxs=0.5, ks=0.003, mumax=0.2, f=0.0,
sgin=0.0, a1=1.0, a2=0.0, pe=0.0, ve=0.0,
yxe=0.48, mt=0.03, yes=0.51, k1=0.0023,
k2=0.007, yo2 = 0.91, gpl=0.007, cl=0.07,
cs=0.0, clsp = 0.0, clp = 0.0, nclp=0.0,
clpmin=100.0, ncl=0.0, clpmax=0.0
logical nflag
constant nflag=.FALSE.
End $ ' of Initial '
Dynamic
  Cinterval Cint = 0.005
  Constant Tstp = 7.5
Derivative
  Algorithm IALG = 5
  Nsteps Nstp = 1
  Minterval Mint = 0.005
  Maxterval Maxt = 0.005
constant vxinit=100.0, vsinit=0.01,
vpinit=0.0, vcinit=0.0, clinit=0.07
vx=integ(((mu*vx)+(a1*yxe*ve*vx)),vxinit)
vs=integ((f*sgin)-((mu*vx)/yxs)-(mt*vx)-((a
2*pe*vx)/yes),vsinit)
vc=integ(((a2*pe*vx)-(a1*ve*vx)),vcinit)
vp=integ(((k1*vx)+(k2*mu*vx)),vpinit)
mu=(s*mumax)/((1+p**2)*(ks+s))
cs=gpl*v
cl=integ((kla*(cs-cl))-((a2*(1/yo2)*mu*vx)-(a
1*(1/eyo2)*mu*vx),clinit)
clp=100*(cl/cs)
clsp=(pcent/100)*cs
demand=(a2*(1/yo2)*mu*vx)+(a1*(1/eyo2)
*mu*vx)
procedural
if (cl.lt.0.0) cl=0.0:clp=0.0
if (cl.gt.100.0) cl=100.0:clp=100.0
  if (vc.lt.0.0) vc=0.0
  if (s.lt.0.0) s=0.0000001
  if (vs.lt.0.0) vs=0.0000001
  pe=0.155+(0.123*a log(s))
  if (pe.lt.0.0) pe=0.0
  if (s.eq.two8)go to sjmp1
ve=0.138-(0.062*p)+(0.0028/(s-(two8)))
  go to sjmp2
sjmp1..ve=(0.138-0.062*p)
sjmp2..if (ve.lt.0.0) ve=0.0
  if (vc.le.0.0) ve=0.0
  a1=1.0 : a2=0.0
  if (s.gt.(two8)) a1=0.0: a2=1.0
end
x1=vx/v : s=vs/v : p=vp/v : ce=vc/v
  if (clp.ge.clpmax) clpmax=clp
  if (clp.le.clpmin) clpmin=clp
procedural
  if ((nclp.lt.10.0).and.(s.ge.two8))low=500:
high=600:mr=550:nflag=.FALSE.
  if ((nclp.lt.10.0).and.(s.lt.two8)) low=18:
high=28:mr=20
end
End $ 'of derivative'
Discrete
  interval tsamp=0.016
procedural
ncl=cl+( noise=gas*GAUSS(0.0,std))
  if (ncl.lt.0.0) ncl=0.0
  nclp=100*(ncl/cs) : timer=timer+t
if(timer.lt.sample) go to jjm2
timer=0.0
if (nflag) go to jjmp1
leror=eror:eror=pcent-nclp
direc=eror-leror:oldk=kla:kla=low
  if (eror.ge.beta) kla=high
  if (eror.lt.-beta) kla=low
if (direc.ge.0.0 .and. eror.ge.-beta .and.
eror.lt.beta) kla=low
if (direc.lt.0.0 .and. eror.lt.beta .and.
eror.gt.-beta) kla=high
if (kla.eq.oldk) go to jmp2
lamp=amp:amp=clpmax-clpmin
clpmax=0.0 : clpmin=100.0
period=2*(t-lastt) : lastt=t
  if (lamp.eq.amp) go to jjj
  count=count+1
jjj..continue
if (count.lt.lims) go to jmp2
nflag=.TRUE. : count=0
  kp=(4*(high-low)/2)/(1.7*pi*amp)
  ti=period/(6.3*pi*vu)
  td=period/(2.6*pi)
jjmp1..continue
leror1=eror1:eror1=clsp-ncl:tot=tot+eror1
kla=(kp*eror1)+((kp/ti)*tot)+(kp*td*(leror1-
eror1)/tsamp)+mr
jmp2..continue
jjm2..continue
end $ 'of procedural'
End $ ' of discete'
  call logd(.TRUE.)
  term(t.ge.tstp)
End $ 'of dynamic'
End $ 'of program'

```

CHAPTER 6.

ON-LINE EXPERIMENTATION.

6.1. INTRODUCTION.

The simulation results presented in the previous chapter illustrate that the concept of the automatic tuning procedure is viable, however this only provides an indication of the general usefulness and applicability of the tuning procedure and its associated software techniques (such as the transfer mechanism from the tuning procedure to the PID controller). This chapter presents the results of on-line implementations of the tuning procedure, using three different processes:

- 1) Batch Bakers' Yeast fermentation,
- 2) Fed-batch Bakers' Yeast fermentation,
- 3) Chemical reaction.

Each of these experiments will be described and a comparison of the application of the automatic tuning procedure with a manually tuned PID controller will be made. For each on-line experiment, the dissolved oxygen concentration was used as the controlled variable and the input air flow rate as the manipulated variable (Figure 6.1). Even at cell densities of 10 g.l^{-1} or less, oxygen limitation can occur [6.1] when a reasonable rate of growth is obtained. For industrial applications, aeration is usually provided by the injection of sterile air under pressure; air is used since it contains 20.9% oxygen while pure oxygen is expensive and requires specialized hardware. The availability of oxygen within the fermenter broth may become limiting for microorganism growth since oxygen has a low solubility in water; typically one cubic metre of water will hold 7-8mg of oxygen [6.2]. If the oxygen concentration in the medium falls below a critical value there may be metabolic changes which lead to microorganism death; for example, if the dissolved oxygen concentration falls below 0.256 mg.l^{-1} (that is, 3.7%) then growth of *Escherichia coli* cells would terminate (Table 6.1). It is sufficient to use the input air flow rate as the manipulated variable with a constant agitation, however the oxygen transfer rate, $K_{L,a}$, is not very sensitive to changes in aeration at high agitation speeds owing to surface aeration effects [6.1]. For the fermentation work presented, the agitation was set at 650 rpm, which although providing some surface aeration, it can be considered negligible

compared to the effects of the input air flow. Thus the primary use of the stirrer was to provide a well mixed broth and to break-up the air bubbles within the fermenter.

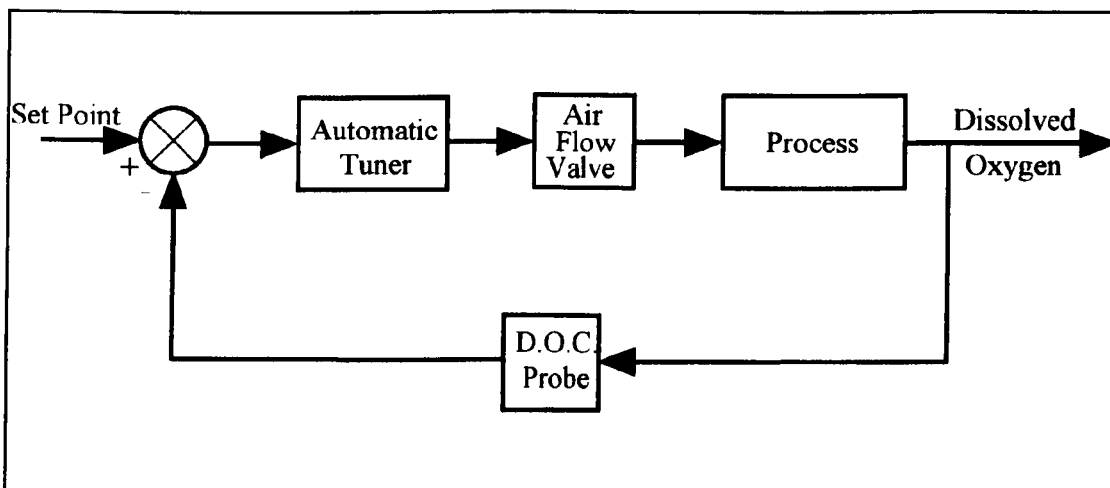


Figure 6.1 Block diagram of dissolved oxygen control loop.

Table 6.1 Oxygen consumption and critical concentration for various microorganisms.

Microorganism	Temperature °C	Critical concentration		Maximum consumption mmol.l ⁻¹ .hr ⁻¹
		mmol.l ⁻¹	% of C'	
<i>Azotobacter</i>	30	0.018	8.2	260
<i>Escherichia coli</i>	37	0.008	3.7	5-8
<i>Yeast</i>	30	0.004	1.8	10-15
<i>Penicillium chrysogenum</i>	24	0.022	10.1	20-30

6.2. SOFTWARE IMPLEMENTATION OF THE TUNING PROCEDURE.

The inclusion of the automatic tuning procedure within the ACSL simulation environment used a particular implementation, whereas the on-line application of the tuner, in conjunction with the MENTOR software, required a slightly different implementation. In particular, the form of the PID algorithm within MENTOR differs from the accepted form. Thus it was necessary to compensate for the MENTOR implementation.

6.2.1. Comparison of PID Implementations.

The standard discrete-PID equation used for the tuning procedure simulation work (Chapter 5) was given by

$$y_{\text{tuner}}(t) = K_p \left[\epsilon(t) + \frac{1}{T_i} \sum \epsilon(t) + T_d \frac{d\epsilon(t)}{dt} \right] \quad (6.1)$$

where K_p is the proportional gain, T_i the integral action and T_d the derivative action. Whereas the equation used within the MENTOR software is

$$y_{\text{mentor}}(t) = \left[\frac{100 \epsilon(t)}{P_B R} + \frac{100 \sum \epsilon(t)}{T_i P_B R} + \frac{100 T_D d\epsilon(t)}{P_B R dt} \right] \quad (6.2)$$

where P_B is the proportional band, T_i the integral action, T_D the derivative action and R the range of the measured process variable. For example, for the pH control loop the range is given by

$$\begin{aligned} R &= \text{Raw High} - \text{Raw Low} \\ &= 13.5 - 1.8 \\ &= 11.7 \end{aligned}$$

That is, the PID equation includes a normalization factor. For the automatic tuning procedure to be included within MENTOR, an equality must be made between the simulation and MENTOR PID algorithms. Additionally, MENTOR requires T_i to be entered in seconds, and T_D in 100 second units (that is, for a derivative action of 200 then $T_D=2.0$); thus the following equalities must be made

$$P_B = \frac{10000}{R K_p}, \quad T_i = 60 T_i, \quad T_D = 0.06 T_d \quad (6.3)$$

Table 6.2 shows the comparison between the PID parameter equations for the simulated automatic tuner and those for the MENTOR tuning; where A is the oscillation amplitude, τ the oscillation period and E the nonlinear element output amplitude. It is these modified relationships which are programmed into the tuning procedure software. It was reported in Chapter 2 that two PC's were used for the on-line experiments; the MENTOR software was executed on the first while the second was used to run the automatic tuning software, called REL_5B. This software provides additional facilities such as data logging, transient response graphing, etc. Since REL_5B runs on a separate computer to MENTOR, the fermentation process information held by MENTOR has to be transmitted to REL_5B via the RS-232 serial communications link as encoded ASCII

REL_5B via the RS-232 serial communications link as encoded ASCII (Figure 6.27). For each analog control loop on the fermentation process, a MENTOR subroutine extracts certain information about the loop from a central database and combines the data into a complete ASCII character string. The character strings for a number of loops are combined and then transmitted along the serial link. The MENTOR database is arranged such that each analog control loop contains exactly 130 ASCII characters, with each piece of information allotted a certain number of characters (illustrated in Appendix C); for example the control loop name, or TAG, is given five characters such as 01D01, even numerical data has a limited character size imposed upon it by converting the numerical information into a combination of alpha-numeric characters, thus the measured value for pH which has a maximum numeric character format of ##.## and the stirrer speed which has the form ####.### both have four ASCII characters assigned to them. Characters 39 & 40 in the database string are used to store logical information about the control loop, such as whether the control action is direct or reverse, or if data logging is to be used. On the second computer, the REL_5B program firstly receives the ASCII string and then extracts the individual data for each control loop; this data then becomes available for storage in a data file and for producing graphical transient responses. The flowcharts which describe the full operation of REL_5B are presented in Appendix D. The automatic tuning procedure operation is carried out within the 'Algorithm,' subroutine of REL_5B, which is described below.

Table 6.2 PID parameter equations.

Simulation	MENTOR
$K_p = \frac{1.7 \pi A}{4 E}$	$P_B = \frac{4000 E}{1.7 \pi A R}$
$T_i = \frac{\tau}{6.3 v \pi}$	$T_i = \frac{60 \tau}{6.3 v \pi}$
$T_d = \frac{\tau}{2.6 \pi}$	$T_D = \frac{0.06 \tau}{2.6 \pi}$

6.2.2. Activating the Tuning Procedure.

The automatic tuning procedure is not continuously active; it lies dormant until the process requires an update of the PID controller parameters. There are three possible methods of starting the retuning phase, namely:

- 1) on demand by the operator
- 2) after a specific time delay
- 3) on process performance

The simulation studies (Chapter 5) indicated that each of these methods were applicable to the process. For the on-line work it was decided to have the tuning procedure activated at the start of the fermentation process and thereafter on demand by the operator. This operator activation is achieved within the REL_5B software by using a keyboard interrupt.

6.2.3. Procedure 'Algorithm'.

The procedure 'Algorithm' (Figure 6.28) begins by calculating the hysteresis nonlinearity values (that is, $\pm E$ and $\pm\beta$) before determining the previous error, nonlinearity output and current error. The hysteresis width, $\pm\beta$, would normally remain constant for any implementation, while the nonlinearity output, $\pm E$, may be modified during a tuning phase. If the tuning procedure is not active or is currently active but has exceeded its predetermined time out period then the software bypasses the procedure and reverts to PID control (Figure 6.28a). However, if the tuning procedure has been initiated by one of the three methods, then the software determines the appropriate output level from the nonlinear element and the time period for which the nonlinear element output has been at $+E$ (Relay On Time) and the time for an output of $-E$ (Relay Off Time). Additionally, the software determines the maximum and minimum process response values and the time at which they occurred (Figure 6.28b and Figure 6.28c). Prior to calculating the new PID controller parameters (K_p , T_i & T_d) the procedure determines the process output oscillation amplitude and period (Figure 6.28d).

The fermentation process has all instrumentation interrogated by MENTOR at 10 second intervals, additionally all control commands are processed at this sample rate. This provides a regular monitoring and control regime for the fermentation

process. The communication between MENTOR and REL_5B occurs at approximately twice the process sample rate, thereby providing the automatic tuning procedure with a reduced data set of the fermentation process; however this does not seem to have posed a problem to the operation of the tuning procedure.

6.2.4. Estimation of Oscillation Period and Amplitude.

For the on-line experimentation, the oscillation amplitude was ascertained by finding the approximate maximum and minimum values of the process response by successive comparison; however this method will only provide the maximum/minimum value at least one sample after the reading is taken. Additionally excessive noise on the measurand causes problems in the accurate determination of the oscillation. This may be overcome by filtering the signal; a number of filters have been investigated [Appendix B] with the chosen filter being the moving average filter given by:

$$x_n' = \frac{x_n + x_{n-1}}{2} \quad (6.4)$$

where x_n' is the filtered value, x_n the current reading and x_{n-1} the previous reading. Having observed and recorded the oscillation's maximum and minimum points, the time at which these occur can be utilised to estimate the oscillation period. The calculated period value is a composite of twice the time between each maximum and minimum value found. Listing 6.1 illustrates the coding used to estimate both the period and amplitude of the oscillatory response. It also shows the code for the calculation of the controller parameters (K_p , T_i and T_d). The estimation of the amplitude and period during a typical tuning phase can be seen in Figure 6.2. The estimation methods used are relatively simple, however their operation is adequate for fermentation process.

6.2.5. Terminating the Tuning Phase.

Having found the controller settings, the PID algorithm must be updated with the new values as quickly as possible; thus it is important that the tuning phase determines the controller parameters quickly. Since the calculation of the controller parameters requires the estimation of the amplitude of the oscillatory

```

AirOut = Eref
IF LastDOC < 0 THEN LastDOC = MeasuredValue
DOC = (MeasuredValue + LastDOC) / 2
DOTError = RequiredDOT - DOC

IF ComputeAlgorithm$ = "FALSE" THEN GOTO tunerend
IF ((TIMER - ATStartTime) / 60) > ATOntime THEN
    Tripflag$ = "TRUE"
    ComputeAlgorithm$ = "FALSE"
    LPRINT "W A R N I N G.....Auto-Tuner Time Out at "; TIMES$
    IF Amp = 0 THEN Tripflag$ = "FALSE"
    IF Amp = 0 THEN LPRINT "Amplitude is zero ..... PID not calculated"
    GOTO tunerend
END IF

REM ----- Auto Tuner goes in here -----
thil = ATN(v) * 180 / pi
bmag = Astar * SIN((thim + thil) * pi / 180)
bp = bref + bmag
bn = bref - bmag
IF (DOC < LastDOC AND direc$ = "UP") THEN
    direc$ = "DOWN"
    maxDOC = LastDOC
    Maxperiod = (TIMER - timmax) / 60
    LastAmp = Amp
    Amp = ABS(maxDOC - minDOC)
    timmax = TIMER
    maxflag$ = "TRUE"
ELSEIF (DOC > LastDOC AND direc$ = "DOWN") THEN
    direc$ = "UP"
    minDOC = LastDOC
    Minperiod = (TIMER - timmin) / 60
    LastAmp = Amp
    Amp = ABS(maxDOC - minDOC)
    timmin = TIMER
    minflag$ = "TRUE"
END IF

AirOut = ep * GainK
IF DOTError > bp THEN AirOut = ep * GainK
IF DOTError < bn THEN AirOut = en * GainK
IF (direc$ = "UP" AND DOTError > bn AND DOTError < bp) THEN AirOut = en * GainK
IF (direc$ = "DOWN" AND DOTError < bp AND DOTError > bn) THEN AirOut = ep * GainK
IF (minflag$ = "TRUE" AND maxflag$ = "TRUE") THEN
    period = (2 * ABS(timmax - timmin)) / 60
    AvPeriod = (AvPeriod + period) / 2
END IF

REM ----- work out the PID controller parameters -----
IF Amp = 0 THEN GOTO ffin
    Emag = (ep - en) / 2
    Range = 100 - 0
PIDkp = (400 * Emag) / (1.7 * pi * Amp * Range)
PIDti = (60 * AvPeriod) / (6.3 * v * pi)
PIDtd = (60 * AvPeriod) / (2.6 * pi)
ffin:
    REL_5B continues from here.

```

Listing 6.1 Program listing for oscillation and period estimation.

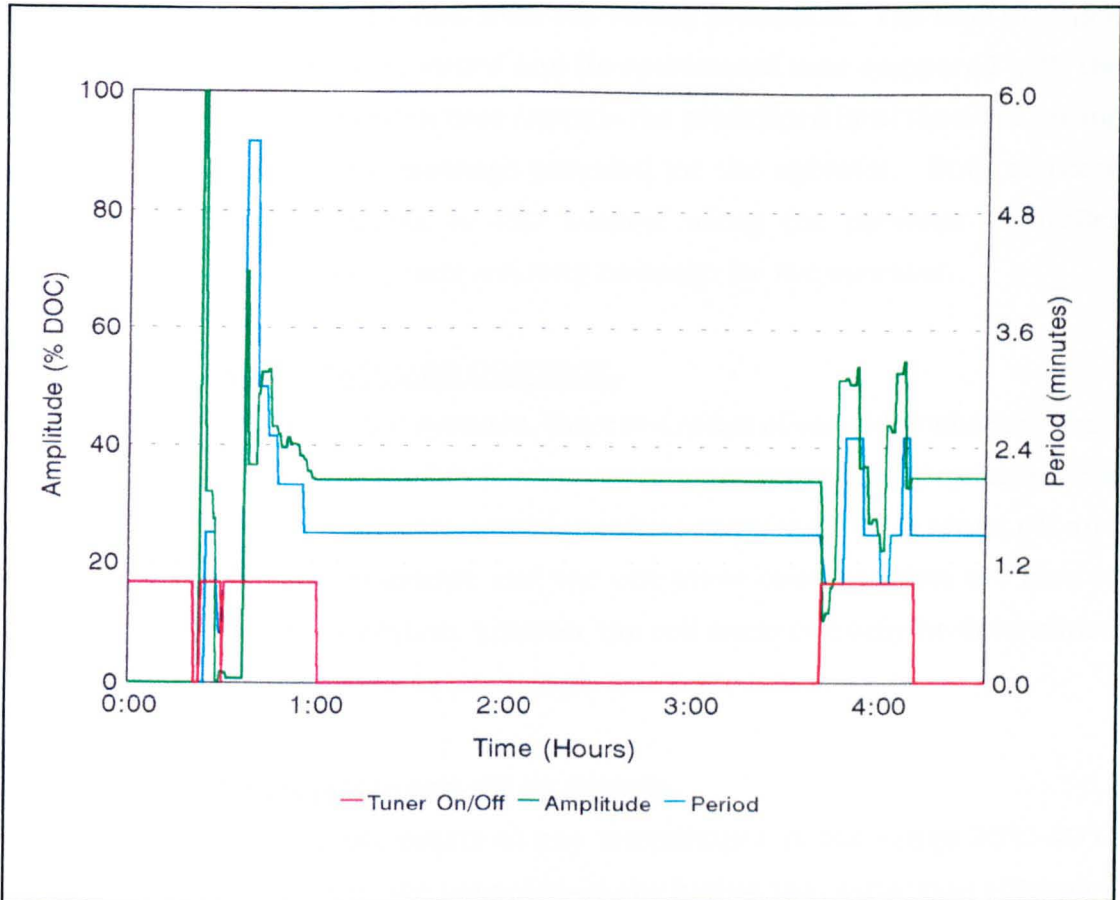


Figure 6.2 Plot of oscillation amplitude and period estimation.

process output, it seemed appropriate to use the changing amplitude values as a means of ascertaining whether the tuning phase is complete. The actual requirement for a successful termination of the tuning procedure is heuristic rather than predefined. For the on-line work conducted, it was decided that three consecutive equal amplitudes with a 10% tolerance would signify that the process was under consistent oscillation and thus an appropriate set of PID parameters may be calculated. The method proved suitable when initially applied on-line, and was adopted for all on-line experiments. The above procedure should provide a successful termination of the tuning procedure, however if three consecutive amplitudes are not approximately equal then oscillation of the process response by the nonlinear element will continue uninterrupted. To prevent this occurring indefinitely, two other termination criteria were included with REL_5B, firstly an operator keyboard interrupt to stop the tuning procedure on demand and secondly a time-out routine. The REL_5B includes a program variable (Time Out) to indicate the maximum time that the

process will be under 'oscillation' from the tuning procedure. The time at which the tuning phase starts is recorded and its operational time compared with the time-out value; if the operation time exceeds the predefined limit then the tuning procedure is halted and a message provided for the operator. Both of these methods return the process to PID control using the previous controller parameters, with an appropriate warning message for the operator.

6.3. FERMENTATION PROCESS CONTROL.

For both batch and fed-batch systems, there is a range of variables which require accurate control to ensure the broth environment is appropriate for optimum cell growth. The variables of primary importance for control are temperature, pH and agitation. The glucose substrate and the cell mass concentration are also of interest during the fermentation, however the cell mass can only be determined off-line some hours after the broth sample has been taken.

6.3.1. Effect of Temperature and pH on Growth.

It is possible to grow most yeasts at any temperature in the range 20°C-40°C [6.3]. In general, the lower the temperature the higher the conversion efficiency of glucose substrate to cell mass, owing to the lower maintenance energy requirement. For the strain of Bakers' Yeast used for the experimental work, the optimum temperature was 31°C. Microorganism growth produces heat, thus the broth temperature was regulated using proportional control on the cold water circulator feed.

Most strains of *S. cerevisiae* grow well at pH values between 3.5 and 7.0, with some restriction on growth occurring at the extremes of this range; gives a good yield at a pH value between 4.5 and 5.0 [6.4]. The use of advanced pH control systems can be applied to estimate the growth rate of Bakers' Yeast during its cultivation in the fermenter [6.5]. The growth rate can be used to both give an indication of biomass present within the fermenter and aid in the optimisation of the process. For the cultivation of *S. cerevisiae*, ammonia was utilised for the nitrogen source as well as providing pH control, with a linear relationship between the ammonia consumption rate and the cell growth rate [6.5]. This can be shown by the chemical reaction involving the ammonium hydroxide used for

pH regulation. The reaction for the control of pH is given by



which produces water and ammonia which is then available as the nitrogen source for the yeast cells, as given by



The graph of the total ammonium added for a batch fermentation has two distinct gradients which correspond to the two different growth rates that occur; that is firstly the consumption of glucose and then the consumption of the produced ethanol (Figure 6.3).

6.3.2. Agitation Control.

The use of the vessel stirrer was primarily to provide a well mixed fermentation broth, although the stirrer does break-up the air bubbles and thus provides an improved oxygen transfer to the broth. The agitation rate was set at 650 rpm with a proportional controller maintaining the set point.

6.4. BAKERS' YEAST FERMENTATION.

6.4.1. Experimental Method.

Each experiment performed, whether batch or fed-batch, followed a predetermined initialisation sequence, starting with the sterilization of the fermenter vessel using the in-situ steam sterilizer. The vessel was primed with 10l of water before the sterilization sequence was started, taking the vessel to a temperature of 121°C for a minimum of 3 hours. The temperature was then reduced and controlled at 38°C in readiness for the start of the fermentation. During the sterilization sequence, appropriate valves were activated to ensure that every part of the fermenter vessel was sterilized. The vessel liquid volume was reduced to a working volume of 8l with a further 0.4l being removed for mixing with the yeast cells. The maintenance chemicals were then added to the broth (Table 6.3) while the temperature was reduced to 31°C for the yeast fermentation.

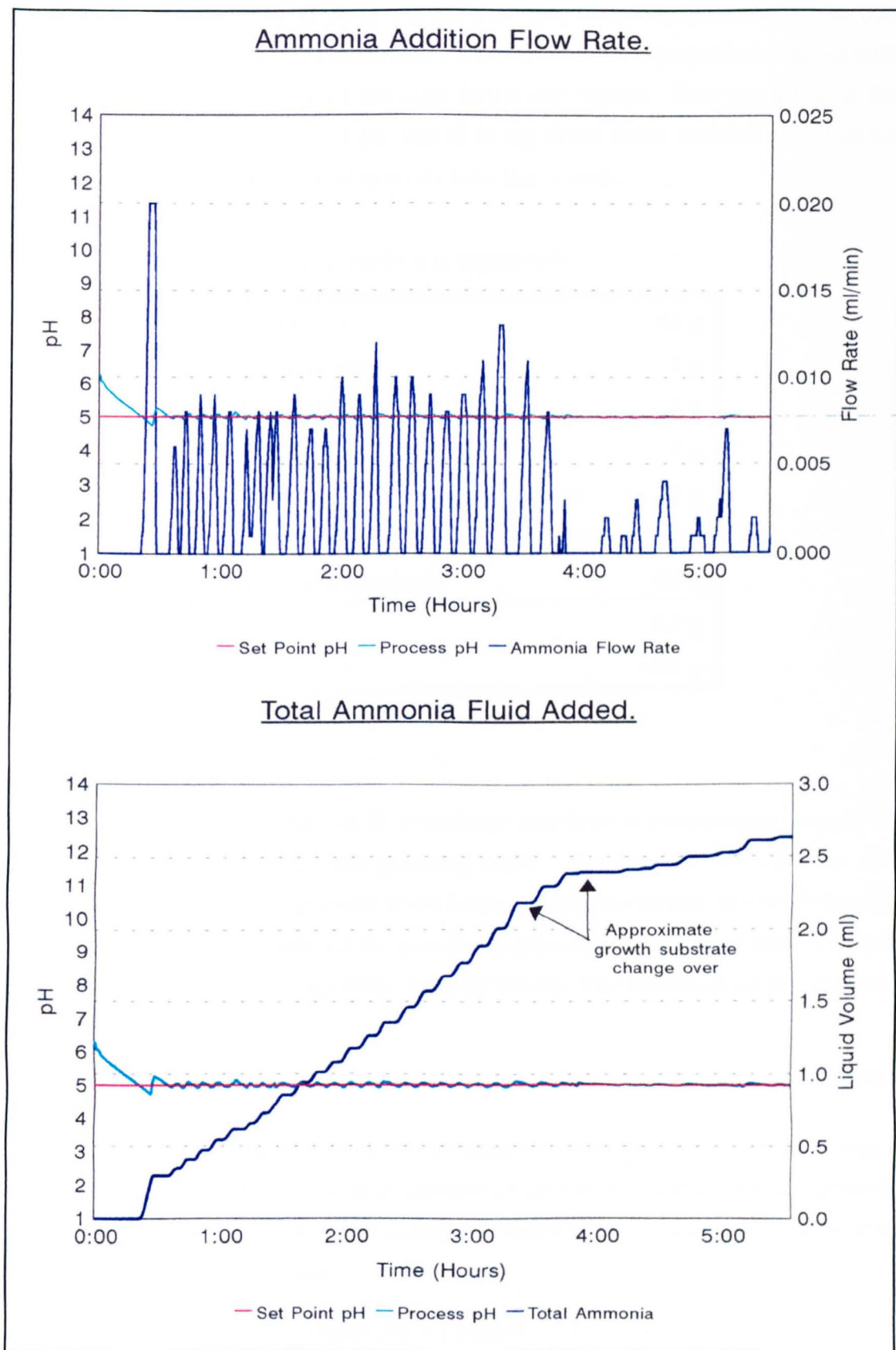


Figure 6.3 Total ammonia added and pH level during a batch fermentation.

The initial yeast concentration of 10g per litre (80g total) was placed into the 0.4l of sterilized water (at 38°C) and left for 10 minutes, after which it was mixed with the water before being placed into the fermenter vessel. This warming of the yeast was required because of the use of freeze dried yeast instead of the usual wet yeast which can be placed directly into the vessel.

Table 6.3 Bakers' Yeast fermentation components.

Yeast extract	20 g
Initial glucose	4 g
Sodium chloride	4 g
Magnesium sulphate	4 g
Potassium dihydrogen phosphate	16 g
Dipotassium hydrogen phosphate	8 g
Ammonium sulphate	40 g
<hr style="border-top: 1px dashed black;"/>	
<i>Yeast</i>	<i>80 g</i>
<i>Feed glucose</i>	<i>632 g</i>

6.4.2. Glucose feed.

The fed-batch fermentation of *S. cerevisiae* requires a continuous supply of glucose to be provided to the growing cells. For this to be used by the fermentation process, the glucose must be supplied directly into the broth liquid. This is conveniently achieved if the powdered glucose is mixed with water, which may then be pumped into the fermentation vessel. The equation for the glucose feed profile is given by:

$$\text{Glucose feed} = 2X_0[e^{\mu t} - 1] \quad (6.7)$$

For the fermentation experiments, the initial cell mass concentration was 10 g/l with an initial volume of 8l. It was assumed that the maximum specific growth rate was $\mu=0.2 \text{ hr}^{-1}$, and that the maximum fermentation time would be 8 hrs. Thus equation (6.7) becomes

$$\begin{aligned} \text{Glucose feed} &= 2 \times 80[e^{0.2 \times 8} - 1] \\ \therefore \text{Glucose feed} &= 632\text{g} \end{aligned} \quad (6.8)$$

Hence the total glucose needed is 632 g, which must be added to the broth in liquid form. The concentration of the glucose in the solution was 30%; thus 1494 g water was required.

For a batch fermentation the glucose was not mixed with water and fed in according to a feed profile; it was placed directly into the fermenter broth immediately after the introduction of the yeast cells into the vessel.

6.4.3. Process Control by MENTOR.

The fermentation process was monitored and controlled using the MENTOR SCADA software (Chapter 2), which includes a method of sequencing process control. The sequence commands allow the operator to detail the type of control to be used (direct digital, cascade or supervisory), when broth samples are to be taken and the set point a variable must follow. The sequence commands for fed-batch fermentations is shown in Listing 6.2, while that for batch fermentations is given in Listing 6.3. The operation of the sequence starts by defining the process as fermentation (line 1), the sequence then indicates which analog control loops have data logging and alarm monitoring (lines 2 & 3). The command 'CONTRLON 01T01,30,30.5,31,31.5,32' (line 4) informs MENTOR to apply PID control onto the temperature loop (01T01) with a set point of 31°C, set point high/low alarms of 31.5/30.5°C and operation high/low alarms at 32/30°C respectively; a similar command provides stirrer speed control at 650 rpm (line 5). The system then waits until the temperature of the fermenter broth rises to a value slightly above 30.5°C (line 6), only once this occurs does the sequence set the input air flow rate to 8 l/min (line 7) to provide a fully aerated fermenter broth. At line 8 the operator is requested to inoculate the broth having previously introduced the nutrient chemicals. The sequence then cascades the pH control loop onto the ammonium hydroxide feed pump (line 9), with the pH given a set point of 5 (line 10). The glucose substrate feed pump is initially given a control set point of zero before being given a set point feed profile to follow (lines 11 & 12); where the desired profile is exponential to allow for maximum cell growth (Figure 6.4). Lines 13-15 provide a loop which informs the operator to take a broth sample once an hour for a maximum of 8 hours. This provides a basic fermentation period which allows for two doublings of the cell mass

concentration from its initial value. After 8 hours the operator response to the question "Finish fermentation ?" (line 16) informs the sequence program to start a shut-down procedure: initially stopping data logging (line 17), switching off alarm monitoring (line 18), followed by terminating all control action (line 19) before finally forcing all valves into their safe positions (line 20) and archiving the created data files onto disk (line 21). The sequence for the batch process follows a similar line, except for the inclusion of a glucose feed profile.

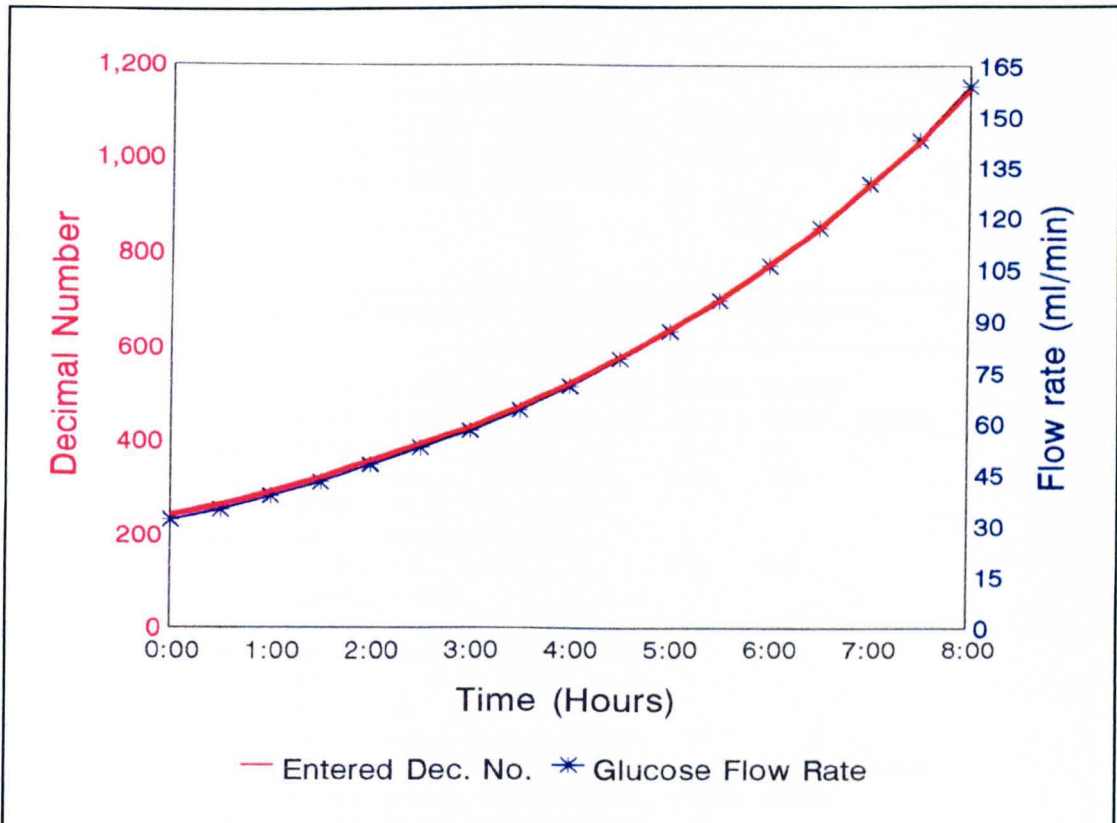


Figure 6.4 Exponential glucose substrate feed profile.

6.5. BATCH FERMENTATION RESULTS.

The two distinct growth phases of a batch fermentation pose a unique problem for the determination of appropriate controller parameters, since any tuning values which are suitable for the first phase will be inappropriate for the second phase and *vice versa*. Additionally once a PID set has been chosen, their effectiveness can only be judged after an 8 hour fermentation. The process is nonlinear, time-varying and non-repeatable thus any comparison of results has to be conducted from a pseudo-aesthetic aspect as opposed from a technical stand-point using quantities such as settling time, overshoot etc.

```

1  FERMENT
2  ALARMON      01S01, 01T01, 01A01, 01J01, 01B01, 01B02
3  LOGGINON    01S01, 01T01, 01A01, 01J01, 01D01, 01B01, 01B02
4  CONTRLON    01T01, 30, 30.5, 31, 31.5, 32
5  CONTRLON    01S01, 600, 645, 650, 655, 700
6  WAIT        01T01, 30.5, +1, 4
7  CONTRLON    01J01, 7.5, 7.9, 8, 8.1, 8.5
8  QUESTION    10    Ready to start ?
9  CASCADE     01A01, 01B02
10 CONTRLON    01A01, 4.5, 4.9, 5, 5.1, 5.2
11 CONTRLON    01B01, 0, 0, 0, 1, 4095
12 PROFILE     01B01, 22
13 QUESTION    11    Has a sample been taken ?
14 HOLD        60
15 REPEAT      8, 13
16 QUESTION    12    Finish fermentation ?
17 LOGGINOF    01S01, 01T01, 01A01, 01J01, 01D01, 01B01, 01B02
18 ALARMOF     01S01, 01T01, 01A01, 01J01, 01B01, 01B02
19 CONTRLOF    01S01, 01T01, 01J01, 01A01
20 SAFE
21 ARCHIVE
22 END

```

Listing 6.2 Sequence commands for a fed-batch fermentation.

```

1  FERMENT
2  ALARMON      01S01, 01T01, 01A01, 01J01, 01B01, 01B02
3  LOGGINON    01S01, 01T01, 01A01, 01J01, 01D01, 01B01, 01B02
4  CONTRLON    01T01, 30, 30.5, 31, 31.5, 32
5  CONTRLON    01S01, 600, 645, 650, 655, 700
6  WAIT        01T01, 30.5, +1, 4
7  QUESTION    10    Ready to start ?
8  CONTRLON    01J01, 7.5, 7.9, 8, 8.1, 8.5
9  CASCADE     01A01, 01B02
10 CONTRLON    01A01, 4.5, 4.9, 5, 5.1, 5.2
11 QUESTION    11    Has a sample been taken ?
12 HOLD        60
13 REPEAT      8, 11
14 QUESTION    12    Finish fermentation ?
15 LOGGINOF    01S01, 01T01, 01A01, 01J01, 01D01, 01B01, 01B02
16 ALARMOF     01S01, 01T01, 01A01, 01J01, 01B01, 01B02
17 CONTRLOF    01S01, 01T01, 01J01, 01A01
18 SAFE
19 ARCHIVE
20 END

```

Listing 6.3 Sequence commands for a batch fermentation.

6.5.1. Manual Tuning.

An initial manual tuning was attempted on a batch fermentation using proportional control only. The result of the controller can be seen in Figure 6.5 which primarily illustrates that although the dissolved oxygen concentration was maintained above the set point value (which can be considered as a minimum critical oxygen concentration for cell growth), this was only achieved by using large amounts of input air. While this type of response may be acceptable for

maximum cell growth, it is wasteful of resources and hence uneconomic. An improvement in the process response was attained after a number of manual tunings of a PID controller (Figure 6.6). The dissolved oxygen concentration response was reduced in level without falling below the set point for any considerable period of time. It can be seen that the dissolved oxygen concentration generally increases after $T=4:00$ hours which coincides with the change to the second growth phase.

It is noticeable that the dissolved oxygen measurement is extremely noisy. It is thought that there are two primary causes of this; firstly there are abrupt changes in the measurement owing to attachment of oxygen bubbles (high reading) or clumps of cells (low readings) to the oxygen probe and secondly the dissolved oxygen control loop possesses high speed dynamics, so that even a relatively small increase in the input air flow rate produces a dramatic increase in the dissolved oxygen measurement. The problem is compounded by the 10 second sampling rate of the MENTOR software. It is also worth noting that the process may be subjected to external disturbances such as the addition of surfactant, which can cause sudden and dramatic changes in the oxygen dissolution value, C' .

6.5.2. Automatic Tuning.

The dissolved oxygen response shown in Figure 6.7 includes a single activation of the tuning procedure during the first growth phase. The process started under manually tuned PID control which maintained the oxygen concentration at an uneconomic maximum. The automatic tuning procedure was manually initiated at $T=0:24$ hours, however this particular tuning was manually terminated after 14 minutes owing to a lack of induced oscillations; with the process subsequently returned to the manually tuned controller. The active period of the automatic tuning procedure is represented by the solid block along the x-axis of the graph. A second tuning phase was started at $T=1:10$ hours and terminated after 74 minutes. The resultant PID controller successfully maintains the level of dissolved oxygen above the set point, using a reduced input air flow, until the start of the second growth phase at approximately $T=4:30$ hours. The performance of the controller during this ethanol consumption phase is poor

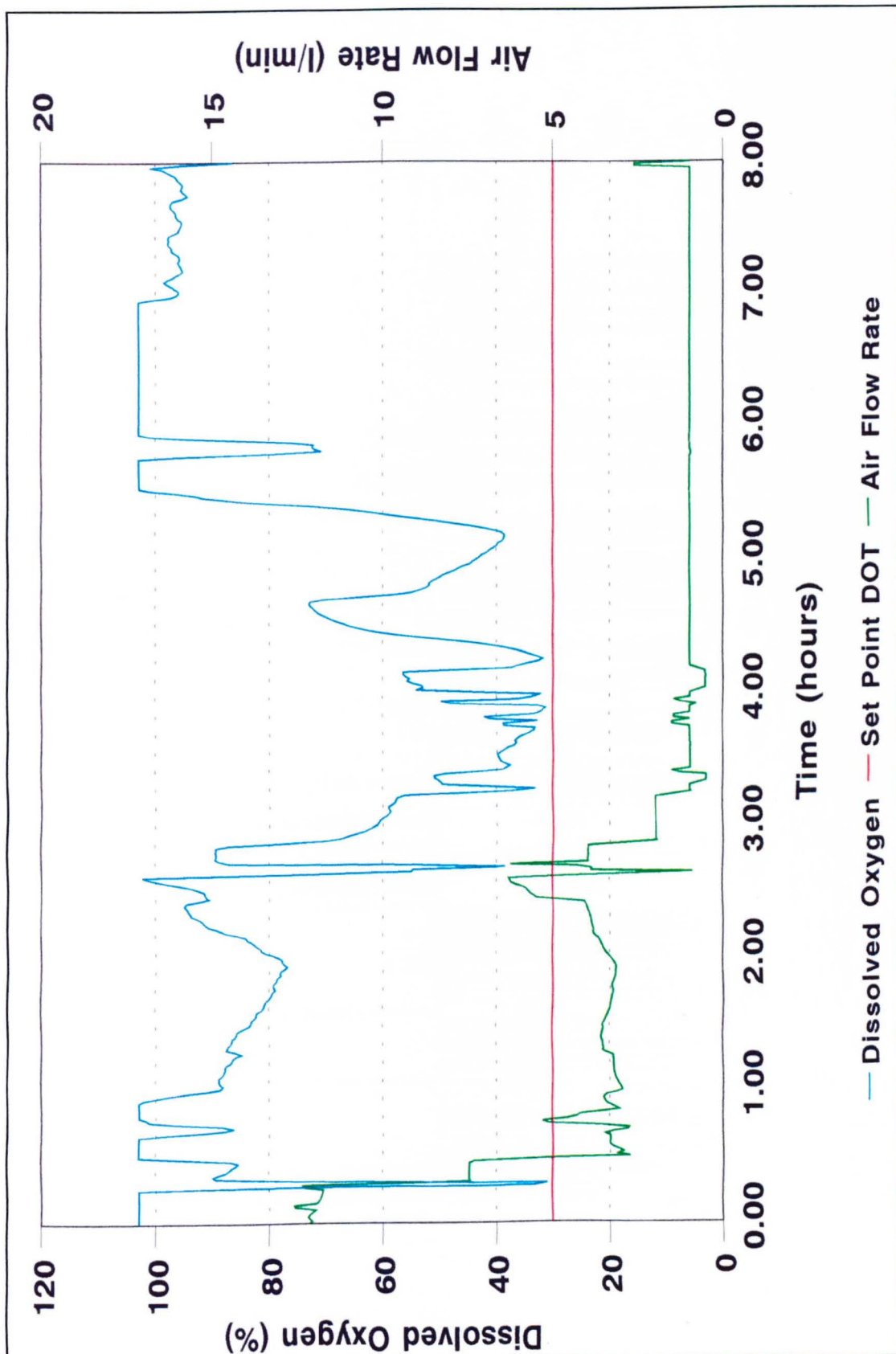


Figure 6.5 Manually tuned proportional controller response.

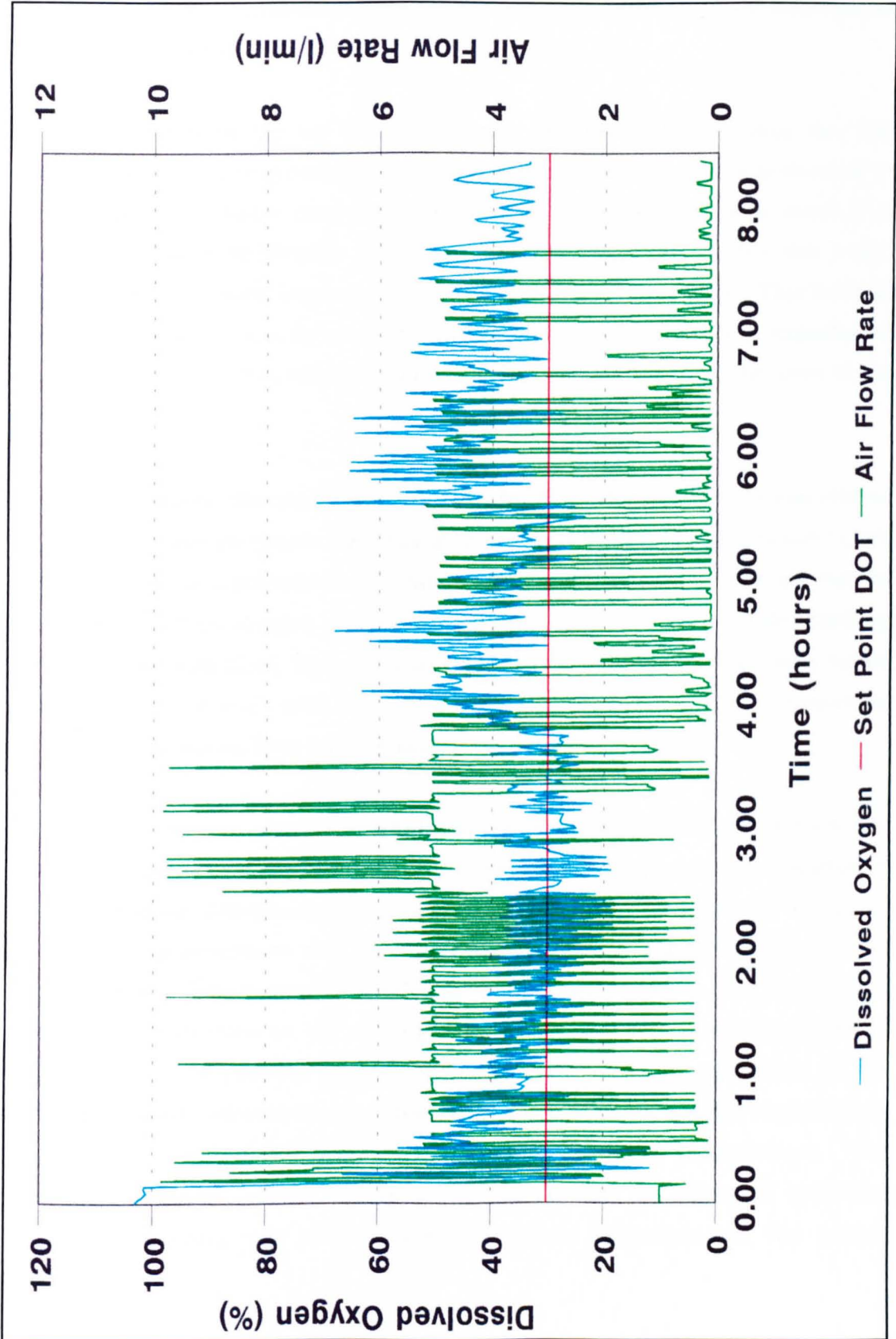


Figure 6.6 Final manually tuned PID controller response.

since it maintains a minimum input air flow rate of 1.0 l/min which contributes to the steady increase in the dissolved oxygen level.

An improvement in the air flow usage can be obtained by tuning the PID controller during both growth phases. The activation of the tuning procedure at the start of the ethanol consumption phase is difficult to achieve since it is almost impossible to identify precisely when the yeast cells enter this state, although the pH control loop can provide an approximate indicator. This method was employed to manually start the tuning procedure during the experiment illustrated in Figure 6.8, which also includes a tuning soon after the start of the fermentation.

From the response, the oscillations induced by the tuning procedure can clearly be seen as sharp increases/decreases in the dissolved oxygen measurement. Both tuning phases provide tuning parameters which allow the PID controller to keep the dissolved oxygen concentration above the set point while utilising minimum input air flow. The response is similar to that for the manually tuned controller (Figure 6.6) with respect to the dissolved oxygen concentration, however the input air flow used is markedly reduced.

The results presented above had a control sampling rate of 10 seconds while the automatic tuning procedure, running on the second computer, had a sampling rate of 1 minute. Obviously this was not ideal, thus the frequency of sampling for the tuning procedure was increased to 30 seconds; with a corresponding increase in the data logging rate. The increased data transfer rate meant that there was a reduction in the tuning time, enabling the tuning procedure to quickly return the process to PID controlled operation. The reduction in the tuning period also allowed the dissolved oxygen concentration to be retuned more frequently, if required, to maintain a satisfactory process performance. The experimental result shown in Figure 6.9 illustrates the effect of both the increased sampling rate and of multiple manual activations of the tuning procedure.

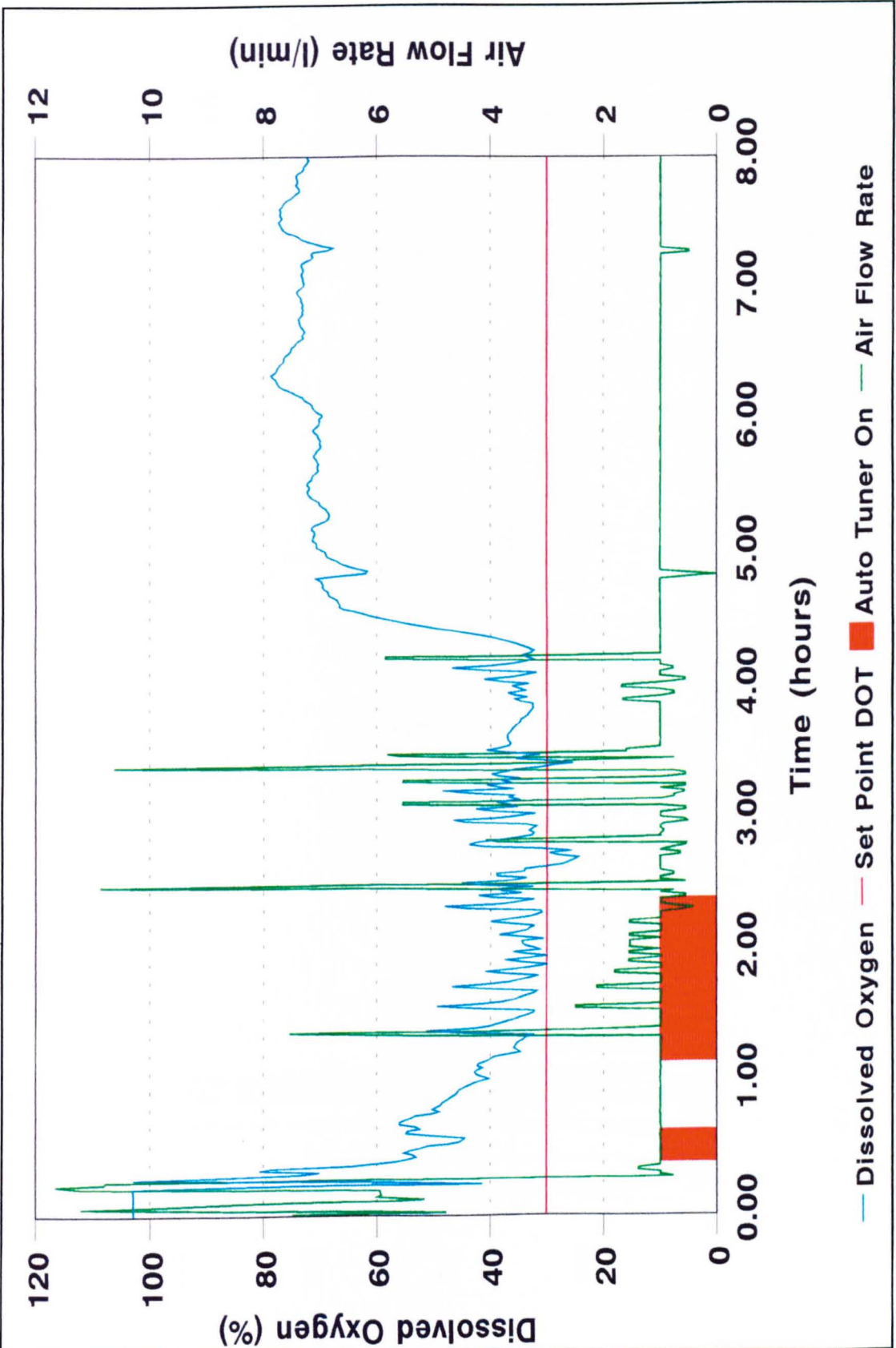


Figure 6.7 Single tuning during a batch fermentation.

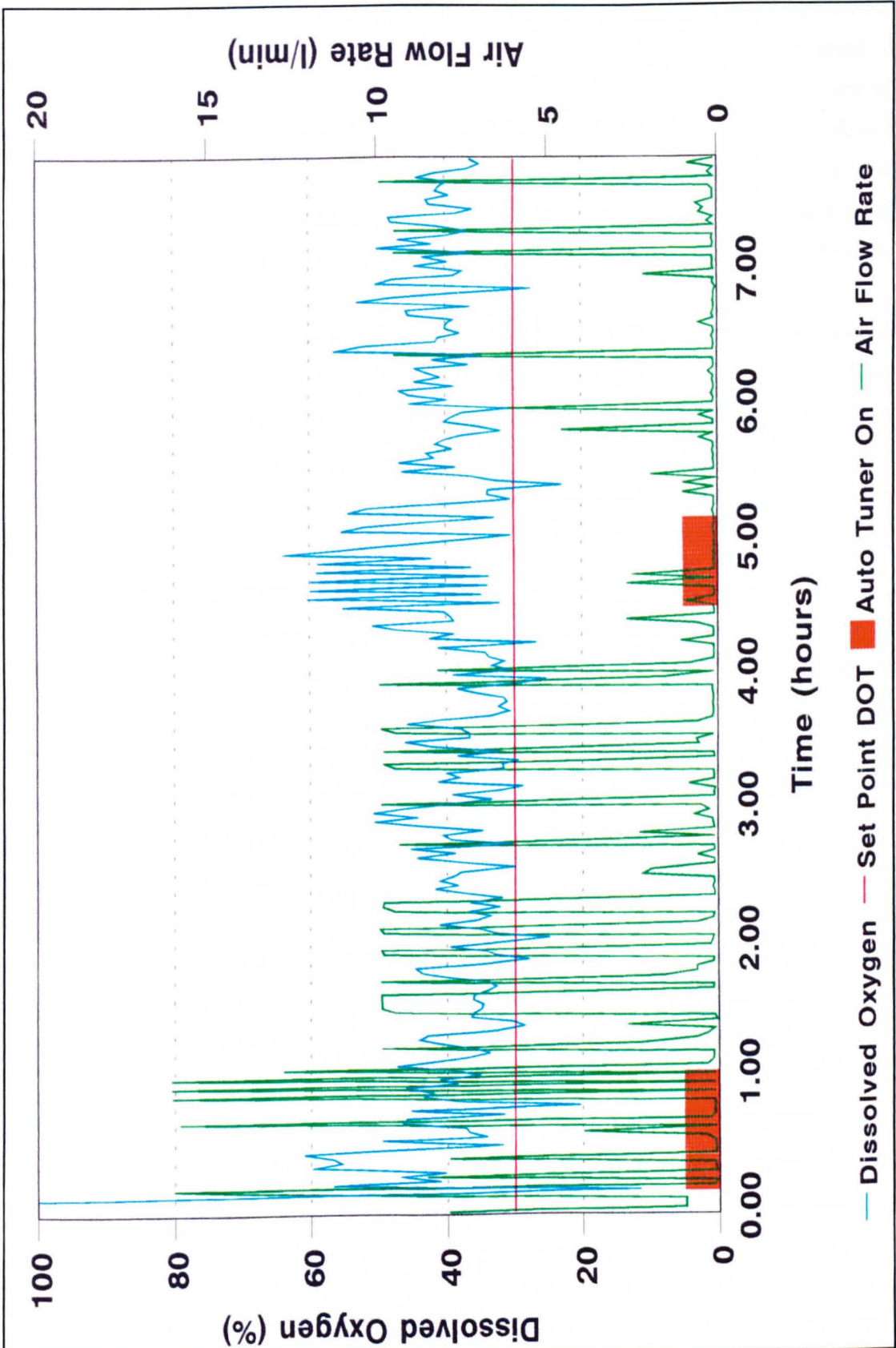


Figure 6.8 Auto-tuning during both growth phases.

The response is similar to previous results in that the dissolved oxygen was maintained above the critical set point level. The process underwent a total of seven manual activations of the automatic tuning procedure; the first two of which were terminated by the time limiting procedure (that is, a time out without obtaining an adequate oscillatory response). The major improvement of this response over previous results is that the regulation of the dissolved oxygen level is much tighter, accomplished with a low input air flow rate at regular intervals.

The next improvement made to the operation of the automatic tuning procedure was the further increase of the sampling rate to 20 seconds (Figure 6.10). This particular result clearly highlights the two distinct growth phases. The changeover for this particular experiment occurred some point after T=3:00 hours, then there is a reduction in the oxygen consumption rate.

6.5.3. Controller Modification.

The various batch experiments performed were successful in terms of maintaining the dissolved oxygen concentration at or above the set point level, however the responses are far from perfect. From observations made, it was noticed that the combination of the tuning procedure, MENTOR and the communication interval was not ideal. The PID controller algorithm was therefore included within the software running on the second PC (REL_5B) to improve overall process performance. This maintained a 20 second sampling rate for both the PID controller and the automatic tuning procedure. This arrangement was used during a batch fermentation with the result obtained given in Figure 6.11. The dissolved oxygen measurements have a marked reduction in the noise content as well as having a response which is much closer to the required set point. The response of the dissolved oxygen, which is initially below the set point, rises with the characteristic of a first order response, after the introduction of a tuned PID controller. Generally, this result can be considered very good, as the dissolved oxygen concentration was maintained at a level suitable for maximum cell growth, with a steady rate of input air flow. A total of four manual activations of the tuning procedure were required for the first growth phase, while a single retuning was adequate for the second growth phase.

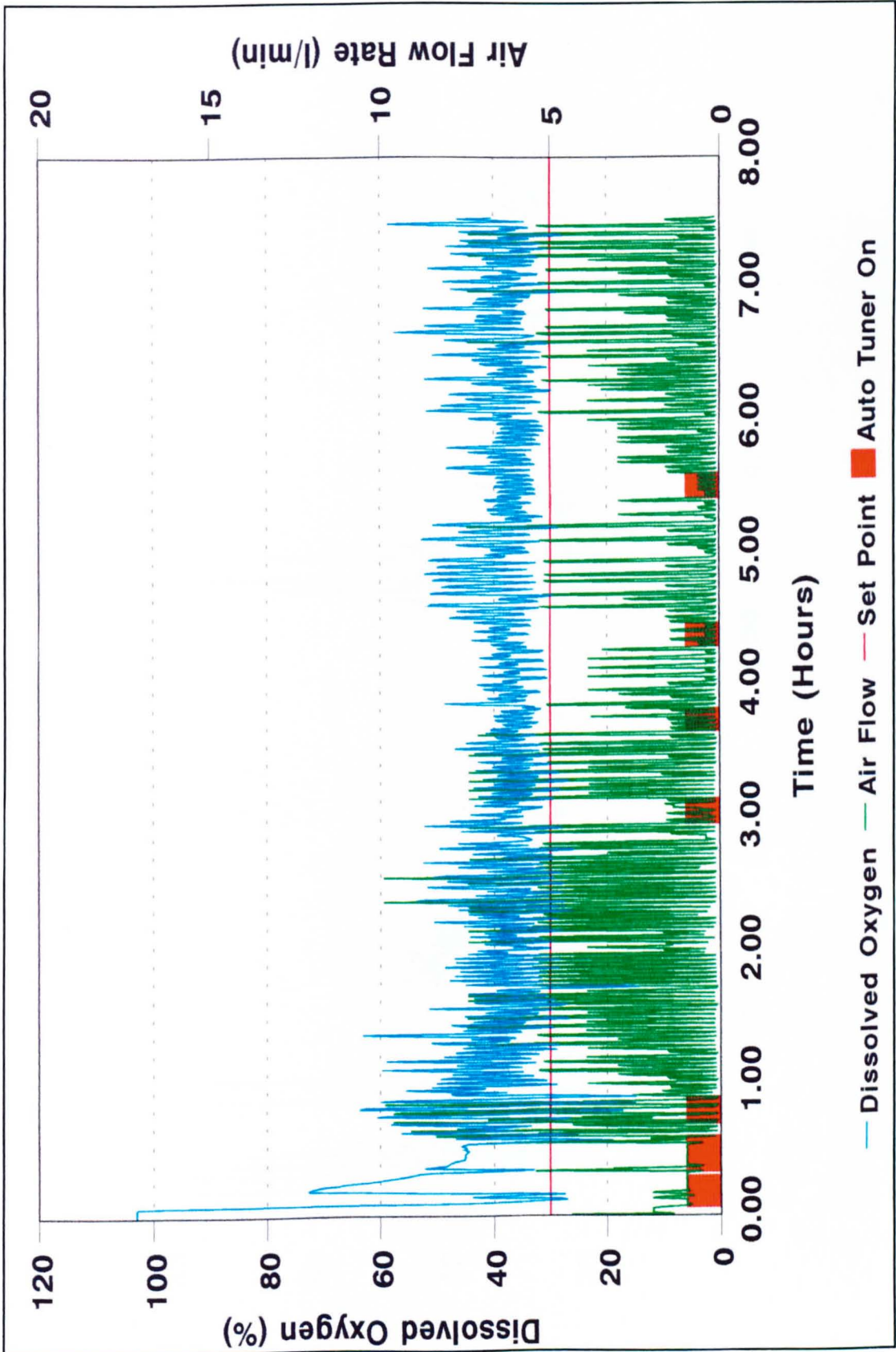


Figure 6.9 Auto-tuning with increased sampling rate.

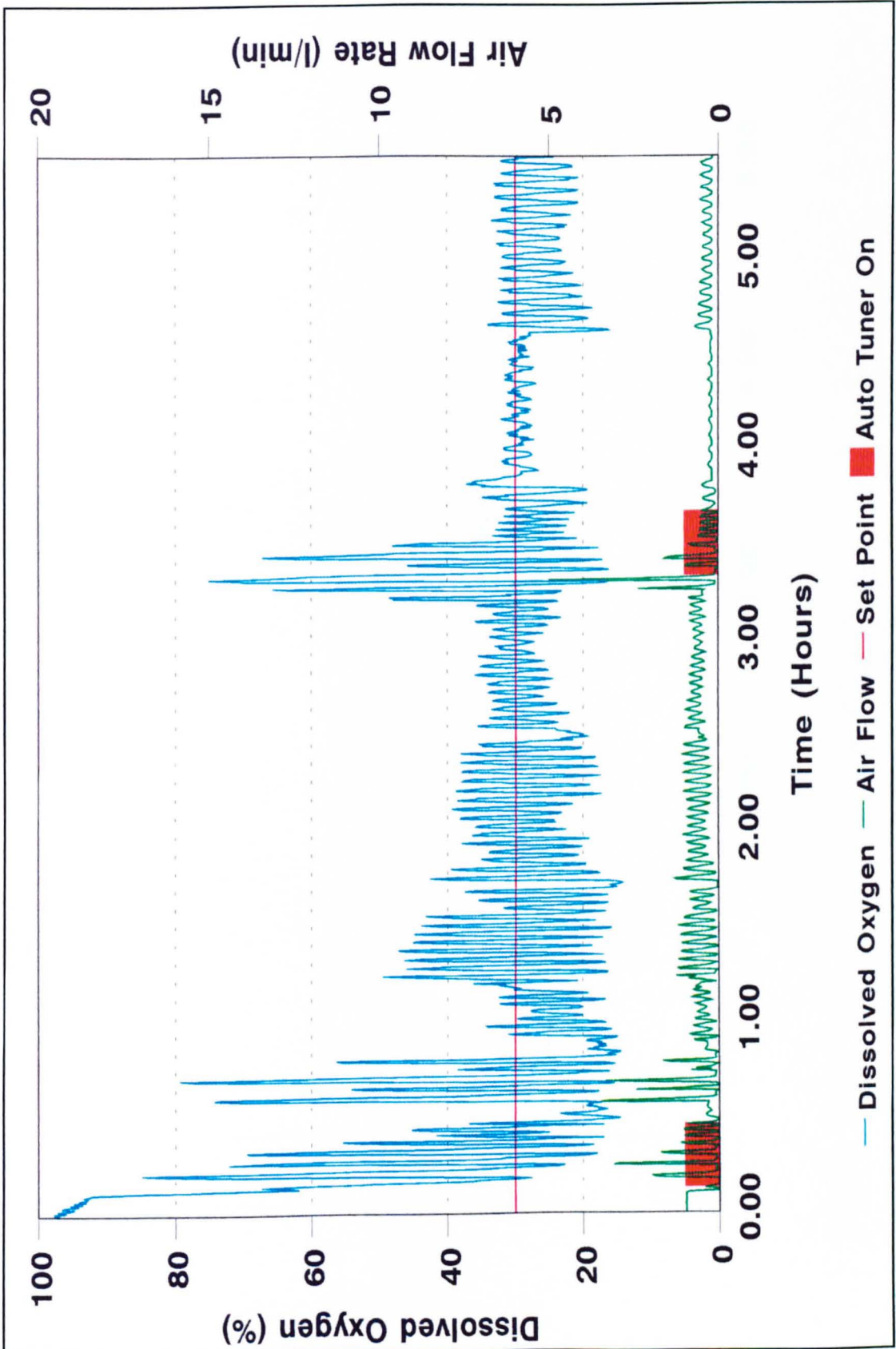


Figure 6.10 Dissolved oxygen response for final sampling rate.

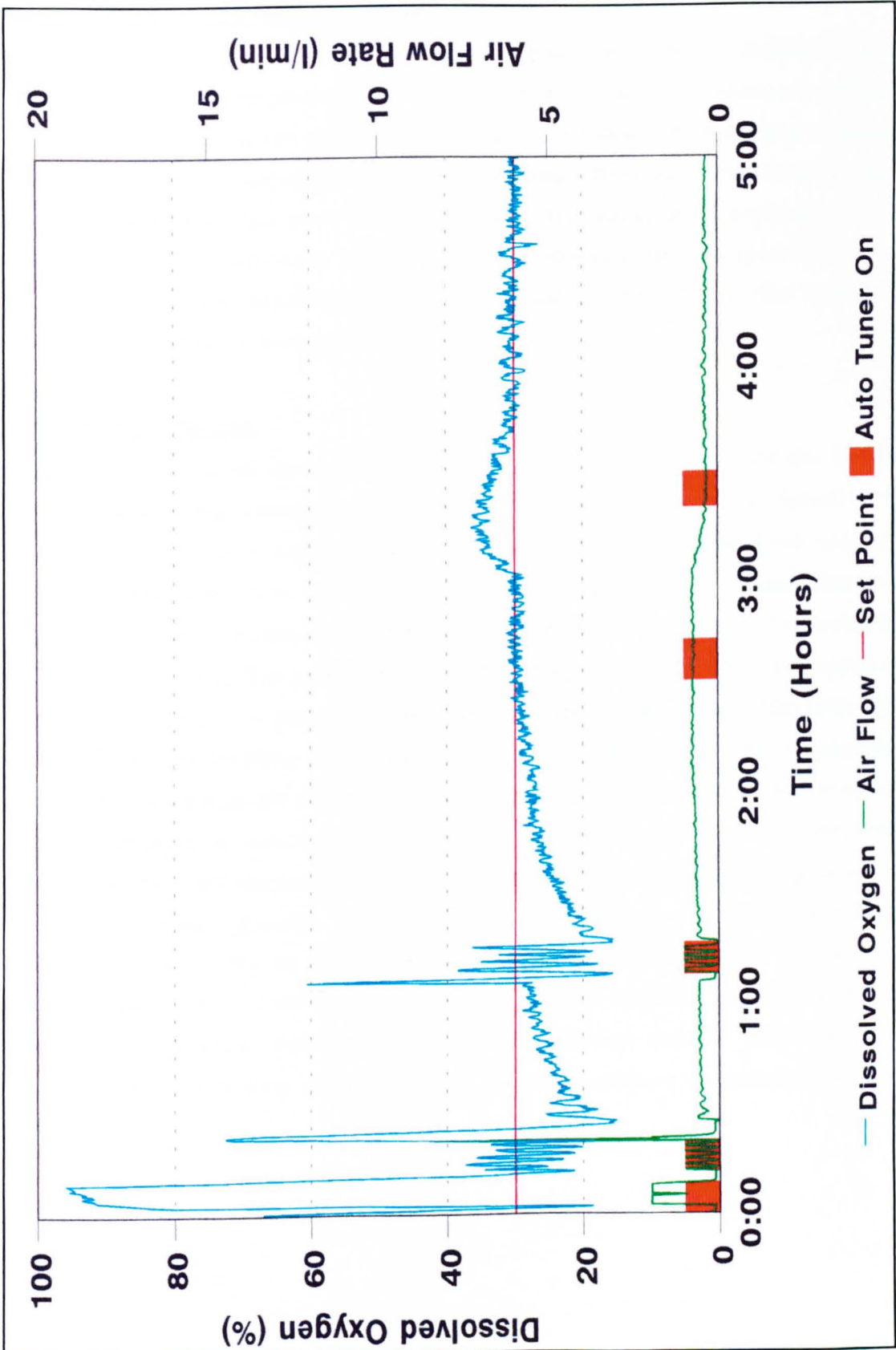


Figure 6.11 Response for controller modification.

6.6. FED-BATCH FERMENTATION RESULTS.

Having successfully applied the automatic tuning procedure to a Bakers' Yeast batch fermentation, the procedure was tested on a fed-batch fermentation. Once again a comparison of the process performance including the tuning procedure will be made with a manually tuned PID controller. The results obtained for the fed-batch fermentations were conducted using the increased sampling rate of 20 seconds for the automatic tuning procedure, however the PID algorithm was executed within the MENTOR software and not combined into the REL_5B software (described in section 6.5.3).

6.6.1. Manual Tuning.

The experience gained from attempting to tune the PID controller for the batch fermentation assisted in manually tuning a fed-batch fermentation, however a few experiments were still required before an acceptable dissolved oxygen concentration profile was obtained (Figure 6.12). The controller maintains the dissolved oxygen concentration above the required set point until approximately T=2:30 hours. After this point there is a slow decrease in the dissolved oxygen concentration which is generally maintained below the set point. The primary cause of the deterioration in the response was that the chosen PID controller parameters were suitable only for the relatively low oxygen demand at the start of a fed-batch fermentation. As the process progresses, there is an exponential increase in the cell mass concentration which requires an increasing oxygen supply to maintain growth. Since the tuning parameters were fixed, the PID controller was unable to provide an adequate air supply for the constantly changing dynamics. This result includes a sudden increase in the dissolved oxygen level around T=6:45 hours; this coincides with a fault on the temperature control loop which resulted in the premature termination of the fermentation.

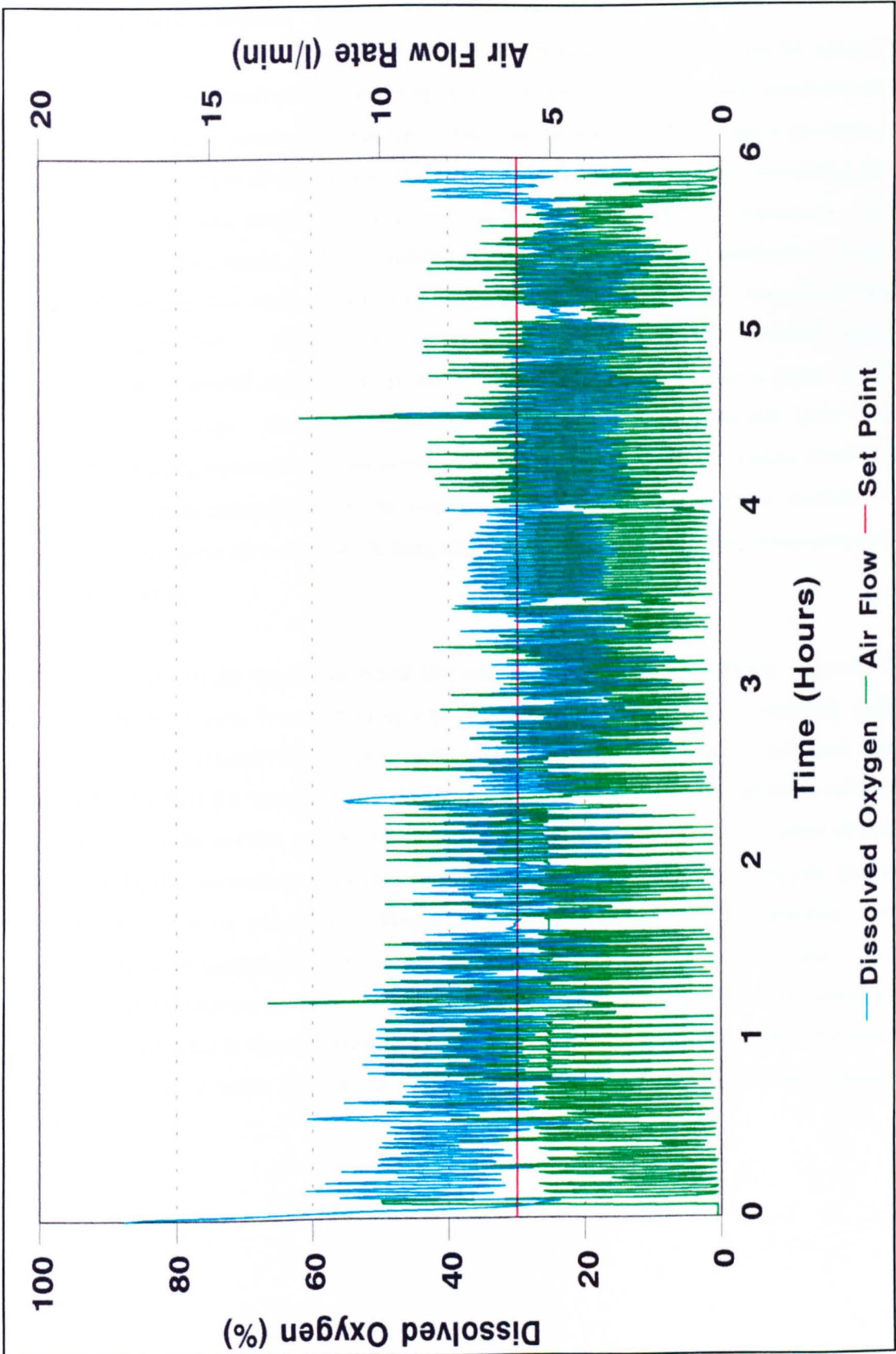


Figure 6.12 Fed-batch fermentation with a manually tuned PID controller.

6.6.2. Automatic Tuning.

The result of four activations of the automatic tuning procedure can be seen in Figure 6.13. The dissolved oxygen response follows the required set point for the duration of the fermentation, although this is achieved only by using a great deal of input air. The first activation of the tuner was terminated after exceeding the operator chosen time limit without detecting three consecutive oscillations. The second tuning produced a PID controller which maintained regulation of the dissolved oxygen for almost 3 hours, at which point a further retuning was manually initiated. This third tuning provided adequate control until approximately T=6:00 hours, when the process was subjected to a loss of the glucose feed pump. Once the glucose feed had been restarted then the automatic tuning procedure was activated a fourth time. It was noted that the dissolved oxygen measurement in conjunction with other process variables, indicated that optimal cell growth had effectively ceased, thus the fermentation was terminated.

The effect of multiple applications of the automatic tuning procedure, on a time basis, to a fed-batch fermentation can be seen in Figure 6.14. During this experiment, the dissolved oxygen concentration was maintained around the required set point for the duration of the fermentation. The high growth rate of the yeast used meant the process had a high oxygen demand. Since none of the auto-tuned PID controllers had optimal parameters, the dissolved oxygen has a slow decrease in its response. Despite the high activity of the process, the oxygen level was maintained by using only a limited amount of input air. The oxygen level increases suddenly at approximately T=6:45 hours corresponding to the point at which the substrate consumption rate exceeded the glucose feed rate. Since the process dynamics had changed dramatically, the fermentation was terminated.

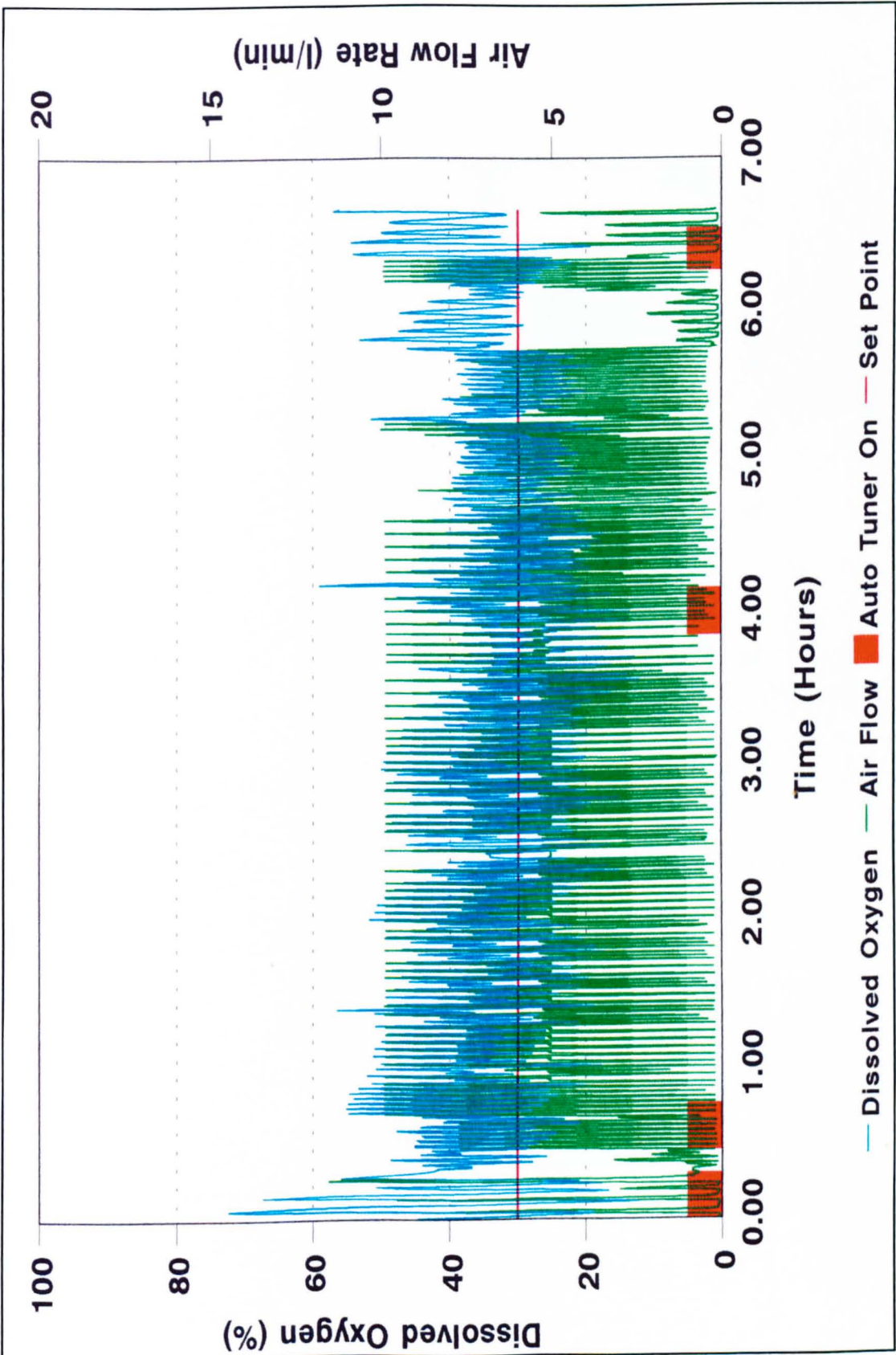


Figure 6.13 Fed-batch fermentation with automatic tuning.

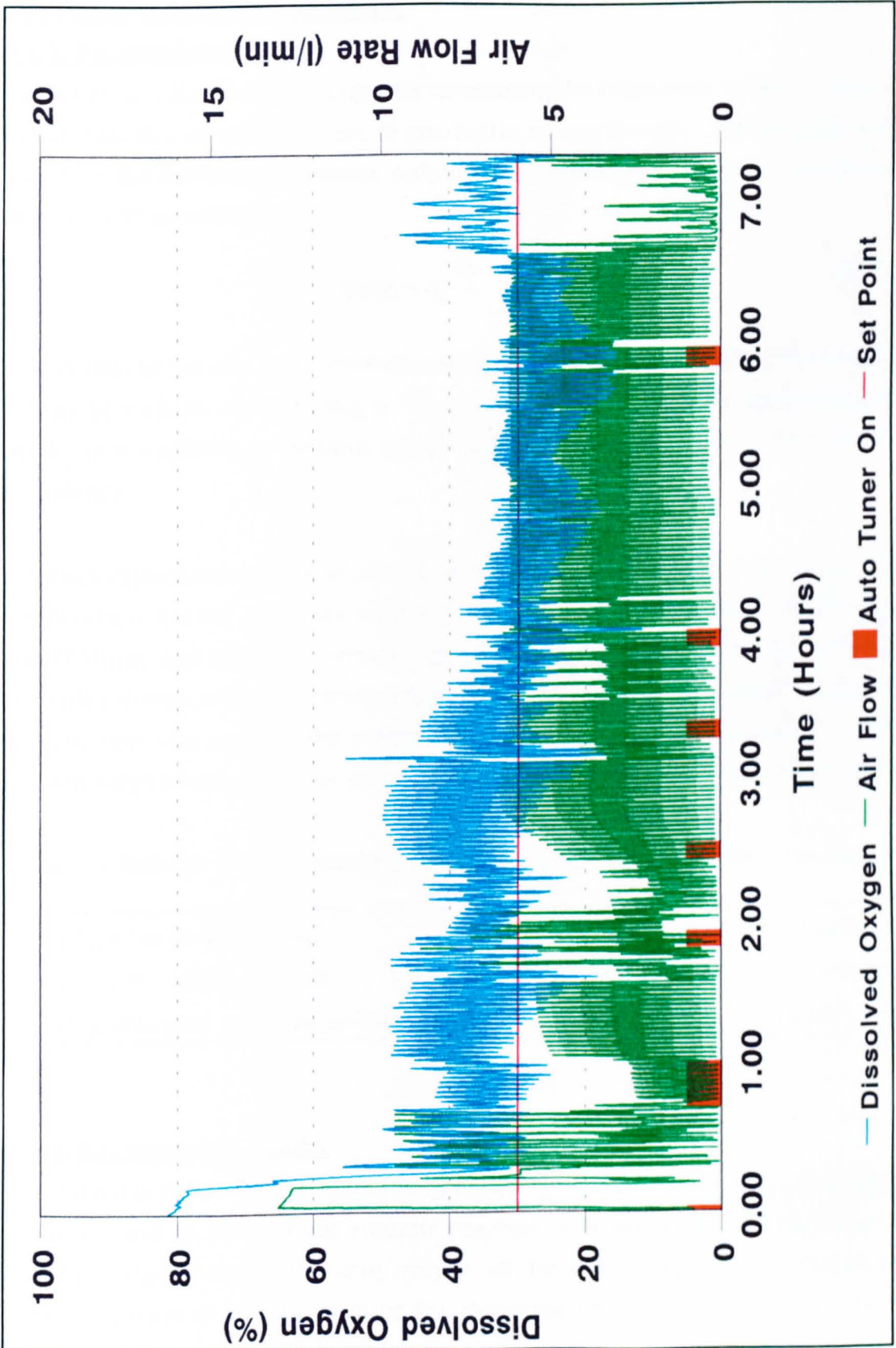


Figure 6.14 Fed-batch fermentation with multiple tunings.

6.7. SODIUM SULPHITE RESULTS.

6.7.1. Experimental method.

Cooper et al [6.6] used a technique for measuring the volumetric oxygen transfer coefficient, K_{La} , in various types of gas-liquid environments. The method was based on the oxidation of sodium sulphite to sodium sulphate in the presence of a catalyst according to



It was decided to use this chemical reaction for further testing the automatic tuning procedure, representing a "black box" process since no mathematical model was available to perform simulation trials; thus there was no *a priori* knowledge.

For each experiment the vessel was filled with 10 litres of ordinary tap water; the temperature control loop was used to maintain the vessel at 25°C, while the vessel stirrer was held at a constant speed during the experiments; the sodium sulphite solution addition rate was altered for some experiments, while the input air flow rate was used as the manipulated variable for each experiment. The sodium sulphite solution was made according to the recipe shown in Table 6.4.

Table 6.4 Sodium sulphite solution recipe (For each litre of solution required).

1.0 litre of distilled water	(H ₂ O)	55.5 mole
63.0 g of sodium sulphite	(Na ₂ SO ₃)	0.5 mole
0.5 g of copper sulphate pentahydrate	(Cu ₂ SO ₄ .5H ₂ O)	2 x 10 ⁻³ mole

6.7.2. Experimental Results.

Although it is theoretically possible to apply the tuning procedure to an unknown process, such as the sodium sulphite reaction, it is advisable to determine a suitable range for the nonlinearity output, $\pm E$, by on-line experiment. The form of the experiment was to monitor the dissolved oxygen concentration while sending a binary (high/low) signal to the input air flow rate with a constant rate

of sodium sulphite addition. A selection of nonlinearity values were investigated with a sodium sulphite addition rate of 1 ml/min, the results for two of these tests are shown in Figure 6.15, and indicate that the chemical reaction mimics the operation of a fermentation process with respect to the dissolved oxygen concentration response. The results also show that the process can be placed into an oscillatory response by the use of two distinct air flow rates, thus it is possible to apply the automatic tuning procedure with the nonlinearity output, $\pm E$, in the range 0.0 l/min up to 5.0 l/min.

6.7.2.a. Manual Tuning.

To determine the suitability of the automatic tuning procedure it is required that the performance of the automatically tuned PID controller be compared with that of a traditionally tuned PID controller. In order to obtain an ideal comparison then it is necessary to either manually tune the PID or to use a defined procedure (such as the Ziegler-Nichols methods) followed by a manual fine tuning. It was decided to perform a full manual tuning at a dissolved oxygen concentration set point of 50%. A total of 12 experiments were performed before an acceptable response was obtained. It is recognised that further testing could have improved the response of the controller, however a compromise has to be made between an ideal response and time spent on tuning. The manually tuned controller was then applied to the process with a dissolved oxygen set point profile: 1 hour at 50% followed by 1 hour at 70% and finally 1 hour at 20% concentration. The result from this experiment is shown in Figure 6.16 where the manually determined controller parameters were:

$$K_p = 2.85 \qquad T_i = 470.0 \qquad T_d = 94.0$$

The dissolved oxygen response is adequate for the 50% set point, although it is somewhat oscillatory. In contrast the step change to 70% produces a fast rise time with minimal overshoot followed by a tight regulation response. The dissolved oxygen response to the step down to 20% is governed solely by the dynamics of the process, however once the set point is reached the controlled response is very oscillatory without falling below the required 20%.

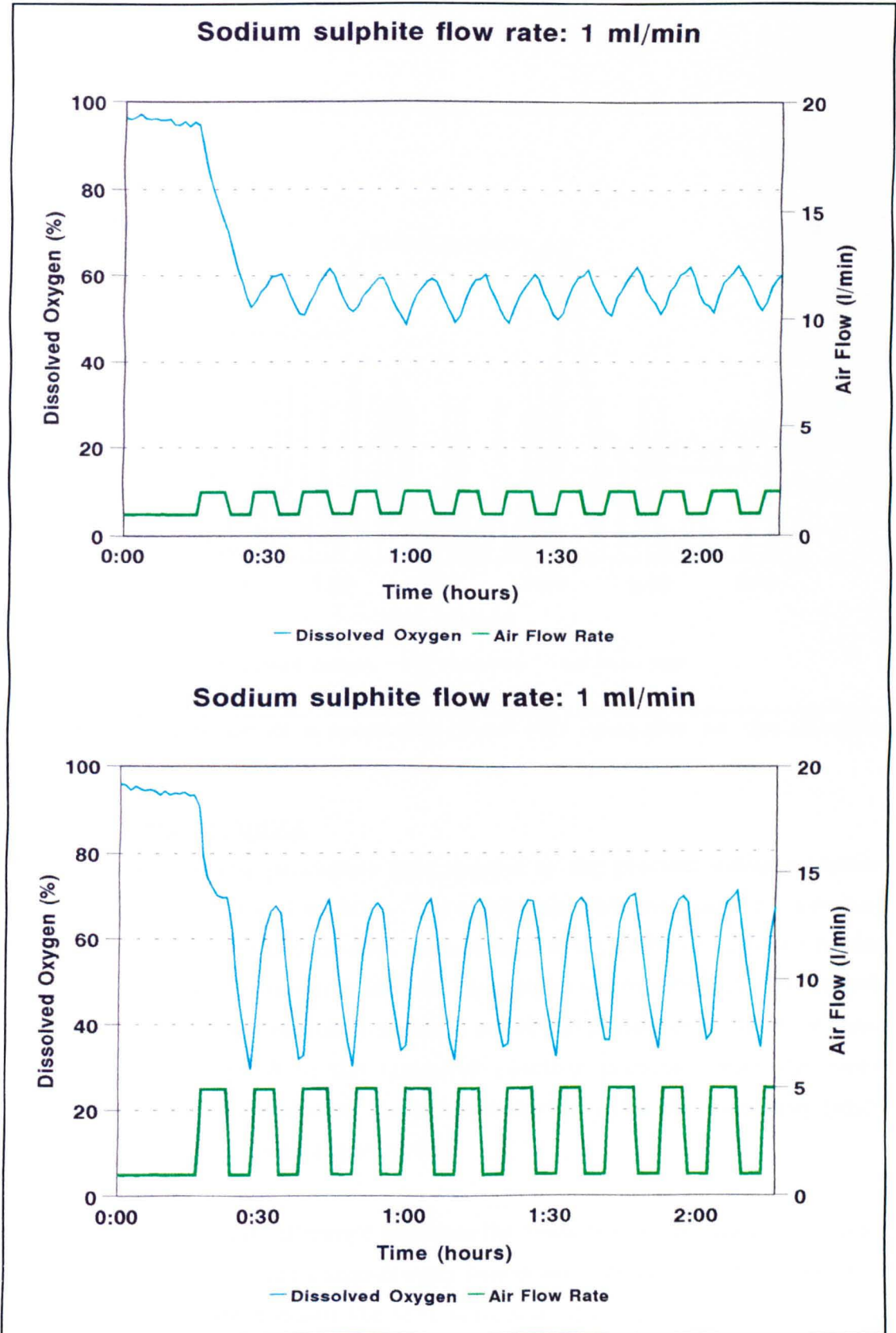


Figure 6.15 Sodium sulphite reaction with binary air flow rate.

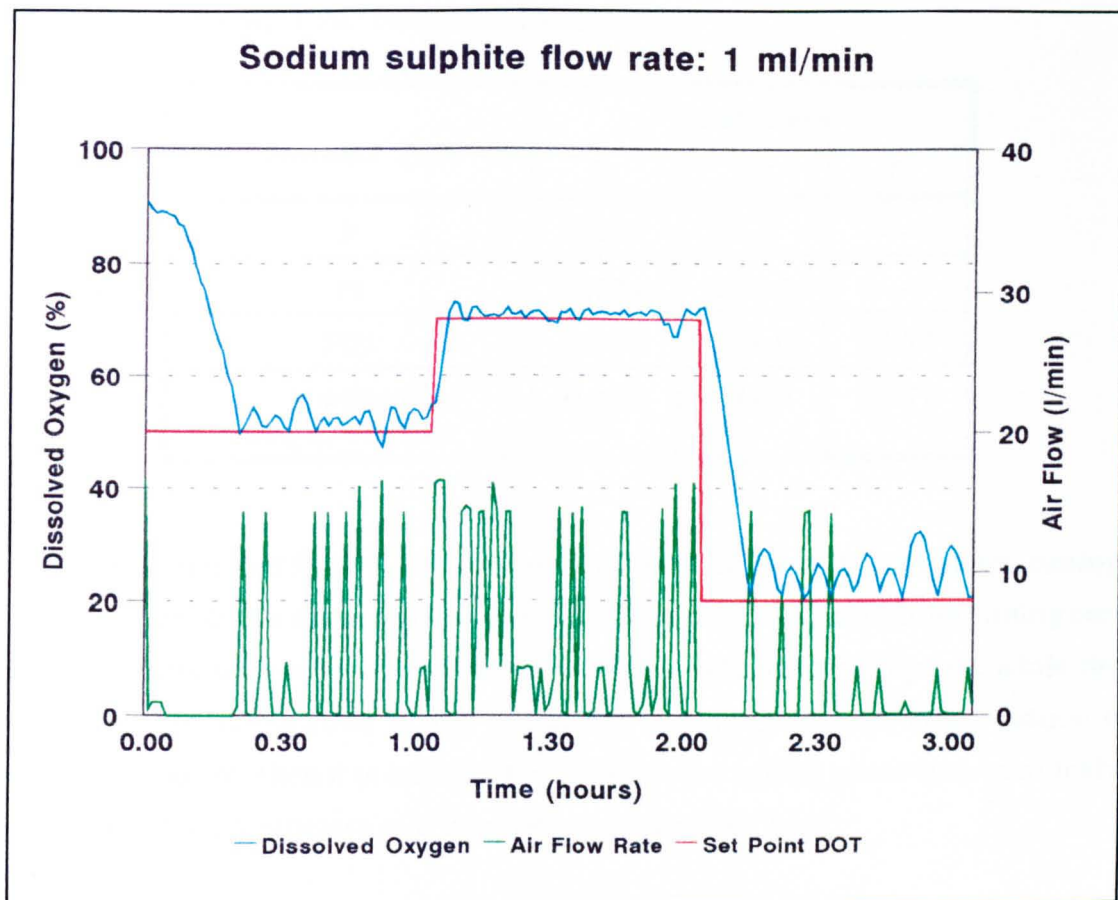


Figure 6.16 Response of a manually tuned PID controller on the chemical reaction.

6.7.2.b. Automatic Tuning.

The automatic tuning procedure was applied to the process using a sodium sulphite addition rate of 1 ml/min. The amplitude and period of the oscillatory response were determined on-line; from which a set of PID controller tuning parameters were determined (Table 6.5). In addition the modified Ziegler-Nichols equations were used to calculate an extra set of PID parameters. Each of these controllers was applied to the chemical reaction process using the same dissolved oxygen concentration set point profile used for the manually tuned controller (Figure 6.17 and Figure 6.18).

There is no significant difference between the response of the manually tuned controller and those of the automatically tuned controllers; each controller has an adequate regulation about the 50% set point with an improvement at 70% although the control about the 20% set point is oscillatory. From these results

Table 6.5 Calculated PID controller parameters.

Controller Type	Parameters		
	K_p	T_i	T_d
P	0.113	-----	-----
PI	0.124	764.0	-----
PID	0.106	244.0	58.77
Modified Ziegler-Nichols	0.162	244.0	58.77

it can be stated that there is no obvious advantage in using the automatic tuning procedure to obtain an improved controlled response. Since manual tuning can take a considerable amount of effort to achieve a satisfactory response while the single on-line application of the automatic tuning procedure can produce a similar response; then it is advantageous to use the tuning procedure to quickly determine the parameters of a user defined controller type.

6.7.2.c. Tuning using Stirrer Speed.

The tuning procedure was also applied to the chemical reaction process using the agitation rate as the manipulated variable. The response of the process to the tuning, at a set point of 60%, can be seen in Figure 6.19. It can be seen that the increase from a stirrer speed of 60 rpm to 300 rpm, for a short time, causes a significant increase in the dissolved oxygen concentration (from 60% to 66%, approximately). Once the stirrer speed returns to the lower value of 60 rpm, the apparent transfer of oxygen continues producing an increase in the dissolved oxygen concentration. This increase eventually reaches a peak after which the oxygen is utilised in the production of sodium sulphate causing a slow reduction in the dissolved oxygen level. Thus, the process displays a typical non-symmetrical oscillatory response. This type of process response prolongs the time that the process is subjected to tuning, although it does not produce a deterioration in the determination of the controller parameters. The effect of applying the resultant auto-tuned PID controller can also be seen in Figure 6.19.

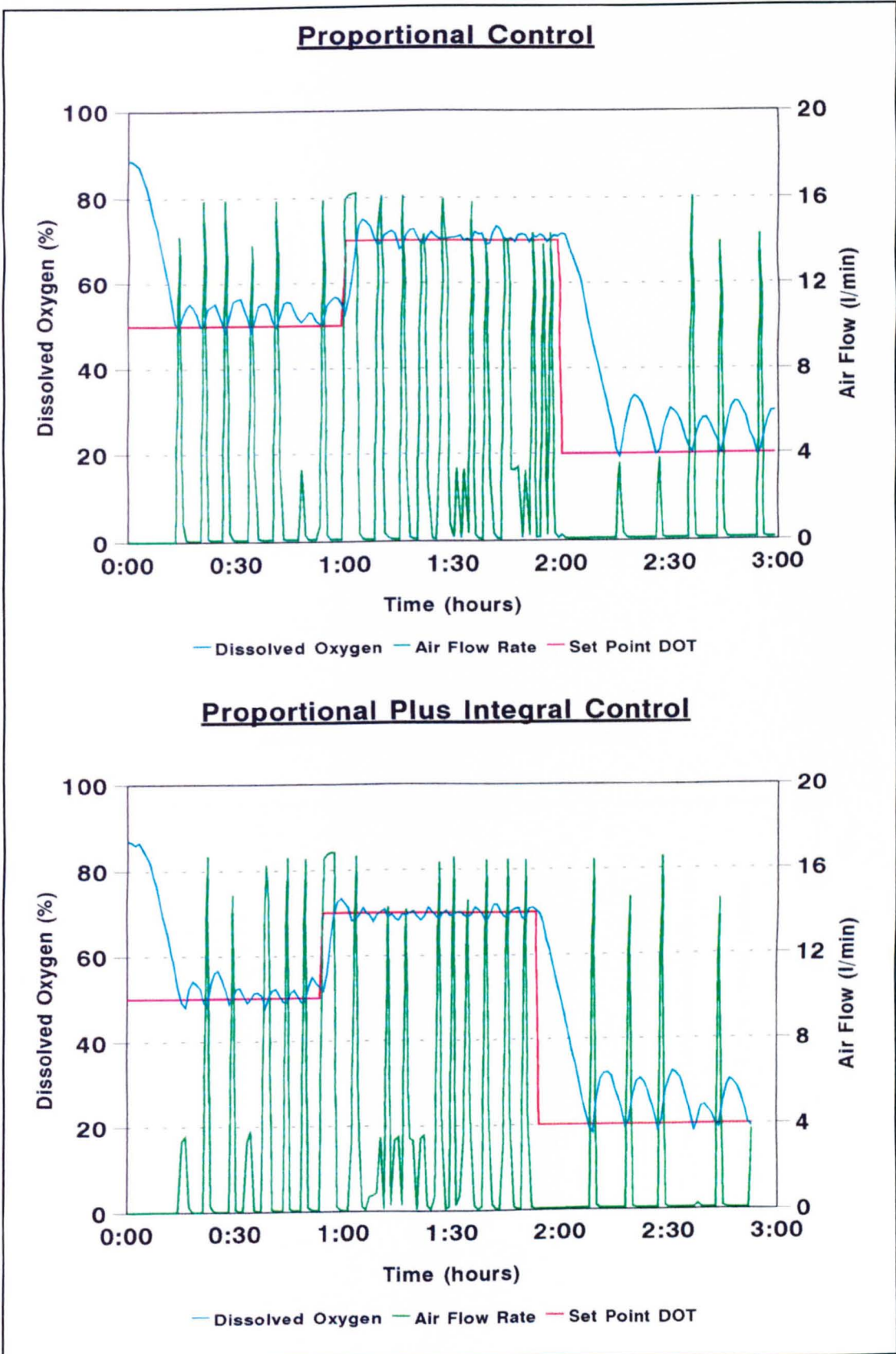


Figure 6.17 Automatically tuned P and P+I controller responses.

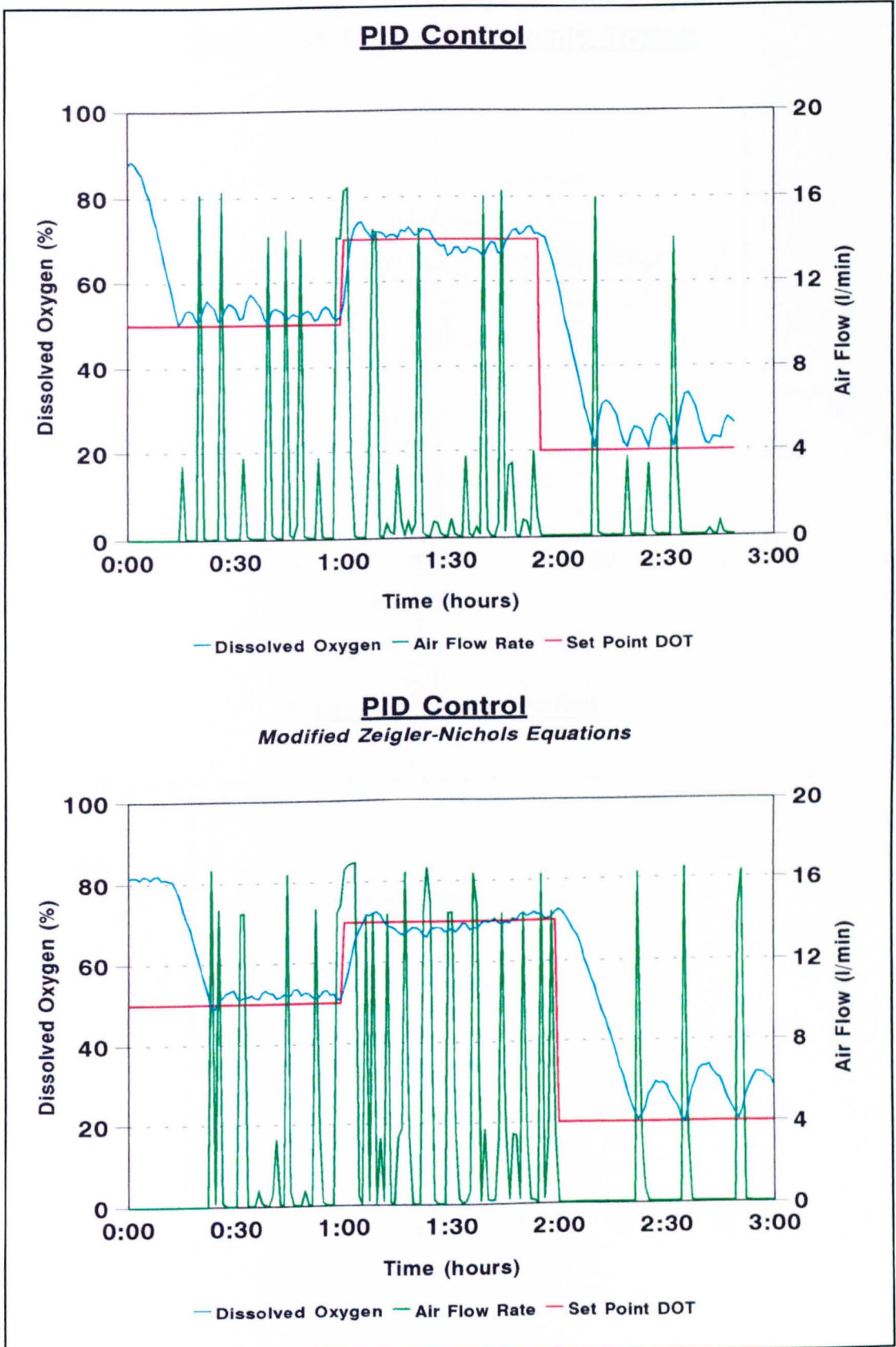


Figure 6.18 Auto tuned PID and modified Ziegler-Nichols PID responses.

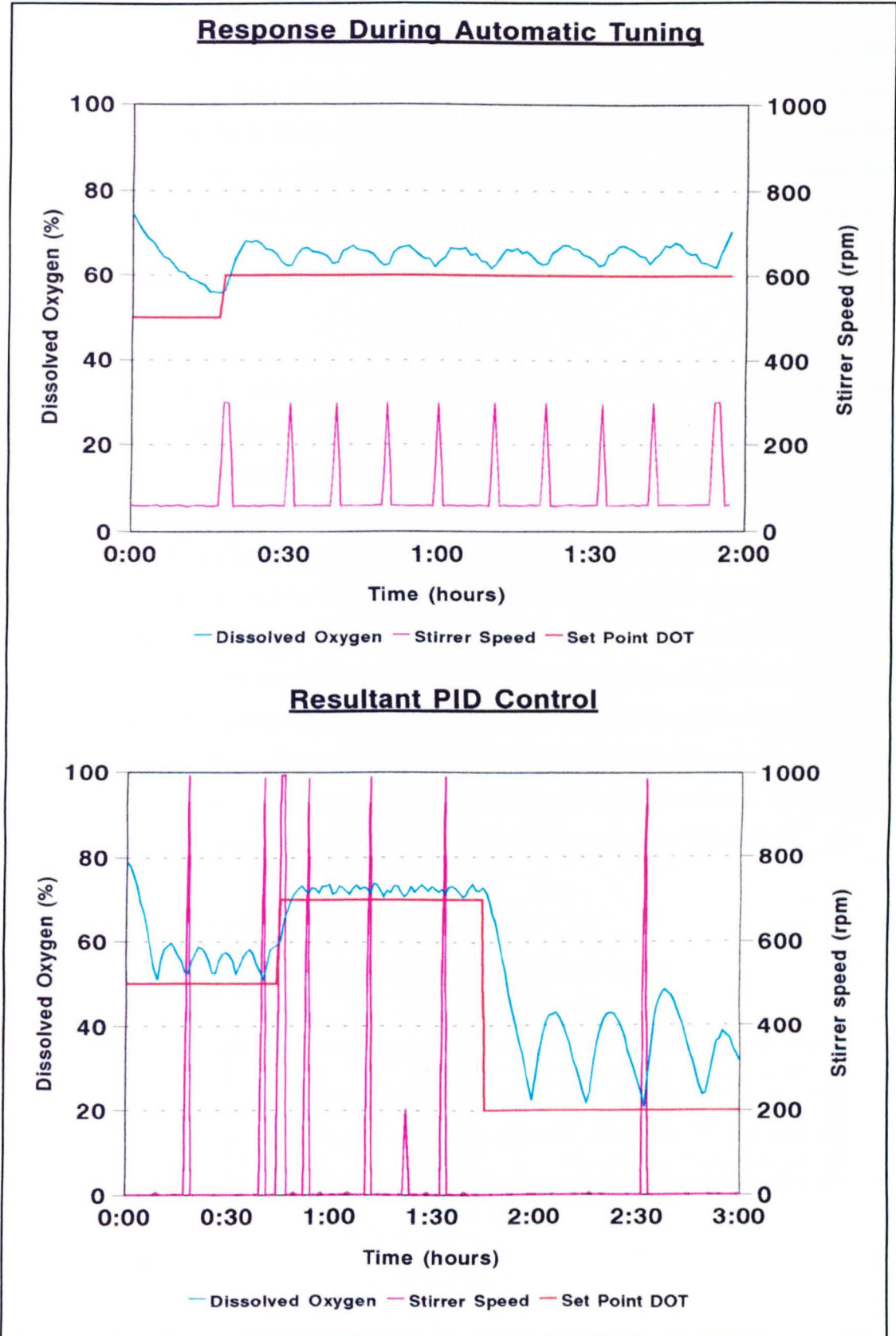


Figure 6.19 Application of automatic tuner using stirrer speed.

6.7.2.d. Effect of Nonlinearity Characteristic.

The three variables which form the nonlinearity are the hysteresis width, $\pm\beta$, the output value, E_{mag} , and the mid-point output, E_{ref} . The primary effect of the hysteresis is to provide some noise rejection capabilities, while E_{mag} provides the driving force for the oscillatory process response. It is possible to use the equations presented in Chapter 3 to determine appropriate values of E and β :

$$E = \frac{\pi A^*}{4}$$

$$\beta = A^* \sin(\phi_n + \phi_i)$$

The practical use of these equations can provide values which are impractical for the process variable being used, and should only be used with caution. If *a priori* knowledge is available for the process, then this should be used to assist in the determination of suitable values for E and β . For the on-line experiments performed, β was chosen as 2.5% dissolved oxygen concentration (that is, a hysteresis width of 5%) to allow some signal noise through but rejecting the majority of the low magnitude noise. A heuristic for determining the value of E is to set it between 2% and 10% of the manipulated variable range; for the input air flow rate this represents 0.5 l/min to 2 l/min (a nonlinearity output change of 1 l/min to 4 l/min). The result shown in Figure 6.20 illustrates the effect of applying a selection of upper and lower nonlinearity output values. The tuning parameters of the resultant PID controllers are presented in Table 6.6.

Table 6.6 Change in nonlinearity output value.

Nonlinearity output	K_p	T_i	T_d	
2 - 3 l/min	3.50	69.2	16.77	Figure 6.21
1 - 2 l/min	6.49	137.7	38.77	Figure 6.22
3 - 6 l/min	0.72	65.4	15.84	Figure 6.23

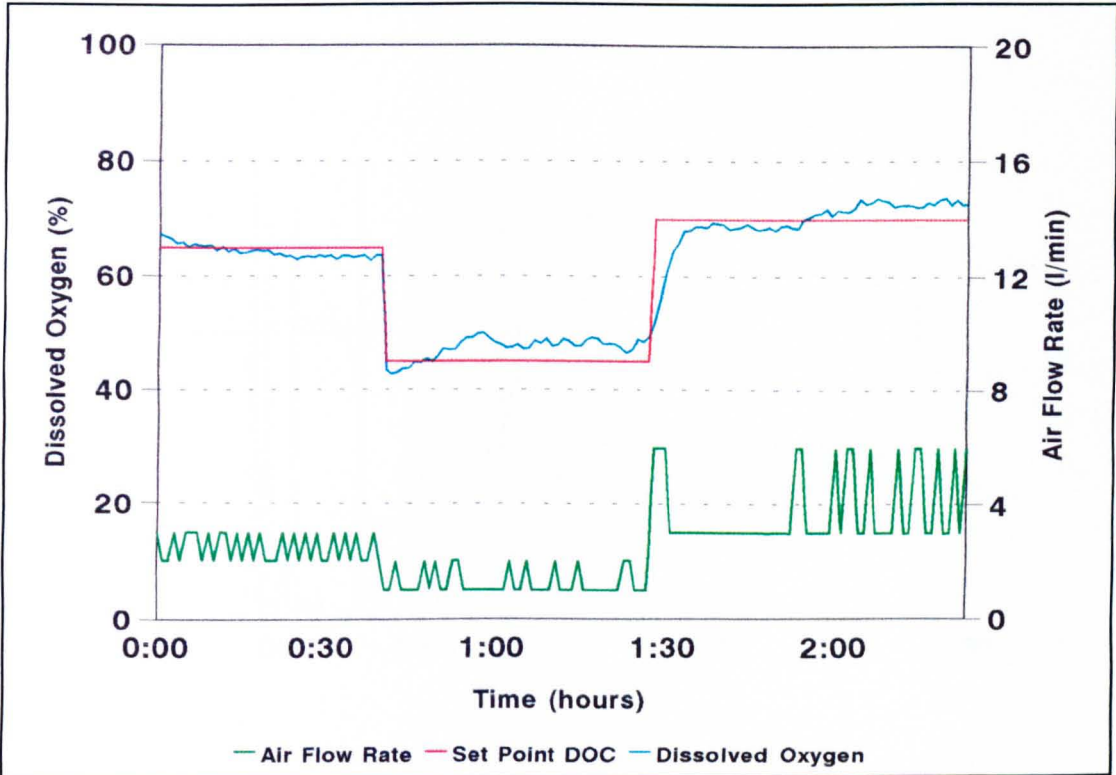


Figure 6.20 Effect on the dissolved oxygen concentration of varying the nonlinearity output.

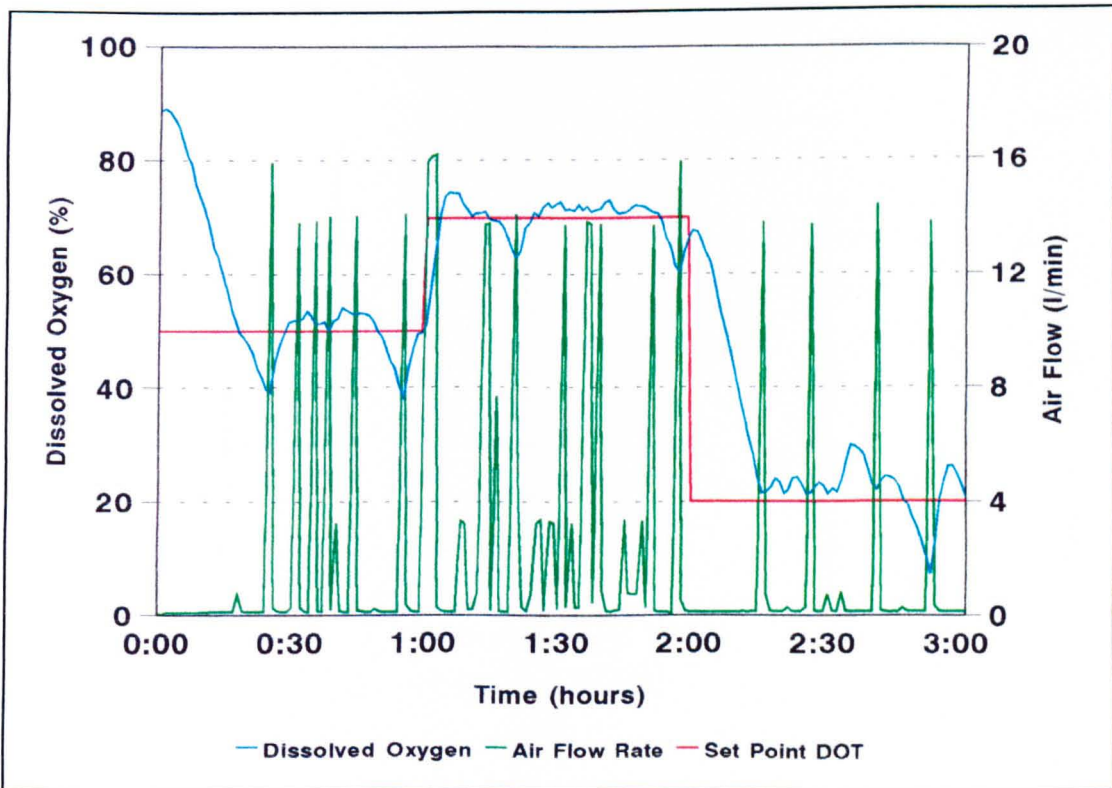


Figure 6.21 Response of auto-tuned controller: 2-3 l/min.

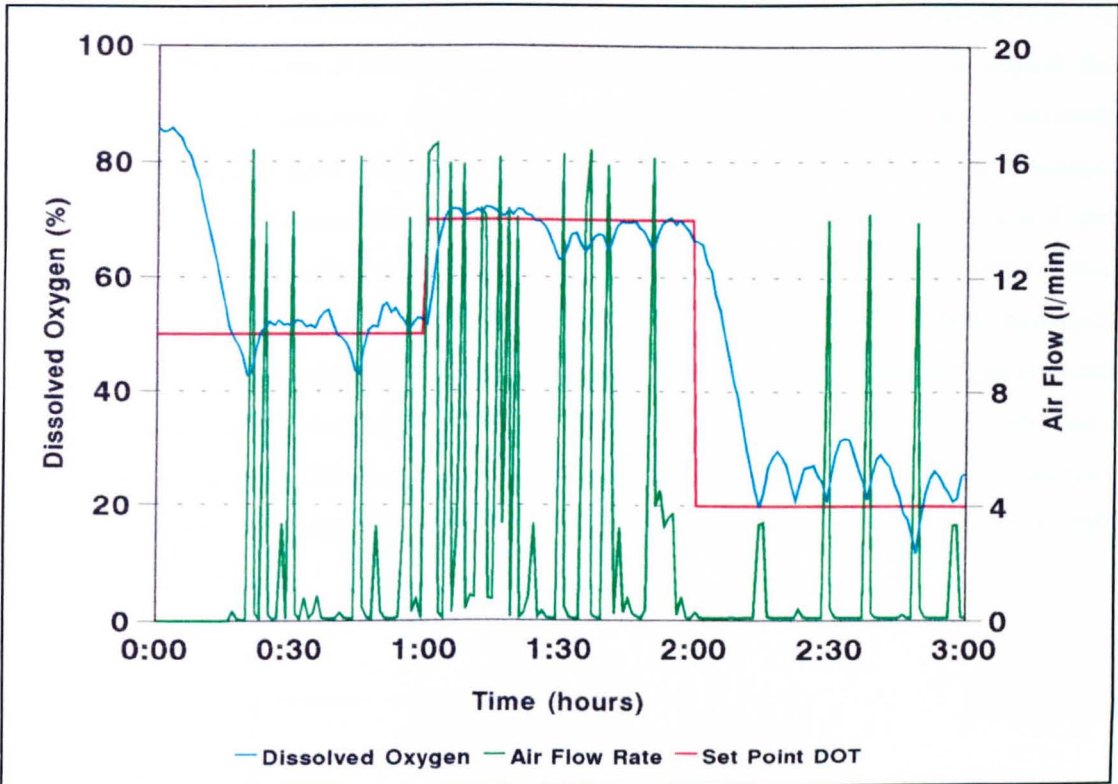


Figure 6.22 Response of auto-tuned controller: 1-2 l/min.

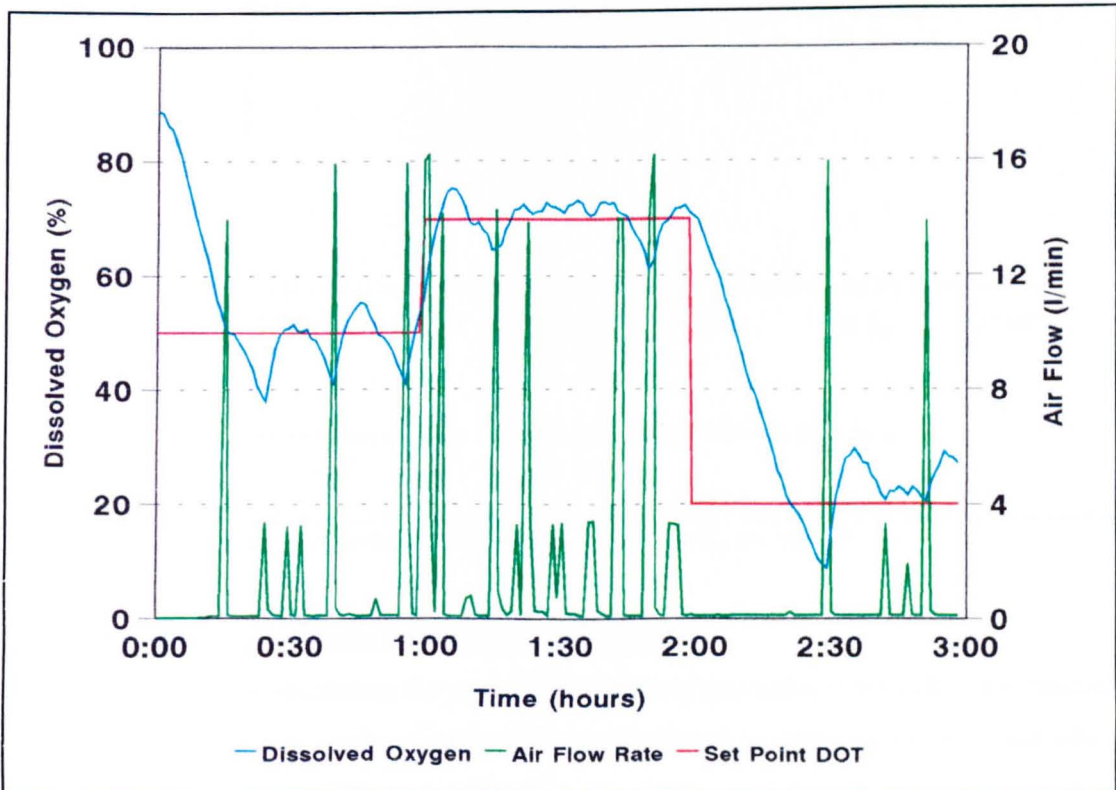


Figure 6.23 Response of auto-tuned controller: 3-6 l/min.

The tuning procedure induces an oscillatory response with an amplitude, A , while the operator can define a minimum oscillation amplitude, A' , to which the process can be subjected. Since the magnitude of the amplitude is directly related to the upper and lower nonlinearity output values, $\pm E$, then it is possible to modify the nonlinearity output to force the process oscillation toward the desired value. A number of techniques exist to accomplish this modification, such as the Regula-Falsi equation described in Chapter 3; however few methods actually work when applied on-line. One method which was investigated with some success involved changing the nonlinearity output values by a predefined percentage. Figure 6.24 illustrates the result of altering the nonlinearity output by $\pm 10\%$, where the original output was 2.6 l/min while the final output levels were 3.5-4.9 l/min.

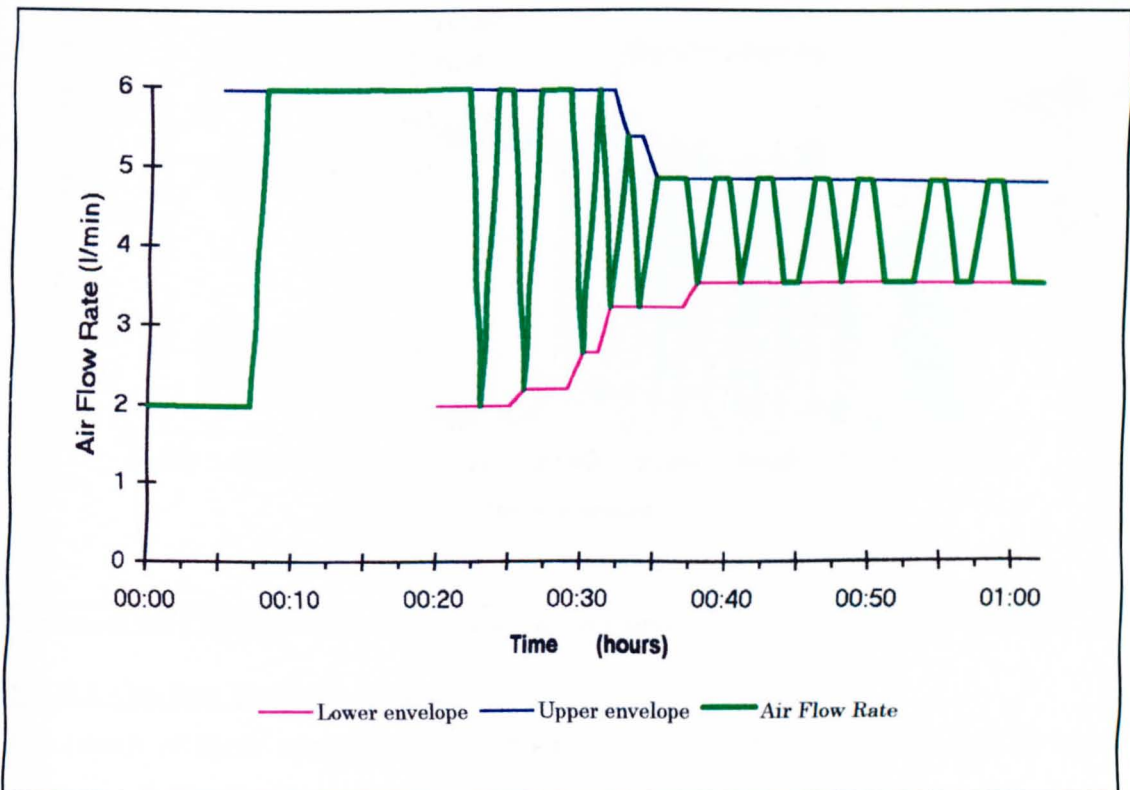


Figure 6.24 On-line adjustment of nonlinearity output value.

6.7.2.e. Change-over from Tuning to PID Control.

The previous tests involving the automatic tuning procedure and the reaction of sodium sulphite have utilised a separate experiment to determine the controller tuning parameters. Further experiments were performed to examine the operation of the change from the tuning procedure to PID control. A typical

result for a sodium sulphite addition rate of 4 ml/min is shown in Figure 6.25, where the tuning phase was started manually. Once the tuning phase was terminated, the PID controller was required to maintain the dissolved oxygen concentration at the required set point profile, where the derived controller parameters were:

$$K_p = 4.082 \qquad T_i = 144.04 \qquad T_d = 34.90$$

The required set point control was achieved with some degree of success at levels of 50% and 70%, although at 20% there was some degradation in the performance of the controller.

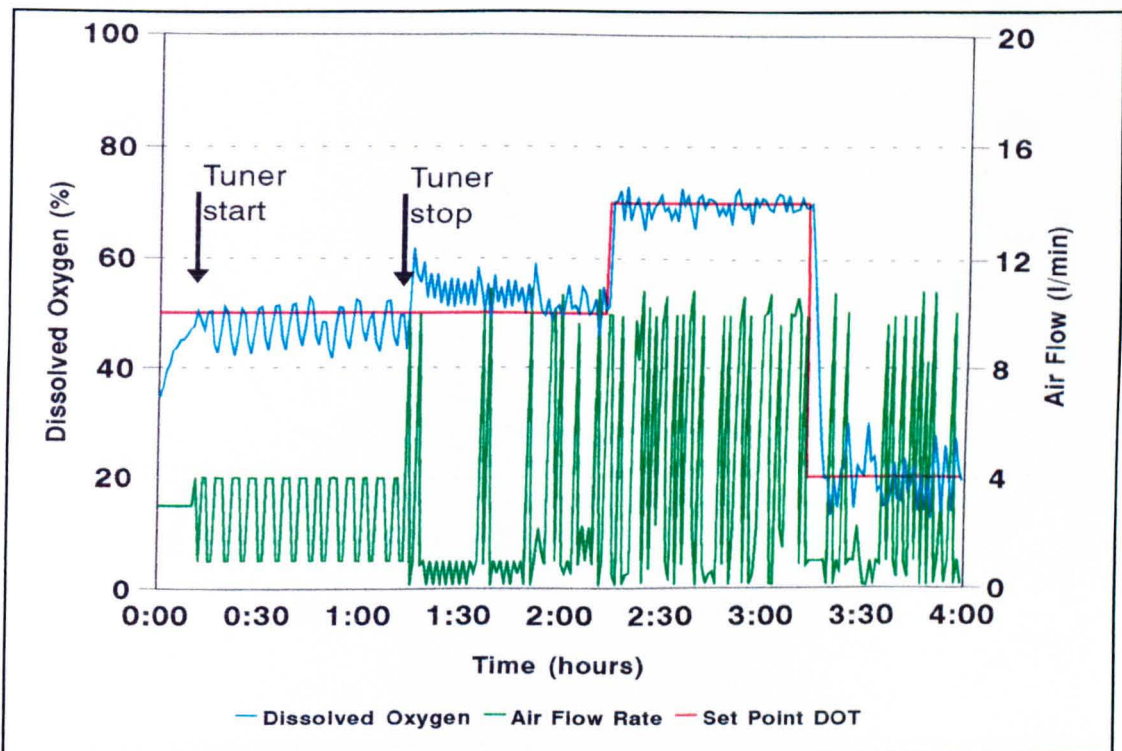


Figure 6.25 Change from automatic tuning procedure to tuned PID control.

6.7.2.f. On-line Multiple Tuning.

The result of three applications of the automatic tuning procedure can be seen in Figure 6.26. The first activation began at the start of the experiment, however it was terminated after 1 hour having been unable to produce an oscillation on the dissolved oxygen concentration. The cause of this unsuccessful tuning was a combination of a low set point value, and too high a value for the lower input air flow rate producing a dissolved oxygen equilibrium value above the required set point. Once this tuning phase was terminated, process control reverted to the MENTOR default of proportional only control (with $K_p=0.5$). The second and

third activations automatically occurred when the dissolved oxygen set point was changed from 20% to 70% and again from 70% to 50%. Both of these tuning phases produced an oscillatory response before switching over to a tuned PID control. The tuning phases provided PID controllers which maintained the dissolved oxygen concentration about the required set point level. The second tuning phase induced oscillations on the dissolved oxygen concentration below the set point owing to the upper nonlinearity output value being less than that necessary for a peak dissolved oxygen measurement above the set point.

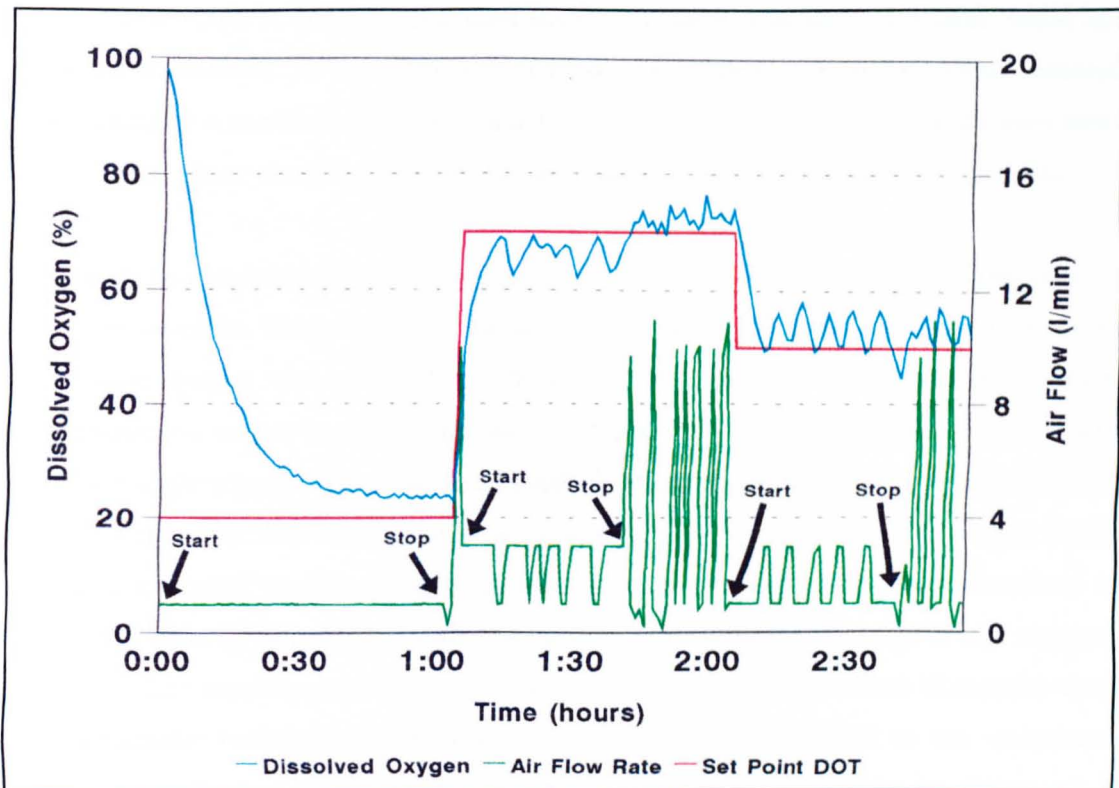


Figure 6.26 Multiple tuning during the sodium sulphite reaction.

Currently the automatic tuner has a sampling rate of approximately 20 seconds, owing to the constraints imposed by the sample rate of MENTOR and the need for communication with the second computer. However, a commercial implementation of the automatic tuner would have the tuning procedure software included within MENTOR and thus enables it to utilize the 10 second sampling rate.

6.8. DISCUSSION.

The fed-batch and batch fermentation results show perturbations on the dissolved oxygen concentration measurements; which are thought to be due to noise caused by the attachment of air bubbles to the dissolved oxygen probe. The work of Nakauoh [6.7] concluded that when an oxygen electrode is used in liquid in a fermenter, the effects of the liquid film on the electrode membrane surface are unavoidable.

From the results it will be seen that there can be a dramatic reaction, from the controlled variable, to the changeover from the tuning procedure to PID control. This could be a problem for some processes, however there seems to be very little that can be done to either rectify the problem or to smooth out the transfer.

Although the sodium sulphite technique is used to evaluate oxygen transfer in agitated vessels, there are limitations on the results obtained. The most important being the use of a chemical reaction to simulate an actual fermentation, since there is almost no evidence to substantiate that sodium sulphite approximates the physical and chemical properties of a fermentation. However the reaction can be used as a test-bed for control methodologies such as the automatic tuning procedure. Since the reaction is purely chemical it offers some degree of repeatability which the fermentation process cannot provide. The results presented for the sodium sulphite reaction illustrate that the automatic tuning procedure can be successfully applied to an unknown process: producing process responses which are comparable to those of a manually tuned controller. The results also highlight some of the operational aspects of the automatic tuning procedure, such as the change over from the tuning phase to tuned PID control or the on-line modification of the nonlinearity output values. The results also show that the tuning procedure can be applied to either of the manipulated variables (air flow rate or stirrer speed) with equal success.

The various on-line results presented for automatically tuned PID controllers compare favourably with those for manually tuned controllers. The automatic tuning procedure cannot produce a greatly improved process response over a

conventionally tuned controller. Firstly, both methods are based on the PID algorithm which suffers from a number of well known drawbacks; such as, fixed tuning parameters which are unsuitable for a nonlinear process and a derivative action which is highly susceptible to noise. Therefore a PID controller cannot accurately control a highly nonlinear time-varying fermentation process. Secondly, the controller parameters determined are based upon the Ziegler-Nichols tuning rules which produce controlled responses which have an overshoot and a 25% damping ratio.

Thus, the role of the automatic tuning procedure is to produce a controlled response which mimics the response obtained from a manually tuned controller: which is the case for the results presented here. The advantage of the automatic tuning procedure over conventional tuning techniques is that while manual tuning requires a number of experiments, the tuning procedure has the ability to determine suitable controller parameters on-line in a relatively short time. Additionally the tuning procedure can be activated a number of times to retune the controller. Thus the process is controlled by a series of different fixed controllers instead of one 'rigid' controller.

6.9. REFERENCES.

- 6.1. Fuch, R. and D.I.C. Wang. Simple system for controlling dissolved oxygen concentration in laboratory fermenter. *Biotechnology and Bioengineering*. Vol. XVI. p. 1529-1536. 1974.
- 6.2. Wiseman, A. *Principles of biotechnology*. Surrey University Press. 1988.
- 6.3. White, J. *Yeast Technology*. Chapman and Hall. 1954.
- 6.4. Reed, G. and H.J. Pepler. *Yeast Technology*. Chapter 5. AVI Publishing Company, USA. 1975.
- 6.5. Shioya, S. Measurement of biological reaction rates using advanced pH control systems. IFAC/ICCAFT 4 Conference. U. K. p.15-22. 1988.
- 6.6. Cooper, C.M., G.A. Fernstrom and S.A. Miller. Performance of agitated gas-liquid contactors. *Ind Eng Chem*. Vol. 36. p. 504-509. 1944.
- 6.7. Nakauoh, M and F. Yoshida. Transient characteristics of oxygen probes and determination of K_{La} . *Biotechnology and Bioengineering*. Vol. XXV. p. 1653-1654. 1983.

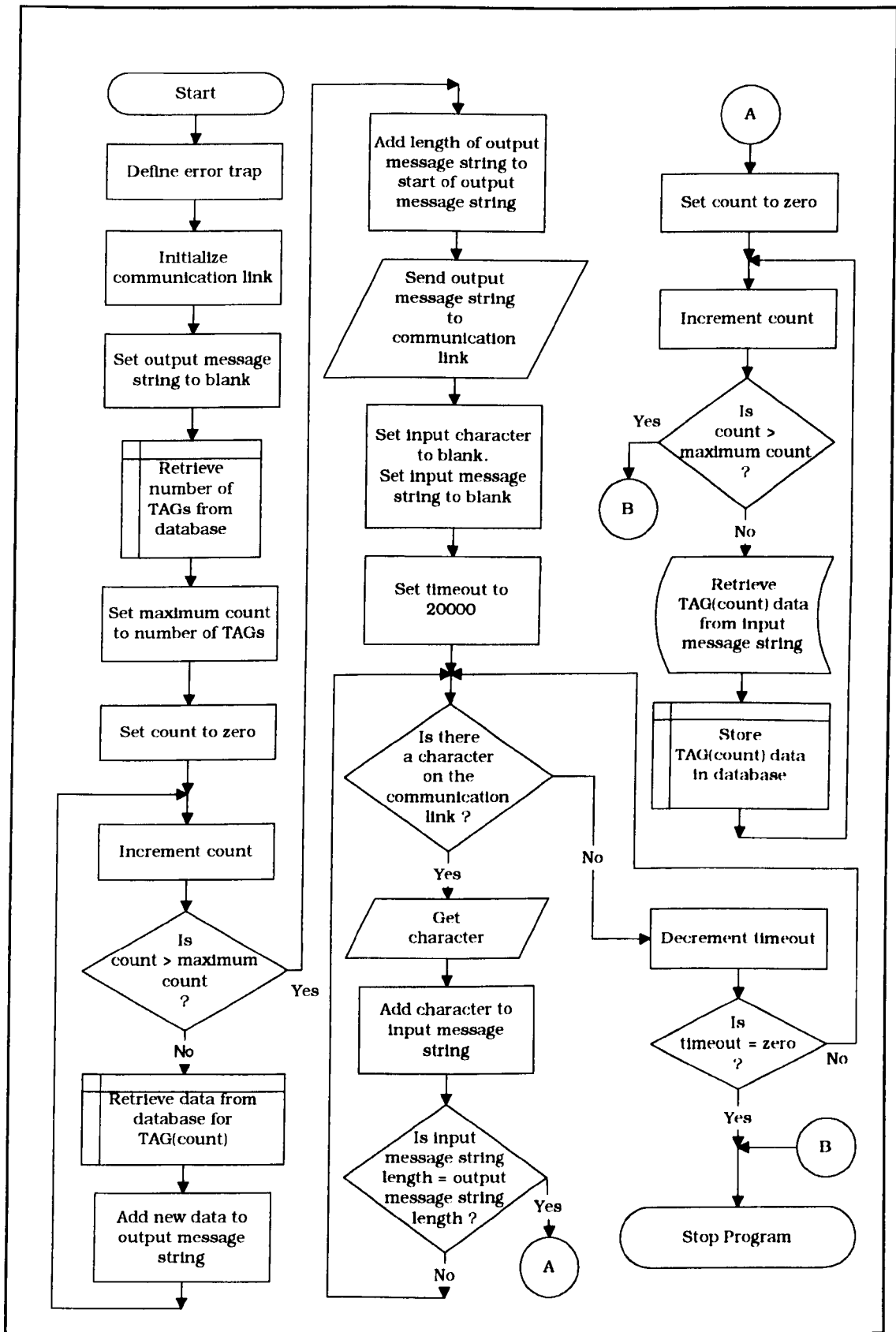


Figure 6.27 Flowchart for the MENTOR to Amstrad communication routine.

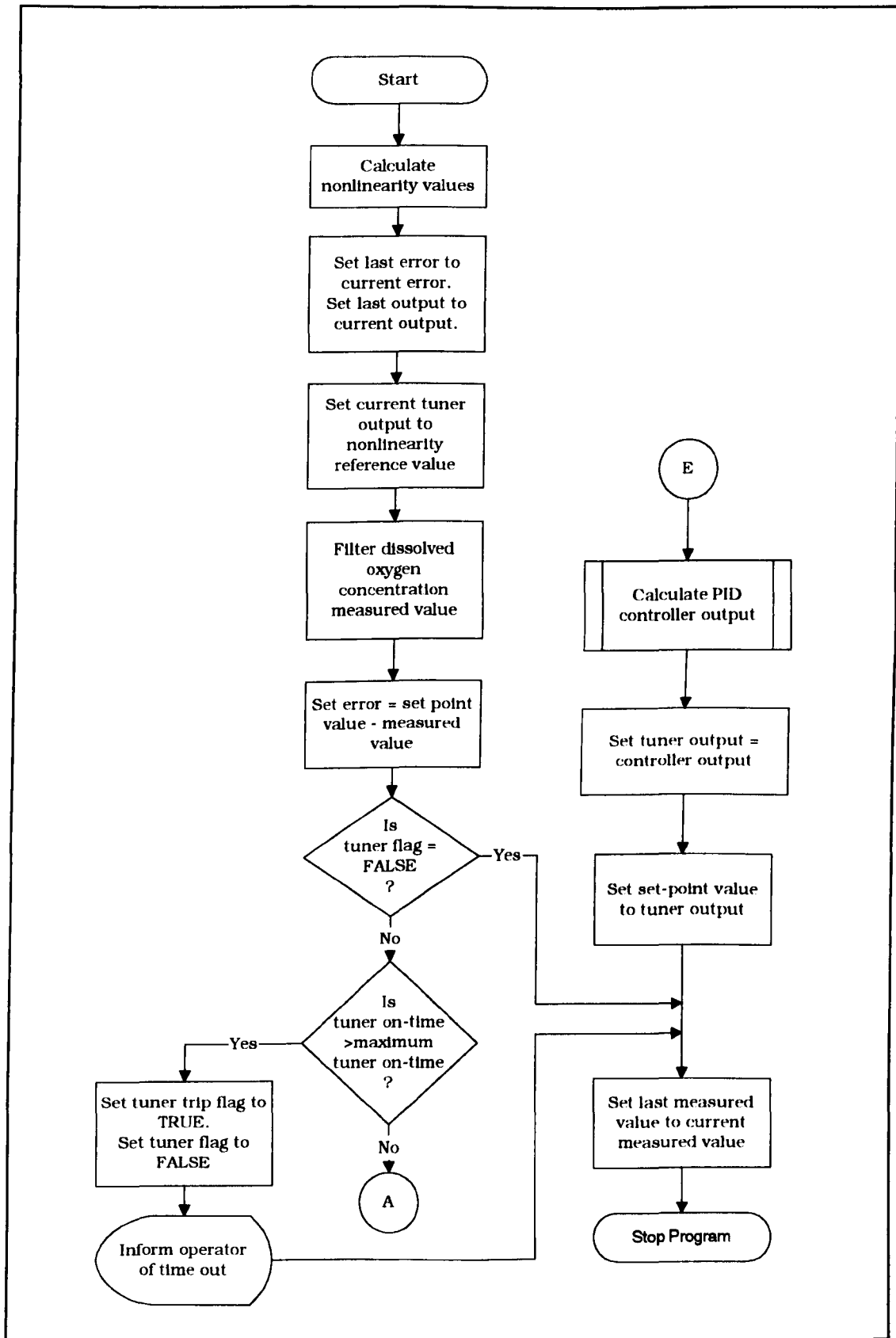


Figure 6.28a Flowchart for the procedure 'Algorithm'.

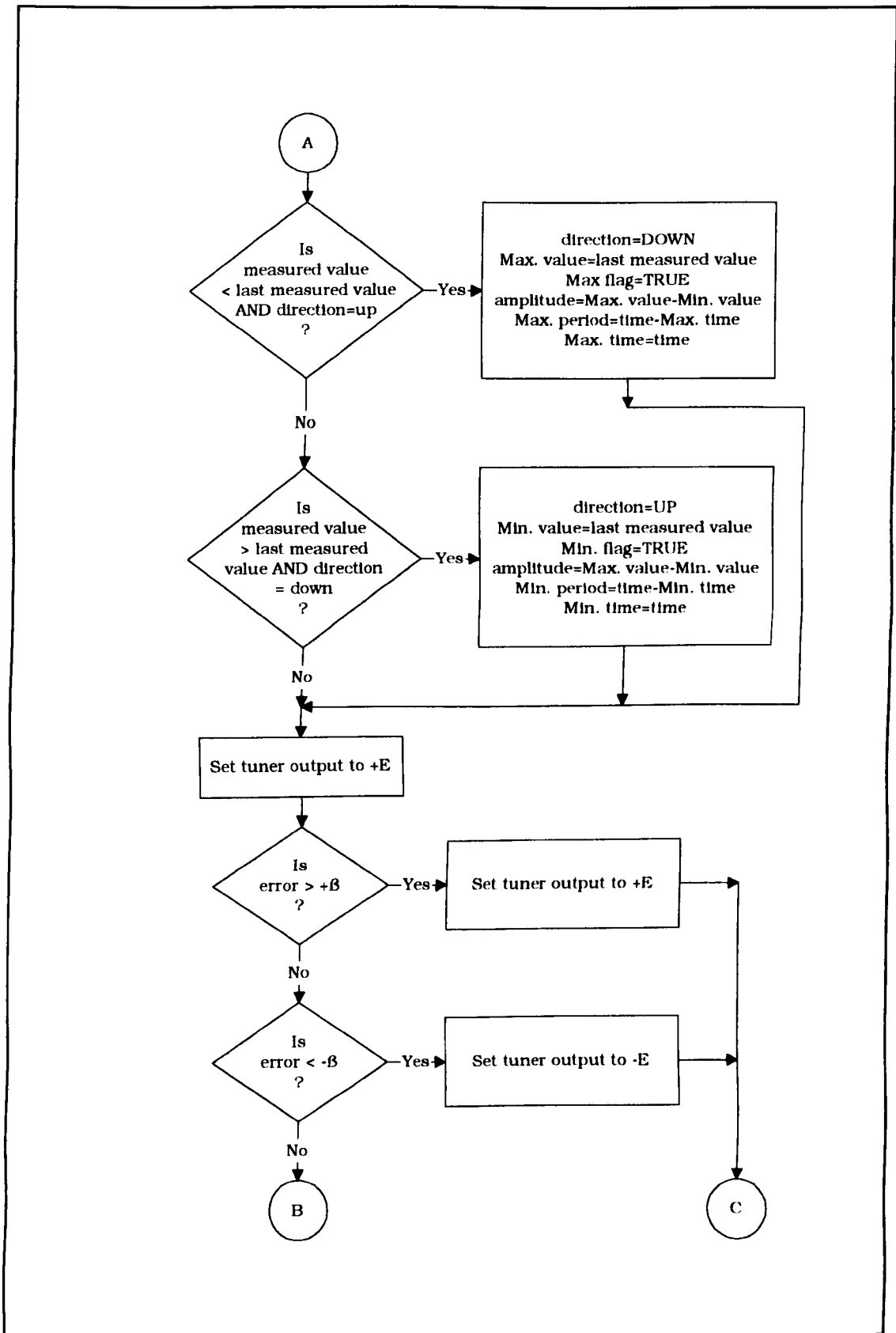


Figure 6.28b Flowchart for the procedure 'Algorithm' (continued).

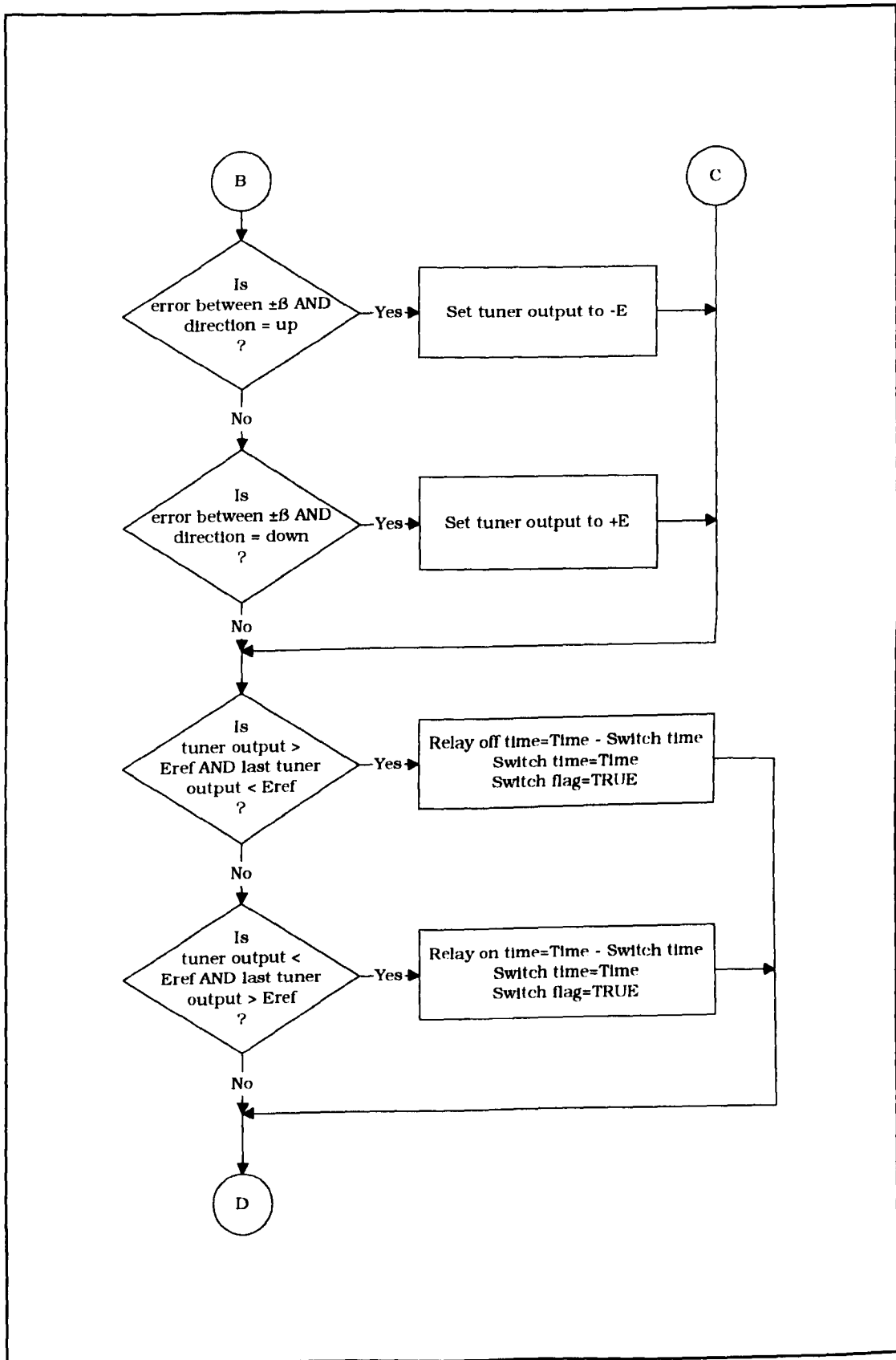


Figure 6.28c Flowchart for the procedure 'Algorithm' (continued).

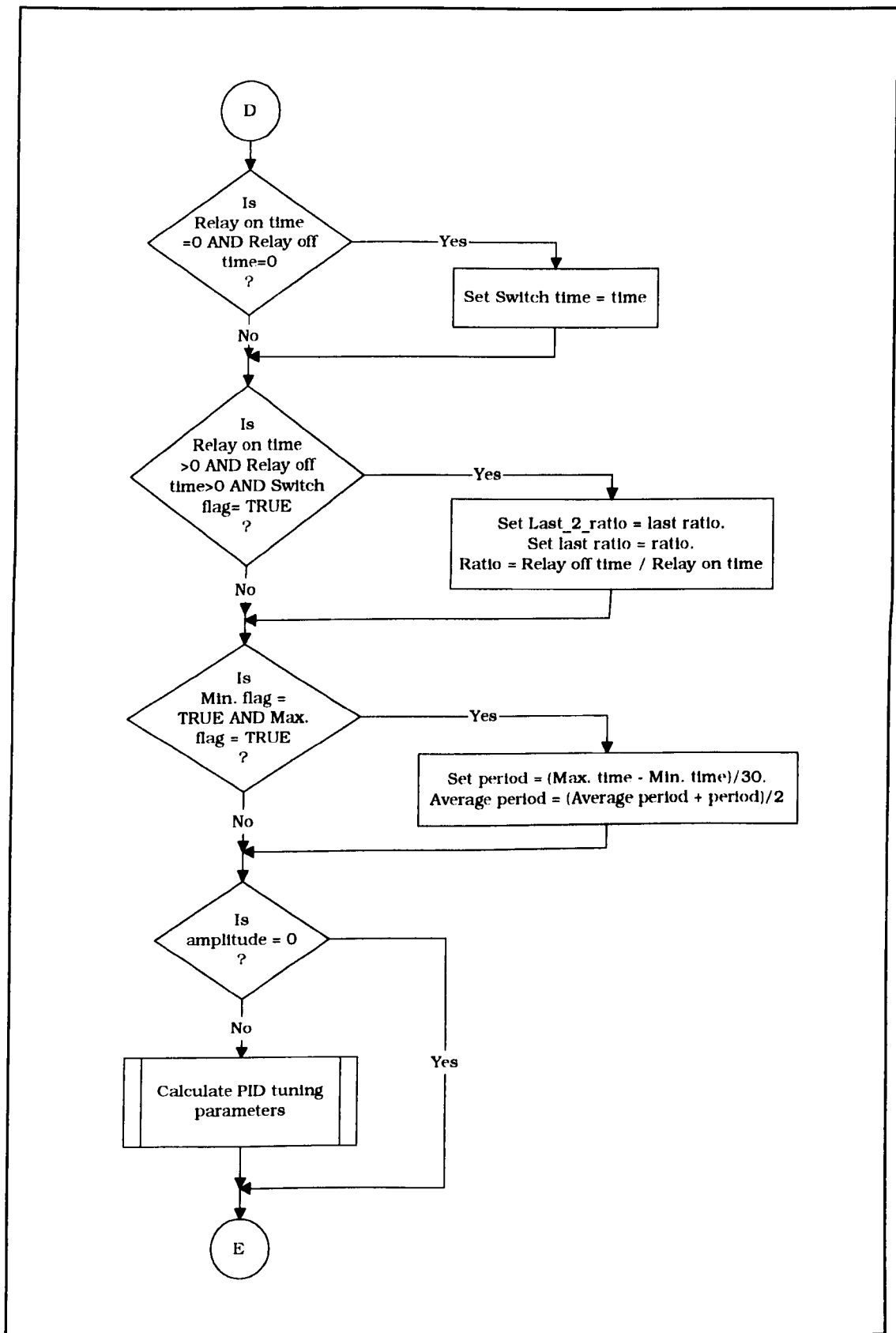


Figure 6.28d Flowchart for the procedure 'Algorithm' (continued).

CHAPTER 7.

CONCLUSIONS AND RECOMMENDATIONS.

7.1. INTRODUCTION.

Since the 1940's, single-loop controllers, such as the PID, have undergone a series of developments from the original pneumatic versions to the current microprocessor implementations. It is only recently that the industrial PID controller has started to have additional elements included, such as adaptation. One of the primary reasons for their development is the availability of inexpensive microprocessors with large computing power. Additionally, plant operators are becoming familiar with advanced control techniques, while the range of suitable applications is increasing, especially newly developed processes for which no *a priori* knowledge is available to assist in controller design. The use of currently available adaptive control algorithms is not straight-forward, especially for the inexperienced user. The use of an adaptive controller means that even more responsibility is passed onto the control system, hence the operator must be confident that he can allow the system, however intelligent, to make unsupervised changes to the tuning parameters of control loops which may be critical to the process plant. The advantage of the described automatic tuning procedure over conventional tuning methods, is that it can be implemented automatically, thus reducing operator training. Additionally, conventional tuning methods provide an acceptable PID controller performance for time invariant feedback loops, at a specific operating point. However problems in the controller performance usually arise with changes in the static or dynamic behaviour of the process. The automatic tuning procedure not only guarantees closed loop stability, but can also easily be understood by practising control engineers. Additionally, the procedure requires little *a priori* process knowledge for a successful implementation.

7.2. DISCUSSION.

It has been the intention of this thesis to investigate the problems of implementing the automatic tuning PID controller on nonlinear and time variant processes which include noisy process variables. One application exhibiting

such characteristics is the control of dissolved oxygen concentration during batch and fed-batch fermentations.

Åström [7.1] has presented the results of an application of the automatic tuner to a laboratory experiment for temperature control using a carbon filament lamp. The lamp temperature was measured with a thermocouple, while the lamp current was controlled using a thyristor system. The automatic tuner worked well for the system, although the response was rather noisy. Åström and Hagglund [7.2] report how the automatic tuner has been applied to temperature control in an industrial sugar refinery, and to liquid-level control in a single tank system. The application of the automatic tuner to temperature control in a distillation column has been presented by Åström [7.3] where the original process had previously been considered poorly controlled. The use of the tuning procedure improved the overall process performance and produced controllers which provided an adequate response during severe disturbances. Radjai *et al* [7.4] used the vessel stirrer speed to determine a suitable PI controller for regulating the redox potential in an amino acid production process, where the effect of the change in input air flow rate on the fermentation process was negligible. A number of other laboratory processes, including liquid flow and pressure control loops, had the automatic tuning procedure applied with some success. All of these processes were primarily linear systems with known process dynamics which were generally first order with dead-time.

This work represents a novel application of the tuning procedure since it is applied to a multivariable and highly nonlinear industrial process. In particular the procedure has been placed on a critical process variable with fast dynamics. The automatic tuning procedure is based upon the Ziegler-Nichols closed-loop tuning technique and was originally developed for second-order systems with a delay. The performance of the closed-loop system, after automatic tuning, is therefore conditional on how close the process is to the approximation.

The theoretical background to the automatic tuning procedure (Chapter 3) relates the phase margin required for the controlled process to the hysteresis width of the nonlinear element. The simulation results for the various linear

transfer functions show that the tuning procedure is capable of providing a solution which approaches the required phase margin. For the case of real nonlinear systems with noise, such as a fermentation process, there is a problem in determining the actual phase margin achieved. Additionally, the equations used to determine the nonlinearity output and hysteresis width, can produce values which are unsuitable for the process variables used: for example, the hysteresis width for a 30° phase margin may be ±10% dissolved oxygen concentration, which provides a noise rejection of 20%. The compromise adopted for the on-line experimentation was to fix the hysteresis width at ±5% dissolved oxygen concentration, which can be designed to a phase margin of 20°.

7.3. CONCLUSIONS OF THE WORK.

There have been a number of new controller algorithms developed recently, which have been suggested as viable replacements for the traditional PID controller; "But are they really better than the PID, which has now been in continuous use for over 40 years?" For industrial process control applications the PID controller is widely preferred; for several reasons, including:

1. For the majority of processes, the use of PID control provides adequate system performance, and is known to be almost as robust as state-space-control with regard to process parameter changes [7.5].
2. Current process engineers are more familiar with the PID controller than with modern control concepts such as self-tuning regulators, Artificial Neural Network control and so on. Hence there is a comprehensive knowledge base on the implementation and tuning of PID controllers.
3. The application of complex controller algorithms requires operator training and retraining.

The advantage of the automatic tuning procedure over adaptive or self-tuning controllers is that it maintains the well known PID algorithm as the controller, while requiring little operator training for its successful use. The automatic tuning procedure can be initiated on-line by a variety of methods, including:

- a) on process start-up;
- b) on operator demand;
- c) on a periodic time-base;
- d) when the controlled variable begins to stray from the required set-point.

Each method has its own obvious implementation. For a process which is highly nonlinear and/or time-varying then it is more convenient to arrange for the tuning procedure to be activated automatically, either after a set time period or when a sustained deviation is detected in the output variable. If, however, the process dynamics change very slowly then the operator should be allowed to decide when to retune the controller. For most processes there will be unknown initial conditions, thus the tuning procedure should be initiated at the start of the process run-time. Each of these methods has been implemented during the simulation work, while the first three have also been applied on-line. Once the tuning phase is complete, an acceptable PID controller is produced, however minor adjustments to the tuning parameters may be necessary to obtain an optimized process response. The nonlinearity induces an oscillatory response on the process variable, however the system remains stable. In fact, stability is ensured by the on-line modification of the nonlinearity output level to maintain the oscillation amplitude below a defined maximum. Once the controller has been retuned, then stability is maintained owing to the use of the PID controller algorithm. The time taken for the tuning procedure to complete the tuning phase is dependent upon the process dynamics; thus for the sodium sulphite reaction a typical retuning took 40 minutes while it was only 15 minutes for a fed-batch fermentation. The transfer time from the PID controller to the tuning procedure and vice versa, is performed almost instantaneously ensuring that the process always has some form of control action applied.

The investigation into the proposed automatic tuning procedure has been carried out in two stages. Firstly, simulation trials were performed to ascertain the operational properties of the procedure; and secondly on-line experiments were performed for both batch and fed-batch fermentations as well as a simple chemical reaction. The results presented in Chapter 5 show how the automatic tuning procedure was successfully validated, developed and fully tested on a range of simulated processes. The fed-batch fermentation model (Model I in Chapter 4) has been taken from Pirt [7.6] and represents a comprehensive yet simple account of the process; while the complex model (Model II) includes the step-change which occurs in the fermentation process dynamics when the glucose substrate has been completely utilised during a batch fermentation.

which produces ethanol as a by-product. The results for the on-line experiments, given in Chapter 6, illustrate that the tuning procedure showed favourable characteristics for both batch and fed-batch fermentations of *S. cerevisiae*, as well as for the chemical reaction when compared to a manually tuned PID controller. Often adaptive controllers are shown to have an improved performance over PID controllers. However, these comparisons are often biased in the sense that the PID scheme used for the comparison might differ from a fine tuned PID controller. An industrially implemented control scheme often might include first hand knowledge of the process gain and linearizing blocks to increase the robustness and improve the process performance. The on-line and off-line results presented within this thesis have contrasted like with like, to provide a fair comparison.

Contrasting the results for the manually fine tuned PID controller on a batch fermentation with the response for a single automatic controller tuning; it can be seen that the tuning procedure is capable of performing as well as a manual tuning. The advantage of the automatic tuning procedure is in the ability to retune the controller during the experiment and thus improve the process performance. A similar conclusion can be drawn by comparing the manually tuned and automatic tuned controller responses for a fed-batch fermentation. The results for the batch and fed-batch fermentations also show that the automatic tuning procedure is capable of the on-line determination of the controller parameters using the period and amplitude of the oscillations induced by the nonlinear element. Further, the results illustrate that the process can be retuned during the experimental period to maintain overall process performance. The fermentation experimental results indicate that the dissolved oxygen concentration measurement has a significant noise element. The fact that the responses of the automatically tuned controllers are as good as the manually tuned controller demonstrate that the automatic tuning procedure is not adversely affected by the noise. This is partly owing to the noise rejection capabilities of the nonlinearity hysteresis width, as well as the general robustness of the tuning method.

A benefit of the automatic tuner over other adaptive or self-tuning controllers is that the tuning procedure is capable of consistently retuning the PID controller for both nonlinear and time-varying processes. This feature can be seen from the batch and fed-batch fermentation results, which also show that the procedure has the ability to cope with batch-to-batch variation in the fermentation process starting conditions. The results of the application of the auto tuner to the sodium sulphite reaction illustrate that the procedure can successfully cope with "black-box" processes.

The tuning procedure does not necessarily offer an improved control method for a process since it is constrained by the structure of the PID algorithm. Thus, if a PID is unsuitable for the control loop then the tuning procedure cannot provide a solution to the control problem. Fortunately, the vast majority of control loops perform adequately under PID control. The automatic tuning procedure provides an on-line method of determining suitable PID controller parameters which can produce a controlled response which is comparable to a manually fine tuned controller. Additionally, the tuning procedure requires little operator training and can determine controller parameters after a 'single attempt', while manual tuning requires a number of experiments. Since the tuning procedure can be used to retune a controller during a experiment, it provides the operator with a method of improving the process performance as time varying dynamics change.

It can be concluded that the work presented in this thesis has been productive in that an automatically tuned PID controller has been developed and successfully applied to the control of dissolved oxygen concentration for a fed-batch fermentation, a batch fermentation and a chemical reaction; in simple terms these represent processes which are time-variant, highly nonlinear and "unknown" respectively.

7.4. RECOMMENDATIONS FOR FURTHER WORK.

There are two broad areas in which additional work may be carried out. Firstly, the operation of the automatic tuning procedure within the confines of biotechnology and fermentation processes, can be investigated further; while the other area of interest is the application of the automatic tuning procedure to other processes, such a multi-input multi-output.

7.4.1. Automatic Tuning Procedure Operation.

The automatic tuning method proposed inherits the limitations of the PID algorithm, also it does not work well for problems where a more complicated control law is required. However, the procedure may be used to produce initialization values for more sophisticated self-tuning controllers. For example, gain scheduling is a powerful method of dealing with nonlinear processes where the controller parameters need to be changed from one known set to another, if process control is to be maintained over a nonlinear range. Implementation of gain scheduling has therefore required a great deal of effort to obtain all the sets of tuning parameters required to adequately control the process for all phases of operation. Using the automatic tuning procedure it may be possible to automate this process, with fermentation processes offering an ideal opportunity to investigate the possibilities of incorporating the automatic tuning procedure and gain scheduling within an Expert System environment.

In [7.7] it is reported that the presented automatic tuning procedure has been applied to numerous laboratory processes and has been found to be very robust. However, the limits of robustness have not been determined by any mathematical analysis; this obviously should be determined.

7.4.2. Application to Other Processes.

It has been shown [7.8] that the nonlinearity tuning method can be extended to multivariable, multi-loop systems. The automatic tuner is placed on one of the loops while the remainder are left open-loop. Once the tuning phase is complete, then the tuning procedure is moved on to the next loop in the system while the tuned loop is placed into closed-loop control. The tuning of the new loop provides a method of determining tuning parameters while the process dynamics

are being altered by the previous loop's controller. This method, of tuning a loop and moving on to the next loop, is continued until all the process loops have been tuned. An obvious use of this concept would be in sequentially tuning the controllers used for input air flow rate and agitation speed, since by the optimum choice of air flow rate and agitation speed the process running costs may be kept to a minimum. This would represent a 2-input-1-output system. Alternatively, Sirisen *et al* [7.9] have suggested a method of using information provided by nonlinearity control to tune a PI controller for a 2x2 system: this requires the oscillation of both loops simultaneously. The effect this would have on a real process is unknown, and should be investigated.

The work carried out has been on a small-scale 20 litre fermenter, whereas industrial usage would be on vessels in excess of 1000 litres. This should not pose a problem, since it has been suggested [7.10] that 20 litre pilot-plant data can be directly scaled up to 100,000 litre vessels. This may be true, however one direct difference is in the measurement systems. When measurements of oxygen partial pressure are carried out at the lower depths of an industrial fermentation vessel, the effect of hydrostatic pressure should be taken into consideration. In the absence of air bubbles there is no effect of hydrostatic pressure on the oxygen partial pressure. In theory this should not affect the operation of the automatic tuning procedure on the dissolved oxygen concentration control loop provided that the data presented to the procedure has been calibrated accordingly, although a number of large scale industrial fermenters use pure oxygen as the input source which could affect the operation of the automatic tuning procedure.

7.5. REFERENCES.

- 7.1. Åström, K.J. Ziegler-Nichols Auto-Tuners. Report CODEN: LUFTD2/(TFRT-3167)/1-025(1982). Lund Institute of Technology, Lund, Sweden. 1982.
- 7.2. Åström, K.J. and T. Hagglund. Automatic tuning of simple regulators for phase and amplitude margin specifications. IFAC Symposium on Adaptive systems in control and signal processing. p. 271-276. 1983.

- 7.3. Åström, K.J. Adaption, auto-tuning and smart controls. International symposium on advanced process supervision and real-time knowledge based control. November, 1988.
- 7.4. Radjai, M.K., R.T. Hatch and C.W. Cadman. Optimization of Amino acid production by automatic self tuning digital control of Redox potential. Biotechnology and Bioengineering Symposium No. 14. p. 657-679. 1984.
- 7.5. Kofahl, R. and R. Iserman. A simple method for automatic tuning of PID controllers based on process parameter estimation. Proceedings of the American Control Conference., p. 1143-48. 1985.
- 7.6. Pirt, S.J. Principles of cell and microbe cultivation. Blackwell Scientific Press. 1975.
- 7.7. Åström, K.J. and T. Hagglund. Practical experiences of adaptive techniques. In 'Advances in adaptive control', Eds: K.S. Narendra, R. Ortega and P. Dorato. p. 243-250. 1991.
- 7.8. Loh, A. P. and C.K. Quek. An approach to multivariable control system design using relay auto-tuning. Proceedings of the Singapore International Conference on Intelligent Control and Instrumentation. IEEE Singapore Section. p. 162-164. 1992.
- 7.9. Sirisenn, H.R., C.C. Hang and V.U. Vasani. Empirical tuning of a class of multivariable control systems. Proceedings of the Singapore International Conference on Intelligent Control and Instrumentation. IEEE Singapore Section. p. 177-182. 1992.
- 7.10. Harrison, J.S. Aspects of commercial yeast production. Process Biochemistry. March. p. 41-45. 1967.

A. DISSOLVED OXYGEN PROBE STEP RESPONSE.

Before any on-line experiments were conducted, the response time of the dissolved oxygen probe was established. This was achieved by recording the output from the probe in reaction to a step change in conditions; firstly with a transition from air (100%) to Sodium Sulphite Solution (0%), and secondly from Sulphite solution (0%) to aerated water (100%). The zero percentage reading (or zero current) was determined by placing the sensor in nitrogen saturated water. The zero current should be as low as possible since it sets the detection limit, for the Ingold sensor used the zero point was between 0.1 and 0.2% of air saturation.

In all, four tests were carried out for each transition, with the values recorded every 20 seconds. The response graphs are shown in Figure A.1 and Figure A.2, illustrating the average values from the tests as well as the maximum and minimum values.

From the results it was found that the probe time-constant is approximately 60 seconds. This probe time-constant is less than the reaction time of Sodium Sulphite, thus the probe should not be the dominant component in the Sodium Sulphite tests. However, the time-constant is much greater than the reaction time of a Bakers' Yeast fermentation, thus the dissolved oxygen probe will be the dominant component in the fermentation experiments.

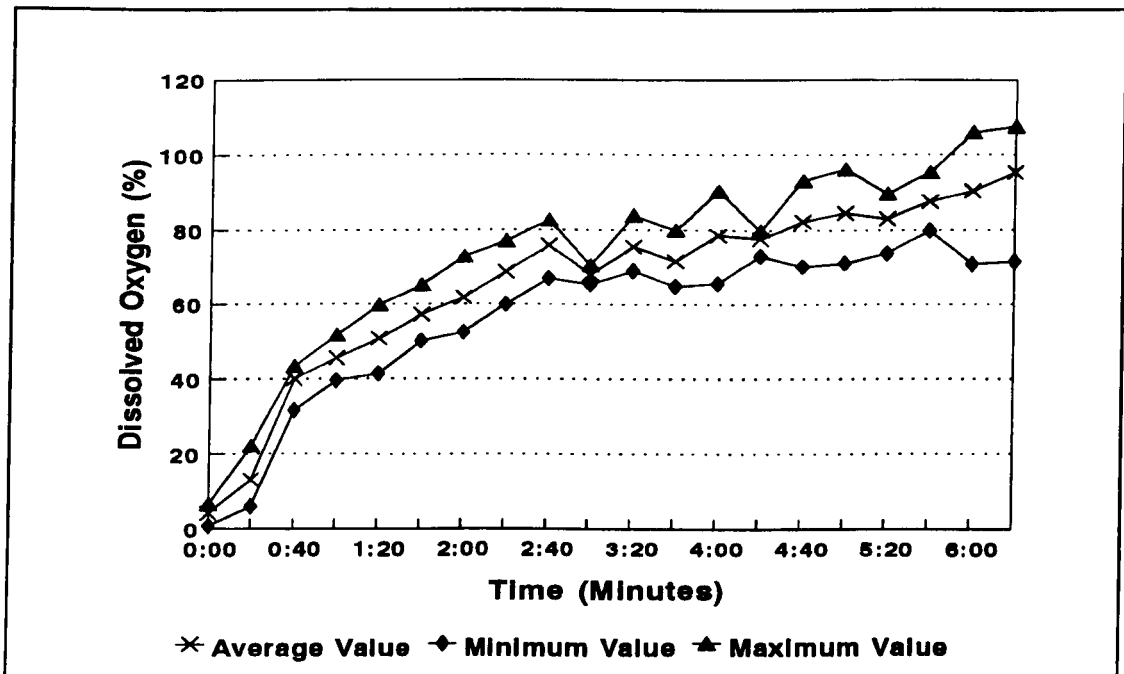


Figure A.1 Probe step response from 0% to 100%.

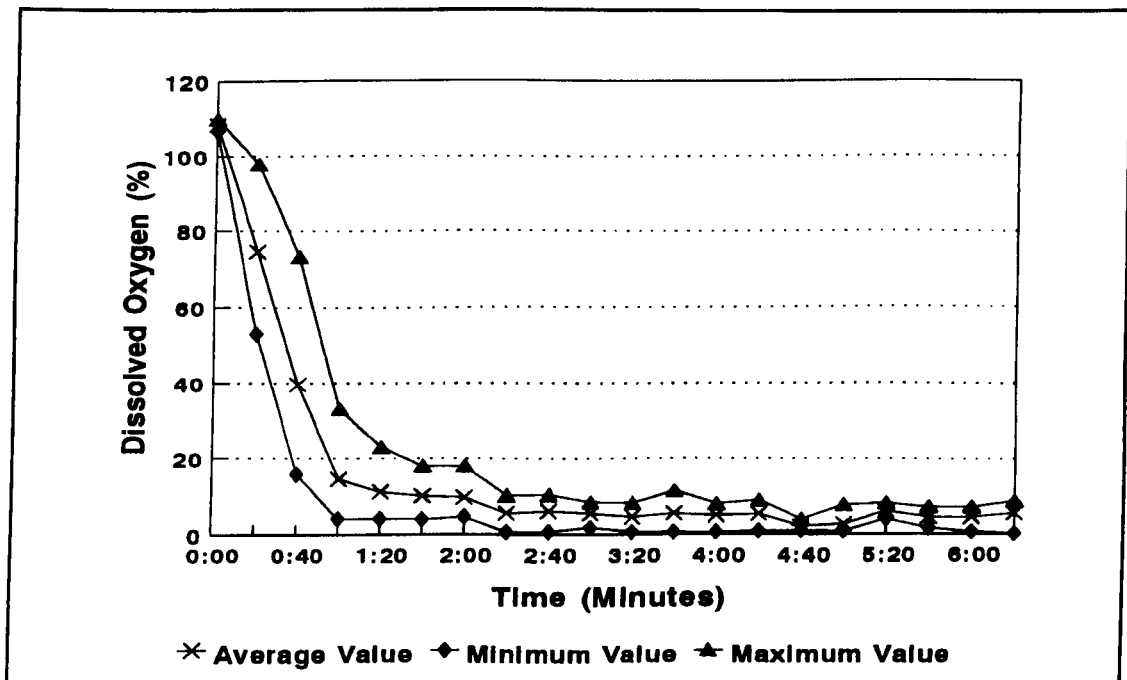


Figure A.2 Probe step response from 100% to 0%.

B. DATA FILTERS FOR NOISE SUPPRESSION.

During a fermentation, the dissolved oxygen concentration measurement is inherently noisy. In addition to small changes caused by the dynamic behaviour of cell respiration, there are spurious measurements owing to either bubbles of oxygen becoming momentarily attached to the probe (producing, for example, a 100% reading), or clumps of cells and/or substrate attaching (for example, reading 0%). Generally these spikes on the dissolved oxygen measurement last for one sample reading only. This type of noise is not desirable for any type of controller especially the automatic tuning procedure, since it introduces false maxima and minima into the amplitude detection procedure.

Thus it is beneficial to reduce - if not remove - these readings from the measurement signal. An obvious method of accomplishing this is to filter the raw data before applying it to the controller. For any system filtering can be both beneficial and problematic, since a filter does not completely remove spikes from the signal, instead it reduces the amplitude of each reading so that the effect of a spike is reduced.

There are a number of possible filters which can be used. One such filter is the regressive filter, given by

$$\hat{x}_n = \alpha x_n + (1 - \alpha)x_{n-1} \quad (\text{B.1})$$

where x_n is the actual measured value, \hat{x}_n is the filtered value and α is the filter constant. For $\alpha=0.0$ then $\hat{x}_n=x_{n-1}$, and for $\alpha=1.0$ then $\hat{x}_n=x_n$. The results of applying equation (B.1) to some on-line dissolved oxygen concentration measurements can be seen in Figure B.1. The results show that α values 0.0 to 0.6 produce \hat{x}_n values which are unrelated to the actual measured values. Since the filter is to be used simply to reduce the effect of extreme measurement noise readings, then these α values are inappropriate, as is $\alpha=1.0$. Therefore, suitable α -values for the regressive filter are 0.7, 0.8 and 0.9.

Another type of simple filter available is known as the moving-average window-filter. These filters can be represented by the generic equation

$$\hat{x}_n = \frac{1}{(k+1)} \sum_{j=0}^k x_{(n-j)} \quad (\text{B.2})$$

The results of applying equation (B.2) to actual on-line data, with $k=1, 2, 3$ & 4 , can be seen in Figure B.2. It can be seen that as the value of k increases there is a reduction in the information contained within the filtered data series. Suitable moving-average window-filters are therefore given by $k=1, 2$.

The filter chosen for the on-line experimental work was given by:

$$\hat{x}_n = \frac{x_n + x_{n-1}}{2} \quad (\text{B.3})$$

which is a form of equation (B.2) with $k=1$. This filter is a balance between the need to reduce the effect of measurement noise and the requirement to have a simple and fast piece of computer code.

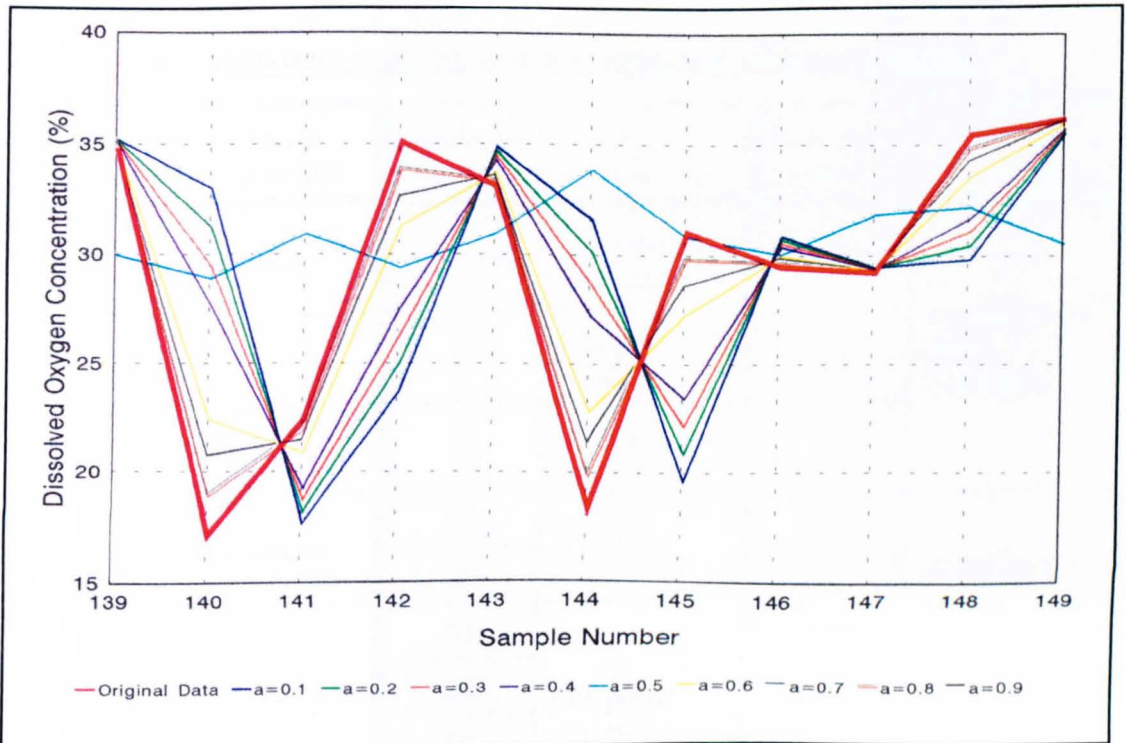


Figure B.1 Regressive filter results.

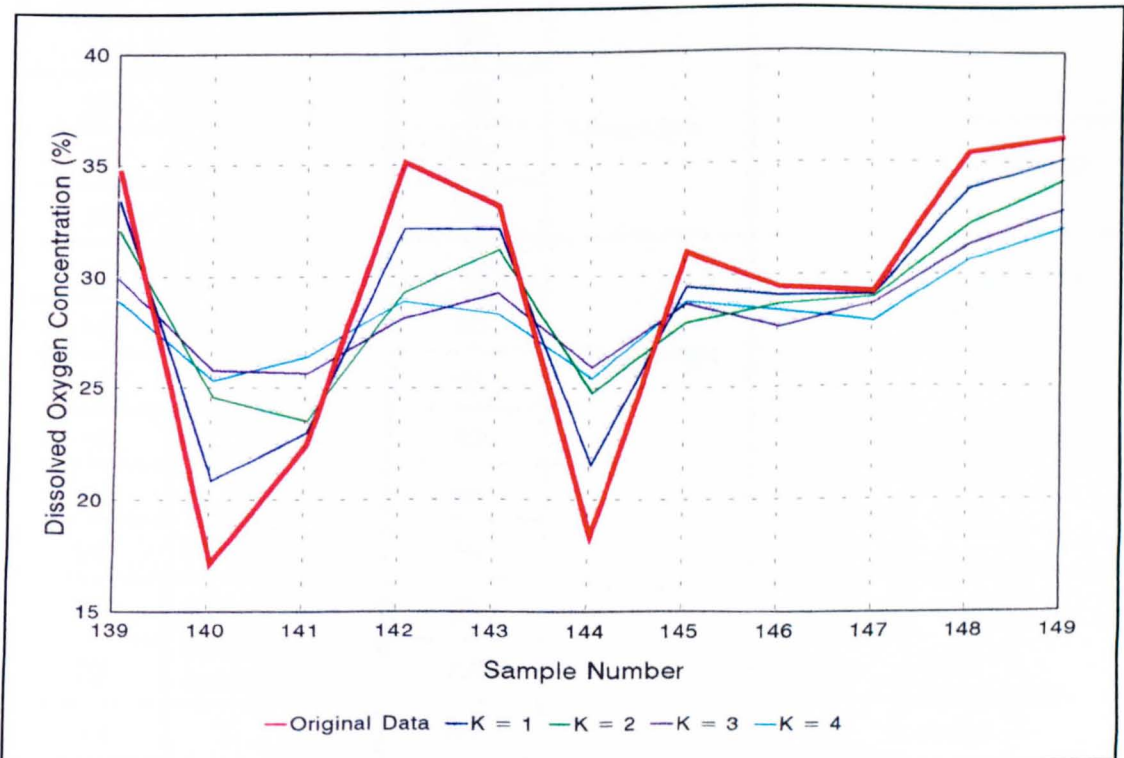


Figure B.2 Moving-average window-filter results.

C. MENTOR ANALOG LOOP DATABASE ARRANGEMENT.

Position Number	Stored Contents	Position Number	Stored Contents	Position Number	Stored Contents
1	Raw low	45	Log rate (in minutes)	87	Proportional gain constant
2		46		88	
3	Raw high	47	Insub number	89	
4		48	Outsub number	90	
5	Raw value	49	Vessel number	91	Integral action constant
6		50		92	
7	Measured value	51	Set point value	93	
8		52		94	
9		53		95	Derivative action constant
10		54		96	
11	Totalised value	55	Range low	97	Output raw low
12		56		98	
13		57		99	Output raw high
14		58		100	
15	Time constant	59	Range high	101	Sum of errors
16		60		102	
17		61		103	
18		62		104	
19	Output value	63	Alarm low	105	Last measured value
20		64		106	
21	Slave - to pointer (of master)	65	Alarm high	107	
22		66		108	
23	TAG number	67	Alarm high	109	Timer for control
24		68		110	
25		69		111	
26		70		112	

27		71		113	
28	Critical number	72	Set point low	114	Slope (derivative term)
		73		115	
29	Text dictionary pointer - word 1	74		116	
30	Text dictionary pointer - word 2	75	Set point high	117	Last output (for supervisory)
31	Text dictionary pointer - word 1	76		118	
32	Text dictionary pointer - word 2	77		119	
33	Text dictionary pointer - units	78	Dead band	120	Last output (for supervisory)
34	Day contact pointer	79		121	
35	Night contact pointer	80		122	
36	Day contact pointer	81	Day contact pointer	123	spare
37	Night contact pointer	82		124	
38	BIT list (See below)	83	Night contact pointer	125	RESEAU TAG
39	Input channel number	84		126	
40	Output channel number	85	127		
41	Input channel number	86	128		
42	Output channel number		129		
43	Output channel number		130		
44	Output channel number				

Bit Position	System Indicator	"1"/"0" Status
1	Status	Critical/Non critical
2	Action	Direct/Reverse
3	Logging	On/Off
4	Totalisation	On/Off
5	Control	On/Off
6	Alarm suppression	On/Off
7	Scanning	On/Off
8	DDC/Supervisory	On/Off
9	Cascade	On/Off
10	Alarm High	
11	Alarm Low	
12	Set point high	
13	Set point low	
14	BAD alarm	
15	Alarm acknowledge	

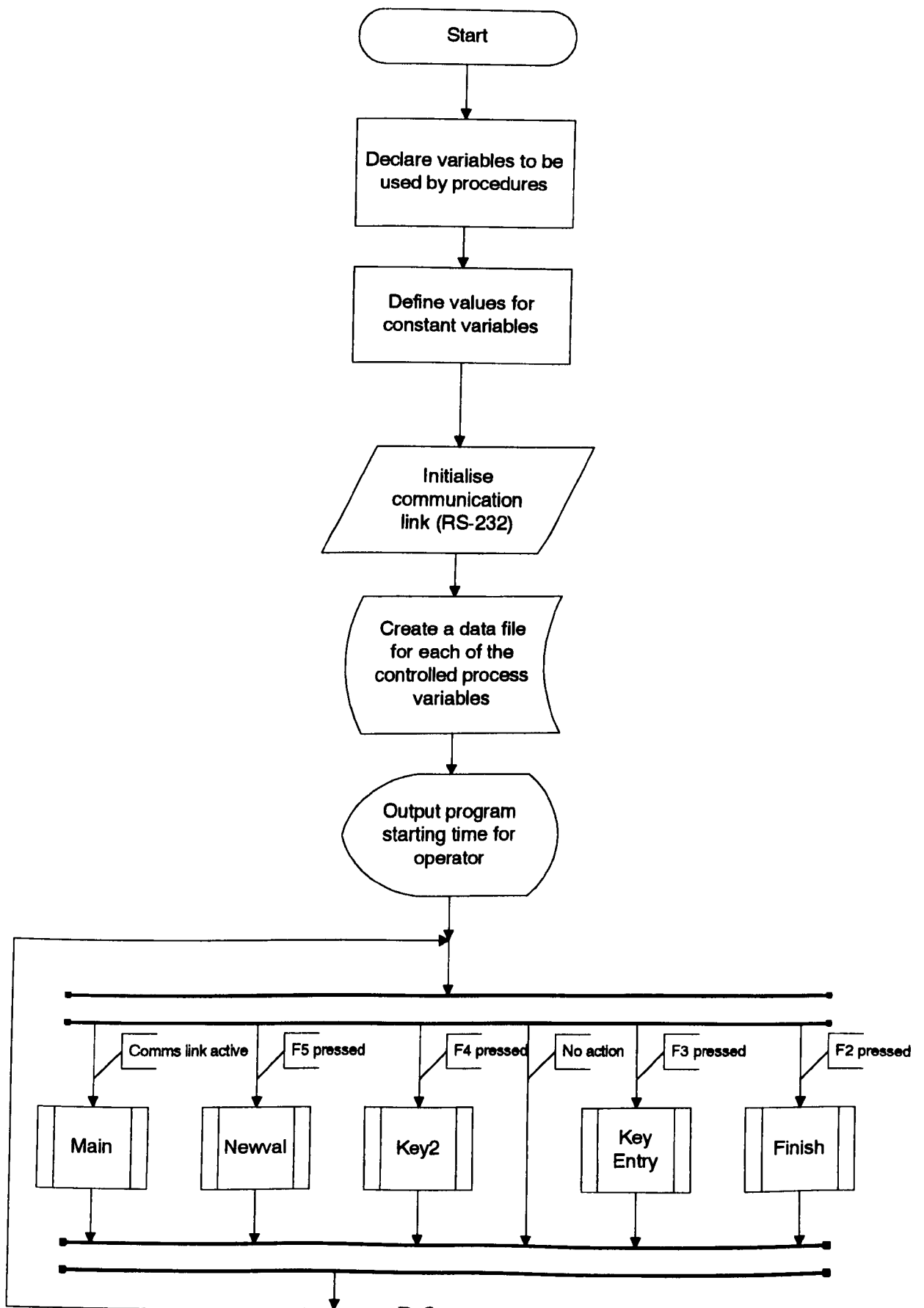
D. AUTOMATIC TUNING PROCEDURE SOFTWARE FLOWCHARTS.

The MENTOR software (described in Chapter 2) was used as the primary on-line control software for the fermenter vessel, while a secondary program was used for the development and implementation of the automatic tuning procedure. This proprietry software was written using the QuickBASIC programming environment, and was executed on the second (Amstrad) of the two Personal Computers used for the on-line experimentation.

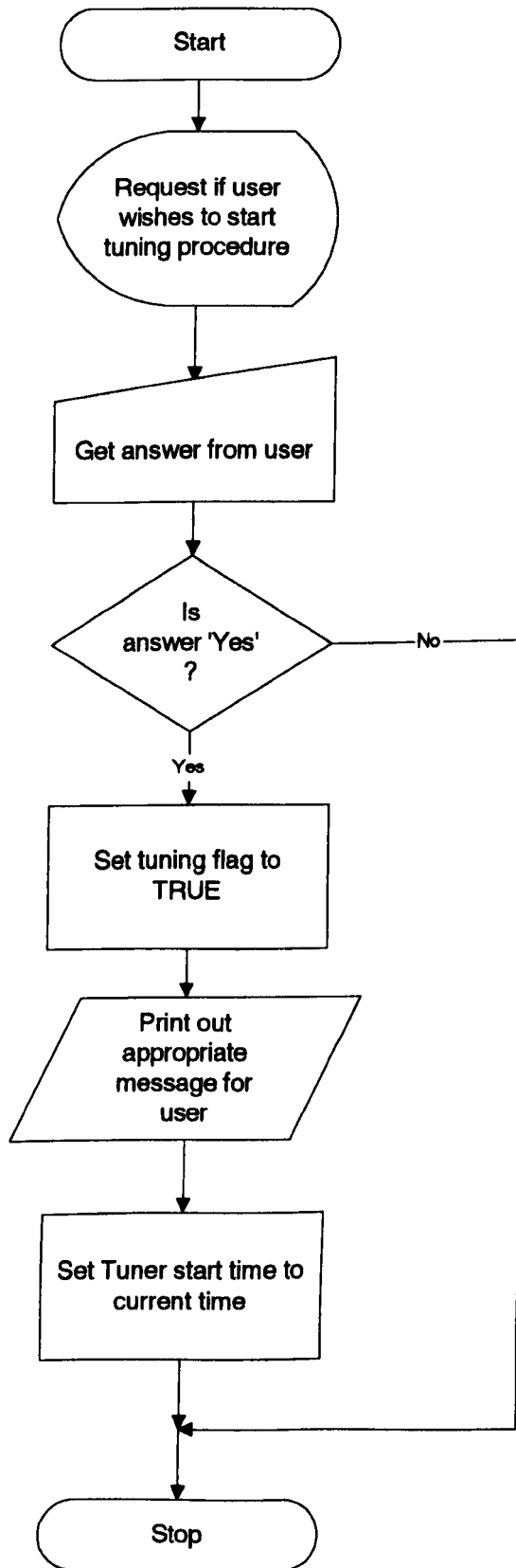
Neither a description of the software nor a program listing will be provided, however the flowcharts for the program are reproduced on the following pages for information.

Initial Program

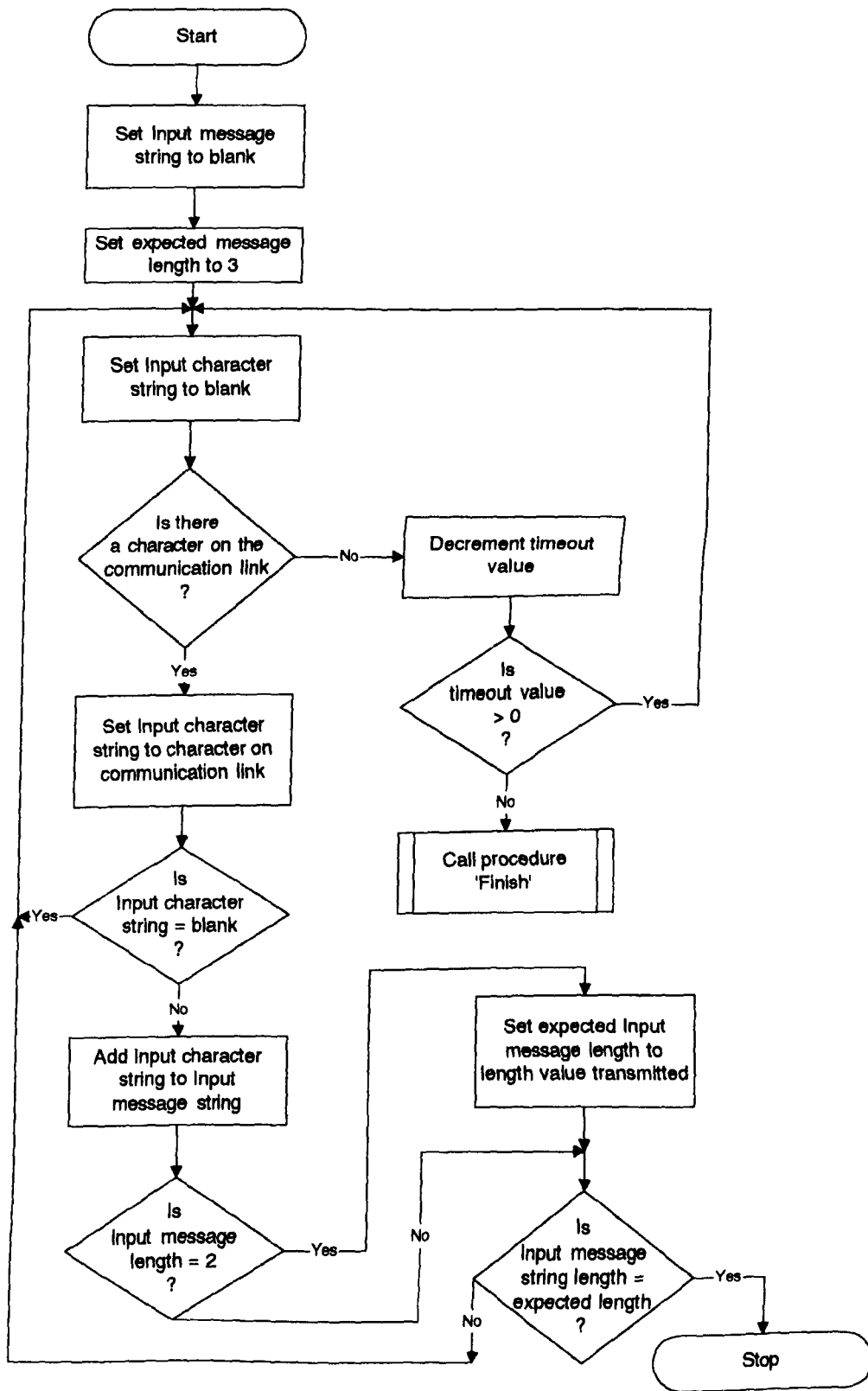
Appendix D



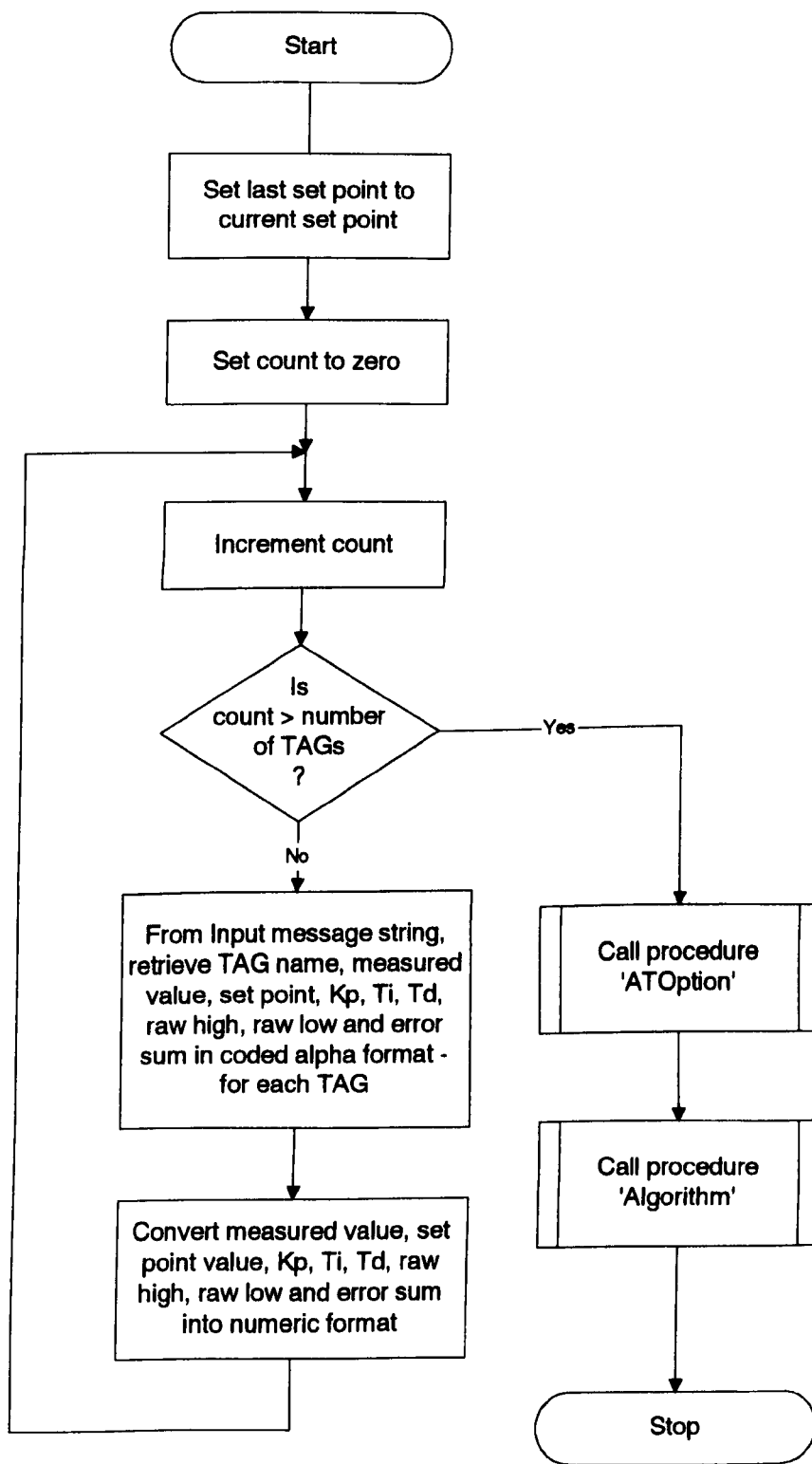
Procedure - Key Entry



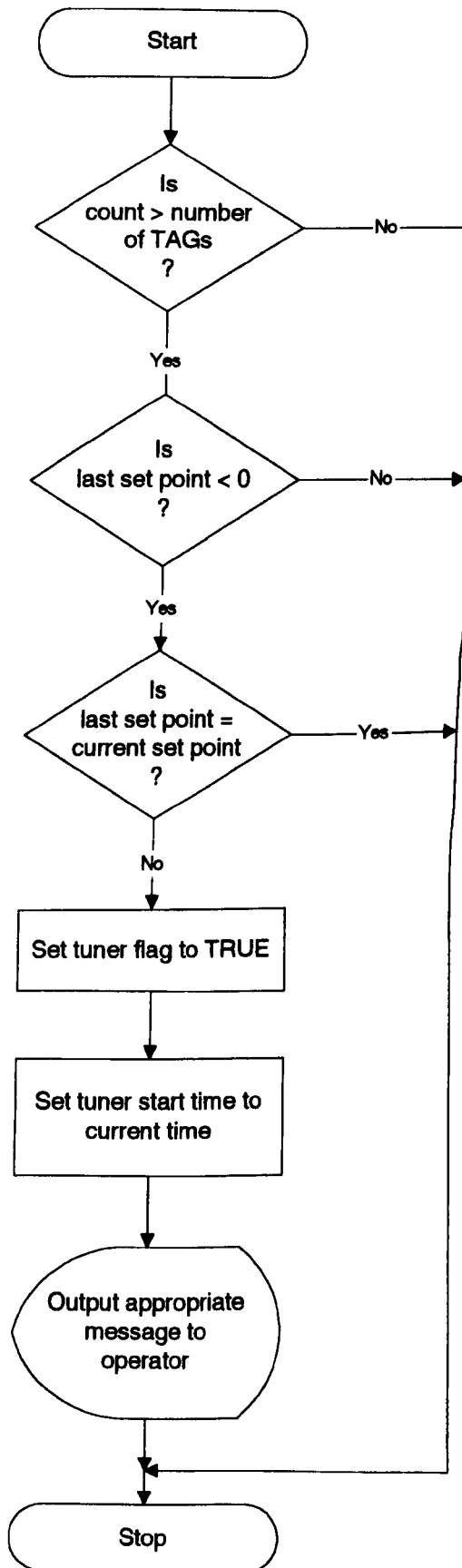
Subroutine - Get Data



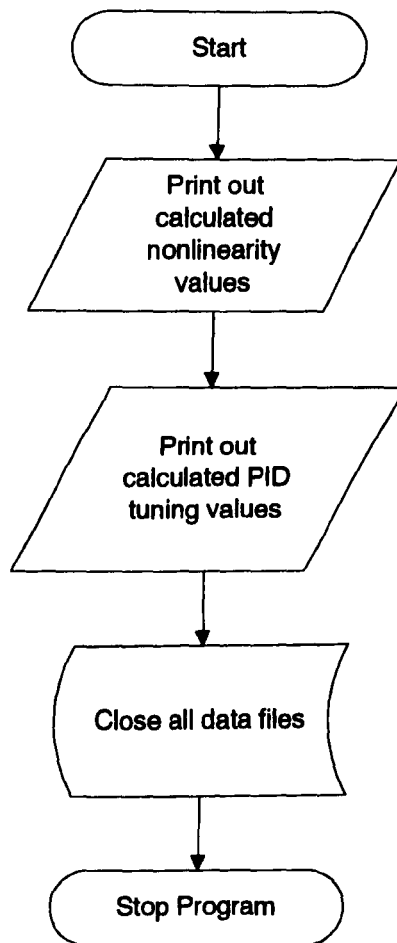
Subroutine - Pull Out



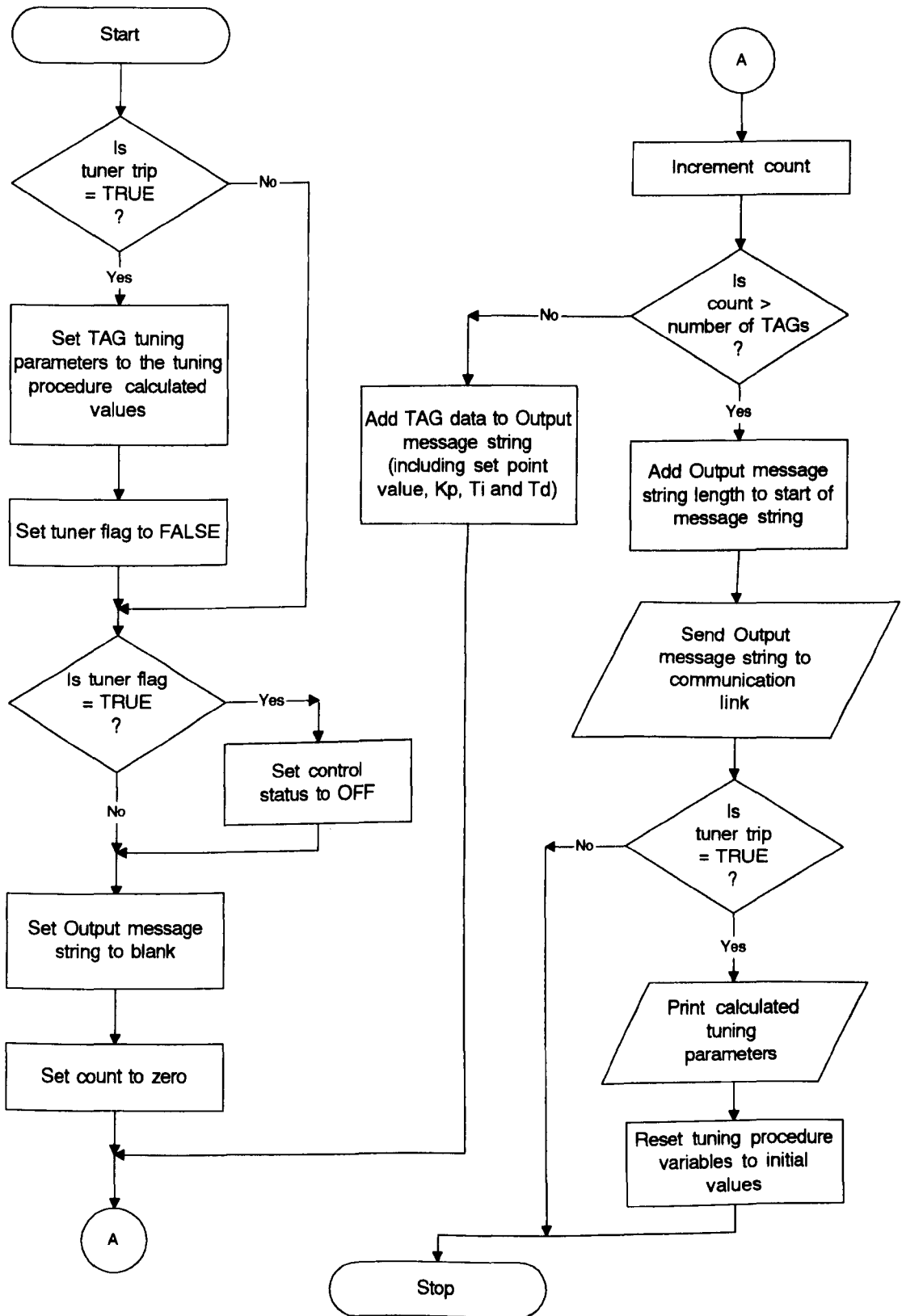
Procedure - ATOption



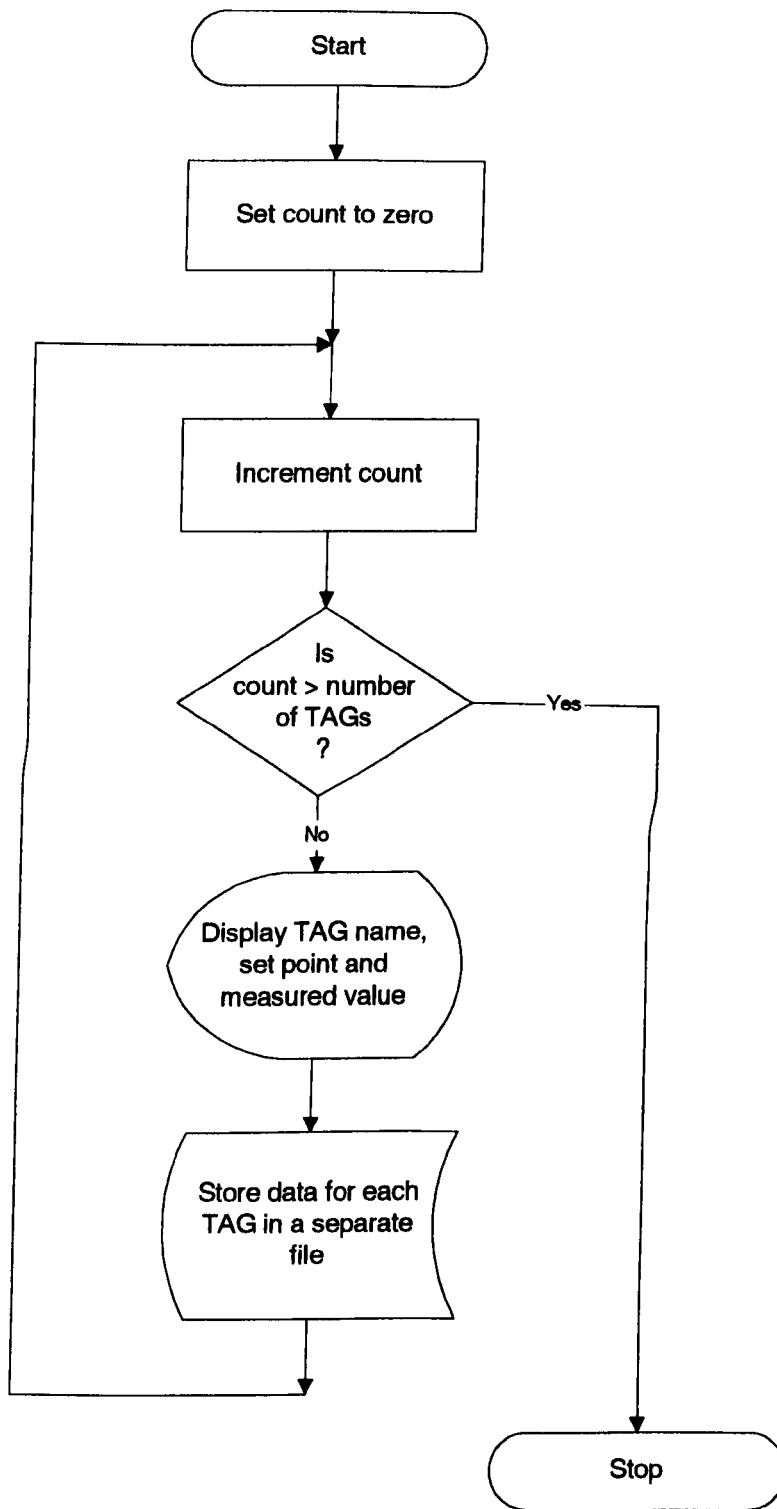
Procedure - Finish



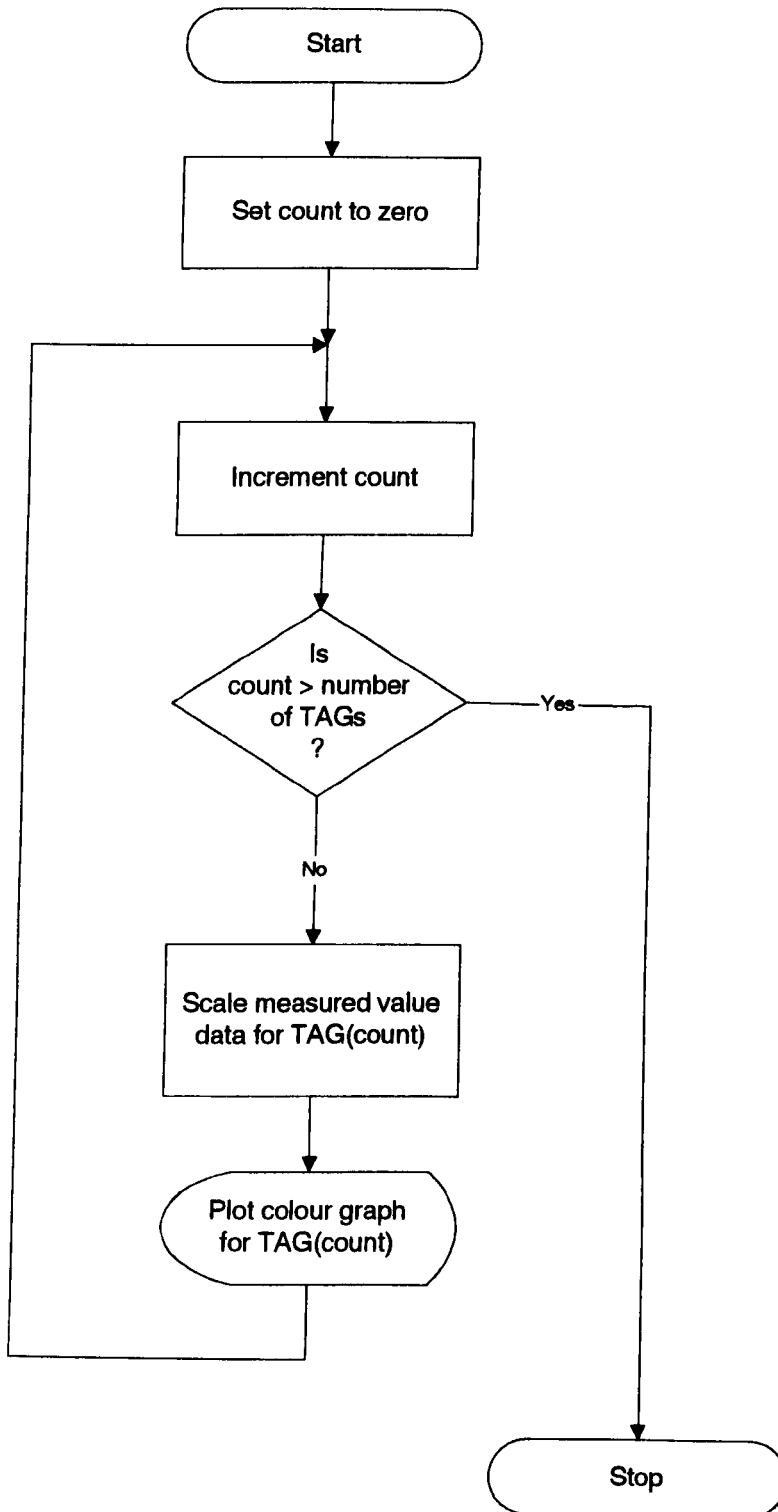
Subroutine - Send



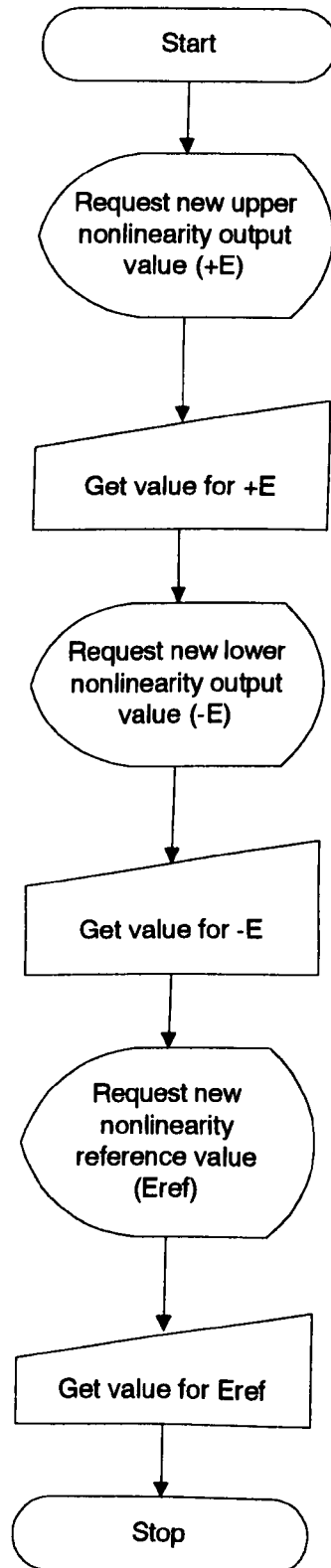
Procedure - Logging



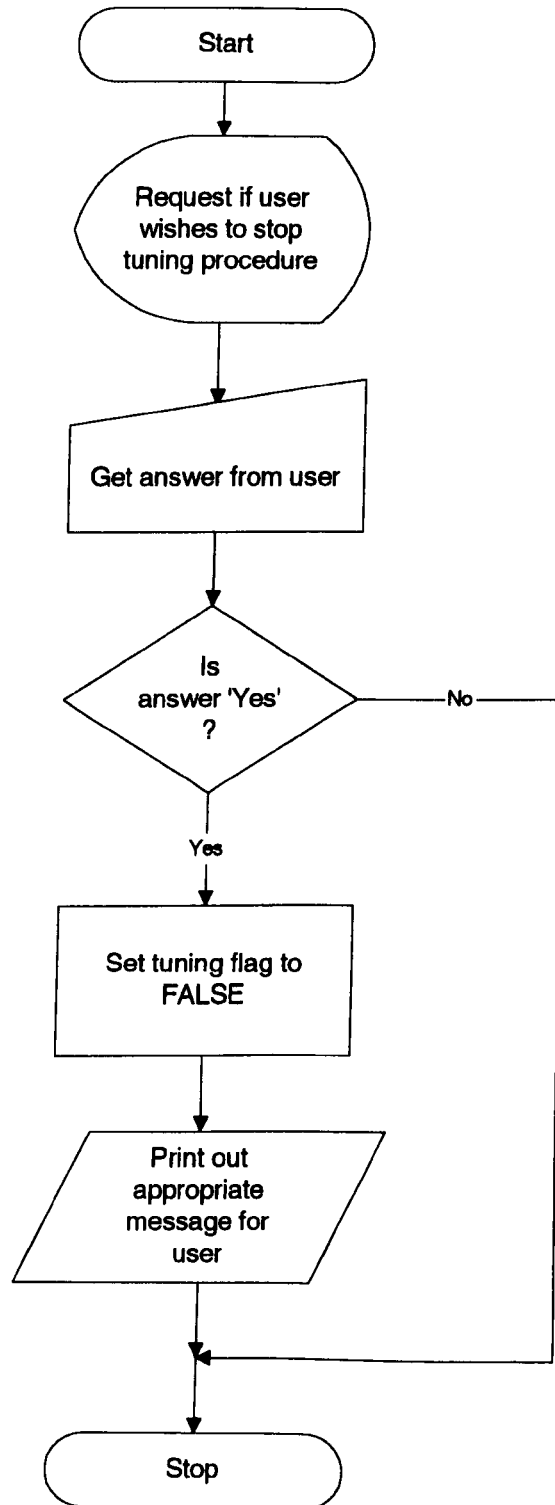
Procedure - Graphing



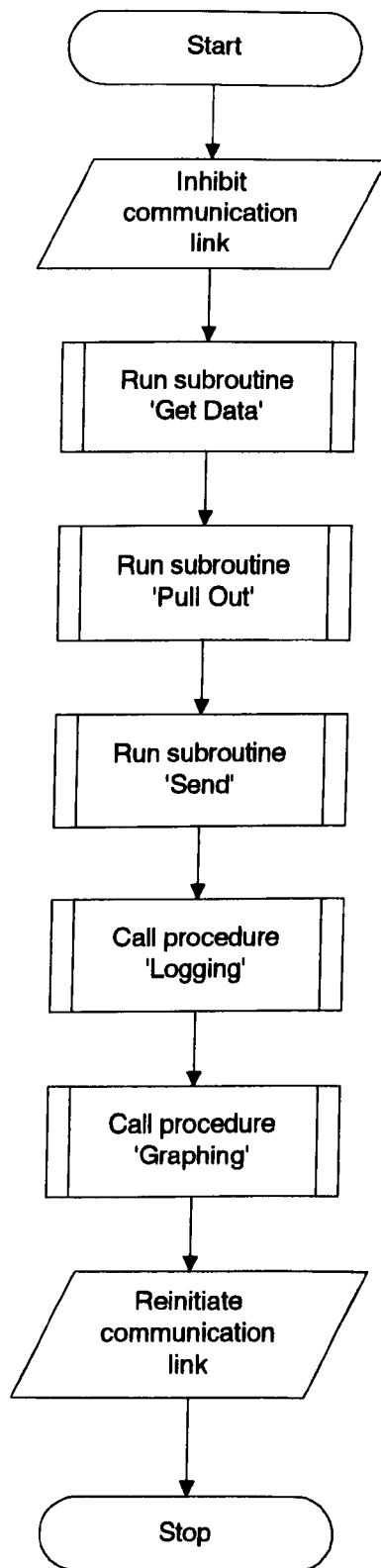
Procedure - Newval



Procedure - Key2



Subroutine - Main



**APPENDIX
NOT COPIED**

**ON INSTRUCTION
FROM
THE UNIVERSITY**